THE ROLE OF *RpoT;3* IN CHLOROPLAST DEVELOPMENT AND GENE EXPRESSION

A Dissertation

by

AGLAIA CHANDLER

Submitted to the Office of Graduate Studies of
Texas A&M University
in partial fulfillment of the requirements for the degree of

DOCTOR OF PHILOSOPHY

August 2005

Major Subject: Biochemistry

THE ROLE OF *RpoT;3* IN CHLOROPLAST DEVELOPMENT AND GENE EXPRESSION

A Dissertation

by

AGLAIA CHANDLER

Submitted to the Office of Graduate Studies of
Texas A&M University
in partial fulfillment of the requirements for the degree of

DOCTOR OF PHILOSOPHY

Approved by:

Chair of Committee,	John E. Mullet
Committee Members,	John A. Howard
	Ryland F. Young
	Alan E. Pepper
	Gregory D. Reinhart
Head of Department,	Gregory D. Reinhart

August 2005

Major Subject: Biochemistry

ABSTRACT

The Role of *RpoT;3* in Chloroplast Development and

Gene Expression. (August 2005)

Aglaia Chandler, B. S.; M. S., Midwestern State University

Chair of Advisory Committee: Dr. John E. Mullet

The real-time PCR assay method was used to quantify the RNA abundance of twenty-eight plastid genes in a range of tissues and developmental stages of *Arabidopsis thaliana*. Three groups of co-regulated genes were identified. Three *trn* genes (Cluster I) showed differential expression in siliques. Genes encoding components of the plastid transcription and translation apparatus, the energetic apparatus as well as two genes encoding components of the plastid protease and acetyl-CoA carboxylase, showed maximum transcript accumulation at the 2-day stage (Cluster IIA and IIB). Finally, the genes encoding components of the photosynthetic apparatus of Cluster III reached maximum transcript abundance in later stages of chloroplast development. This coordinated expression of plastid genes reflects the presence of regulatory mechanisms that modulate plastid gene expression in different plant tissues and developmental stages.

We identified an *Arabidopsis* mutant, *rpoZ191*, in which a T-DNA is inserted in the *RpoT;3* gene encoding the plastid–targeted phage-type NEP enzyme. The mutant displays a general reduction in growth, as well as a delay in greening and in chloroplast development. Real-time PCR analysis of plastid RNA accumulation showed that the *RpoT;3* mutation caused a significant decrease in plastid transcript accumulation at the 2-day stage and a smaller inhibition at the 5-day stage. No major effects of the *RpoT;3*

mutation on the accumulation of plastid transcripts was observed in mature seeds and 5-day roots. Additionally, plastid transcript accumulation in mutant siliques was not significantly different from the wild-type, except for *trnfM-CA*U and *trnW-CCA*, which showed enhanced transcript levels. Taken together, these data indicate that the RpoT;3 NEP enzyme plays an important role in the overall transcription of plastid genes during the early phases of chloroplast and leaf differentiation. Furthermore, a functional RpoT;3 is required for the activation of selected nucleus-encoded plastid-localized proteins. However, the enhanced activity of RpoT;3 during the early stages of chloroplast differentiation is not due to an increase in *RpoT;3* mRNA abundance. We suggest that post-transcriptional mechanisms (e.g. phosphorylation, specificity factors) activate the transcription of plastid RpoT;3 - transcribed genes during the early stages of plastid development.

DEDICATION

This dissertation is dedicated to my ever-supporting daughters, Dolores Chandler and Nadia Chandler.

ACKNOWLEDGMENTS

First of all, I would like to thank my advisor, Dr. John E. Mullet for providing me with the opportunity to conduct my dissertation research under his guidance and support. I am also grateful to the members of my graduate committee, Dr. Ryland F. Young, Dr. Gregory D. Reinhart, Dr. Alan E. Pepper, and Dr. John A. Howard for their constructive criticism and encouragement. The laboratory of Dr. Ryland F. Young has also provided me with equipment essential for my work. Additionally, I would like to express my appreciation to present and past members of the Mullet laboratory including Dr. Daryl Morishige, Dr. Karen Thum and Dr. Christina Buchanan for their technical advice. I would also like to acknowledge the Microscopy and Imaging Center at Texas A & M University for their collaboration in the microscopy analysis. I am especially grateful to E. Ann Ellis who performed the transmission electron microscopy studies. Finally, I would like to thank other present and past members of the Biochemistry and Biophysics Department: Dr. Terrence Pinkerton from the Wilde laboratory and Dr. Monique Paricharttanakul from the Reinhart laboratory for their friendship and for sharing many enjoyable occasions. Additionally, I would like to thank Dr. Karel Riha and J. Matthew Watson from the Shippen laboratory and Dr. Liz Summer from the Young laboratory for their helpful discussions in the course of this investigation.

TABLE OF CONTENTS

TABLE OF CONTENTS (CONTINUED)

LIST OF FIGURES

LIST OF FIGURES (CONTINUED)

LIST OF TABLES

LIST OF TABLES (CONTINUED)

CHAPTER I

INTRODUCTION

PLASTIDS

Plastids of higher plants are a diverse group of prokaryotically-derived organelles that perform a range of different functions essential for plant growth and development. They are involved in numerous metabolic processes including photosynthesis, nitrogen assimilation (Staehelin and Newcomb, 2000), and the synthesis of starch (Gibbs, 1971), lipids, amino acids (Goodwin, 1971) as well as pigments, pyrimidines, terpenes, tetrapyroles and plant hormones (Goodwin, 1971; Neuhauss and Emes, 2000). Plastids exist in a number of different forms with different functions. Although they differ in internal structure, all plant plastids have two envelope membranes, ribosomes, a small genome, and are self-replicating. In addition, all plastids contain a variable number of osmiophilic plastoglobuli, which are filled with lipids and / or carotenoids (Mühlethaler, 1971; Neuhaus and Emes, 2000). Two major groups of plastids are recognized: the non-photosynthetic plastids and the photosynthetic plastids (reviewed in Mullet, 1988; Bowsher and Tobin, 2001). Non-photosynthetic plastids include proplastids, etioplasts, and a wide range of specialized plastids such as leucoplasts, chromoplasts and gerontoplasts. Small undifferentiated proplastids are the progenitors of all types of

---

This dissertation follows the style of The Plant Cell.

plastids. They have little internal structure (Bogorad, 1967, Mühlethaler, 1971) and are present in shoot and apical meristems (Possingham, 1980). Etioplasts are plastids found in cotyledons and leaves of plants grown in the dark and are characterized by the presence of crystalline prolamellar bodies and few thylakoid membranes (Possingham, 1980, Staehelin, 2003). Leucoplasts are colorless plastids that function primarily in the storage of starch, oils and protein granules (Mühlethaler, 1971; Neuhaus and Emes, 2000). Leucoplasts specializing in starch storage are called amyloplasts and are common in seeds and roots as well as in storage tissues such as cotyledons, endosperm, and tubers (Possingham, 1980; Thomson and Whatley, 1980). Proteoplasts are leucoplasts that contain stored proteins and are found in seeds and embryonic tissues whereas elaioplasts store oil droplets and lipids and are common in the epidermal cells of some mononocotyledonous plants (Mühlethaler, 1971). Finally, chromoplasts and gerontoplasts are non-photosynthetic plastids that are characterized by the presence of degenerating thylakoids and a large number of plastoglobuli (Thomas and Whatley, 1980; Mancera *et al.,* 1999). The carotenoid-containing chromoplasts are responsible for the yellow, orange or red color of fruits, flowers and certain roots (Thomson and Whatley, 1980; Neuhaus and Emes, 2000) whereas gerontoplasts are engaged in sequestering degraded materials in senescent leaves (Mancera *et al.,* 1999). The photosynthetic, chlorophyll-containing chloroplasts are found in all green plant tissues including leaves, cotyledons, stems as well as immature flowers and fruit pods (Bowsher and Tobin, 2001; Neuhauss and Emes, 2000). They are specialized for photosynthesis (Mullet, 1993) and contain three different membranes: the thylakoid membrane, the inner membrane of the envelope and the outer membrane of the envelope. These membranes enclose three aqueous

compartments: the thylakoid lumen, the stroma, which contains enzymes involved in CO_2 fixation as well as the chloroplast DNA, and the intermembrane space between the inner and the outer membrane (Figure 1). Photosynthetic electron transport, which generates the reducing power and ATP necessary for carbon fixation as well as nitrogen and sulfur assimilation, is associated with the chloroplast thylakoid membranes and occurs through a series of thylakoid bound, multisubunit protein complexes to which chlorophyll and other pigments are bound.

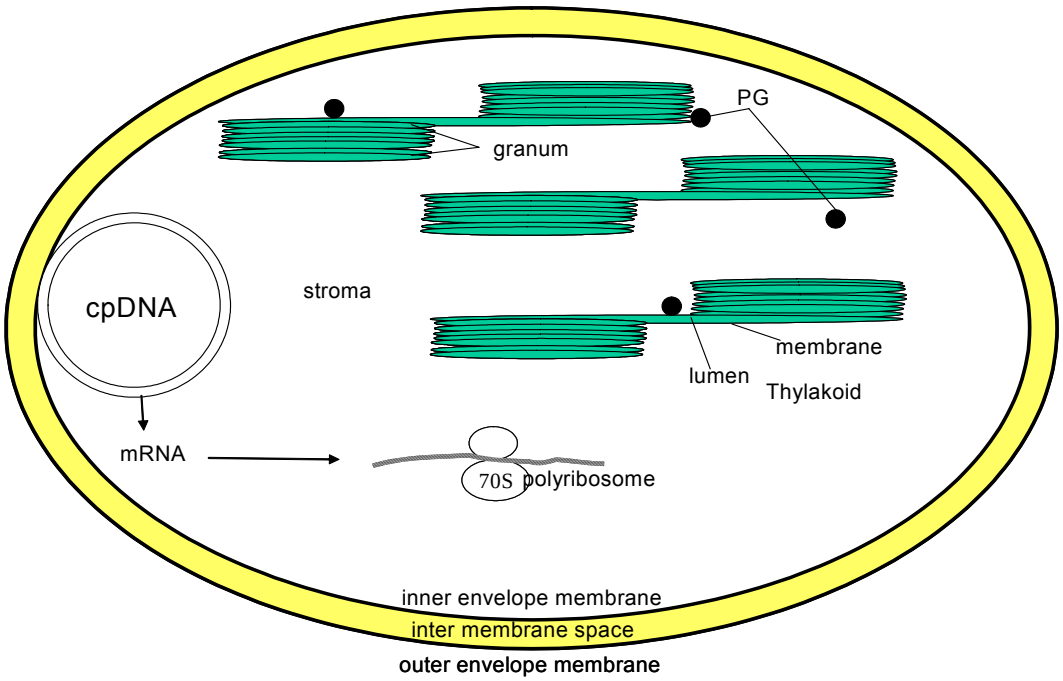

Figure 1. Schematic diagram illustrating a typical chloroplast.

Two envelope membranes (outer and inner) surround the chloroplast stroma, within which stacked grana of thylakoid vesicles can be seen. Thylakoid vesicles enclose another aqueous phase in their lumen. There are also DNA molecules, tRNA molecules, bacterial-like ribosomes and lipid- and/or carotenoid-containing plastoglubuli (PG) in the stroma.

PHOTOSYNTHESIS

In the simplest terms photosynthesis is the process by which photosynthetic organisms (green plants, algae and cyanobacteria) trap the energy of sunlight and form ATP and NADPH, which they use as energy sources to make carbohydrates and other organic compounds from CO_2 and H_2O. As a byproduct, the photosynthetic pathway generates oxygen molecules whose release is largely responsible for the oxygen-rich atmosphere characteristic of our planet today. The general process, which in green plants occurs in chloroplast, encompasses two discrete stages designated the “light” and “carbon fixation” or “dark” reactions of photosynthesis. The “light reactions”, which consist of electron and proton transfer reactions, occur only when plants are illuminated (see Lawlor, 1993; Hall and Rao, 1994; Whitmarsh, 1998). During these reactions, energy from sunlight is used to carry out the photochemical oxidation of H_2O to form O_2, and reduces the oxidized form of the electron carrier NADP generating NADPH. Light energy is also used to generate a pH gradient, which is used to synthesize ATP from ADP and Pi, a process known as photophosphorylation. In the carbon fixation reactions, which occur in both light and darkness, ATP and NADPH are used to reduce CO_2 to form starch and sucrose, the principal end products of CO_2 metabolism during photosynthesis. Absorption of light and all of the light reactions occur within or on the chloroplast thylakoid membranes. The ATP and NADPH produced by these reactions are released into the surrounding stroma, where all of the carbon fixation reactions occur. The actual reaction that fixes CO_2 into carbohydrates is catalyzed by the enzyme ribulose 1,5-biphosphate carboxylase / oxygenase, or Rubisco. The enzyme is a multimeric protein complex present in the chloroplast stroma and consists of 16

subunits, organized into eight large subunits (LSU) encoded by the plastid gene *rbcL* and eight small subunits (SSU) encoded by a small family of nuclear genes (*RbcS*).

The light reactions are mediated by a series of four multisubunit protein complexes located in the chloroplast thylakoid membrane (Figure 2). These multisubunit complexes, which include the photosystem II (PS II) complex, the cytochrome b_6/f complex, the photosystem I (PS I) complex, and the ATP synthase complex, consist of up to 20 polypeptides and over 200 cofactors and comprise the photosynthetic electron transport chain and photophosphorylation apparatus. Photosystem I and II are pigment-multiprotein complexes that trap and utilize light energy for the oxidation of H_2O and subsequent transport of electrons. The two photosystems are structurally distinct; each is a complex of many chlorophyll molecules, cytochromes, carotenoid pigments, and other electron-transporting proteins that have specific orientations in the thylakoid membranes. The PS II complex is located preferentially in the stacked thylakoid membranes while PS I is found mainly in the unstacked membranes (Anderson and Anderson, 1980; Goodchild *et al.,* 1985; Vallon *et al.,* 1985; Vaughn *et al.,* 1983). Each photosystem consists of the associated light-harvesting antennae and the reaction center proteins, which have an absorption maximum at 680 nm (PS II) and 700 nm (PS I). The antennae, which consist of a large number of protein-bound chlorophyll molecules (Chl-a and Chl-b), absorb photons and transfer their energy to the reaction centers. In addition to the chlorophylls, the light-harvesting antennae of the two photosystems also contain a number of carotenoids that protect against excess light energy (Cogdell and Frank, 1987; Demmig-Adams, 1990; Havaux and Niyogi, 1999). Upon absorption of a photon, delocalized π electrons

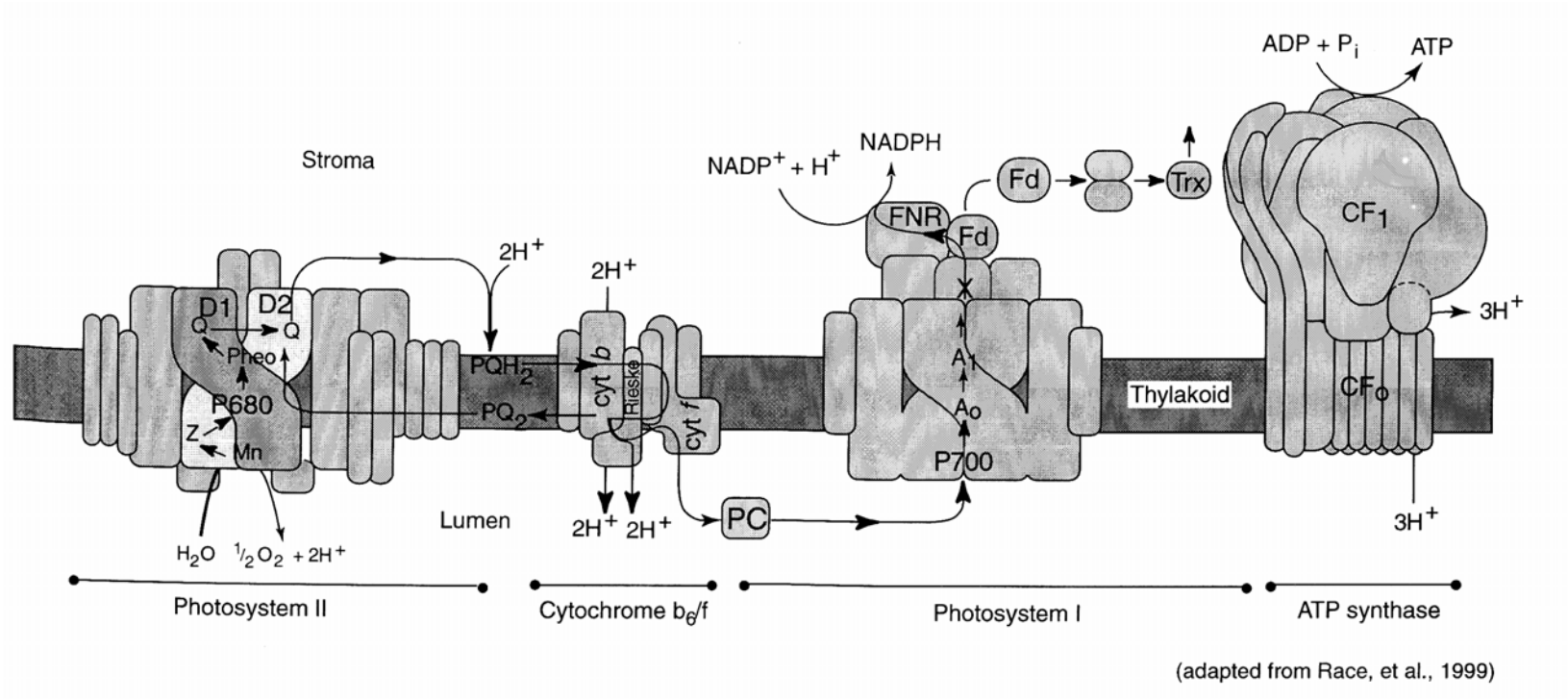

Figure 2. Schematic diagram of the chloroplast thylakoid membrane showing the arrangement of the photosynthetic electron transport and photophosphorylation apparatus.

The location and structure of the major components of the photosynthetic electron transport and photophosphorylation apparatus, PS II, cytochrome b_6/f, PS I and ATP synthase are shown and labeled accordingly. Transport of electrons between PS II and the cytochrome b_6/f complex is mediated by plastoquinone (PQ) and that between the cytochrome b_6/f complex and PS I by plastocyanin (PC). Splitting of water takes place in the lumen while NADPH and ATP formation occurs in the stroma. The ATP synthase utilizes the electrochemical gradient of protons pumped into the lumen for the synthesis of ATP. The flow of electrons and the translocation of protons across the thylakopid membrane are represented by arrows.

present in the double bonds of the chlorophyll tetrapyrrole ring are elevated from the unexcited state to the excited first state π^*, resulting in excited Chl* molecule. Chl* transfers its energy through resonance energy transfer to a neighboring Chl with a lower energy state. This excitation energy is then channeled into P680 (PS II) and P700 (PS I) reaction centers chlorophylls and used for primary charge separation. Each antenna is composed of an inner and an outer part. The outer part is composed of the light harvesting complexes (LHCs) that collect the light and are formed by nucleus-encoded polypeptides whereas the inner antenna consists of the core complexes that conduct the excitons collected in the outer antenna into the photosynthetic reaction centers. In PS I, the reaction center and the inner antenna are combined into a single chlorophyll-protein complex that consists of two polypeptides encoded by the plastid genes *psaA* and *psaB* that bind chlorophyll a and β-carotene. The outer antenna of PS I (LHC I) is composed of dimers of Lhca proteins encoded by the nuclear genes *Lhca1-4* (Jansson, 1999). PS II is a complex multimeric protein assembly composed of at least 20 protein subunits (Barber *et al.,* 1997; Wollman *et al.,* 1999). It contains the reaction center proteins D1 and D2 encoded by the plastid genes *psbA* and *psbD* as well as the inner antenna, which consists of the plastid-encoded polypeptides CP43 and CP47. The outer antenna of PS II (LHC II) is composed of trimers of Lhcb proteins encoded by the nuclear genes *Lhcb1-3* that transfer energy to the reaction center proteins through three small chlorophyll-binding proteins, Lhcb4 (CP29), Lhcb5 (CP26) and Lhcb6 (CP24). Photosystem I utilizes light energy absorbed predominantly by chlorophyll a to drive electron transport from the cytocrome b_6/f complex to ferredoxin and then $NADP^+$, while photosystem II utilizes light energy absorbed by chlorophyll a and b to drive electron transport from water to the plastoquinone pool.

The transfer of electrons from H_2O to $NADP^+$ involves three of the thylakoid bound, multisubunit protein complexes - photosystem II (PS II), which functions as water:plastoquinone oxidoreductase, the cytochrome b_6/f complex, which acts as a plastoquinone:plastocyanin oxidoreductase and photosystem I (PS I), which functions as plastocyanin:ferredoxin oxidoreductase. Photosynthetic electron transport starts with the capture of light energy by the chlorophyll molecules of the light harvesting chlorophyll-protein complex (LHC II) associated with PS II. This energy is transferred by resonance energy transfer to the reaction center complex (P680) of PS II. Excited P680 transfers an electron to pheophytin (Phe, a chlorophyll a with its two Mg^{2+} replaced by two protons). The electron transport process causes P680 to become positively charged. $P680^+$ withdraws one electron from a tyrosine residue in the D1 protein which then regains the donated electron from water through the oxygen-evolving (water-splitting) complex located in the thylakoid lumen. This protein complex, which contains a cluster of manganese ions, binds two water molecules and extracts a total of four electrons from them releasing $4H^+$ and O_2. The electrons are passed on to oxidized P680 reaction center while the four protons are pumped from the stroma into the thylakoid lumen. The released O_2 diffuses out of the chloroplast. Reduced pheophytin transfers its electron to a series of plastoquinone molecules (Q_A and Q_B) associated with PS II proteins which are thus converted to semiquinones. Q_B – semiquinone is then reduced to quinol and accepts two protons from the stromal surface of the thylakoid membrane forming a plastoquinol (PQH_2). Reduction of Q_B to PQH_2 requires two electrons and two H^+, which are acquired from Q_A and the solvent water, respectively. PQH_2 dissociates from PS II and diffuses within the thylakoid membrane where the

cytochrome b_6/f complex is located while an oxidized plastoquinone from the thylakoid bound plastoquinone pool takes its place.

The cytochrome b_6/f complex, which is comprised of nucleus- as well as plastid-encoded protein subunits, consist of the heme-containing cytochrome f (encoded by the plastid gene *petA*), a 2Fe-2S Rieske protein, one 2 heme-containing cytochrome b_6 (encoded by the plastid gene *petB*) and one bound plastoquinol. The complex is involved in the electron transfer from PS II to PS I that contributes to the generation of much of the electrochemical proton gradient which drives ATP synthesis (Lawlor, 1993; Whitmarsh, 1998). The flavoenzyme ferredoxin (flavodoxin)-NADPH reductase (FNR), encoded by the nuclear gene *PetH*, is also involved in the cytochrome b_6/f-mediated electron transfer between the two photosystems (Whitelegge *et al.,* 2002). During the cytochrome b_6/f-mediated electron transfer, the reduced plastoquinone is oxidized in the Q-cycle by the cytochrome b_6/f complex and two protons are released into the lumen of the thylakoid. From cytochrome b_6/f, electrons move one at a time to plastocyanin (PC), a copper-containing mobile protein in the thylakoid lumen (Lawlor, 1993; Whitmarsh, 1998). Plastocyanin that has been reduced by the cytochrome b_6/f complex diffuses through the lumen of the thylakoids and binds to PS I. Electrons from reduced PC are transferred to the oxidizing side of the PS I complex. Chlorophyll molecules at the PS I reaction center (P700) are excited by transfer of light energy from the light harvesting chlorophyll-protein complex associated with PS I (LHC I), and an electron is transferred to an adjacent electron acceptor, A_0, while an electron obtained from the reduced PC reduces the oxidized chlorophyll. The electron that was extracted from P700 is passed along via phyloquinone (A_1) and three 4Fe-4S clusters, FX, FA and FB to the soluble Fe-S protein ferredoxin (Fdx), which is located in the stromal compartment of the

chloroplast (Lawlor, 1993; Whitmarsh, 1998). From ferredoxin, electrons are transferred one at a time, to $NADP^+$ by the Fdx-$NADP^+$ reductase (FNR) producing NADPH, a mobile electron carrier.

During the passage of each electron through the system, protons generated by water and plastoquinone oxidation are pumped from the stroma into the thylakoid lumen generating a proton gradient across the thylakoid membrane. The chloroplast ATP synthase is the component of the thylakoid membranes that couples the synthesis of ATP with the proton gradient generated by the light-dependent electron transport reactions. The thylakoid bound enzyme uses the proton gradient for the phosphate group transfer to generate ATP from ADP and Pi. The complex, which is located exclusively in the unstacked thylakoid membranes (Miller and Staehelin, 1976; Allred and Staehelin, 1985), consists of several different nucleus- and plastid-encoded polypeptides organized into a membrane-embedded, intrinsic part, CF_0, and an extrinsic part, CF_1, which contains the catalytic site. One of the functions of the CF_0 components is to provide a mechanism for proton transport across the membrane to the CF_1 component which then covalently attaches inorganic phosphate to ADP, generating ATP (Lawlor, 1993; Hall and Rao, 1994; Whitmarsh, 1998).

Besides this non-cyclic electron transfer described above, cyclic electron transfer can also take place where the electrons from the excited photosystsem I are fed into the cytochrome b_6/f complex and transferred back to PS I. Under these conditions, NADPH is not formed and the energy released is only used for the synthesis of ATP. It has been suggested that the function of cyclic electron transport is to adjust the rates of ATP and NADPH formation by synthesizing extra ATP when there is an accumulation of NADPH (Bendall and Manasse, 1995). Cyclic electron transport has

been shown to occur *in vivo* in the bundle sheath chloroplasts of certain C_4 plants (Herbert *et al.,* 1990; Asada *et al.,* 1993) as well as in cyanobacteria (Carpentier *et al.,* 1984) and algae (Maxwell and Biggins, 1976; Ravenel *et al.,* 1994). Despite the fact that cyclic and linear electron transfers share certain electron carriers such as plastoquinone (PQ), the cytochrome b_6/f complex and plastocyanin (reviewed in Bendall and Manasse, 1995), the exact pathway of electron flow from PS I to the the cytochrome b_6/f complex is not completely understood. Two pathways have been proposed to operate in the cyclic electron transfer. One of these pathways involves a putative ferredoxin quinone reductase (FQR) while the other involves the plastid NADH dehydrogenase complex (Endo *et al.,* 1997; 1998; reviewed in Peltier and Cournac, 2002). The NADH complex, which has been shown to have an NADH:plastoquininone oxidoreductase activity (Sazanov *et al.,* 1998), is homologous to complex I of bacteria and mitochondria. The complex is abundant in the non-appressed thylakoid membranes where the PS I and the ATP synthase complexes are also located (reviewed in Peltier and Cournac, 2002). Based on its similarity to the *E. coli* complex I, the plastid NADH complex is thought to be comprised of a membrane-bound domain encoded by the plastid genes *ndhA, B, C, E, F, G*, a connecting portion that consists of a series of proteins encoded by the plastid genes *ndhH, I, J, K* and an NADH-binding domain whose subunits have not been identified (Friedrich and Scheide, 2000; reviewed in Peltier and Cournac, 2002; Lennon *et al.,* 2003). Evidence supporting the role of the NADH complex in the flow of electrons from NADPH or ferredoxin to plastocyanin includes studies carried out in *Synechocystis*, which showed that the NADH complex participates in both cyclic electron flow as well as repiratory flow (Mi *et al.,* 1995). In addition, the NADH complex was found to be more abundant in the bundle sheath

chloroplasts of C_4 plants, which have a high cyclic electron activity, than in the mesophyll chloroplast where cyclic electron activity is low (Kubicki *et al.,* 1996). Although the exact role of the NADH complex in the cyclic electron flow has not yet been established, it has been suggested that the complex might be involved either directly and/or indirectly. In the first scenario, the flow of electrons from NADPH or ferredoxin to plastoquinone could proceed via the NADH complex. In the second scenario, the NADH complex could facilitate the initiation of the cyclic electron transfer by regulating the redox state of the plastoquinone pool through its function in chlororespiration (reviewed in Nixon, 2000; Peltier and Cournac, 2002). According to the concept of chlororespiration, a term coined by Bennoun (1982) to describe the activity of a putative respiratory chain in plastids, the NADH complex reduces the plastoquinone pool, which is then oxidized by molecular oxygen through a chloroplast terminal oxidase. This electron transfer would then generate an electrochemical gradient across the thylakoid membrane. Recent evidence to support the model of chlororespiration has come from the identification of the plastid-localized IMMUTANS (IM) protein (Carol *et al.,* 1999; *Wu et al.,* 1999). The IM protein, which is also involved in carotenoid biosynthesis, has sequence similarity to mitochondrial alternative oxidases and is localized to the stromal lamellae where the NADH, PS I and ATP complexes are also located (Lennon *et al.,* 2003). In additrion, the fact the IM protein, like the *ndh*-encoded polypeptides, is present in early expanding and senescing leaves as well as in etioplasts, which lack PS II activity, is consistent with a role in cyclic electron flow and or chlororespiration (Martín *et al.,* 1996; Catalá *et al.,* 1997; Lennon *et al.,* 2003).

PLANT AND PLASTID DEVELOPMENT DURING SEED GERMINATION AND SEEDLING ESTABLISHMENT

Plastid differentiation is tightly coupled with temporal and spatial changes of plant development. During seed formation, a plant embryo passes through several discrete stages from a single-celled zygote to a fully mature embryo (Mansfield and Briarty, 1991; Goldberg *et al.,* 1994). During these stages which include the globular, the heart-shaped, the torpedo and the walking-stick phases, the embryo differentiates into two major embryonic organ systems: the hypocotyl-radicle region or the axis and the cotyledons. The axis contains the root meristem, which will give rise to the tissues of the main root, and the shoot meristem, which will produce all the tissues of the main plant stem, including the leaves (Figure 3A). The cotyledons are modified leaves that are initially responsible for synthesizing and storing nutrients such as lipids, proteins and carbohydrates. They develop with the rest of the embryo and arrest when the seed enters dormancy. Upon germination, the cotyledons resume growth and either remain below ground (hypogeal) or, more commonly, spread out above soil level (epigeal) and become photosynthetically active (Lovel and Moore, 1970). In plants with epigeal cotyledons such as *Arabidopsis thaliana*, germination, which takes place within 24 hours after imbibition, is followed by a period of 2-3 days of heterotrophic growth during which the seedling uses its stored reserves (Eastmond and Graham, 2001). Depending on the availability of light, *Arabidopsis* seedlings follow two distinct developmental patterns (Figure 3B and 3C). In darkness, etiolated seedlings follow skotomorphogenic development characterized by elongated hypocotyls, folded and unexpanded cotyledons and apical hooks. In the presence of light, seedlings follow photo-

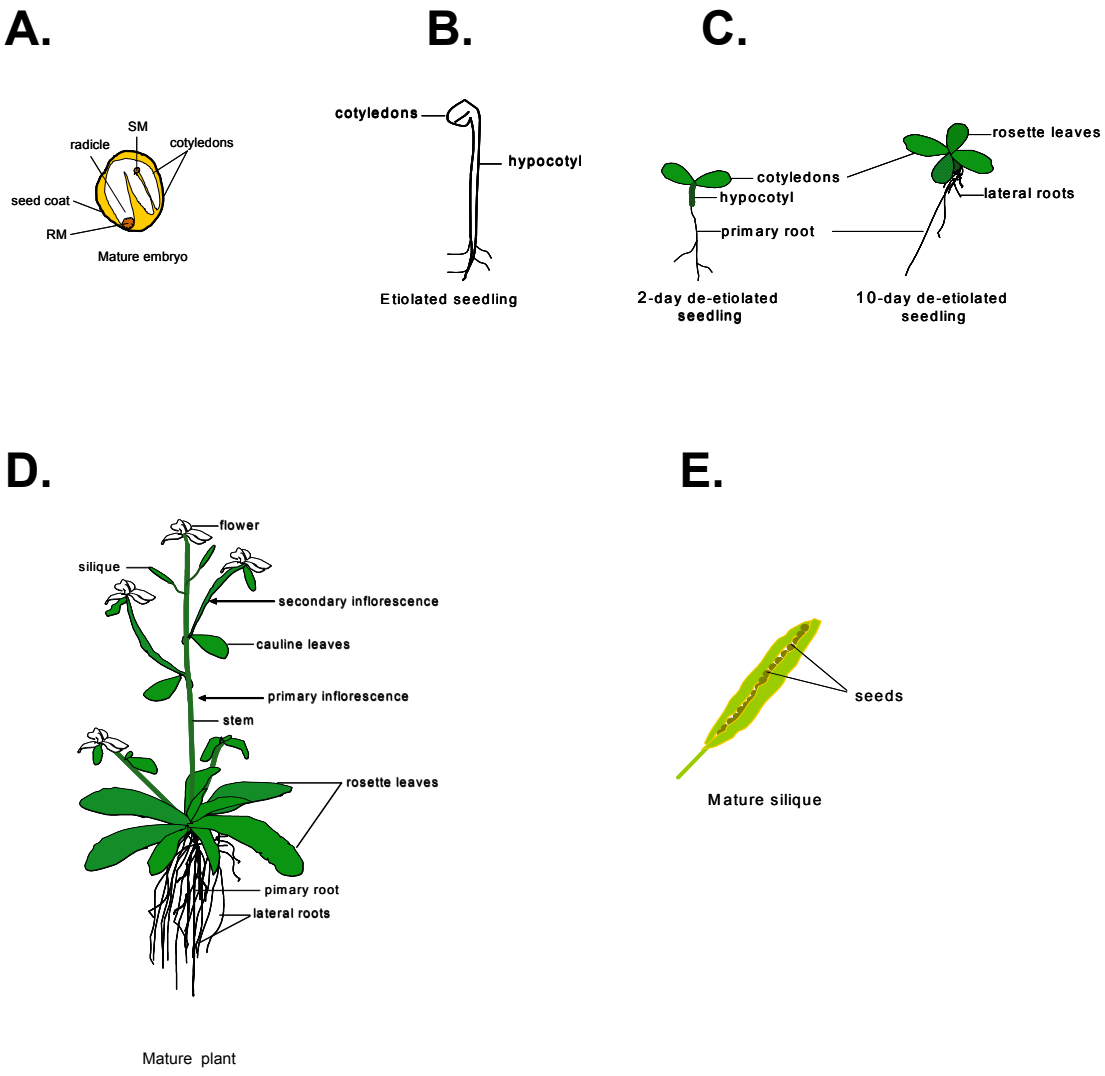

Figure 3. Developmental stages of *Arabidopsis thaliana*.

(A) Schematic representation of a mature embryo. SM and RM refer to shoot meristem and root meristem, respectively (Adapted from Goldberg *et al.,* 1994).
(B) Schematic representation of a skotomorphogenic seedling (Adapted from Franhauser and Chory, 1997).
(C) Schematic representation of a photomorphogenic seedling (Adapted from Franhauser and Chory, 1997; Anderson and Wilson, 2000).
(D) and **(E)** Schematic representation of a mature Arabidopsis plant (D) and siliques (E) (Adapted from Anderson and Wilson, 2000).

morphogenic development or de-etiolation (for review see Chory, 1992). During seedling emergence under light conditions, the cotyledons expand considerably and become photosynthetic followed by the development of the first pair of true leaves that arise from the apical meristem (Bakalova-Stoynova *et al.,* 2004; von Arnikm and Deng, 1996). The cotyledons continue to grow and photosynthesize and senesce only after the plant develops true leaves and bolts. Depending on growth conditions, *Arabidopsis* seedlings will produce 10 to 14 vegetative rosette leaves followed by a period of flower production that begins 21-23 days post-germination (Boyes *et al.,* 2001). The plant continues to produce secondary and tertiary inflorescences as the siliques develop (Figure 3D). This period is characterized by leaf senescence and maturation of the siliques (Figure 3E), which contain from 30 to 60 seeds per silique (Chory, 1992; Anderson and Wilson, 2000).

Plastids proliferate by division of pre-existing plastids that are passed on to daughter cells at cell division and to subsequent generations by maternal inheritance (reviewed in Connett, 1987; Gillham, 1991; Tilney-Bassett, 1978). The different forms of plastids are, to some extent, interconvertible and all arise from proplastids (Figure 4) that are present in embryonic and meristematic cells (Mühlethaler, 1971; Mullet, 1988). Plastid differentiation is determined, to a large extent, by the tissue in which the plastid resides as well as the stage of cellular development. During development and in response to environmental conditions, plastid composition and volume change and organelles differentiate into various specialized plastids. Moreover, a diverse population of plastid forms and functions may be present within a single organ (Bowsher and Tobin, 2001). Plastid differentiation pathways include proplastid and chloroplast interconversions during embryogenesis (Schultz and Jensen, 1968; Mansfield and

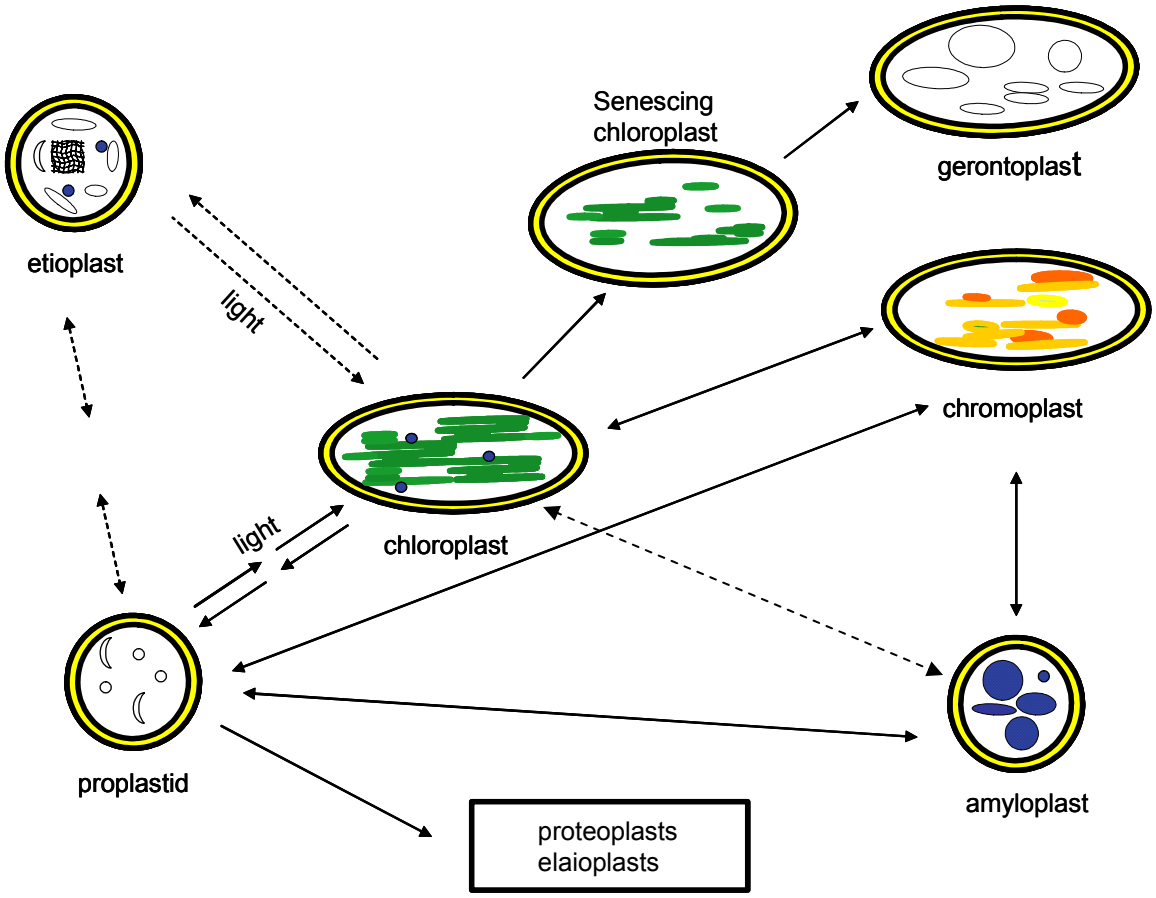

Figure 4. Schematic diagram illustrating the interrelating pathways of plastid development.

In the course of a plant life cycle, plastids develop into clearly distinct types: amyloplasts in storage tissues and roots, chloroplasts in green tissue, chromoplasts in flowers, fruits and certain roots, etc... The various plastid types originate from undifferentiated proplastids found in meristematic cells as well as from the interconversion of plastid types (Adapted from Thomas and Whatley, 1980; Staehelin and Newcomb, 2000).

Briarty, 1991), chloroplast differentiation during leaf formation (Mullet, 1988) and cotyledon emergence (Mansfield and Briarty, 1996), leucoplast differentiation in petals (Pyke and Page, 1998), plastid formation during root development (Whatley, 1983), amyloplast differentiation in storage tissues such as roots, tubers and seeds (Thomson and Whatley, 1980), chromoplast differentiation in fruits and flowers (Marano *et al.,* 1993) and gerontoplast formation in aging leaves (Mancera *et al.,* 1999). In the developing embryo, greening begins during the transition from the undifferentiated globular stage to the heart-shaped embryo, and the initiation of greening is associated with the development of chloroplasts. After the torpedo stage, chloroplasts begin to lose their photosynthetic membranes and dedifferentiate into proplastids (Schultz and Jensen, 1968; Mansfield and Brarty, 1991). The mature embryos and cotyledons of the seeds contain proplastids, which develop into chloroplasts within the preformed cotyledons or into amyloplasts in roots (reviewed in von Arnin and Deng, 1996; Possingham, 1980). In the absence of light, proplastids of the cotyledons develop into etioplasts, characterized by the presence of a paracrystalline prolamellar body and the accumulation of the chlorophyll precursor photochlorophillide (von Arnin and Deng, 1996; Sperling *et al.,* 1998). When exposed to light, the etioplasts differentiate into chloroplasts by rapidly accumulating chlorophyll-containing photosynthetic membranes and the associated proteins (Mayfield, 1990; Staehelin, 2003). In roots, chloroplast development is repressed and proplastids differentiate into starch-accumulating amyloplasts in the root cap whereas proplastids in the root tips remain undifferentiated unless they are exposed to light for prolonged periods of time when they may develop into chloroplasts (reviewed in von Arnin and Deng, 1996; Possingham, 1980). Plastid development in leaves occurs in coordination with cell and organ differentiation

(reviewed in Mullet, 1988; Fujie, 1994). During leaf development, proplastids located in the meristematic cells of the shoot apex differentiate into chloroplasts through a process that involves an increase in volume and membrane expansion (Possingham, 1980; Mullet, 1988). The meristematic activity in monocotyledonous plants such as barley or wheat is confined to the base of the leaf. Consequently, a gradient of cells and plastids is created that result in physical separation of the various stages of development along the length of the leaves with the undifferentiated cells and proplastids at the base of the leaf and mature cells along with differentiated plastids at the tip of the leaf (Robertson and Laetsch, 1974; Gandar and Hall, 1988). Leaf development in monocots such as barley and wheat occurs both in the presence and absence of light. In the absence of light, the proplastids of monocots differentiate into non-photosynthetic etioplasts which upon illumination develop into photosynthetically competent chloroplasts (Possingham, 1980). In contrast, primary leaf development in dicotyledonous plants such as *Arabidopsis* is inhibited in the absence of light (Butler, 1967). Upon illumination, the meristematic cells divide and develop into cells of the leaf concomitant with differentiation of proplastids into chloroplasts (Fujie *et al.*, 1994). Generally, greening in both dicots and monocots implies the transition from proplastids or etioplasts to chloroplasts in the presence of light and is characterized by rapid synthesis of chlorophyll along with formation of thylakoids and grana stacking (Bogorad, 1968; Lebedev and Timko, 1998). Conversely, during leaf senescence, which is characterized by the transformation of chloroplasts into gerontoplasts, the organized chloroplast granal stacks and chlorophylls are lost and the photosynthetic apparatus within the chloroplast begins to disassemble with a concomitant decrease in photosynthetic activity (Mancera-Zavaleta *et al.,* 1999; Lu *et al*., 2001).

PLASTID GENOME ORGANIZATION

Plant cells contain a variable number of plastids as well as DNA molecules depending on the cell type (Bendich, 1987; Rodermell, 2001). It has been estimated that meristematic cells contain from 10 to 20 proplastids (Juniper and Clowes, 1965; Cran and Possingham, 1972; Lyndon and Robertson, 1976) whereas mesophyll cells contain 100 or more chloroplasts with 22-900 identical genomes per plastid (Thomas and Rose, 1983; Bendich, 1987). Although plastid genomes are usually represented as momomeric circular molecules, they occur in both circular and linear monomeric as well as multimeric conformations (Deng *et al.,* 1989; Bendich and Smith, 1990; Backert *et al.,* 1995; Lilly *et al*., 2001; Oldenburg and Bendich, 2004). The DNA molecules are organized in functional units called plastid nucleoids that contain over 10 copies of cpDNA complexed with proteins as well as RNA (Kuroiwa, 1991; reviewed in Sato *et al.,* 1999b). Proplastids contain 1-2 nucleoids per organelle located at the center of the plastid. In developing chloroplats, the number of nucleoids increases and they are associated with the inner membrane whereas in mature chloroplasts, plastid nucleoids decrease in size and are associated with the thylakoid and envelope membranes (reviewed in Mullet, 1988; Sato *et al.,* 1999b; Mache and Mache-Lerbs, 2001; Maliga, 2004). Plastid genomes of higher plants range in size from 120 to 200 kb, encoding approximately 120 genes (Mullet, 1988; Palmer, 1985; Igloi and Kössel, 1992; Sugiura, 1992; Gruissem and Tonkyn, 1993). A feature of the chloroplast DNA found in most higher plants is the presence of a large inverted repeat (IR) which ranges from 6 to 76 kb in length (Palmer, 1985). All the large inverted repeats in the chloroplast DNA of land plants and algae contain a complete set of rRNA. The segments of the IR are separated

by one large and one small single-copy region (LSC and SSC, respectively). Pea, broad bean, alfalfa and pine chloroplast lack IR (Sugiura, 1992).

The first physical map of plastid DNA was constructed for maize in 1976 (Bedbrook and Bogorad, 1976) and the first chloroplast gene was cloned in 1977 (Bedbrook *et al.*, 1977). The entire nucleotide sequence of the plastid DNA is now established for twelve plants (reviewed in Wakasugi *et al.,* 2001; Odintsova and Yurina, 2003) including tobacco (Shinozaki *et al*, 1986), liverwort (Ohyama *et al,* 1986), rice, (Hiratsuka *et al*, 1989), maize (Maier, 1995), *Arabidopsis thaliana* (Sato *et al.,* 1995), black pine (Wakasugi *et al.,* 1994), and *Porphyra purpurea* (Reith and Munholland, 1995). The average plastid genome contains between 108 and 122 different genes most of which are conserved among the various plant species (Wakasugi *et al.,* 2001). These genes can be grouped into two major classes (see Table 1): genes encoding products involved in transcription and translation (~ 55 genes encoding RNA polymerase subunits, tRNAs, rRNAs, ribosomal proteins) and genes encoding proteins of the photosynthetic apparatus (~ 40 genes encoding components of photosystem I (PS I), photosystem II (PS II), the ATP synthase, the cytochrome b_6/f complex, and the large subunit of Rubisco). The plastid genome of land plants also contains 30 conserved open reading frames (ORFs) of largely unknown function. Eleven of them are homologous to genes encoding subunits of the mitochondrial NADH dehydrogenase (Palmer, 1991). Isolation of the NADH dehy-drogenase complex and targeted mutagenesis of tobacco *ndh* genes have confirmed that plastid *ndh* genes encode a functional NADH dehydrogenase complex (Sazanov *et al.,* 1998; Guera *et al.*, 2000; Kofer *et al.,* 1998; Shikanai *et al.,* 1998; Burrows *et al*., 1998). Approximately ten open reading frames are conserved between different

Table 1. Genes encoded by *Arabidopsis thaliana* plastid genome

Gene products	Genes
A. Genes for the Genetic System	
RNA polymerase	*rpoA, B, C1, C2*
Ribosomal RNAs	*rrn4.5, 5, 16, 23*
50S ribosomal subunits	*rpl2, 4, 6, 20, 22, 23, 32, 33, 36*
30S ribosomal subunits	*rps2, 3, 4, 7, 8, 11, 12, 14-19*
tRNAs	*trnA(ugc), C(gca), D(guc), E(uuc), F(gaa), G(gcc), G(ucc), H(gug), I(cau), I(gau), K(uuu), L(caa), L(uaa), L(uag), fM(cau), M(cau), N(guu), P(ugg), Q(uug), R(acg), R(ucu), S(ccu), S(gga), S(uga), T(ggu), T(ugu), V(gac), V(uac), W(cca), Y(gua)*
B. Genes for the Photosynthetic Apparatus	
Photosystem I subunits	*psaA, B, C, I, J*
Photosystem II subunits	*psbA, B, C, D, E, F, H, I, J, K, L, M, N,T*
Cytochrome b6/f subunits	*petA, B, D, G*
ATP synthase subunits	*atpA, B, E, F, H, I*
Rubisco	*rbcL*
C. Genes for Other Functions	
NADH dehydrogenase subunits	*ndhA, B, C, D, E, F, G, H, I, J, K*
ATP-dependent protease	*clpP*
Acetyl-Co-A carboxylase β subunit	*accD*
Maturase	*matK*
Unknown	*ycf1, 2, 3, 4, 5, 6, 7, 8, 9, 10; orf76*

This table is based on information from Sato *et al.,* 1999a.

species, and are designated *ycfs* for hypothetical chloroplast open reading frame (reviewed in Wakasugi *et al.,* 2001). In addition, plastid genomes code for small non-coding RNAs (Marker *et al.,* 2002). Fourteen to eighteen plastid genes are interrupted by single introns that range in size from 0.3 kb to 2.5 kb. One exception is the *rps12* gene which contains two introns and requires *trans* splicing to produce a mature RNA (Odintsova and Yurina, 2003).

In accordance with the hypothesis that plastids are of endosymbiotic origin, many plastid genes (~ 60%) are organized in complex gene clusters which bear a striking resemblance to bacterial operons (Table 2). These gene clusters contain multiple promoters as well as multiple RNA-processing sites and are co-transcribed as polycistronic pre-RNAs that are subsequently processed into shorter RNAs giving rise to complex RNA populations (Kanno and Hirai, 1993; Mullet, 1993). Steps involved in RNA processing include intron splicing, cleavage in the intergenic region, maturation of 5′ and 3′ ends as well as RNA editing (reviewed in Monde *et al.,* 2000). Genes with common function are often co-localized in operons allowing for co-regulation of groups of genes and coordinated production of subunits for specific protein complexes (Sugiura, 1992; Gruissem and Tonkyn, 1993). Some of these operons are comprised of genes involved only in photosynthesis (*psbB-psbH-petB-petD*) whereas others contain genes involved only in transcription (*rpoB-rpoC1-rpoC2*) and / or translation (*rrn* and *rpl23-rpoA* operons). In addition, some plastid gene clusters include genes encoding subunits of different complexes. For example, the *ndhB* gene encoding a subunit of the NADH dehydrogenase complex is co-transcribed with *rps12* and *rps7* encoding ribosomal protein subunits whereas *psaA* and *psaB* encoding PS I subunits are part of a transcription unit that contains *rps14* encoding a ribosomal protein subunit. The 30-33

Table 2. Examples of plastid gene clusters

Gene Cluster	Products
A. Gene clusters encoding components with related functions	
rpoB-rpoC1-rpoC2	Plastid RNA polymerase subunits (PEP)
trnE-trnY-trnD	tRNAs
16S-*trnI-trnA*-23S-4.5S-5SrRNA	rRNAs and tRNAs
atpI-atpH-atpF-atpA	ATP synthase subunits
B. Gene clusters encoding components with different functions	
rpl16-rpl14-rps8-rpl36-rps11-rpoA	Ribosomal proteins and PEP subunit α
rps12-rps7-ndhB	Ribosomal protein and NADH dehydrogenase subunits
psaA-psaB-rps14	PSI and ribosomal protein subunits
clpP-5′rps12-rpl20	Protease and ribosomal protein subunits
ndhA-ndhI-ndhG-ndhE-psaC-ndhD	PSI and NADH dehydrogenase subunits
accD-psaI-ycf4-ycf10 -petA	Acetyl-Co-A carboxylase β subunit, PSI subunit, two hypothetical proteins and Cyt subunit
psbD-psbC-ycf9-trnG	PSII subunits, hypothetical protein and tRNA

This table is based on information from Gruisem and Tonkyn, 1993; Mullet, 1993; Meurer *et al.,* 1996; Sato *et al.,* 1999a.

plastid tRNA genes are transcribed either as polycistronic or monocistronic RNAs and are located within tRNA gene clusters as well as within or at the end of heterogeneous gene clusters. Two tRNA genes (*trnI(gau)* and *trnA(ugc)* are found within the *rrn* operon

located in the inverted repeat (IR) region of the plastome. All plastid-encoded tRNAs code for functional tRNAs that participate in protein synthesis. Interestingly, $tRNA^{Glu}$ (UUC) encoded by the *trnE* gene is also involved in the synthesis of 5-aminolevulinic acid, which is a precursor in heme and chlorophyll biosynthesis (Jahn *et al.,* 1992).

Although plastids contain an autonomous genome, its size is sufficient to encode only a subset of the structural and functional proteins that are necessary for synthesis of plastid membranes and for carrying out diverse light and dark reactions of photosynthesis. Of the estimated 2500-3100 different proteins found in various types of plastids (Pesaresi *et al.,* 2001) less than one hundred are encoded by the plastid genome. As a consequence, much of the information required for plastid biogenesis resides in the nuclear genome. Nuclear genes encode subunits of each protein complex involved in photosynthesis, pigment, lipid and amino acid biosynthetic enzymes, as well as components of the organelle's transcriptional and translational machinery (Table 3). In addition, the nucleus encodes a large number of auxiliary factors involved in regulating the expression of plastid genes (Barkan and Goldschmidt-Clermont, 2000).

Plastid development requires coordinated expression of plastid and nuclear genes and it is generally accepted that chloroplast development is controlled by genetic information encoded in the nucleus. However, evidence also suggests that plastids influence the expression of nuclear genes involved in plastidogenesis (Mayfield and Taylor, 1984; Taylor, 1989; Oelmüller *et al.*, 1986; Oellmüller and Mohr, 1986; Mullet, 1993). Several distinct plastid signals have been identified (reviewed in Brown *et al*., 2001; Surpin et al., 2002; Gray *et al*., 2003).

Table 3. Nuclear and plastid genes encoding subunits of the photosynthetic protein complexes

Polypeptide complex	Plastid genes	Nuclear genes
SSU (RUBISCO)		[1]*RbcS* multigene family
LSU (RUBISCO)	[2]*rbcL*	
LHC I		[3]*Lhca1.1, 2.1, 3, 4, 5*
LHC II		[3]*Lhcb1.1, 1.2,1.3,1.4,1.5, 2.1, 2.2,2.4, 3, 4.1, 4.2, 4.3,5, 6*
PS II	*psbA, B, C, D, E, F, H, I, J, K, L, M, N, T*	*PsbO, P, Q, R, S, W*
cyt b_6/f	*petA, B, D*	*PetC, E*
PS I	*psaA, B, C, I, J*	*PsaD, E, F, H, K, L*
ATP synthase	*atpA, B, E, F, H, I*	*AtpC, D, G*

Adapted from Table 1 and Table 2 in Pakrasi, 1995 unless otherwise indicated.
[1] Coruzzi *et al.,* 1983; Kuhlemeier *et al.,* 1979.
[2] Coen *et al.,* 1977; Bedbrook *et al.,* 1979.
[3] Frisco *et al.,* 2004.

The putative chloroplast signals required for expression of certain photosynthesis-related nuclear genes have been speculated to be RNAs, plastid proteins and metabolites produced by plastids (reviewed in Oelmüller, 1989; Taylor, 1989; Susek and Chory, 1992). *Arabidopsis* mutants*,* referred as *gun* (genomes uncoupled) mutants, have been identified that express nuclear genes encoding plastid proteins in the absence of chloroplast development (Susek *et al.*, 1993; Mochizuki et al., 1996). Genetic analysis of several *gun* mutants suggests that chlorophyll precursors can act as plastid-derived signals and that perturbations of the tetrapyrole biosynthetic pathway

might be involved in the generation of this “plastidic signal” causing transcriptional repression of nuclear genes encoding plastid-localized proteins (Mochizuki et al., 2001). In addition, the plastid redox state and sugars have been implicated in the plastid-to-nucleus signaling (reviewed in Brown *et al*., 2001). Moreover, expression of several nuclear genes involved in chloroplast biogenesis is known to be controlled by light via several photoreceptors that include the phytochromes (Thompson *et al.,* 1983; Quail, 1991; Smith, 1995), the photochlorophyllide holochrome (Thompson and White, 1991), the blue light/UV-A photoreceptors such as cryptochrome (Ahmad and Cashmore, 1993; Kaufman, 1993; Short and Briggs, 1994), and photosynthetic redox potentials (Danon and Mayfield, 1994; Kim *et al*., 1993b). A complex network of molecular interactions couples output from the photoreceptors to plastid and cell development. The nuclear proteins DET and COP, for instance, repress nuclear and chloroplast gene expression in the dark (reviewed in von Arnim and Deng, 1996). In addition, positive activators are also involved in the signaling network (Li *et al.,* 1995; Wang *et al.,* 1997).

THE TRANSCRIPTIONAL AND TRANSLATIONAL APPARATUS OF PLASTIDS

The transcription and translation machinery of plastids is similar to that of prokaryotic organisms. Plastids, for instance, contain 70S ribosomes, which are characteristic of prokaryotic organisms, rather than 80S ribosomes found in the cytoplasm of plant and animal cells. The 50S ribosomal subunit is made up of ribosomal RNA molecules of 23S, 5S, and 4.5S while the 30S subunit is made up of an RNA molecule of 16S. Ribosomes also contain 54-74 ribosomal proteins that are encoded by both the plastid and the nuclear genomes. Many of the elements characteristic of the prokaryotic

translation system such as initiation factors as well as an *E. coli*-like Shine-Dalgarno sequence are also present in plastids (reviewed in Subramarian *et al.,* 1991; Stern *et al.,* 1997).

Transcription in plant plastids is mediated by at least two types of RNA polymerases. The plastid-encoded polymerase (PEP), has a multi-subunit structure that closely resembles the eubacterial RNA polymerase whereas the nucleus-encoded phage type polymerase (NEP) is a single-subunit RNAP similar to that of the mitochondria (reviewed in Hess and Börner, 1999).

THE PLASTID-ENCODED RNA POLYMERASE

The bacterial-type multisubunit RNA polymerase (PEP) is encoded by the plastid genes *rpoA*, *rpoB*, *rpoC1*, and rpoC2. PEP is composed of α_2 (38 kDa), β (120 kDa), β' (85 kDa) and β'' (185 kDa) subunits and is similar to the *E. coli* RNA polymerase, except that the plastid β' and β'' subunits correspond to the amino- and carboxy-terminal domains of the bacterial β' subunit, respectively (Gruissem and Tonkyn, 1993). The sequence as well as the organization of the operon encoding these genes is conserved between bacteria and plastids. For example, *rpoB*, *rpoC1* and *rpoC2* are colocalized in one operon whereas *rpoA* is part of another operon that includes genes for ribosomal proteins (Sugiura, 1992). Studies suggest that mustard (*Sinapsis alba*) contains two different soluble polymerase activities, termed PEP-A and PEP-B (reviewed in Hess and Börner, 1999; Allison, 2000). Pfannschmidt and Link (1994) have determined that the two forms differ in terms of subunit composition (13 subunits for PEP-A and 4 subunits for PEP-B), functional properties (PEP-B is sensitive to the inhibitor of

prokaryotic transcription rifampicin, whereas PEP-A is not), and abundance (PEP-A is the predominant form in chloroplasts, whereas PEP-B is found mainly in etioplasts and in immature plastids during greening). N-terminal sequencing and MALDI-MS characterization of the purified PEP-A enzyme have indicated that PEP-A contains the *rpo* gene products. In addition, PEP-A was converted into the rifampicin sensitive PEP-B form in a phosphorylation-dependent manner (Pfannschmidt *et al.*, 2000). A model has been proposed according to which PEP consists of a catalytic core and polymerase-associated factors. The core complex recruits different factors depending on the type of tissue, developmental stage, and environmental cues (Pfannschmidt and Link, 1997). For example, studies have shown that two types of PEP-A polymerase are present in the different developmental zones of wheat leaves: a tip-type PEP, which is activated by light, and a base-type PEP, which is not light-activated. The two PEP-A forms have different promoter recognition properties and are believed to be associated with different factors (Satoh *et al.,* 1999). Candidates for the polymerase-associated factors include a number of nucleus-encoded plastid-localized σ-like factors (SLF). Sigma-like factors have been identified in rice (Tozawa *et al.,* 1998), mustard (Kesterman *et al.,* 1998), wheat (Ito *et al.,* 1999), maize (Tan and Troxler, 1999; Lahiri and Allison, 2000), and *Arabidopsis thaliana* (Isono *et al.,* 1997b; Tanaka *et al.,* 1997) through sequence similarity to bacterial σ^{70}-type factors. At least six different SLF gene family members have been identified in *Arabidopsis* and five members in maize (reviewed in Allison, 2000; see also Table 4).

In bacteria, recognition of a promoter sequence is aided by sigma factors that interact in a reversible way with core subunits of RNA polymerase to form a holoenzyme. Bacteria contain a number of different sigma factors that are involved in

the expression of specific sets of genes (reviewed in Helmann and Chamberlin, 1988). Two major families of sigma factors are known to occur in eubacteria: the σ^{70} (RpoD) family (Lonetto *et al.,* 1992; Gruber and Bryant, 1997) and the σ^{54} (RpoN) family (Kustu *et al.,* 1989; Collado-Vides *et al.,* 1991). However, most of the bacterial sigma factors belong to the σ^{70} –family and are involved in expression of genes during exponential growth (reviewed in Wösten, 1998). The σ^{70} – family is further subdivided into three different groups which are functionally and structurally related (Lonetto *et al.,* 1992). Group I contains the primary sigma factors and are essential for cell survival.

Table 4. Plant sigma-like factors (the names in parenthesis represent the new nomenclature for the *Arabidopsis* sigma factors as presented by Kanamaru *et al.,* 2001)

Organism	**Gene name**
Arabidopsis (*Arabidopsis thaliana)*	*sigA* (*SIG1*)
	sigB (*SIG2*)
	sigC (*SIG3*)
	sigD (*SIG4*)
	sigE (*SIG5*)
	sigF (*SIG6*) [1]
Maize (*Zea mays)*	*sig1*
	sig2
	sig3
	sig1
	sig2
Mustard (*Sinapsis alba*)	*Sig1*
Wheat (*Triticum aestivum*)	*sigA*
Rice (*Oryza sativa*)	*rsigA*

Adapted from Table 1 in Allison, 2000 unless otherwise indicated.
[1] Fujiwara *et al.,* 2000.

They are found in all known eubacteria (Gruber and Bryant, 1997) and are involved in the transcription of genes expressed in exponentially growing cells. Group II contains sigma factors that are very similar to the primary sigma factors in amino acid sequence but are nonessential for exponential cell growth. Finally, group III contains the alternative sigma factors that differ in amino acid sequence from the primary sigma factors. These alternative sigma factors are involved in the transcription of specific genes that are expressed during certain physiological or developmental conditions such as sporulation and heat shock (reviewed in Helmann and Chamberlin, 1988; Wösten, 1998). Based on sequence comparison of σ^{70} family members, four highly conserved amino acid regions have been identified (Helmann and Chamberlin, 1988; Lonetto *et al.,* 1992). Region 1 is the least well conserved whereas region 2, whose crystal structure has been determined (Malhotra *et al.,* 1996), is the most highly conserved portion. These regions have been subdivided further and a number of functions have been associated with them. For example, subregion 1.1, which is found only in the primary sigma factors, is involved in DNA binding and initiation of transcription whereas subregion 1.2 is involved in open complex formation (Wilson and Dombroski, 1997). Regions 2.1, 2.2, and 3.1 are thought to be involved in binding of sigma factors to the core RNA polymerase while region 2.3 is involved in DNA melting (Chan *et al.,* 1996). Regions 2.4 and 4.2 are believed to be involved in recognition and binding of the –10 and –35 promoter elements, respectively while region 3.2, which is less conserved, is thought to be involved in binding the RNA polymerase core enzyme (reviewed in Wösten, 1998). Finally, region 4.1 is believed to be involved in binding transcriptional activators during initiation (Li *et al.,* 1994; Kuldell and Hochschild., 1994*)* whereas region 2.5 was shown to be involved in contacting nucleotides at positions –14 and –15

in *E. coli* promoters (Voskuil *et al.,* 1995) and the 5′-TG-3′ motif of extended –10 promoters. A histidine residue at position 455 may participate in the recognition of the motif while a glutamate residue at position 458 is believed to interact with the motif (Barne *et al.,* 1997).

All of the plant sigma-like factors have substantial sequence similarity to the conserved regions 2, 3, and 4 of eubacterial sigma factors. In addition, there is a higher degree of similarity between the conserved C-terminal domains of different plant sigma-like factors than there is within their NH_2-terminal regions. In fact, within the C-terminal domain, the degree of similarity to the *E. coli* σ^{70} of the six *Arabidopsis* and the five maize SLFs ranges from 32% to 38%, which is similar to that between bacterial alternative and primary sigma factors (reviewed in Allison, 2000). Moreover, the glutamate residue at position 458 of region 2.5 of bacterial sigma-70, which recognizes the extended –10 box, is conserved in all plant SigA and SigB proteins whereas the histidine residue at position 455 is conserved in SigA and SigB from *Arabidopsis* and in SigA from mustard, wheat, and rice (Morikawa *et al.,* 1999). Phylogenetic analysis (Allison, 2000) based on sequence comparison of 15 higher plant sigma factors show the existence of three clusters with the SigA cluster members further subdivided into monocot and dicot groups. The SigA cluster contains SLF from all the plant species for which sequences have been published. In addition, *SigA* transcripts from *Arabidopsis* were found to be the most abundant of the six Arabidopsis SLF transcripts (Tanaka, *et al*., 1997; Kanamaru *et al.,* 1999). Consequently, SigA group members are believed to constitute the plant analogues of the primary sigma factors of *E. coli* while *Arabidopsis* SigE, which has the least sequence similarity to the other factors, may represent a plant factor similar to the group 3 bacterial members (Allison, 2000). Direct evidence for the

function of the sigma gene products has been obtained from overexpression studies of the mustard Sig1 and *Arabidopsis* SigB proteins. In the case of mustard Sig1, the overexpressed protein was able to stimulate transcription initiation when used in heterologous reconstitution experiments with *E. coli* core RNA polymerase and the mustard plastid *psbA* promoter (Kesterman *et al.,* 1998). In the case of the *Arabidopsis* SigB protein, the C-terminal domain of SigB was fused to the NH_2-terminus of *E.coli* sigma-70. The fusion protein, which was overexpressed in *E.coli*, was able to complement the *E. coli* thermonsensitive *rpoD* mutants (Hakimi, *et al.,* 2000).

THE NUCLEUS-ENCODED RNA POLYMERASE

The second plastid-localized polymerase is encoded by the nuclear genome and has sequence similarity to the single-subunit mitochondrial and phage T3/T7 RNA polymerases (reviewed in Hess and Börner, 1999). This nucleus-encoded polymerase (NEP) is encoded by the nuclear gene *RPOZ* (*RPOT;3*) and has a predicted molecular mass of 112 kDa (Hedtke *et al.,* 1997). In land plants, *RPOT* genes have been identified in *Arabidopsis thaliana* (Hedtke *et al.,* 1997), *Chenopodium album* (Weihe *et al.,* 1997), maize (Young *et al.,* 1998; Chang *et al.,* 1999) and wheat (Ikeda and Gray, 1999). In *Arabidopsis* three closely related *RPOT* genes have been identified (reviewed in Hess and Börner, 1999). The genes have been cloned and characterized (Hedtke *et al.,* 1997). *RPOT;*1 is targeted to the mitochondria whereas *RPOT;3* is targeted exclusively to the plastids (Hedtke *et al.,* 1997, 1999). *RPOT;2*, on the other hand, is targeted to both the mitochondria and the plastids (Hedtke *et al.,* 2000). Furthermore, studies on the transcription of the *rrn* operon from spinach chloroplast suggest the existence of

another nucleus-encoded polymerase (NEP-2). The activity of this polymerase was found to be different from both PEP and NEP activities (Bligny *et al.,* 2000).

PLASTID PROMOTERS

Plastid promoters have been classified into PEP, NEP, and exceptional promoters (reviewed in Hess and Börner, 1999). However, many plastid genes and operons are transcribed from more than one promoter, which may be recognized by different RNA polymerases (see Table 5). For example, the *atpB* gene of *Zea mays*, the tobacco *atpI/H/F/A* operon, and the *clpP* gene of tobacco have been shown to contain such mixed promoters. The maize *atpB* gene, for instance, has two transcription initiation sites relative to the coding region: one at nucleotide position –298 recognized by PEP and a second one at –601 recognized by NEP (Silhavy and Maliga, 1998a). The *clpP* gene of tobacco, on the other hand, has three transcription initiation sites at –53, -173, and –511 recognized by NEP and a fourth one at position –95 recognized by PEP (Hajdukiewicz *et al.*, 1997; Sriraman *et al.,* 1998a) whereas the *atpI/H/F/A* operon has one initiation site at position -130/-131 recognized by PEP and one at position –208/-212 recognized by NEP (Hajdukiewicz *et al.,* 1997).

The PEP promoters, which are recognized by PEP in association with different sigma factors, are found in many plastid genes and contain prokaryotic-like –10 (TATAAT) and –35 (TTGACA) consensus type (CT) promoter elements (Kapoor *et al.,* 1997). These CT promoters have an architecture that shows considerable similarity to the bacterial –10/-35 σ^{70}-type promoters (Hawley and McClure, 1983) and have been shown to function in *E. coli* (Gatenby *et al.,* 1981; Bradley and Gatenby, 1985; Boyer and Mullet, 1986). As in bacteria, there are also many variants of the CT promoters in

plastids. For instance, extended –10 promoters, where the –35 promoter element is not required for transcription initiation, have also been reported in plastids. In bacteria, a TGn motif located upstream of the –10 element has been shown to be involved in transcription initiation of these promoters (reviewed in Bown *et al.,* 1997). A similar motif has been found to be important for the transcription of the wheat *psbA* promoter in the light (Satoh *et al.,* 1999.) In addition, the activity of the light-dependent *psbD* promoter was shown not to require the –35 element (Kim *et al.,* 1999; Nakahira *et al.,* 1998). Instead, the activity of the *psbD* promoter was found to be dependent on two upstream blocks of conserved elements (Allison and Maliga, 1995; Kim and Mullet, 1995; To *et al.,* 1996; Satoh *et al.,* 1997; Nakahira *et al.,* 1998; Kim *et al*., 1999).

NEP promoters, also called nonconsensus type II (NCII) promoters (Kapoor *et al.,* 1997), do not contain the CT promoter elements and are thought to be recognized and utilized by NEP. There are three types of NEP promoters: class Ia promoters, class Ib promoters, and class II promoters. Class Ia promoters contain the sequence 5′-YRT-3′ [Y = (T, C), R = (A, G)] near the transcription initiation site whereas class Ib promoters contain both the YRT-box and the sequence 5′-GAA-3′ further upstream. Class II promoters, on the other hand, lack any similarity to class Ia and Ib NEP promoters (reviewed in Weihe and Börner, 1999; Hess and Börner, 1999). Analysis of the RNA species present in experimental systems such as the ribosome-deficient plastids (Hübschmann and Börner, 1998; Silhavy and Maliga, 1998a), tobacco *Δrpo* plants lacking PEP (Allison *et al.,* 1996; Hajdukiewicz *et al.,* 1997; Serino and Maliga, 1998; Liere and Maliga, 1999), non-photosynthetic plastids from tobacco BY-2 cells (Kapoor *et al.,* 1997; 1999), and a rice embryogenic cell culture (Silhavy and Maliga, 1998b) has identified NEP-dependent transcription initiation sites (see Table 5).

Table 5. Transcript accumulation patterns of plastid genes in various mutants lacking PEP activity (parenthesis indicate uncharacterized promoters) [a]

Gene	Gene Product	Transcript Level	Predicted Promoter Type	Reference
rbcL	Large subunit of RUBISCO	*Ŧ#§Barely Detectable	PEP	Allison *et al.* (1996), Serino and Maliga (1998), De Santis-Maciossek (1999), Krause *et al.* (2000), Silhavy and Maliga, (1998a,1998b), Hess *et al.* (1993)
psaA-psaB-rps14 transcription unit	Photosystem I subunits, 30S ribosome subunit	*Barely Detectable	PEP	Fish *et al.* (1985), Berends *et al.* (1987), Chen *et al.* (1993), Hajdukiewicz *et al.* (1997),De Santis-Maciossek (1999)
psaJ	Photosystem I subunit	†Low	PEP	Nagashima *et al.* (2004)
psbA	Photosystem II subunit	*#§Barely Detectable	PEP	Allison *et al.* (1996), De Santis-Maciossek (1999), Silhavy and Maliga (1998a), Hess *et al.* (1993)
psbB,C,D,E	Photosystem II subunits	*Barely Detectable	PEP	Allison *et al.* (1996), Hajdukiewicz *et al.* (1997), Krause *et al.* (2000)
psbD-256	Photosystem II subunit	†Barely Detectable	-35 /-10-like sequences (PEP)	Hanaoka *et al.* (2003)
petB	Cytochrome b6/f subunit	*Barely Detectable	(PEP)	Hajdukiewicz *et al.* (1997), Krause *et al.* (2000)
ndhA	NADH oxidoreductase subunit	*Barely Detectable †Elevated	-35 /-10-like sequences (PEP)	Matsubayashi *et al.* (1987), Hajdukiewicz *et al.*(1997), Hanaoka *et al.* (2003)

Table 5. (continued).

Gene	Gene Product	Transcript Level	Predicted Promoter Type	Reference
trnE-UUC-trnD-GUC-trnY-GUA transcription unit	Glu-tRNA (UUC), Asp-tRNA (GUC), Tyr-tRNA (GUA)	†(Severely-Slightly-Slightly) Reduced	-35 /-10-like sequences (PEP)	Kanamaru *et al.* (2001), Hanaoka *et al.* (2003)
trnF-GAA	Phe-tRNA (GAA)	Not determined	-35 /-10-like sequences (PEP)	Kanamaru *et al* .(2001)
trnfM-CAU	fMet-tRNA (CAU)	†Normal	Unknown	Hanaoka *et al.* (2003)
trnM-CAU	Met-tRNA (CAU)	†Reduced	-35 /-10-like sequences (PEP)	Kanamaru *et al.* (2001), Hanaoka *et al.* (2003)
trnG-GCC		†Normal	Unknown-no –-35 /-10-like sequences	Kanamaru *et al.* (2001)
trnS-GGA	Ser-tRNA (GGA)	Not determined	-35 /-10-like sequences (PEP)	Kanamaru *et al.* (2001)
trnQ-UUG	Gln-tRNA (UUG)	Not determined	-35 /-10-like sequences (PEP)	Kanamaru *et al.* (2001)
trnV-UAC	Val-tRNA (UAC)	†Severely Reduced	-35 /-10-like sequences (PEP)	Kanamaru *et al* (2001), Hanaoka *et al.* (2003)
trnW-CCA	Trp-tRNA (CCA)	†Normal	Unknown-no -35 /-10-like sequences	Kanamaru *et al.* (2001)
rpl16-----rps11-rpoA transcription unit	50S and 30S ribosomal proteins, PEP subunit	§†Elevated	(NEP)	Hess *et al.* (1993), Alison *et al.* (1996), Hanaoka *et al.* (2003)

Table 5. (continued).

Gene	Gene Product	Transcript Level	Predicted Promoter Type	Reference
rpoB-rpoC1-rpoC2 transcription unit	PEP subunits	§#†Elevated	NEP(Ia)	Hess *et al.* (1993), Silhavy and Maliga (1998a), Liere and Maliga (1999), Hanaoka *et al.* (2003)
rps2	30S ribosomal protein CS2	§Normal	NEP(Ia)	Hess *et al.* (1993), Weihe and Börner (1999)
rps15	30S ribosomal protein CS15	§Normal †Elevated	(NEP)	Hess et al. (1993), Hanaoka *et al.* (2003)
rps16	30S ribosomal protein CS16	*Normal-low	NEP(Ib)	Neuhaus *et al.(*1989), Hajdukiewicz *et al* (1997), Weihe and Börner (1999)
rpl23	50S ribosomal protein CL23	§Elevated	NEP(Ib)	Hübschmann and Börner (1998), Weihe and Börner (1999)
rpl33-rps18 transcription unit	30S and 50S ribosomal proteins	*Elevated	(NEP)	Hajdukiewicz *et al.* (1997)
accD	Acetyl-Co-carboxylase subunit	*†Elevated	NEP(Ia)	Hajdukiewicz *et al.* (1997) Liere and Maliga (1999, Hanaoka *et al.* (2003)
ycf2	Putative ATPase	*Elevated	(NEP(Ia))	Hajdukiewicz *et al.* (1997) Liere and Maliga (1999)
atpB	ATP synthase subunit	*Normal #Low	3PEP / 1NEP(Ib)	Hajdukiewicz *et al.*(1997), Serino and Maliga (1998), Kapoor *et al.*(1997), Krause *et al.*(2000), Liere *et al.*(2004), Silhavy and Maliga (1998a)
atpI/H/F/A transcription unit	ATP synthase subunits	§£Reduced *Normal (complex band pattern)	2PEP / 1NEP(Ib)	Hess *et al.* (1993), Allison *et al.* (1996), Miyagi *et al.* (1998)

Table 5. (ontinued).

Gene	Gene Product	Transcript Level	Predicted Promoter Type	Reference
clpP	Protease subunit	*#§†Elevated (complex band pattern) ₸ Normal	1PEP / 3NEP(Ia, Ib, II)	Hajdukiewicz *et al.*(1997), Serino and Maliga (1998) Silhavy and Maliga (1998a, 1998b),Sriraman *et al*.(1998a), Hanaoka *et al.* (2003)
ndhB	NADH oxidoreductase subunit	*Normal-High (complex band pattern)	-35 /-10-like sequences (PEP / NEP)	Matsubayashi *et al.* (1987),Hajdukiewicz *et al.* (1997)
ndhF	NADH oxidoreductase subunit	*Normal-High	-35 /-10-like sequences (PEP /NEP)	Matsubayashi *et al.* (1987), Hajdukiewicz *et al.* (1997)
ndhJ	NADH oxidoreductase subunit	*Normal-High	(PEP / NEP)	Legen *et al.*(2002)
rrn16	Ribosomal RNA	*Normal †Elevated	1PEP / 1NEP(Ib)	Vera and Sugiura (1995), Allison *et al.* (1996), Serino and Maliga (1998), Sriraman *et al.*(1998b), Hanaoka *et al.* (2003)
rpl32	50S ribosomal protein CL32	£Normal (band intensity ratio reversed)	1PEP / 1NEP(Ib)	Vera *et al.* (1992, 1996), Weihe and Börner (1999)
ycf3-psaA-psab-rps14 transcription unit	Putative factor for assembly and/or stability of PSI, photosystem I subunits, 30S ribosomal protein CS14	*Elevated	1PEP / 1NEP(Ib)	Fish *et al.* (1985), Berends *et al.* (1987), Chen *et al.* (1993), Krause et al. (2000), Summer et al. (2000), Legen *et al.*(2002)

[a] Adapted from Hess and Börner, 1999
*data obtained from tobacco *⊿rpo* plants
₸data obtained from non-green plastids of rice embryogenic cell culture
#data obtained from *Zea mays jojap* mutant plants
§data obtained from *Hordeum vulgare albostrian* mutant plants
† data obtained from *Arabidopsis sig2-1* mutant plants
£data obtained from nonphotosynthetic plastids of cultured tobacco BY-2 cells

Systematic dissection of the tobacco P*rpoB-345* and *PatpB-290* promoters has shown that these sequences are indeed functional NEP promoter elements (Liere and Maliga, 1999; Kapoor and Sugiura, 1999).

Exceptional promoters include promoters that differ from the known PEP and NEP promoters (reviewed in Hess and Börner, 1999; Cahoon and Stern, 2001). For example, the *trnR1* and *trnS1* promoters lack 5′ upstream promoter elements. Instead, they contain elements that are similar to the ones recognized by RNA polymerase III (Galli *et al.,* 1981). Another exceptional promoter is the tobacco *PclpP-53* NEP promoter. This promoter was shown to contain a 30 bp region that is conserved in liverworts, conifers, and in the dicots *Arabidopsis thaliana*, spinach, and tobacco. The sequence is also present in the monocot rice but is transcriptionally silent (Shiraman *et al.,* 1998). In addition, the PC promoter of the spinach plastid operon *rrn* encoding 16S rRNA genes has no homology to any of the PEP or NEP promoters (Iratni *et al.,* 1997). This promoter overlaps with two different PEP promoters and has been shown to be recognized by a third polymerase, NEP-2, in association with the transcription factor CDF2. Interaction of CDF2 with PEP leads to repression of transcription from the *rrn*-PC promoter (Bligny *et al.,* 2000).

REGULATION OF PLASTID GENE EXPRESSION

Plastid gene expression is regulated by environmental cues such as light, developmental cues, cell type as well as a variety of trannscriptional and post-transcriptional mechanisms (reviewed in Mullet, 1988, Rochaix, 1992; Igloi and Kössel, 1992; Gruissem and Tonkyn, 1993; Link, 1996; Stern, 1997; Alison, 2000).

Transcriptional activity in plastids has been proposed to be regulated by DNA copy number (Aguettaz *et al.*, 1987), changes in plastid DNA conformation (Stirdivant *et al.,* 1985; Lam and Chua, 1987; Thompson and Mosig, 1987), and DNA modification (Ngernprasirtsiri *et al.,* 1988; Kobayashi et al., 1990). In addition, mechanisms that result in changes of plastid RNA polymerase activity as well as changes in the relative ratios of the different plastid polymerases may be involved in the regulation of plastid transcription. These mechanisms may include promoter strength, differential usage of promoter elements, regulatory factors, and modification of these regulatory factors (Mullet, 1988; Link, 1996).

Plastid genes have promoters with diverse architecture that modulate activity. Moreover, the structure of the promoter regions has been shown to constitute an important determinant of the relative transcriptional activities of individual genes. Stronger promoters, for instance, are transcribed at higher rates than the weaker promoters (Gruissem and Zurawski, 1985). In addition, point mutations in consensus promoter sequences have been shown to influence the rates of transcription (Hanley-Bowdoin and Chua, 1987). This is similar to prokaryotic systems where variations in the sequence of the consensus -10 and –35 promoter elements result in reduced promoter activity due to a decrease in the affinity of the RNA polymerase for the promoter (McClure, 1985; Fassler and Gussin, 1996).

Differential utilization of promoter elements has been documented for the spinach *rrn* operon and the *psbD-psbC* operon. In the case of the spinach *rrn* operon, which contains three different promoter elements: P1, PC, and P2, transcription is regulated by the transcription factor CDF2 that interacts with two different RNA polymerases. Interaction of CDF2 with NEP-2 activates transcription of the *rrn* at the PC

promoter whereas interaction of CDF2 with PEP inhibits *rrn* transcription (Mache *et al.,* 1997; 2000; Bligny et al., 2000). In *Arabidopsis*, transcripts for the *psbD-psbC* operon have been shown to originate at positions located 190, 256, 550 and 950 upstream of the *psbD* translation start codon (Hoffer and Christopher, 1997; Hanaoka *et al*., 2003). Two different sigma factors (SIG2 and SIG5) have been shown to be involved in mediating transcription from the multiple *psbD* promoters. The promoter for -256 transcription is recognized by SIG2 whereas the promoter for -950 transcription (*psbDLRP*) is recognized by SIG5 whose expression is specifically induced by blue light through the cryptochrome-dependent signaling pathway (Hanaoka *et al.,* 2003; Mochizuki *et al*., 2004; Nagashima *et al.,* 2004; Tsunoyama *et al*., 2004; reviewed in Toyoshima *et al.,* 2005).

The overall goal of this study is to extend knowledge of the mechanisms controlling plastid gene expression. This will be accomplished by focusing on the contribution of nucleus-encoded RpoT;3 phage-type RNA polymerase (T3-NEP) to the transcription of plastid genes. The specific objectives of this research are: (1) to develop a cost-effective, real-time PCR assay method suitable for high-throughput quantitative analysis of plastid transcript abundance; (2) to quantify RNA abundance for a subset of plastid genes in various tissues and developmental stages of *Arabidopsis thaliana*; (3) to determine the role of T3-NEP in the expression of plastid genes in a range of tissues and developmental stages of *Arabidopsis thaliana*; (4) to determine the role of T3-NEP in the coordinated expression of plastid and nuclear genes encoding plastid proteins; and (5) to investigate the expression of RpoT;1. RpoT;2 and RpoT;3 NEP enzymes in a range of tissues and developmental stages of *Arabidopsis thaliana*.

CHAPTER II

DEVELOPMENT OF REAL-TIME PCR ASSAYS FOR EXAMINATION OF GENES INVOLVED IN CHLOROPLAST DEVELOPMENT AND FUNCTION

INTRODUCTION

Traditionally, methods used to quantify mRNA levels included techniques based upon hybridization, such as Northern blotting, in situ hybridization and RNase protection assays. All these traditional methods provide useful information about the size, integrity, and localization of transcripts. However, these methods can be laborious, involving a number of reaction steps. In addition, their low sensitivity requires large quantities of starting material and makes them unsuitable for detection of rare mRNAs or mRNAs from small amounts of tissue (Bustin, 2000). The introduction of reverse transcription (RT)-PCR-based assays (Becker-André and Hahlbrock, 1989; Wang *et al*., 1989; Gilliland *et al*., 1990) has enabled rapid-throughput, high-sensitivity quantification of RNA levels. PCR-based assays for the quantification of mRNA offer distinct advantages over traditional methods in that they use minimal amounts of starting material thus allowing researchers to gain important insights into the expression patterns of low abundant transcripts in specific tissues. The technique consists of three parts: (1) synthesis of cDNA from RNA by reverse transcription (RT), (2) amplification of a specific cDNA by PCR, and (3) detection of the amplified product.

Reverse Transcription (RT)

The RT reaction uses an RNA template (typically either a total or poly(A) RNA sample) a primer, rNTPs and a reverse transcriptase (MMLV-RT or AMV-RT). The first step when using RT-PCR for mRNA analysis is RNA isolation. The RNA should be of high quality and free from genomic DNA contamination (DNAse treated). Next, a single-strand complementary DNA copy (cDNA) of the RNA is produced. First-strand cDNA synthesis reactions may be primed using random hexamers, oligo (dT), or sequence-specific primers. The least specific primers are the random hexamer primers which contain all possible nucleotide combinations of a 6-base oligonucleotide and bind to all RNAs present generating short, partial-length cDNAs. Oligo(dT) primers are more specific than random hexamers and anneal to the poly (A) tails of eukaryotic mRNAs. Since RT reactions primed with random hexamers or oligo(dT) primers can be used for different PCR assays, each with different gene-specific primers, this method increases the number of genes that can be assayed from a single RNA sample (Morrison *et al.,* 1998; Bustin, 2000). The most specific primers for the RT step are antisense gene-specific primers, which hybridize to specific RNA target sequences and can subsequently be used for PCR in combination with the equivalent gene-specific sense primers. The use of sequence-specific primers for rare messages increases specificity and decreases background that is a common occurrence with random hexamers and oligo(dT) primers. However, product yield depends upon the choice of RT primer and upon the efficiency of the primers used in the amplification reaction (Bustin, 2000).

PCR

Following the RT reaction, the cDNA is amplified by PCR. Components of the PCR, in addition to the cDNA, include dNTPs, buffer, thermostable DNA polymerase, and gene-specific primers. The primers determine the sequence and the length of the amplified product (amplicon) whose size should be, ideally, between 50 and 150 bp so that extension times can be short (15 s) thus increasing the efficiency of the PCR reaction (Bustin, 2000). For accurate quantitation, it is important to avoid coamplification of genomic DNA. Designing intron-spanning primers for PCR allows DNA contamination to be assessed because intron-containing DNA will give a different size amplification product than will a spliced product. For intron-less genes, a control RT-PCR without reverse transcriptase needs to be performed.

Amplification Product Detection

For RT-PCR quantification to be accurate, the reaction must be analyzed in the linear range of amplification before the products reach the PCR plateau and components of the reaction mixture become limiting. There are two broad classes of amplification product detection: “end-point” measurements of product and “real-time” monitoring of product formation. In end-point RT-PCR, which detects the amount of final product amplified, the linear range of amplification is empirically determined by amplifying equivalent amounts of cDNA for different numbers of PCR cycles (Dozois *et al*., 1997; Nakayama *et al*., 1992) or by amplifying cDNA dilutions for the same number of PCR cycles (Horikoshi *et al*., 1992). The detection of PCR products is then accomplished

through the use of fluorescent intercalating dyes such as ethidium bromide or SYBR Green (Higuchi *et al*., 1993; Schneeberger *et al*., 1995), through measurement of incorporated radioactivity by autoradiography or phosphor imaging (Hanson *et al.,* 1996) or through hybridization-based protocols, such as Southern blots. All these techniques require numerous processing steps and time-consuming post-PCR manipulations. Real-time PCR detection of product formation first pioneered by Higuchi *et al.* (1992) monitors PCR product accumulation in the thermal cycler as it progresses and ensures detection during the linear range of amplification without the need for extra steps. In contrast to the end-point method, real-time PCR collects data throughout the PCR process, rather than at the end of the PCR. In addition, real-time PCR quantitation eliminates the need for post-PCR processing, thus increasing the throughput and minimizing the errors in sample manipulation for end-point quantification.

Detection Chemistries for Real-time PCR

All real-time PCR systems rely upon the detection and quantitation of a fluorescent reporter, the signal of which increases in direct proportion to the amount of PCR product in a reaction (Higuchi *et al.,* 1993). A variety of fluorescence-based chemistries have been developed for the “real-time” detection of the amplification products, including methods that rely on FRET or fluorescence resonance energy transfer (Stryer, 1978; Cardullo *et al.,* 1988)), such as TaqMan probes, molecular beacons, hybridization probes, and scorpions or nonspecific dsDNA-binding dyes, such as SYBR Green (reviewed in Bustin, 2000; 2002). The most popular methods include the fluorogenic TaqMan hydrolysis probes (Heid *et al.,* 1996) and the dsDNA-binding dye SYBR Green

I (Wittwer *et al.,* 1997; Morrison *et al.,* 1998). The TaqMan method is based on the 5´ nuclease assay first described by Holland *et al.* (1991) and uses a fluorescent dual-labeled oligonucleotide probe that anneals to the PCR target sequence flanked by the PCR forward and reverse primers. The probe is labeled at the 5´ with a fluorescent dye (6-FAM, TET, VIC or JOE) and a quenching dye (6-carboxy-tetramethyl-rhodamine [TAMRA] at the 3´ end. In an intact probe, the energy of the excited fluorescent dye is transferred to the quenching dye with minimal emission of fluorescence (Livak *et al.,* 1995). During PCR amplification, as the primer is extended, the 5′→3′ exonuclease activity of Taq DNA polymerase degrades the probe liberating the fluorescent dye molecule increasing its fluorescence yield. The amount of fluorescence emitted increases in each cycle and is proportional to the amount of PCR product produced which can be used to determine the initial amount of the DNA template. A reliable method for designing the appropriate combination of primers and TaqMan probes is based on the Primer Express software from Applied Biosystems (Foster City, CA, USA), which designs primers with equal melting temperature values (T_m) of 58-60^{0}C, and probes with a T_m value of 68-70^{0}C.

A second detection method involves the use of the DNA-specific SYBR Green I dye to visualize and discriminate DNA products with differing melting-curve profiles. SYBR Green I is a minor groove binding dye that binds only to dsDNA and has low fluorescence yield when unbound. During the PCR process, the dye binds to all double-stranded PCR products, including primer-dimers and other nonspecific products that may be generated during the reaction resulting in a net increase in fluorescence. Since the amount of fluorescent signal is proportional to the amount of PCR product generated, SYBR Green I dye can be used to monitor the amplification of any double-

stranded DNA sequence. However, because the SYBR Green I chemistry detects all double-stranded DNA, target product quantification is most accurate when the occurrence of nonspecific by products is minimized. Dissociation or melting curve analysis of samples containing the target template as well as no-template control (NTC) samples is usually performed after a completed PCR in order to verify the specificity of amplification. With this method ds-DNA fluorescence is measured as the temperature is increased in small increments (usually 0.1-0.5^{0}C/s) from 60^{0}C to 95^{0}C. Plotting the rate of fluorescence change with changing temperature (-dF/dT) as a function of temperature gives a melting curve whose shape and position vary according to the GC content, length and sequence of the target template. This profile can be used to discriminate among amplification products that are less than 2^{0}C apart in melting temperature (Ririe *et al.,* 1997). Ideally, experimental samples should yield a single sharp peak at the melting temperature of the amplicon, whereas controls with no template will not generate a significant fluorescent signal (Figure 5B). This result indicates that the products are specific and that SYBR Green I fluorescence is a direct measure of accumulation of the product of interest. On the other hand, the presence in the no-template sample of a peak with a melting temperature lower than that of the specific product generated with template is typical of primer-dimer formation and indicates that there is not enough discrimination between specific and non-specific reaction products. To obtain meaningful data, careful design of primers and reaction conditions is necessary.

Both the TaqMan and the SYBR Green detection methods give comparable results when properly optimized (Schmittgen and Zakrajsek, 2000) and the choice depends on the specific purpose of the study and economic considerations.

Instrumentation

There are several instruments capable of detecting a wide range of fluorescence chemistries in real-time and providing a plethora of options for any experiment (Bustin, 2000; 2002; Giulietti et al., 2001; Klein, 2002). Although they differ substantially in price, they all detect the accumulation of PCR products by monitoring fluorescent signals that are then graphed as amplification plots of normalized fluorescence (ΔR_n) versus cycle number. A cycle threshold (C_T) value is obtained by determining the point on the amplification plot at which a significant increase in the ΔR_n is first detected. The C_T, which always occurs in the exponential phase of the amplification, is inversely proportional to the starting amount of target template; the higher the initial amount of template, the lower the C_T value (Figure 5A). The general advantage of the real-time PCR technique over the end-point methods is that it avoids the bias associated with the evaluation of the total product generated at the end of the PCR reaction when different amounts of starting material can yield similar amounts of amplification product due to the consumption of reagents (Freeman *et al.,* 1999).

The first commercially available real-time thermal cycler was the ABI Prism Sequence Detection System (SDS) from Applied Biosystems (Foster City, CA) which can be used for detection based on hydrolysis probes, ds-DNA binding dyes and molecular beacons. The instrument consists of a 96-well thermal cycler connected to a laser with an excitation range of 500-660 nm. The fluorochrome in the PCR solution is excited by a laser which is distributed to all samples via optical fibers. The emitted fluorescence is subsequently detected by a charged-coupled devise camera (CCD)

A

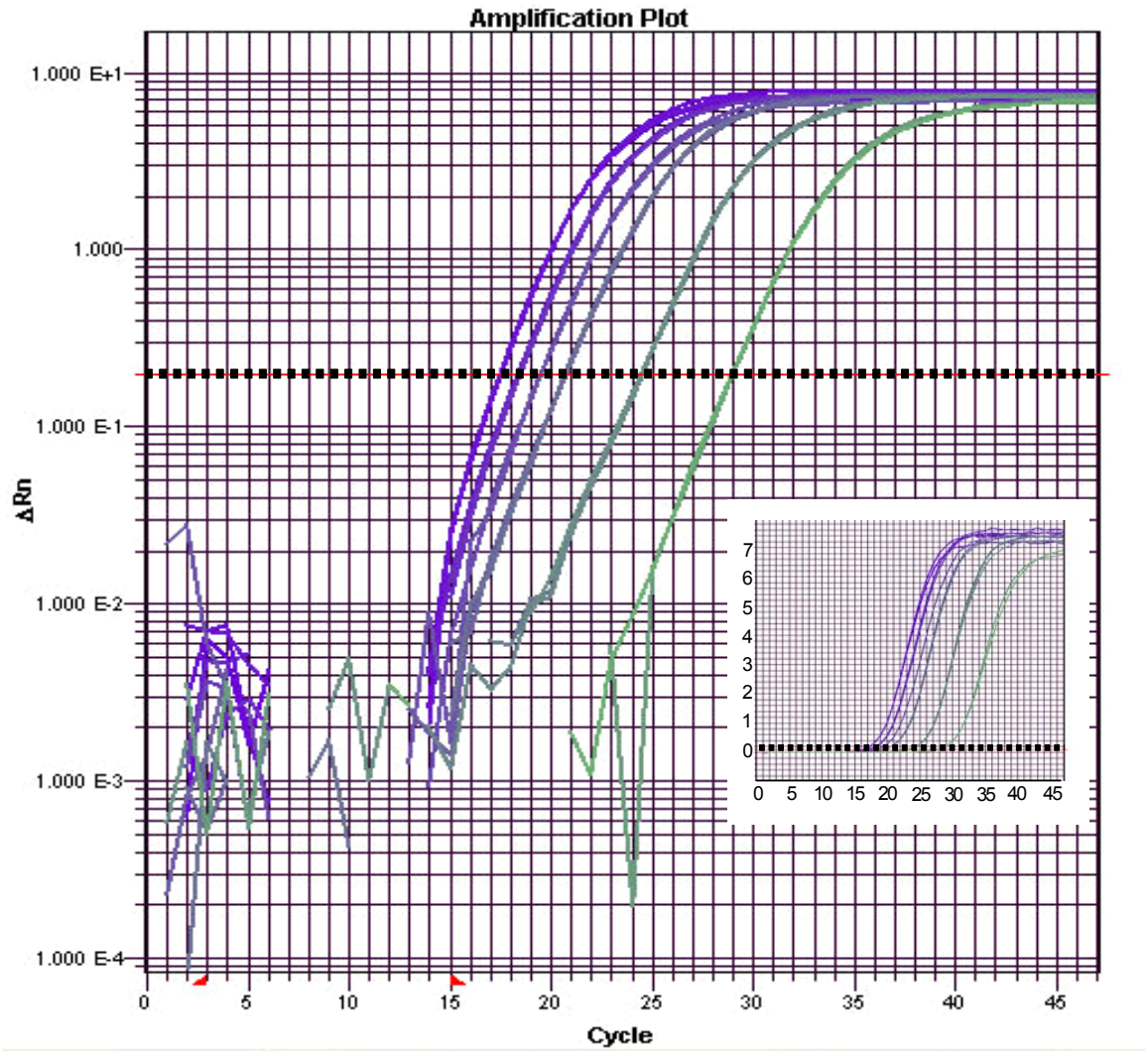

Figure 5. Example of SYBR Green I results representing amplification plots and melting curves from serial dilutions of template cDNA.

Samples of cDNA obtained from total RNA isolated from 23-day old *A. thaliana* rosette leaved were diluted and employed for real-time PCR analysis. Each cDNA dilution corresponding to 20 ng, 10 ng, 5 ng, 2.5 ng, 0.25 ng and 0.025 ng of reverse transcribed mRNA was tested in triplicate. The entire series of cDNA was amplified by 47 cycles of the PCR using primers for the *ndhB* plastid-encoded mRNA and SYBR Green I detection.
(A) Amplification plots from the ABI Prism 7900 HT Sequence detection System showing cycle number versus normalized fluorescence values (ΔR_n). The line in the exponential phase of the log ΔR_n plot (see also linear view-inset) represents the threshold cycle (C_T) – the cycle at which the fluorescence reaches a threshold value ten times the standard deviation of baseline emission and is inversely proportional to the starting amount of target template.

B

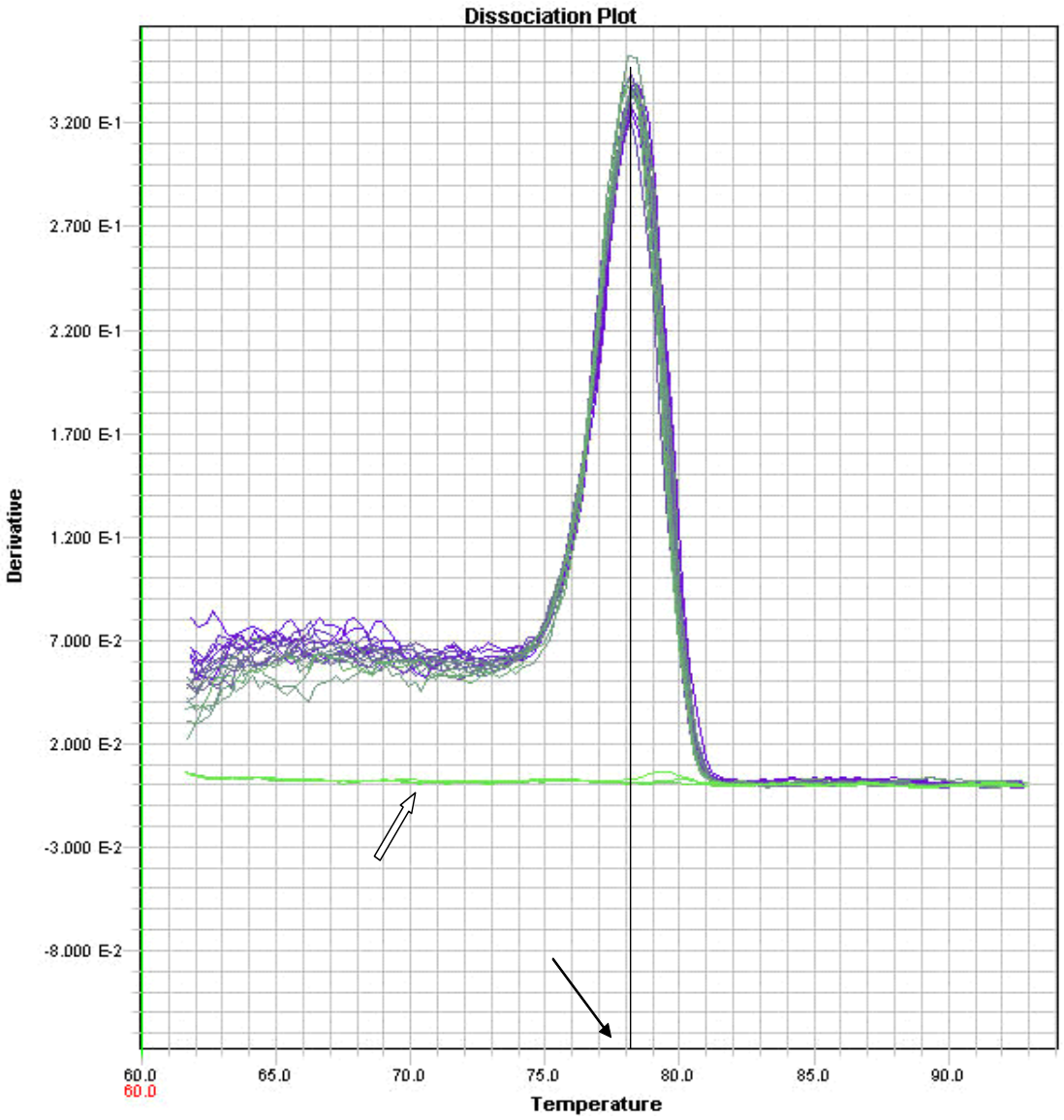

Figure 5. (continued).

(B) Derivative melting curve profile for the *ndhB* primers and the same cDNA dilutions (temperature versus fluorescence [-dF/dT]). All reactions show one sharp and fully overlapping melting peak indicating the specificity of the *ndhB* primers. Open arrow indicates the melting curve with no peaks for the NTC controls. Closed arrow indicates the T_m of the specific *ndhB* product.

for analysis by the software's algorithm and the results can be viewed and analyzed after the amplification run is complete. At the end of each reaction, the recorded fluorescence intensity is normalized to the emission of the internal passive reference dye carboxy-X-rhodamine (ROX^{TM}; Applied Biosystems) present in the SYBR Green and TaqMan PCR master mixes (Applied Biosystems) and plotted as the normalized reporter signal minus background (ΔR_n = Rn^+ [the R_n^+ value of a reaction containing all components] - R_n^- [baseline value detected in the unreacted sample or no-template control (NTC]).

Other established instruments include the halogen-based 96-sample Gene Amp 5700 SDS and the laser-based 384-sample ABI Prism 7900 HT SDS from Applied Biosystems (Foster City, CA, USA), the LightCycler from Roche Molecular Biochemicals (Mannheim, Germany), which uses 20-µL capillaries and allows analysis of the data while PCR amplification is still in progress, and the 96-sample iCycler iQ from Bio-Rad Instruments (Hercules, CA), which is able to multiplex four different fluorophores per sample. Some recently launched instruments are the Smart Cycler (Cepheid, Sunnyvale, CA, USA), which contains 16 different modules and can be operated with hybridization probes, TaqMan probes, molecular beacons, scorpions or SYBR Green I, the ABI Prism 7000 (Applied Biosystems, Foster City, CA, USA), which uses a tungsten-halogen lamp and 96-well plates, the Rotor-Gene 2000 (Corbett Research, Sydney, Australia), which uses standard microfuge tubes, and the Mx4000 (Stratagene, La Jolla, CA, USA), which has a detection range of 350-830 nm, accommodates 96-well plates, 8-strip tubes or individual tubes and is able to detect a variety of fluorescence chemistries.

Principles of Real -Time PCR

Accurate quantitation of mRNA levels by real-time PCR is affected by the efficiencies of both the reverse transcription (RT) step and the PCR amplification step. Although the efficiency of the RT step, which is measured as the percentage of RNA transcribed into cDNA, is affected by differences in nucleotide sequences, it is relatively consistent for a given target (Hayward *et al.,* 1998). During the PCR step, the cDNA is amplified exponentially via cycles of denaturation, annealing, and extension. Theoretically, with each PCR cycle, the amount of DNA doubles according to the equation $X = X_0 2^n$, where X is the amount of amplified target after n amplification cycles and X_0 is the initial amount of template (Wiesner, 1992; Higuchi *et al.,* 1993; Peccoud and Jacob, 1998). Although 100% efficiency results in doubling of the number of amplicon molecules after each amplification cycle, in practice, amplification efficiencies vary, ranging from 0 to 1. Consequently, the PCR equation becomes $X = X_0(1+E)^n$, where E is the amplification efficiency or fold amplification per cycle and E=1 corresponds to 100% efficiency (Freeman *et al.,* 1999; Liu and Saint, 2002). From the above equation the initial amount of template (X_0) can be calculated if the amplification efficiency is known. For real-time PCR, the equation can be written as $X_{CT}= X_0(1+E)^{CT}$, where C_T is the threshold cycle when the emission intensity of the amplification product measured by the real time instrument is recorded as statistically significant above the background noise reflecting the early exponential increase in the PCR product during the log phase and X_{CT} is the number of template copies present after C_T thermocycles. This equation can be converted into the form $\log X_0 = -\log(E+1)C_T + \log X_{CT}$ where there is a linear relationship between C_T and log of the initial amount of template (X_0) when X_{CT} is fixed

and the efficiency is constant. Using a standard curve constructed by amplification of known amounts of template (X_0) and plotting the C_T values against the initial template concentration, a straight line is obtained with a slope of –[1/log(1 + E)] from which the efficiency (E) of the PCR reaction can be estimated via the equation $E = 10^{(-1/slope)} -1$ (Rasmussen, 2001; Rutledge and Côté, 2003). Alternatively, the equation for real-time PCR kinetics can be written as $X_{CT}= X_0E^{CT}$, where E is the amplification efficiency which is ideally 2. By converting this equation into the linear form $CT = - (1/logE) * \log X_0 + (\log X_{CT} / \log E)$, the PCR efficiency can be then estimated from the slope of the standard curve via the equation $E = 10^{(-1/slope)}$ (Ramakers *et al.,* 2003).

Amplification efficiency is affected by a number of variables including sample contaminants from RNA extraction, template concentration, length and sequence, primer sequence, polymerase, buffer composition and PCR cycle profile (Larzul *et al.,* 1988; Arezi *et al.,* 2003). Among the above parameters, the length of the amplicon and the performance of the PCR primers are most important for a successful amplification reaction. Thus, a careful optimization of the PCR parameters and primers leads to reactions with higher amplification efficiencies and less variability (Lehmann, 2001; Karsai *et al.,* 2002; Yeung *et al.,* 2004).

Quantitation of Results

Because amplification is exponential, small differences in sample-to-sample concentration and loading influence product accumulation. Consequently, RT-PCR – based methods of RNA quantitation rely on normalization to correct for differences in input RNA and efficiencies of reverse transcription. Accepted methods used for

normalization of RNA amounts include quantification of the RNA by optical density or fluorescence assay (Jones *et al.,* 1998) and real-time PCR analysis of housekeeping genes, such as glyceraldehydes-3 phosphate dehydrogenase (GAPDH), β-actin and 18Sr RNA (Bustin, 2000). Finding a suitable housekeeping gene for normalization, however, requires additional steps to ensure that the experimental conditions do not alter their expression levels (Suzuki *et al.,* 2000; Schmittgen and Zakrajsek, 2000; Giulietti *et al.,* 2001). Once a suitable housekeeping gene has been identified, the transcripts of the housekeeping gene are quantified along with the transcripts of the target gene. The target value is then divided by the value of the normalizer to obtain a normalized target value that is independent of the amount of starting material.

Two methods are commonly used to quantify the results obtained by real- time PCR: absolute quantification and relative quantification. Absolute quantification is based on the construction of an absolute standard curve of threshold cycle (C_T) versus initial input and determines the precise copy number of the transcript (for instance, known amounts of *in vitro* transcribed RNA amplified under identical conditions to that of the sample). This is a very labour-intensive method and its accuracy relies heavily on the accuracy of standard quantification (Freeman *et al.,* 1999; Giulietti *et al.,* 2001). Relative quantification involves the comparison of mRNA abundance of the target gene to a reference gene or calibrator, such as a non-treated control (Livak, 1997; Morison *et al*., 1998; Bustin, 2000). Two major approaches of relative quantification, the standard curve and the comparative threshold or C_T method, are currently in use (Livak, 1997). In the standard curve method, cDNA plasmids are used as standards and the amounts of target and housekeeping gene are calculated from their respective standard curves. Next, the value obtained for the gene of interest is normalized to the value determined

for the housekeeping gene and then divided by the normalized value of the reference target gene. This method assumes that the diluted samples of the gene of interest are amplified with the same efficiency and results in a relative quantification because it does not take into account the variations in efficiency of the reverse transcription step. The comparative C_T method uses arithmetic formulas to calculate relative expression levels compared to a calibrator (Livak, 1997; 2001). With this method, the amount of target (X) is normalized to a housekeeping gene (H) or normalizer and related to a calibrator (C) sample, which can be any sample chosen to represent 1X expression of the target gene. The method, first outlined by Livak (1997), results in the calculation of a fold change using the formula $2^{-\Delta\Delta CT}$ and relies on the assumptions that (1) the target and normalizer genes have approximately equal amplification efficiencies and (2) there is a constant amplification of approximately 1 in the early exponential phase of the PCR reactions when the C_T values are determined. With these assumptions, the value of the target gene relative to the value of the housekeeping gene chosen can be obtained from the expression $X_{CT}/ H_{CT} = [(X_0 * (1 + E_X)^{CT_X}) / (H_0 * (1 + E_H)^{CT_H})] = K$, where X_{CT} is the number of target copies present after C_T thermocycles, X_0 is the initial amount of target copies, E_X and E_H are the amplification efficiencies of target and housekeeping gene, respectively and K is a constant. Since $E_X = E_H = E$, the above equation becomes $K = X_{CT}/ H_{CT} = [(X_0 * (1 + E)^{CT_X}) / (H_0 * (1 + E)^{CT_H})]$ or $K = (X_0/H_0) * (1 + E)^{CT_X - CT_H}$ which can be written as $K = X_N * (1 + E)^{\Delta CT}$ where X_N equals X_{CT}/ H_{CT} and $\Delta C_T = C_{T\,(target)} - C_{T\,(normalizer)}$. An example of how the ΔC_T value is obtained is shown in Figure 6A. Rearranging and dividing the normalized value of the target by the normalized value of the calibrator (C), the expression $(X_{CT\,(target)} / X_{CT\,(calibrator)}) = [(K * (1 + E)^{-\Delta CT(\,target)}) /$

$(K * (1 + E)^{- \Delta CT(\text{calibrator})})]$ is obtained which can be written as $(X_{CT\ (target)} / X_{CT\ (calibrator)}) = (1 + E)^{- \Delta\Delta CT}$, where $\Delta\Delta C_T = \Delta C_{T\ (target)} - \Delta C_{T\ (calibrator)}$. Since the amplification efficiencies of amplicons properly designed and optimized according to specifications given by Applied Biosystems (Relative quantitation of gene expression, User Bulletin # 2) is assumed to be equal to 1, the above expression becomes: $(X_{CT\ (target)} / X_{CT\ (calibrator)}) = 2^{-\Delta\Delta CT}$ and represents the fold change in expression of the target gene in the experimental sample relative to the expression level of the same gene in the calibrator sample. Alternatively, the relative expression of a gene can be presented using a modification of the $2^{-\Delta\Delta CT}$ method (Schmittgen and Zakrajsek, 2000; Livak and Schmittgen, 2001). In this case, the relative amounts of target and calibrator are presented as $2^{-\Delta CT}$, where $\Delta C_T = CT_{(target)} - C_{T\ (normalizer)}$ and one ΔC_T equals to twofold difference in initial template concentration, $X_1 = X_0(1+1)^1 = 2 X_0$, where X_0 is the initial amount of template at cycle 0, X_1 is the amount of template at cycle 1 and $E_X = 1$ as presented in the manual for TaqMan Human Endogenous Control Plate (Applied Biosystems, Foster City, CA). Although, the comparative C_T method eliminates the need for standard curves as well as the dilution errors associated with the construction of the curves, the method can only be used if the amplification efficiencies of both the target gene and the housekeeping gene are approximately equal. Thus when using the $2^{-\Delta\Delta CT}$ method, validation experiments need to be performed. In these experiments, a dilution series of input template is generated and amplified in triplicate with primers for both the target and the housekeeping gene. If the efficiencies of both amplicons are approximately equal, the ΔC_T should change little over the dilution range and the absolute value of the slope of the log input amount versus ΔC_T plot should be close to zero (Figure 6B). Alternatively, the average C_T values for each dilution of the target and the housekeeping

genes are plotted against the log of cDNA input and from the slopes of the regression lines the amplification efficiencies are estimated (Figure 6C).

In this study, we have evaluated the effectiveness of relative quantification of target gene transcripts in comparison to a reference gene transcript. Our objective was to evaluate the use of the comparative C_T method for quantitating expression of plastid-localized genes in RNA from a variety of plant organs. The specific aims were: (1) establishment of rapid and simple methods for isolation of high- quality RNA from small amounts of various *A. thaliana* tissues; (2) selection of well-performing real-time PCR primers for the target genes; (3) selection of an appropriate housekeeping gene to account for differences in RNA load; (4) development of appropriate real-time PCR protocols using SYBR Green I detection and validation of $2^{-\Delta\Delta CT}$ method for relative quantification; (5) evaluation of the accuracy and reproducibility of the real-time PCR method.

A

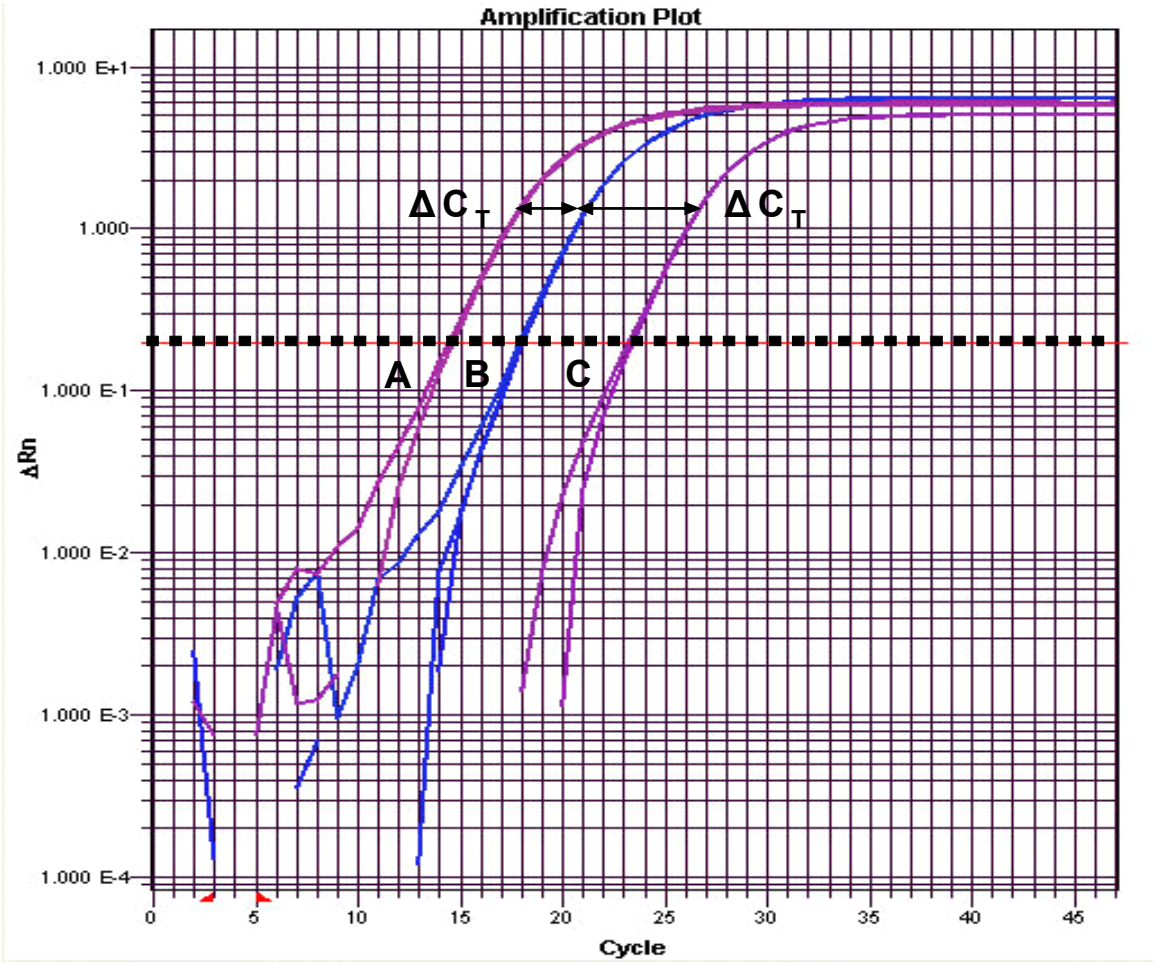

Figure 6. The $2^{-\Delta\Delta CT}$ method.

(A) Example of calculation of the difference (ΔC_T) between the C_T values of the target and the normalizer. Screen-capture from the ABI Prism 7900 HT SDS software representing plots of the ΔRn versus cycle number obtained from SYBR Green detection of the plastid-encoded *rps14* mRNA. Triplicate samples of a cDNA input corresponding to 10 ng of reverse transcribed total RNA obtained from 23-day old *Arabidopsis* rosette leaves were employed as a template for real-time PCR analysis using primers for the *18S rRNA* (A), *rps14* (B), and *Apt* (C) genes. Data for the *rps14* mRNA were normalized relative to cytoplasmic *18S rRNA* and *Apt* levels according to the formula $\Delta C_T = C_{T\ sample} - C_{T\ normalizer}$. The line represents the threshold cycle (C_T) determined by setting a fixed threshold above the baseline.

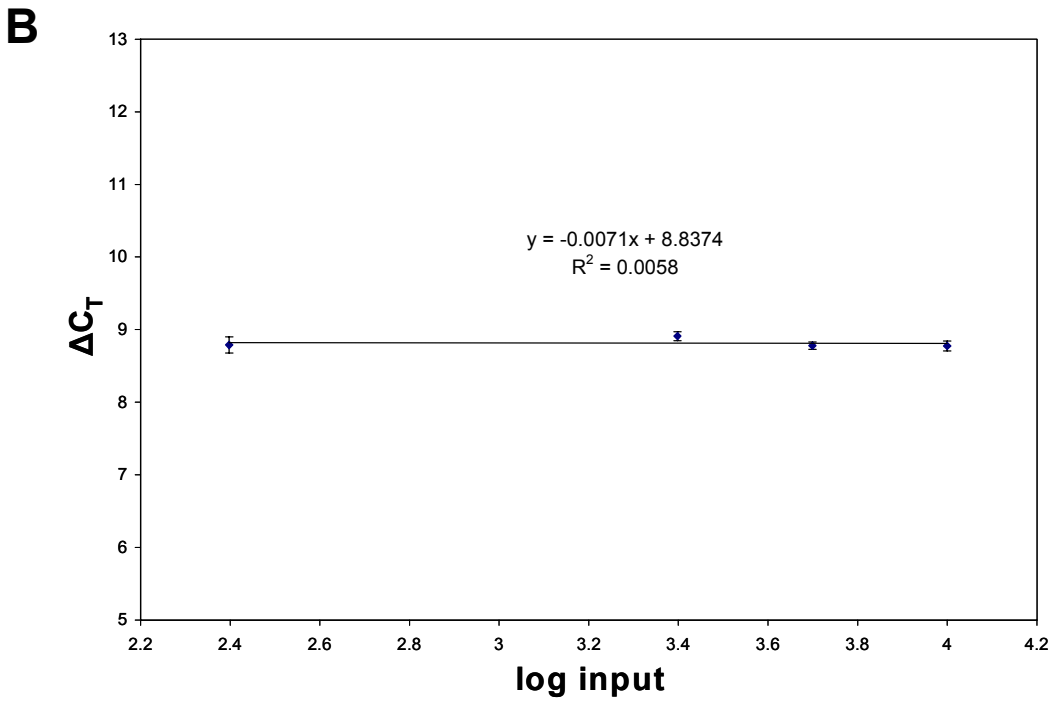

Figure 6. (continued)

(B) and (C) Examples of validation experiments for the $2^{-\Delta\Delta CT}$ method. Dilutions of cDNA corresponding to 10 ng, 5ng, 2.5 ng, and 0.25 ng of reverse transcribed mRNA were amplified by real-time PCR using primers for the nucleus-encoded plastid-localized *petH* gene and detected by SYBR Green I chemistry. The same dilution series was amplified using primers for the cytoplasmic *18S rRNA* and detected using TaqMan chemistry. ΔC_T values obtained by subtracting average C_T values of *18S rRNA* from *petH* were plotted against log input **(B).** Average C_T values of three replicates of each dilution for the *petH* and *18S rRNA* genes were plotted against log input **(C)**

RESULTS

Optimization of RNA Extraction and DNase Treatment Protocols

We compared three commercial kits for RNA extraction from the following *Arabidopsis* tissues: siliques, seeds, seedlings, rosette leaves and roots. The RNeasy Plant Mini Kit (Qiagen, Valencia, CA) and the Tri Reagent (Molecular Research Center, Inc., Cincinnati, OH) proved satisfactory for isolating undegraded RNA from seedlings, rosette leaves and roots but not for RNA extraction from seeds and siliques whereas the Concert Plant RNA Reagent (Invitrogen, Carlsbad, CA) yielded high quality RNA from seeds and siliques. Yields for the RNeasy and the Tri Reagent methods were 25-45 µg per 100 mg of tissue for seedlings and rosette leaves and 3-6 µg per 100 mg of tissue for roots. The purity of the RNA isolated was judged by the $A_{260/280}$ ratios which ranged between 1.9 and 2.0, indicating minimal protein contamination. Analysis of RNA integrity by electrophoresis showed minimal RNA degradation as judged by the intactness of ribosomal RNA bands. Yields of RNA for the Concert Plant RNA Reagent were 2–3 µg per 10-20 µL of dry seeds and 6-10 µg per 100 mg of siliques. Spectrophotometric and gel analysis showed that the isolated RNA was relatively free of contaminants and of high integrity as indicated by $A_{260/280}$ ratios of 1.8 – 2.0 and the 28S:18S rRNA ratio.

To identify the extent of DNA contamination in the RNA samples obtained using the Concert (Invitrogen) and the Tri Reagent (Molecular Research Center) methods, the isolated RNA was reverse transcribed and used as a template for real–time PCR analysis followed by melting curve analysis along with no-template controls (NTC). The

results obtained from the melting curve analysis showed the presence of specific products in the no-template controls indicating the presence of DNA (data not shown). For removal of DNA, three DNase I treatment methods were compared: the column-based DNase I method (Qiagen), the DNA-free method (Ambion), which uses a novel DNase inactivation reagent that does not need to be removed from the RNA sample, and the method described by Huang *et al.* (1996). With the first two methods, DNase I treatment is performed as a separate step during or after RNA isolation whereas with the third method, treatment is performed in the same reaction tube as the reverse transcription of RNA before addition of reverse transcriptase followed by a heat denaturation step at 75^0C for 5 min. To investigate the effectiveness of the different DNase treatments at removing contaminating DNA, the DNase-treated samples were reverse-transcribed simultaneously and used as templates for real-time PCR analysis using SYBR Green I detection followed by melting curve analysis of samples containing either the target template or no-template control (NTC). The results of the melting curve analysis indicated that only the column-based DNase I method (Qiagen) produced a single peak for the target template and no product in the no-template control demonstrating the absence of detectable amounts of contaminating DNA. Thus, the column-based DNase I method (Qiagen) was used for DNase I treatment of all the RNA samples employed in the real-time PCR assays.

Selection of PCR Primers and Housekeeping Gene

Primer pairs were designed for thirty-six target gene sequences and two housekeeping genes of *Arabidopsis thaliana*. The target genes included plastid genes encoding

components of the transcription and translation apparatus (rpoA, *rpoC1*, encoding subunits of the plastid-encoded RNA polymerase (PEP); *rps14*, *rps15*, *rps16*, encoding subunits of the 30S ribosomal protein; *rpl32*, encoding a subunit of the 50S ribosomal protein; *rrn16*, encoding 16S rRNA; *trnC-GCA*, *trnE-UUC*, *trnfM-CAU*, *trnS-GCU*, *trnV-GAC* and *trnW-CCA*), plastid genes encoding components of the NADH dehydrogenase complex (*ndhA*, *ndhB*, *ndhF* and *ndhJ*), plastid genes encoding components of the ATP synthase complex (*atpA* and *atpB*), a plastid gene encoding a component of the cytochrome *b6/f* complex (*petA*), plastid genes encoding Photosystem I components (*psaA*, *psaB*, *psaJ*), plastid genes encoding Photosystem II components (*psbA*, *psbD*, *psbDLRP*), *rbcL*, encoding the large subunit of RUBISCO, plastid genes encoding components involved in other metabolic processes (*accD*, encoding the carboxytransferase subunit of acetyl-CoA carboxylase, *clpP*, encoding the proteolytic subunit of an ATP-dependent protease) and nuclear genes encoding plastid- and / or mitochondrial proteins (*Lhca 1*, encoding a chl a/b binding protein of PSI, *Lhcb 1.2*, encoding a chl a/b binding protein of PSII, *RbcS*, encoding the small subunit of RUBISCO, *PetH*, encoding ferredoxin-NADP+ oxidoreductase (FNR), *RpoT;1*, encoding a mitochondrial RNA polymerase, *RpoT;2*, encoding a plastid / mitochondrial RNA polymerase, *RpoT;3*, encoding a plastid-localized RNA polymerase). The housekeeping genes included the 18S ribosomal RNA (*rRNA*) gene and the *Apt* gene, encoding adenine phosphoribosyltransferase (APRT).

All primers except primers for the *rps16*, *18S rRNA* and *trn* genes were designed using the Primer Express ® v2.0 software (Applied Biosystems, Foster City CA). Primers for the *rps16* and *trn* genes were designed with the online Primer3 program (http://www.genome.wi.mit.edu/cgi-bin/primer/primer3_www.cgi) (Rozen and

Skalettsky, 2000) of the Whitehead Institute (Cambridge, MA, USA) following the same guidelines provided by the Primer Express software. All primers were designed with a melting temperature (T_m) of 58-60^{0}C to allow the use of identical temperature cycle conditions for PCR amplification for all target genes. Amplicon lengths were designed to be between 50 and 150 bp except for the amplicon generated by the 18S rRNA primers which were included in the TaqMan Ribosomal RNA Control Reagents kit (Applied Biosystems) and were designed to produce a product of 187 bp.

To assess the suitability of the 18S rRNA and adeninephosphoribosyl-transferase (*Apt*) as normalizers for relative quanitification, the cDNAs obtained from *Arabidopsis* siliques, seeds, 2-day seedlings, 35-day leaves and 5-day roots were amplified by real time PCR using gene-specific primers for 18S rRNA and *Apt*. As shown in Figure 7 and Table 6, the abundance of 18S rRNA per total RNA was relatively constant in all tissues analyzed with a mean C_T value of 11.24 $\pm$ 0.32 (CV_{CT} = 2.8%, n=5). In contrast, the expression levels of *Apt* varied to some extent across tissue types with a mean C_T value of 22.69 $\pm$ 2.02 (CV_{CT} = 8.9%, n=5) and ΔC_T values that varied significantly from zero.

Table 6. Abundance of 18S rRNA and *Apt* RNA in various *A. thaliana* tissues[a]

Housekeeping gene	Tissue	Mean C_T	ΔC_T
18S rRNA	seeds	11.30 ± 0.07	0.00 ± 0.10
	siliques	10.86 ± 0.11	-0.44 ± 0.13
	2-day seedlings	11.14 ± 0.05	-0.16 ± 0.09
	35-day rosette leaves	11.73 ± 0.06	0.43 ± 0.09
	5-day roots	11.17 ± 0.09	-0.13 ± 0.11
Apt	seeds	26.22 ± 0.09	0.00 ± 0.13
	siliques	22.20 ± 0.07	-4.02 ± 0.11
	2-day seedlings	21.69 ± 0.05	-4.53 ± 0.10
	35-day rosette leaves	22.15 ± 0.04	-4.07 ± 0.10
	5-day roots	21.17 ± 0.09	-5.05 ± 0.13

[a]Three replicate PCRs were performed with cDNAs corresponding to 10 ng of total RNA from *Arabidopsis* seeds, siliques, 2-day seedlings, 35-day rosette leaves and 5-day roots. The same cDNA samples from each tissue were amplified with primers for 18S rRNA or *Apt* on the same run and the amount of PCR product was detected using TaqMan chemistry for 18S rRNA and SYBR Green chemistry for *Apt*. The ΔC_T values were determined by subtracting the average C_T value of the seeds from the average C_T value of the corresponding tissue.

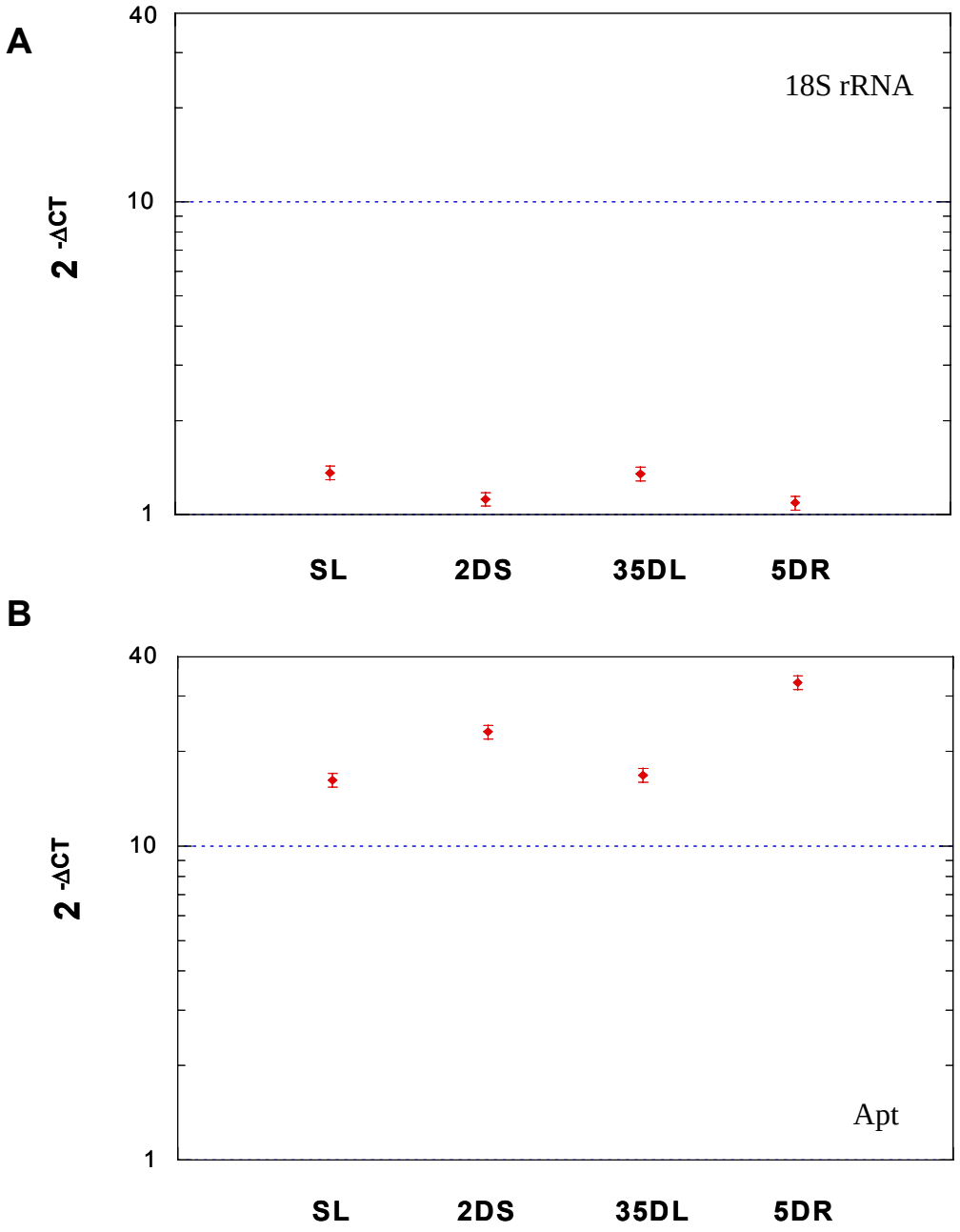

Figure 7. 18S rRNA and *Apt* RNA abundance in various *Arabidopsis* tissues relative to seeds.

Equivalent amounts of total RNA isolated from seeds, siliques (SL), 2-day seedlings (2DS), 35-day rosette leaves (35DL) and 5-day roots (5DR) were converted to cDNA and analyzed by real-time PCR as described in Table 6. The results are presented as $2^{-\Delta CT}$, where $\Delta C_T = (C_{T\ sample} - C_{T\ seeds})$.
(A) Real-time PCR of cDNA synthesized using 18S rRNA primers.
(B) Real-time PCR of cDNA synthesized using *Apt* primers.

Optimization of Real-time PCR

The specificity of the RT-PCR products was verified by electrophoretic analysis of the products in NuSieve® 3:1 agarose gel (BioWhittaker Molecular Applications, Inc., Rockland, ME, USA) and melting curve analysis. For the acquisition of melting curve profiles, every quantitative PCR run contained no-template controls for each primer set. Non-specific amplification products were detected in 25% of the forty primer sets investigated. In these cases, new primer sets were synthesized and retested until primers that specifically amplified target DNA were identified. PCR efficiencies were determined for both the housekeeping genes and the target genes. This was done by exporting the C_T values of a cDNA dilution series into a Microsoft Excel spreadsheet, and calculating the slope for each run using linear regression of log input versus C_T. The slope (m) is related to amplification efficiency by the formula $E = 10^{[-1/m]}$ (Rasmussen, 2001). Finally, to validate the use of the $2^{-\Delta\Delta CT}$ method, which assumes that the amplification efficiency of the target gene and the internal control (normalizer) gene are the same, the ΔC_T ($C_{T\ normalizer} - C_{T\ target}$) from the same run was calculated and plotted against the log input cDNA. If two amplicons have similar efficiencies, linear regression should reveal a slope of approximately zero (Livak, 1997; Livak and Schittgen, 2001). Various template dilution combinations were tested in different runs in order to identify the optimum amount of template cDNA that would yield detectable signals for all target genes investigated. The results indicated that a cDNA input of 100 ng, 80 ng and 50 ng modified the amplification efficiencies of genes with highly abundant transcripts, such as 18S rRNA, *rrn16*, *psbA*, and r*bcL* whereas a 10 ng cDNA template yielded detectable signals for all the genes tested with minimal effect on

amplification efficiency. Table 7 shows the slopes and efficiencies for twelve target genes and two housekeeping genes. The cDNA dilution employed for the examples shown include 10 ng, 5 ng, 2.5 ng, and 0.25 ng for *atpB*, *rps15* and *rpl32*; 20 ng, 5 ng, 2.5 ng, 2 ng, 0.2 ng, and 0.02 ng for *rpoT;3*; 20 ng, 10 ng, 5 ng, 2.5 ng, 2 ng, 0.2 ng, 0.02 ng and 0.01 ng for *trnE-UUC* and *ndhB*; 10 ng, 5 ng, 2.5 ng, 2 ng, 0.2 ng, and 0.02 ng for *trnW-CCA*; 20 ng, 10 ng, 5 ng, 2.5 ng, 0.25 ng, 0.025 ng, and 0.0025 ng for *Lhcb 1.2*; 5 ng, 2.5 ng, 1.25 ng, 0.625 ng, 0.1 ng, and 0.02 ng for rps16; 10 ng, 2 ng, 0.4 ng, 0.08 ng, 0.05 ng, and 0.01 ng for *psbDLRP*. The amplification efficiencies of housekeeping genes and target genes were calculated from the slopes of plots of log input versus average C_T obtained from the same run (see Figures 8 & 9 for examples) according to the equation $E = 10^{[-1/slope]}$ (Rasmussen, 2001). Thirteen out of thirty-six target genes investigated were found to have slopes significantly different from the slopes of 18S rRNA and / or *Apt.* New primers were designed for these genes and retested. Only primers that exhibited differences in PCR efficiencies of less than 0.08 from the efficiencies of the respective housekeeping genes were used for further investigation. As shown in Table 7, slopes for 18S rRNA varied from -3.437 to -3.901 (E varies from 1.80 to 1.95) and from -3.601 to -4.026 for *Apt* (E varies from 1.77 to 1.90) whereas slopes of the target genes ranged from -3.253 to -3.952 (E ranges form 2.03 to 1.79). Also shown in Table 7 are the slopes obtained from the plots of C_T differences (ΔC_T) between the samples and the two housekeeping genes investigated versus log cDNA dilution (see also Figures 8 & 9 for examples of plots). As it can be seen from the examples shown in Table 7, the ΔC_T slopes for 18Sr RNA vary from -0.08 to 0.18 whereas for *Apt* slopes vary from -0.24 to 0.42 with the remaining target genes showing values between these ranges.

Table 7. Determination of PCR efficiency for representative plastid and nuclear genes[a]

Primer	Slope sample	Eff. sample	Slope 18S	Eff. 18S	Slope log input vs. ΔC_T	Slope Apt	Eff. Apt	Slope log input vs. ΔC_T
rps15	-3.446	1.95	-3.437	1.95	-0.01	-3.601	1.90	0.22
rps16	-3.872	1.81	-3.819	1.83	-0.05	-3.634	1.88	-0.24
rpl32	-3.477	1.94	-3.437	1.95	-0.04	-3.601	1.90	0.19
trnC-GCA	-3.253	2.03	-3.437	1.95	0.18	-3.672	1.87	0.42
trnE-UUC	-3.936	1.79	-3.901	1.80	-0.04	-4.026	1.77	0.09
trnW-CCA	-3.793	1.84	-3.834	1.82	0.04	-3.880	1.81	0.09
atpB	-3.513	1.93	-3.437	1.95	-0.08	-3.663	1.88	0.15
ndhB	-3.813	1.83	-3.901	1.80	0.09	-4.026	1.77	0.21
psbD LRP	-3.385	1.97	-3.546	1.91	0.16	ND	ND	ND
clpP	-3.849	1.82	-3.805	1.83	-0.04	ND	ND	ND
Lhcb 1.2	-3.952	1.79	-3.901	1.80	-0.05	-4.026	1.77	0.07
RpoT;3	-3.717	1.86	-3.765	1.84	0.05	-3.697	1.86	-0.02

[a] Total RNA was isolated from 23-day old rosette leaves and converted to cDNA. The reverse transcribed total RNA was serially diluted and employed as template for real-time PCR analysis. Average C_T values of three replicates of each sample were plotted versus $\log_{10}$ of the known starting template concentration in the dilution series. The corresponding real-time PCR efficiencies were calculated according to the equation: $E = 10^{[-1/\text{slope}]}$. In addition, the slope log input vs. ΔC_T was determined by plotting the ΔC_T values obtained by subtracting the average C_T values of each sample from the average C_T values of *18S rRNA* and Apt from the same run versus $\log_{10}$ of the known starting template concentration in the dilution series.

A

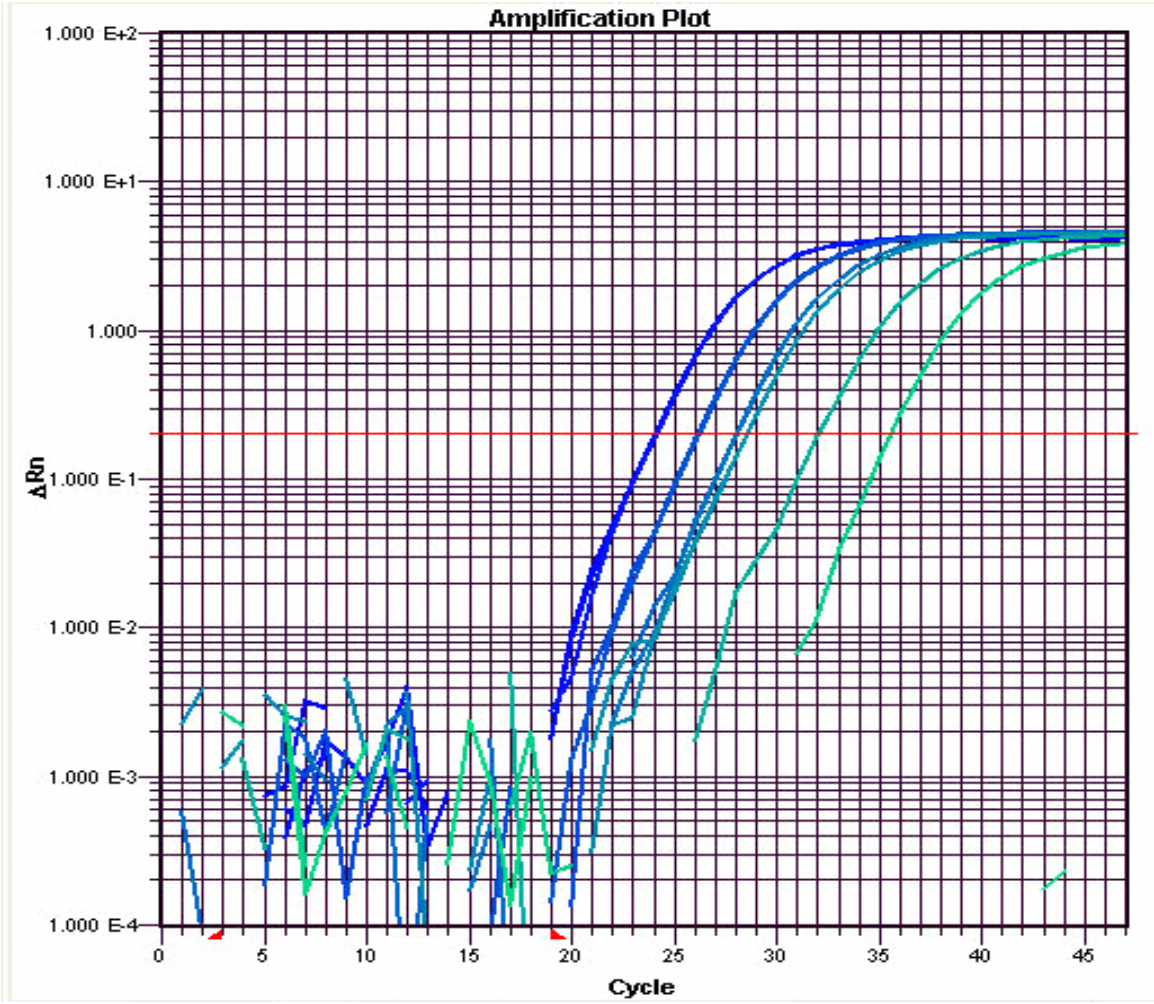

Figure 8. Calculation of amplification efficiency for the *RpoT;3* product.

Three replicate amplification reactions were conducted for each cDNA dilution (20 ng, 5 ng, 2.5 ng, 2 ng, 0.2 ng, and 0.02 ng) using primers for *RpoT;3,* 18S rRNA and *Apt* genes. The amount of PCR product was detected using TaqMan chemistry for 18S rRNA and SYBR Green chemistry for *Apt* and *RpoT;3*.
(A) Output of the amplification run used for the construction of the standard curves showing the plot of ΔRn versus cycle number obtained from the SYBR Green detection of *RpoT;3* mRNA.

B

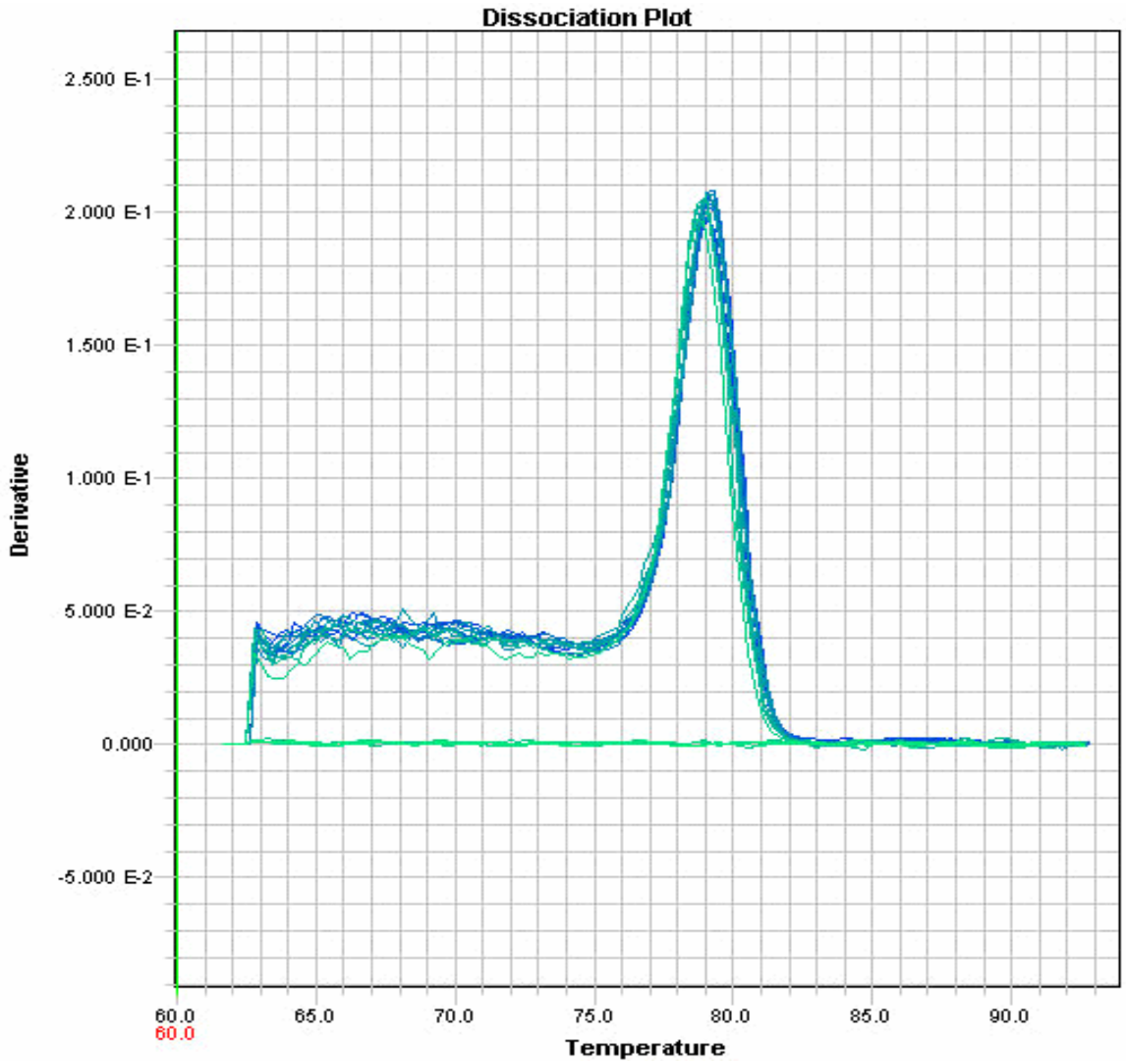

Figure 8. (continued).

(B) Melting curve analysis showing the specificity of the *RpoT;3* primers (sharp overlapping peaks) and the melting curve with no peaks for the NTC controls (flat line).

C

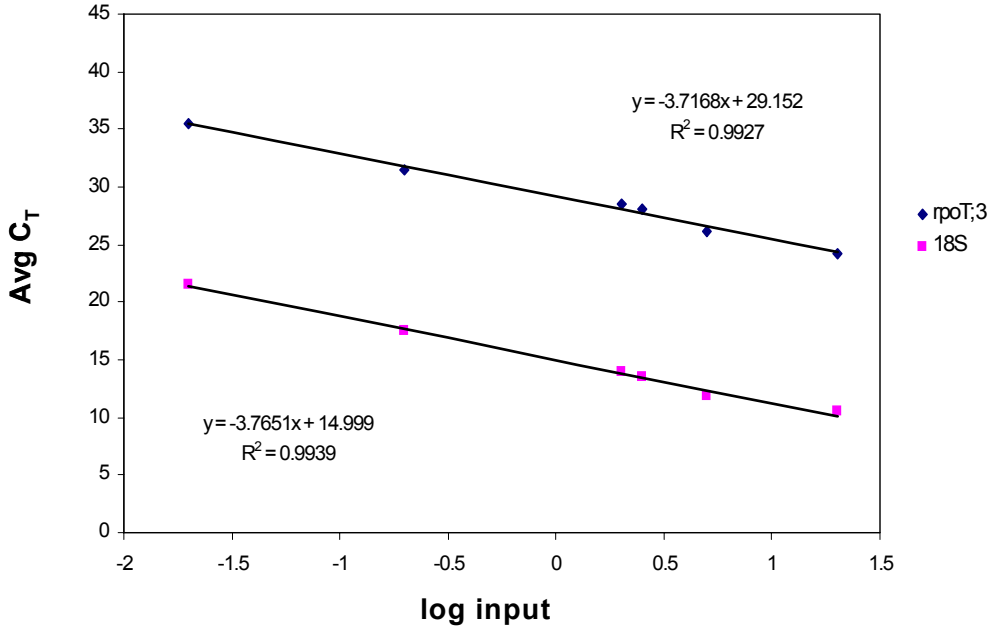

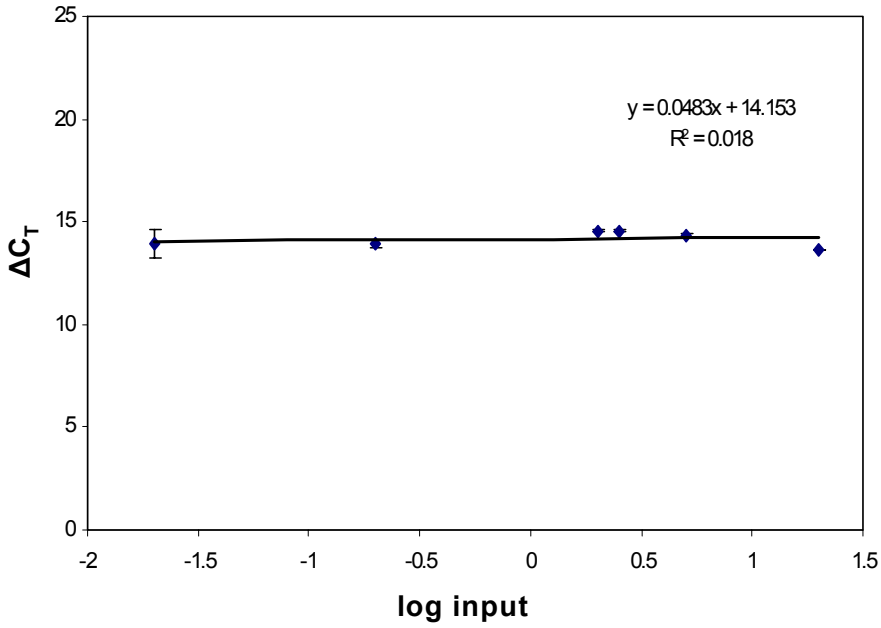

Figure 8. (continued).

(C) Top: the resulting standard curves generated by plotting the log input against the average C_T values of three replicates for each dilution for *RpoT;3* and 18S rRNA with the corresponding regression equations shown. Bottom: standard curves generated by plotting the log input against the ΔC_T values obtained by subtracting average C_T values of 18S rRNA from average C_T values of *RpoT;3*.

D

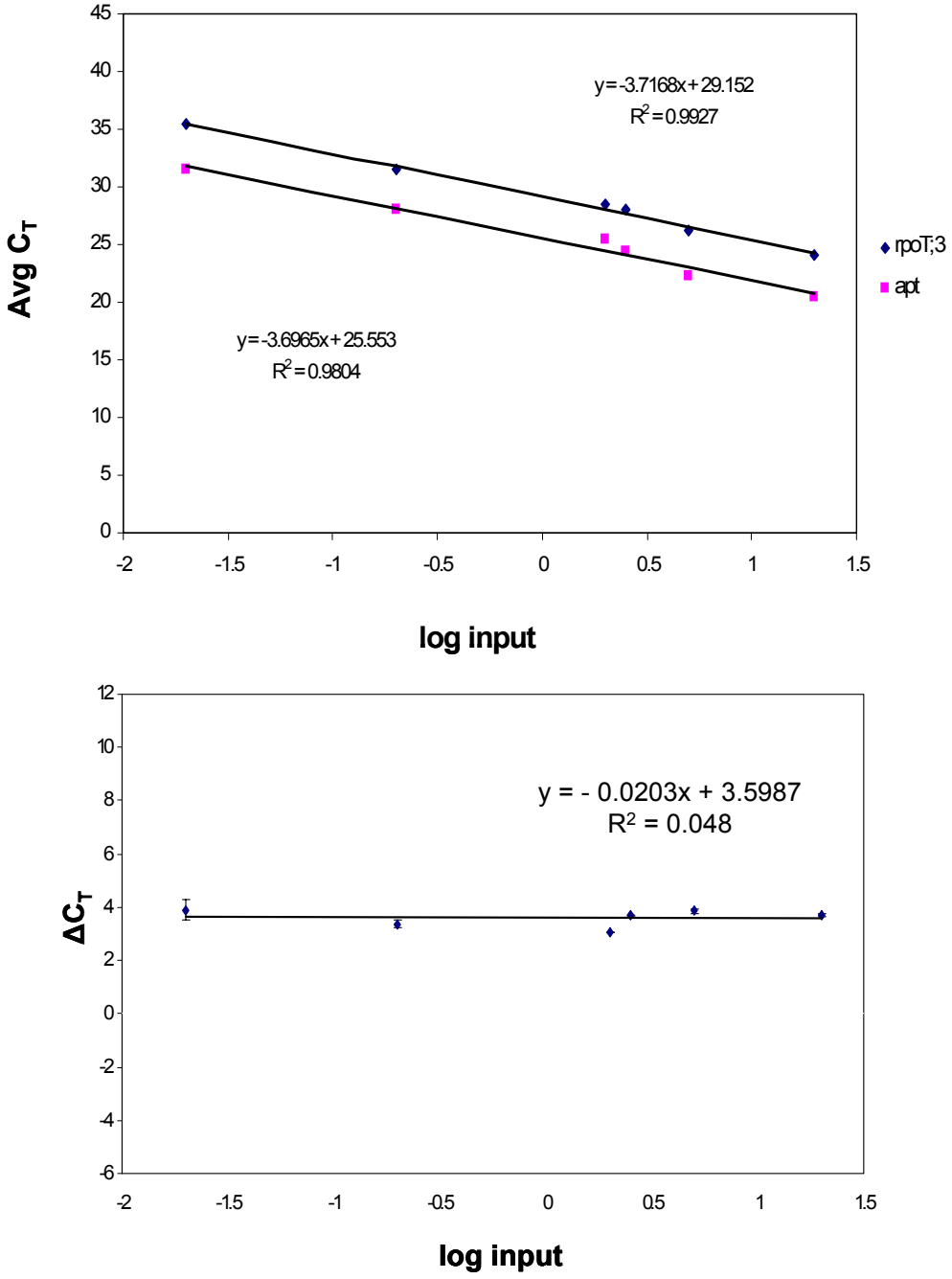

Figure 8. (continued).

(D) Top: the resulting standard curves generated by plotting the log input against the average C_T values of three replicates for each dilution for *RpoT;3* and *Apt* with the corresponding regression equations shown. Bottom: standard curves generated by plotting the log input against the ΔC_T values obtained by subtracting average C_T values of *Apt* from average C_T values of *RpoT;3*.

A

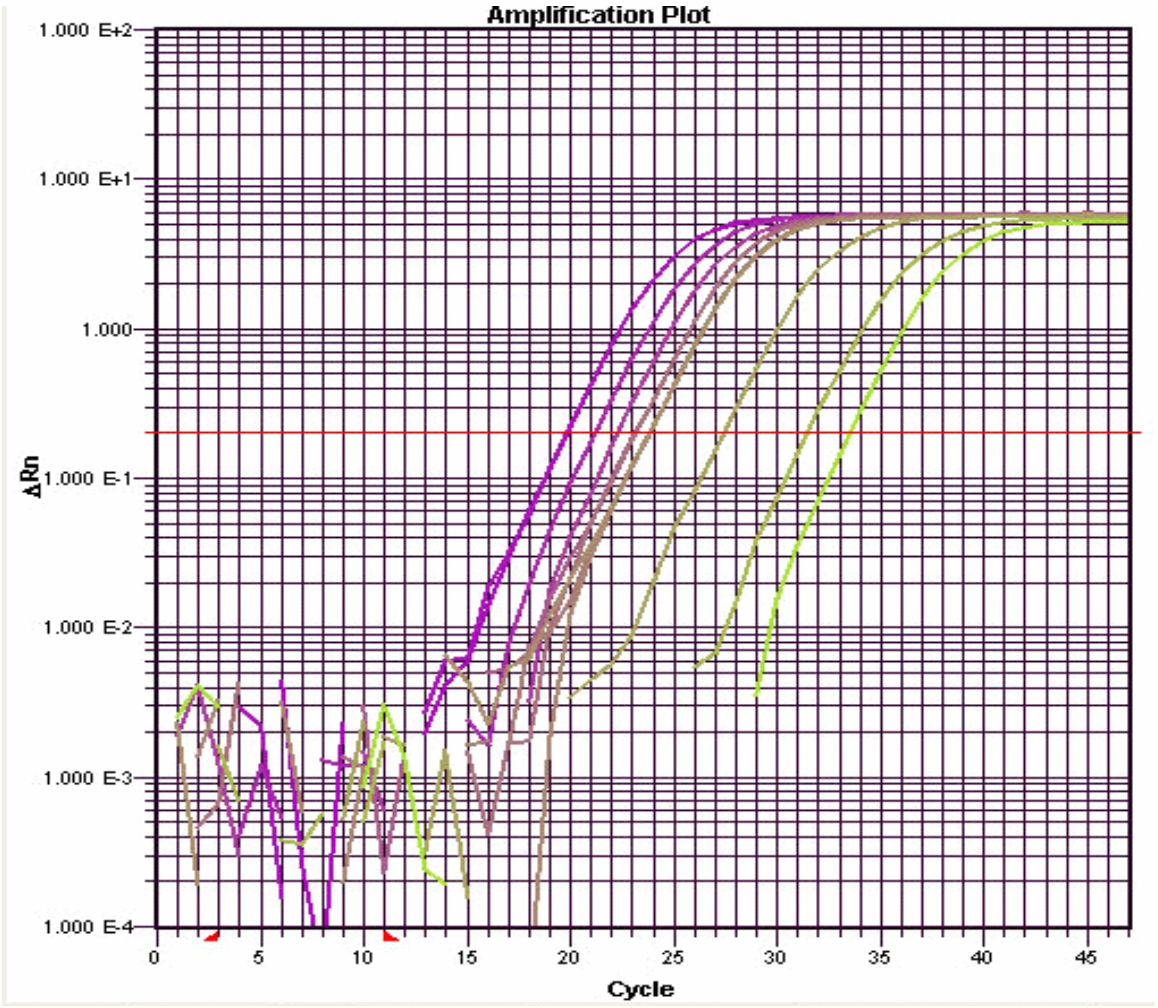

Figure 9. Calculation of amplification efficiency for the *trnE-UUC* product.

Triplicate samples of a cDNA dilution series (20 ng, 10 ng, 5 ng, 2.5 ng, 2 ng, 0.2 ng, 0.02 ng, and 0.01 ng) were assayed by real-time PCR as described in Figure 8 using primers for *trnE-UUC*, *18S rRNA* and *Apt* genes.
(A) Plot of ΔRn versus cycle number obtained from the SYBR Green detection of trnE-UUC mRNA.

B

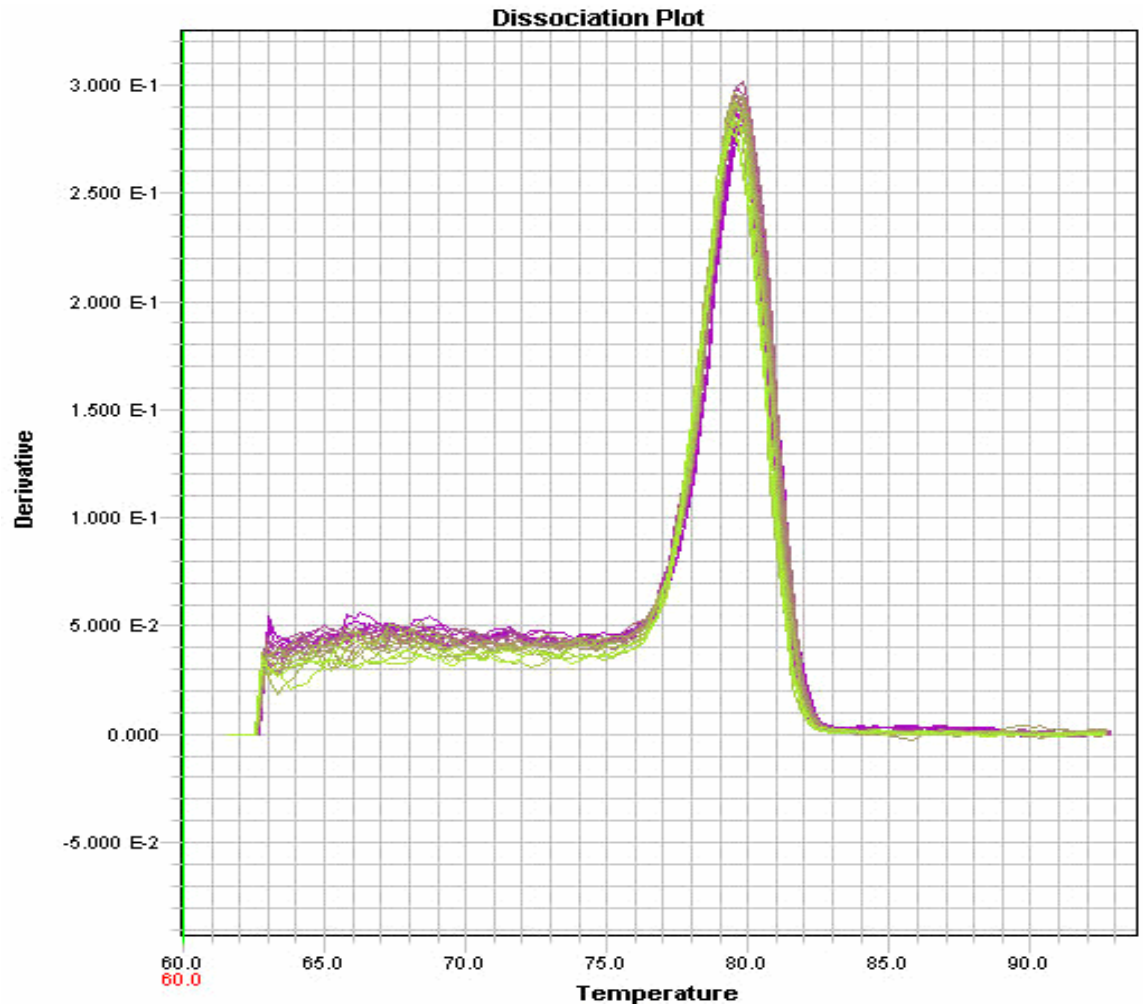

Figure 9. (continued)**.**

(B) Melting curve profile of the *trnE-UUC* product.

C

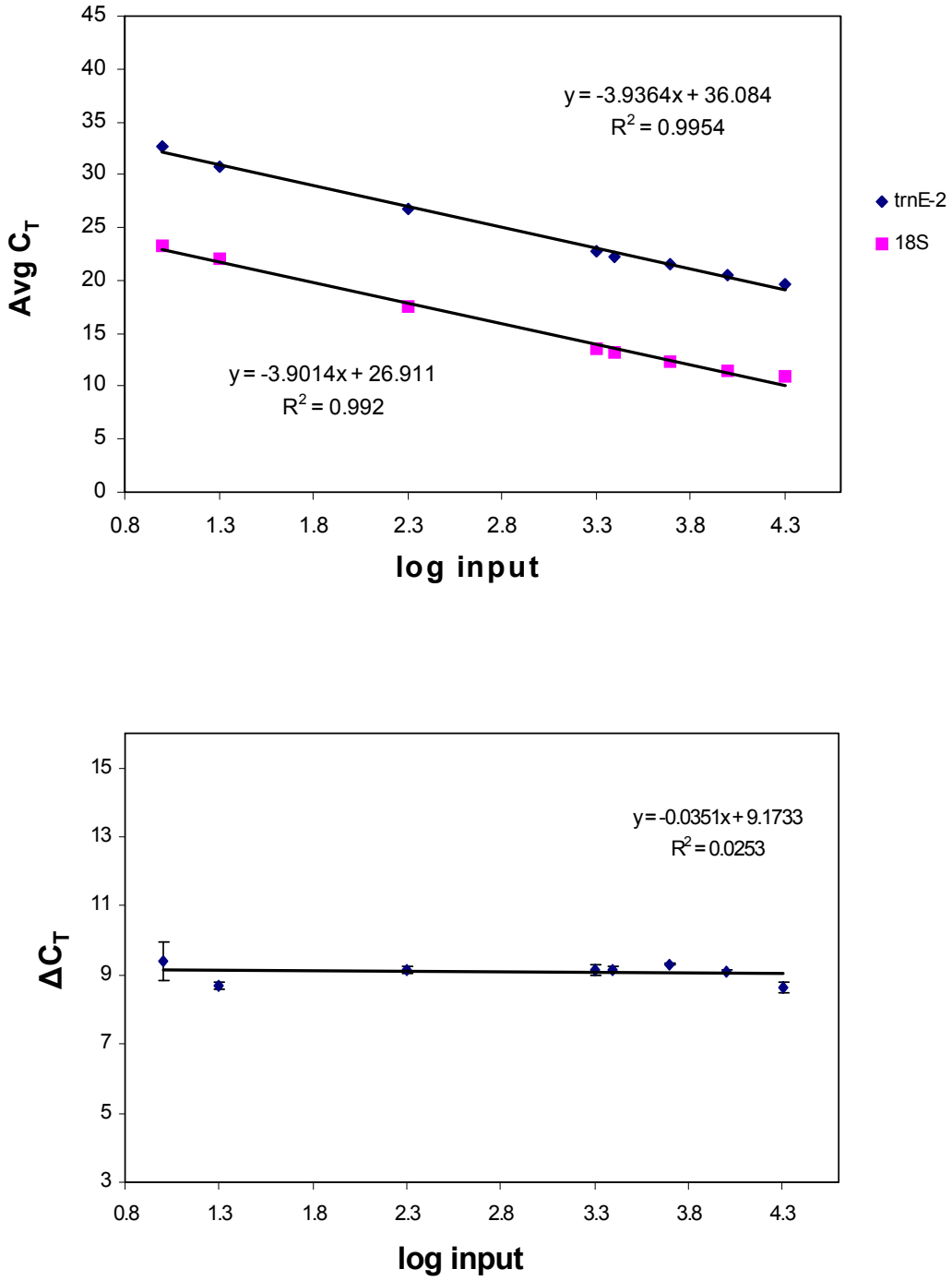

Figure 9 (continued).

(C) Top: the resulting standard curves generated by plotting the log input against the average C_T values of three replicates for each dilution for *trnE-UUC* and 18S rRNA with the corresponding regression equations shown. Bottom: standard curves generated by plotting the log input against the ΔC_T values obtained by subtracting average C_T values of 18S rRNA from average C_T values of *trnE-UUC*.

D

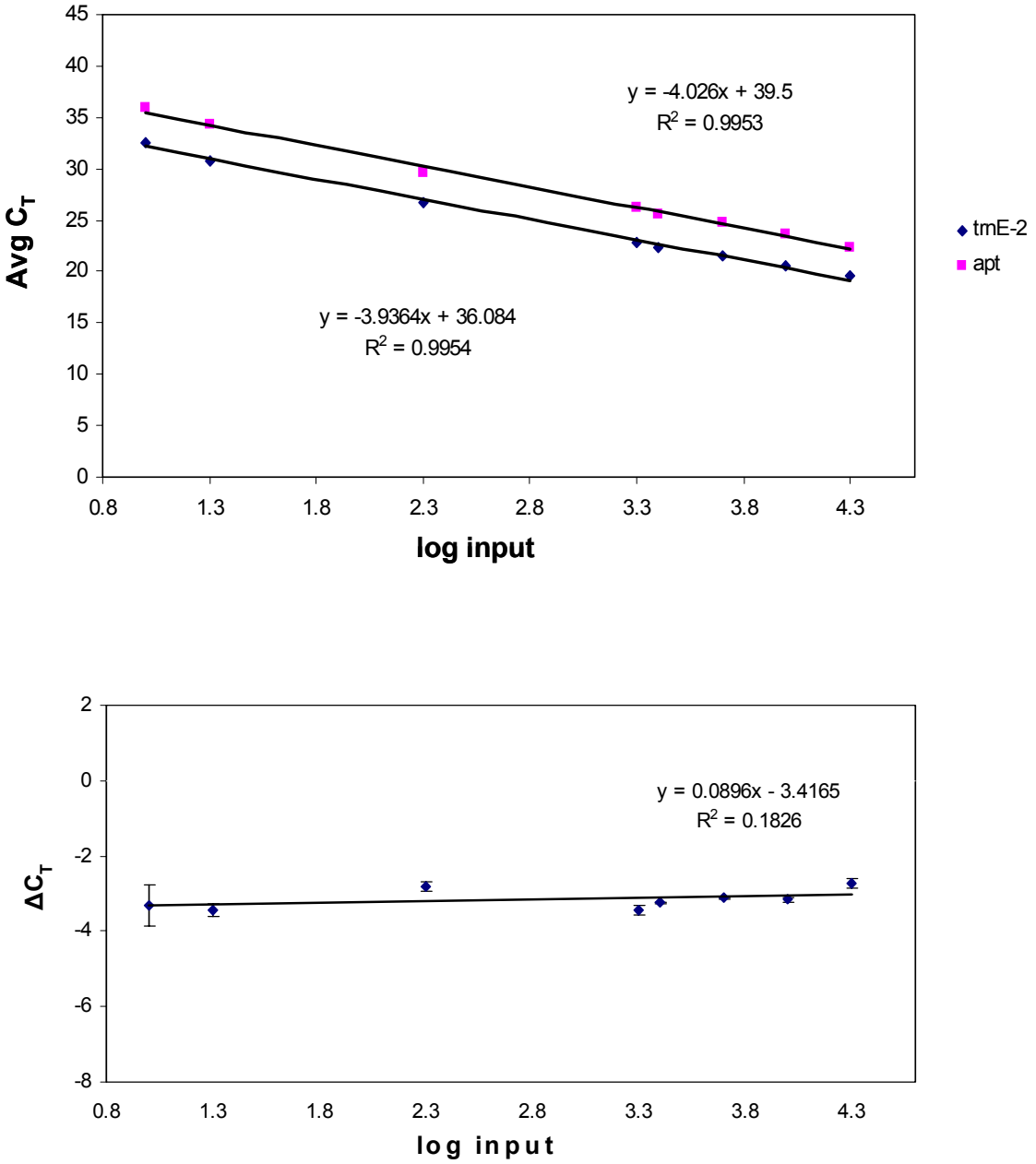

Figure 9 (continued).

(D) Top: the resulting standard curves generated by plotting the log input against the average C_T values of three replicates for each dilution for *trnE-UUC* and *Apt* with the corresponding regression equations shown. Bottom: standard curves generated by plotting the log input against the ΔC_T values obtained by subtracting average C_T values of *Apt* from average C_T values of *trnE-UUC*.

Intra- and Inter-assay Variation

The intra-assay precision of the real-time PCR assay was evaluated by amplifying serial dilutions of cDNA in three replicates followed by PCR using primers for *trnW-CCA*, *ndhB*, *Apt* and 18S rRNA.

Table 8. Intra-assay precision of real-time PCR assays[a]

Primers	Input (ng)	Mean C_T (n=3)	CV (%)	2^{-CT}	CV (%)	ΔC_T 18S	$2^{-\Delta CT}$ 18S ($x10^{\Delta 3}$)	ΔC_T apt	$2^{-\Delta CT}$ *apt*
trnW-CCA	10	21.23	0.51	$4.06x10^{-7}$	7.37	9.79	1.13	-2.47	5.53
	5	22.20	0.14	$2.08x10^{-7}$	2.15	9.93	1.02	-2.44	5.41
	2.5	23.14	0.10	$1.08x10^{-7}$	1.55	10.04	0.95	-2.50	5.67
	2.0	23.74	0.04	$7.13x10^{-7}$	0.73	10.13	0.89	-2.53	5.76
	0.2	27.48	0.55	$5.35x10^{-9}$	10.3	9.92	1.03	-2.08	4.22
	0.02	32.41	0.52	$1.76x10^{-10}$	11.6	10.27	0.81	-1.86	3.64
	0.01	33.18	0.18	$1.03x10^{-10}$	5.76	9.91	1.04	-2.81	7.01
ndhB	10	17.22	0.19	$6.56x10^{-6}$	2.31	5.81	17.85	-6.48	89.34
	5	18.20	0.06	$3.31x10^{-6}$	0.80	5.95	16.23	-6.43	86.06
	2.5	19.17	0.25	$1.70x10^{-6}$	3.29	5.99	15.78	-6.48	89.20
	2.0	19.55	0.19	$1.30x10^{-6}$	2.60	5.91	16.63	-6.72	105.3
	0.2	23.31	0.34	$9.32x10^{-8}$	0.27	5.69	19.41	-6.25	76.17
	0.02	27.46	0.26	$5.41x10^{-9}$	5.01	5.38	23.95	-6.81	112.2
	0.01	28.59	0.33	$2.35x10^{-9}$	6.38	5.38	24.08	-7.40	169.0

Table 8. (continued).

Primers	Input (ng)	Mean C_T (n=3)	CV (%)	2^{-CT}	CV (%)
18S rRNA	10	11.41	0.57	3.68×10^{-4}	4.52
	5	12.26	0.49	1.99×10^{-4}	4.15
	2.5	13.18	0.55	1.08×10^{-4}	5.07
	2.0	13.64	0.68	7.86×10^{-5}	6.39
	0.2	17.62	0.53	4.97×10^{-6}	6.36
	0.02	22.08	0.42	2.26×10^{-7}	6.46
	0.01	23.21	0.25	1.05×10^{-7}	2.57
Apt	10	23.70	0.07	7.34×10^{-8}	1.20
	5	24.63	0.42	3.86×10^{-8}	7.36
	2.5	25.65	0.63	1.91×10^{-8}	10.80
	2.0	26.27	0.31	1.24×10^{-8}	5.71
	0.2	29.56	0.33	1.27×10^{-9}	6.71
	0.02	34.27	0.33	4.83×10^{-11}	7.97
	0.01	35.99	0.41	1.47×10^{-11}	10.20

[a] Three replicate PCRs for seven target concentrations were performed on identical cDNA obtained from total RNA extracted from 23-day old *Arabidopsis* rosette leaves. The cDNA was amplified using primers for *trnW-CCA*, *ndhB*, 18S rRNA or *Apt* and the amount of PCR product produced was detected using SYBR Green chemistry except for the 18S rRNA product which was detected using TaqMan chemistry. CV represents percent standard deviation in C_T generated from replicate amplifications. ΔC_T represents the mean C_T value of the normalizer (18S rRNA or *Apt*) subtracted from the mean C_T value of the target (*trnW-CCA* or *ndhB*).

The standard deviation in C_T of replicate amplifications (Table 8) ranged from 0.01 to 0.17 cycles for *trnW-CCA* (CV_{CT} from 0.04% to 0.55%), 0.01 to 0.09 cycles for *ndhB* (CV_{CT} from 0.06% to 0.34%), 0.06 to 0.09 cycles for 18S rRNA (CV_{CT} from 0.25% to 0.68%), and 0.02 to 0.16 cycles for *Apt* (CV_{CT} from 0.07% to 0.62%). When the individual C_T values were converted to the linear form equal to 2^{-CT}, the standard deviation of replicate amplifications ranged from 5.95×10^{-12} to 3.00×10^{-8} for *trnW-CCA* (CV_{CT} from 0.73% to 11.6%), 1.50×10^{-10} to 3.00×10^{-7} for *ndhB* (CV_{CT} from 0.27% to 6.38%), 2.70×10^{-9} to 1.66×10^{-5} for 18S rRNA (CV_{CT} from 2.57% to 6.46%), and 1.50×10^{-12} to 2.84×10^{-9} for *Apt* (CV_{CT} from 1.20% to 10.2%). Next, the variation in the normalized values of *trnW-CCA* and *ndhB* PCR products over the seven cDNA concentrations examined was assessed by subtracting the mean C_T values of 18S rRNA or *Apt* from the mean C_T values *trnW-CCA* and *ndhB* (see ΔC_T columns in Table 8). For *trnW-CCA,* the mean ΔC_T value relative to 18S rRNA was 10.00 ± 0.16 ($CV_{\Delta CT}$ = 1.6%) whereas the mean ΔC_T value relative to *Apt* was -2.38 ± 0.31 ($CV_{\Delta CT}$ = 13.2%). For *ndhB*, the mean ΔC_T value relative to 18S rRNA was 5.73 ± 0.26 ($CV_{\Delta CT}$ = 4.5%) whereas the mean ΔC_T value relative to *Apt* was -6.65 ± 0.38 ($CV_{\Delta CT}$ = 5.7%). Finally, the variation in the amounts of *trnW-CCA* and *ndhB* relative to 18S rRNA or *Apt* was evaluated by expressing the normalized ΔC_T values for each dilution of *trnW-CCA* and *ndhB* as $2^{-\Delta CT}$ (see $2^{-\Delta CT}$ columns in Table 8). The relative amount of *trnW-CCA* to 18S rRNA was 0.98 ± 0.11 ($CV_{(2^{-\Delta CT})}$ = 10.8%) whereas the relative amount of *trnW-CCA* to *Apt* was 5.32 ± 1.10 ($CV_{(2^{-\Delta CT})}$ = 20.7%). The relative amount of *ndhB* to 18S rRNA was 19.13 ± 3.54 ($CV_{(2^{-\Delta CT})}$ = 18.5%) whereas the relative amount of *ndhB* to *Apt* was 103.9 ± 31.2 ($CV_{(2^{-\Delta CT})}$ = 30.0%).

Inter-assay variation was investigated in two different experimental runs performed on 2 days using the same cDNA samples with different 2X SYBR Green PCR Master Mix (Applied Biosystems, Foster City, CA). Each cDNA was amplified in three replicates using primers for *psaB, psbDLRP*, and 18S rRNA with identical cDNA samples obtained from 6-day seedlings and primers for *clpP*, *rbcL*, *rpoA*, *rrn16*, and 18S rRNA with identical cDNA samples obtained from 12-day cotyledons. Overall, the inter-run standard deviations in mean C_T values ranged from 0.04 to 0.21 cycles and resulted in CV_{CT} values that ranged from 0.36% to 1.90% whereas the CV for the inter-run mean $2^{-\Delta CT}$ values ranged from 3.18% to 25.77% (Table 9). To examine the effect of this variation on the relative amount of transcript calculated using the comparative C_T method, the fold difference between the ΔC_T values obtained from the two runs was computed and expressed as $2^{-\Delta\Delta CT}$. As seen in Table 9, a $CV_{(2-\Delta CT)}$ value of 3.18% corresponded to 1.05 fold difference in expression with a low of 1.01X and a high of 1.08X whereas a $CV_{(2-\Delta CT)}$ value of 25.77 corresponded to 1.45 fold difference in expression with a low of 1.39X and a high of 1.50X. We also looked at the inter-run variation using cDNAs obtained from different RNA samples extracted from different batches of 6-day old seedlings. The samples were reverse transcribed simultaneously and employed for real-time PCR using primers for *psaB*, *psbDLRP* and 18S rRNA. The CV_{CT} value for *psaB* was 5.24% and resulted in a $CV_{(2-\Delta CT)}$ of 14.41% which translated into a difference in expression of 1.11 fold with a low of 0.94X and a high of 1.30X whereas the corresponding values for *psbDLRP* were CV_{CT} = 3.76% with a $CV_{(2-\Delta CT)}$ of 14.09% and a fold difference of 1.22 (1.04 -1.44).

Table 9. Inter-assay variation (n = 2) of ABI Prism 7900 HT real-time PCR[a]

A. Twelve-day cotyledons

Primers	Mean C_T (n=2)	CV (%)	Combined $2^{-\Delta CT}$ 18S	CV (%)	Fold difference ($2^{-\Delta\Delta CT}$)
clpP	17.40 ± 0.14	0.82	0.033 ± 0.008	24.20	1.41 (1.36-1.46)
rbcL	11.75 ± 0.17	1.40	1.62 ± 0.05	3.18	1.05 (1.01-1.08)
rpoA	18.20 ± 0.12	0.65	0.019 ± 0.001	6.38	1.09 (1.05-1.14)
rrn16	8.70 ± 0.17	1.90	13.59 ± 3.50	25.77	1.45 (1.39-1.50)
18S	12.44 ± 0.21	1.69			

B. Six-day seedlings

Primers	Mean C_T (n=2)	CV (%)	Combined $2^{-\Delta CT}$ 18S	CV (%)	Fold difference ($2^{-\Delta\Delta CT}$)
psaB	13.81 ± 0.21	1.55	0.252 ± 0.018	7.34	1.18 (0.93-1.50)
psbDLRP	20.00 ± 0.14	0.70	0.0036 ± 0.0002	6.69	1.10 (0.97-1.24)
18S	11.86 ± 0.04	0.36			

[a] Determination of variation was done in 5 ng of reverse transcribed total RNA from 12-day cotyledons and 10 ng of reverse transcribed total RNA from six-day seedlings. Triplicate samples of cDNA were assayed by real-time PCR in two replicate amplification runs using primers for *clpP*, *rbcL*, *rpoA, rrn16, psaB, psbDLRP* and 18S rRNA. The amount of PCR product produced was detected as described in Table 8. ΔC_T represents the mean C_T value of 18S rRNA subtracted from the mean C_T value of the target gene. $\Delta\Delta C_T$ represents the ΔC_T value for one gene obtained from run 2 subtracted from the ΔC_T value for the same gene obtained from run 1. The range given in parenthesis for the $2^{-\Delta\Delta CT}$ column was determined by evaluating the $2^{-\Delta\Delta CT}$ with $\Delta\Delta C_T$ + s and $\Delta\Delta C_T$ – s, where s represents the standard deviation of the $\Delta\Delta C_T$ value.

DISCUSSION

The study of gene function requires sensitive, precise and reproducible measurements of gene expression levels. Many traditional methods of gene expression analysis, such as Northern blot hybridization are limited by the number of samples that can be analyzed simultaneously as well as by the requirement for high concentrations of starting template and thus large amounts of tissue (Bustin, 2000). Real-time PCR is a powerful and sensitive methodology to amplify and detect low amounts of mRNA and offers the potential for rapid and quantitative high-throughput screening (Wang *et al*., 1989; Freeman *et al*., 1999). Some of the current uses for real-time PCR include validation of microarray results (Rajeevan *et al.,* 2001), estimation of transgene copy number in transformed plants (Ingham *et al*., 2001), zygozity testing in transgenic plants (Schmidt and Parrott, 2001), analysis of cytokine gene expression and determination of bacterial or viral loads (Bustin, 2002). Recently, Czechowski *et al.,* (2004) have developed a library of RT-PCR primers for over 1,400 *Arabidopsis* transcription factor genes which were subsequently used for the identification of putative root- and shoot-specific transcription factor genes.

In the present study, we investigated the suitability of real-time quantitative PCR using SYBR Green to monitor the relative expression of genes in various tissues of *Arabidopsis thaliana*. The intent of this study was to develop a cost-effective, real-time PCR assay suitable for high-throughput quantitative gene expression studies. Therefore, we investigated the use of the comparative C_T or $2^{-\Delta\Delta CT}$ method because it permits higher throughput than the standard curve method by eliminating the need for standard samples when looking at expression levels relative to a reference control

(Giulietti *et al*., 2001). To further simplify the quantification of many different targets, we monitored product formation with SYBR Green I instead of the more specific TaqMan assay which requires a separate fluorescent-labeled probe in addition to the forward and reverse primers. Our objectives included the identification of the most rapid and cost- effective method of isolating high-quality RNA from the siliques, seeds, seedlings, rosette leaves and roots of *Arabidopsis thaliana*, selection of an appropriate housekeeping gene that could be used to correct for experimental variations across all tissues and target genes investigated, selection of primers with the highest amplification efficiencies for thirty-eight plastid- and nucleus-encoded mRNAs, and determination of the precision and the reproducibility of the RT-PCR assay.

Efficient extraction of high quality RNA from a variety of plant tissues is an important first step for the analysis of gene expression by real-time PCR. Unfortunately, RNA extraction from plant tissues such as seeds is troublesome in many cases, possibly due to high content of secondary metabolites, polysaccharides or other compounds that bind and / or co-precipitate with the RNA (Ruuska and Ohlrogge, 2001). Several methods are described in the literature for the isolation of RNA from such tissues that are reported to give RNA of good quality (Tesniere and Vayda, 1991; Chung et al., 1995; Woodhead, 1997). However, these methods are extremely laborious and time consuming. In this study, we compared three commercial RNA extraction kits in order to identify the most effective method of isolating high quality RNA from *Arabidopsis* siliques, seeds, seedlings, rosette leaves and roots. Only the Concert Plant RNA Reagent (Invitrogen, Carlsbad, CA) yielded undegraded RNA from siliques and seeds whereas the RNeasy Plant Mini Kit (Qiagen, Valencia, CA) and the Tri Reagent (Molecular Research Center, Inc., Cincinnati, OH) yielded high quality RNA

from seedlings, rosette leaves and roots but not from seeds and siliques. Although all three methods are fast allowing simultaneous processing of a large number of samples, the Tri Reagent (Molecular Research Center, Inc., Cincinnati, OH) was chosen for real-time PCR assays for all tissues except for siliques and seeds because of the reduced cost and the higher flexibility regarding the amount of tissue used for the RNA extraction.

The kits investigated above claim to allow the isolation of high-quality, DNA-free RNA. However, melting curve analysis of no-template controls indicated that there were unacceptable levels of DNA contamination in all the RNA preparations. Consequently, all the RNA samples were treated with DNase I to remove the contaminating DNA prior to using them for real-time PCR quantitation.

Several housekeeping genes have been used as internal controls for quantitative RT-PCR assays (Bustin, 2000; Giulietti et al., 2001; Dean et al., 2002). In this study we evaluated the suitability of 18S rRNA and adeninephosphoribosyltransfe-rase (*Apt*) abundance for normalization in real-time PCR. The 18S rRNA has been used effectively in many quantitative gene expression studies from various organisms including plants and its levels have been shown to be a constant fraction of total RNA among samples from different tissues or different experimental treatments (Burleigh, 2001; Schmittgen and Zagrajsek, 2001; Hedtke *et al*., 2002). The *Arabidopsis Apt* gene was chosen because it is a single copy, constitutively expressed gene with a low level of expression (Moffatt *et al.,* 1994). In order to find the most appropriate internal control for our quantitative real-time PCR assay, we examined the level of 18S rRNA and *Apt* mRNA in *Arabidopsis* siliques, seeds, 2-day seedlings, 35-day rosette leaves and 5-day roots using the $2^{-\Delta CT}$ method first described by Schmittgen and Zakrajsek (2000). We

found that the levels of *Apt* decreased in seeds compared to the rest of the tissues whereas the levels of 18S rRNA remained relatively constant across all tissues examined (see Table 6 and Figure 5).

When optimizing the SYBR Green real-time PCR for each individual target gene, it is important to confirm the specificity and the efficiency of the amplification. We designed primer sets for forty plastid and nucleus-encoded target mRNAs. Melting curve analysis indicated that high levels of primer dimers were formed in the non-template controls of 25% of the primer sets investigated (10 out of 40 sets of primers). For some genes, avoidance of the primer dimers proved difficult even with several attempts to adjust concentrations and ratios of the primers. Consequently, new sets of primers were designed and examined for the presence of a single melt peak in the respective reactions. The relative amplification efficiencies of the primers selected for the target and housekeeping genes were determined from the slopes of the plots of the log of starting template concentration versus C_T values. The investigated transcripts showed amplification efficiencies in the range 79-100%. It is notable that slopes of plots of log input versus C_T used to determine the efficiency of amplification for the housekeeping genes investigated varied from -3.437 to -3.901 for 18S rRNA (E varies from 1.80 to 2.03) and from -3.601 to -4.026 for *Apt* (E varies from 1.77 to 1.90). Many things can cause this variation. The amplification efficiency of target DNA in different samples has been shown to vary (Meijerink, *et al.,* 2001; Liu and Saint, 2002). In addition, preparation of different dilution series introduces variation. The selected primers for both the target genes and the housekeeping genes were also examined for comparable amplification efficiencies by determining how the ΔC_Ts vary with the log of template dilution. A linear regression line with a slope not significantly different from

zero indicates equal amplification efficiencies between the target gene and the housekeeping gene. We tested all target genes and found that the ΔC_T slopes of the target genes for 18S rRNA varied from -0.08 to 0.18 whereas for *Apt* the ΔC_T slopes varied from -0.24 to 0.42. Thus, 18S rRNA was considered a better choice for use with the $2^{-\Delta\Delta CT}$ method. Table 10 in the Materials and Methods lists the final primer sets used in this study as well as their product lengths.

Many studies have reported that the coefficient of variation (CV) in C_T values of replicate reactions within the same run is usually small ranging from 0% to 5% (Heid *et al*., 1996; Gerard *et al.*, 1998; Winner *et al.,* 1999; Bustin, 2000). However, as Schmittgen and Zakrajsek, (2000) point out, the CV calculated from raw C_T values, which represent exponential terms determined from a log–linear plot of fluorescence signal versus the cycle number does not accurately depict the variation among replicate reactions. Although the standard deviation or CV in C_T produced from replicate amplifications can provide an estimate of reproducibility, a more accurate presentation of the variation in the extent of amplification, which ranges from 10% to 30% (*Heil et al*., 2003), is obtained when the individual C_T values are converted to a linear expression, such as 2^{-CT} (Livak and Schmittgen, 2001). In the present study, the intra-assay precision of replicate amplifications of cDNA serial dilutions for four different genes was investigated using both the raw C_T values and the 2^{-CT} form. When calculated from the raw C_T values, the CV ranged from 0.04% to 0.52% for *trnW-CCA*, 0.06% to 0.34% for *ndhB*, 0.25% to 0.68% for 18S rRNA, and 0.07% to 0.62% for *Apt*; however, when the 2^{-CT} form was used, the CV ranged from 0.73% to 11.6% for *trnW-CCA*, 0.27% to 6.38% for *ndhB*, 2.57% to 6.46% for 18S rRNA, and 1.20% to 10.2% for *Apt*. We also determined the CV in the amounts of *trnW-CCA* and *ndhB* relative to 18S rRNA or *Apt*

calculated from the formula $2^{-\Delta CT}$, which transforms the logarithmic C_T data to linear values. The CV in the case of *trnW-CCA*, and *ndhB* RNAs relative to 18S rRNA was 10.8% and 18.5%, respectively whereas the CV in the case of *trnW-CCA*, and *ndhB* RNAs relative to *Apt* was 20.7% and 30.0%, respectively.

The reproducibility and degree of quantitative variation using SYBR Green I fluorescence in conjunction with the $2^{-\Delta\Delta CT}$ method was also assessed for inter-test experiments with identical cDNA samples as well as different cDNAs obtained from different RNA samples. Although the inter-run variation in the C_T values of the identical cDNA samples was small with a CV_{CT} ranging from 0.36% to 1.90%, when the inter-run mean $2^{-\Delta CT}$ values were computed, the variation was much larger with CV values ranging from 3.18% to 25.77%. When the fold change in RNA abundance between runs was expressed as $2^{-\Delta\Delta CT}$, the fold difference in expression ranged from 1.05X (1.01-1.08) to 1.45X (1.39-1.50). Similar results were obtained for the cDNAs prepared from different RNA samples. Overall our findings indicate that the quantitative real-time PCR assays developed here have an acceptable level of reproducibility and that differences in gene expression levels of ≥ 2-fold can be quantified.

In summary, we have shown that when adequately designed, applied and validated, real-time PCR using SYBR Green I fluorescence dye is a rapid, sensitive, and high throughput method for quantitative measurements of gene expression. In addition, our investigations of accuracy, sensitivity and precision indicate that the $2^{-\Delta\Delta CT}$ method is valid for gene expression comparison and yielded reproducible results for the target genes that were examined in this study.

MATERIALS AND METHODS

Plant Growth

Arabidopsis thaliana ecotype Col-0 seeds were planted in large flats containing Metro-Mix 360 (Scots - Siera Horticultural product Co., Marysville, OH). After a cold treatment at 4^0 C for 48 hours, the seeds were transferred to a controlled environmental chamber and grown at 23^0 C under continuous light (120 μE m^{-2} s^{-1}). White light was obtained from fluorescent light tubes (F72T12/CW; Philips) and incandescent light bulbs (60W; General Electric). *Arabidopsis* plants were watered with 0.5x Hoagland's solution and grown for twenty-three days after which mature rosette leaves were harvested, immediately frozen in liquid nitrogen and stored at -80^0 C until further use.

Arabidopsis seeds were surface sterilized in 95% ethanol for one minute followed by a ten minute incubation in 100% bleach (5.25% sodium hypochlorite-LABBCO, Inc., Houston, TX) + 0.0001% Tween-20. Seeds were washed three times in sterile water and plated on media containing 1x Murashige and Skoog salts and vitamin mixture (Gibco-BRL) 1% sucrose, 0.5 g L-1 2-[N-Morpholino]ethanesulfonic acid (MES) and 0.8% phytagar (Gibco-BRL). The plates were placed at 4^0 C for 48 hours and then transferred to continuous white light (40 μE m^{-2} s^{-1}). Two-day old seedlings, six-day old seedlings, 12-day cotyledons as well as five-day old roots were harvested, frozen in liquid nitrogen and stored at 80^0 C until further use. After fifteen days, some *Arabidopsis* seedlings were transferred to soil whereas others were transferred to fresh plates. Rosette leaves from 35-day old plants as well as siliques from 34-day old plants

transferred to soil after a fifteen-day period of growth on plates were harvested, frozen in liquid nitrogen and stored at 80^0 C until further use.

RNA Isolation and Reverse Transcription

Total RNA from 23-day old leaf tissue was extracted using either the RNeasy Plant Mini Kit (Qiagen, Valencia, CA) with elution for ten minutes in 30 μL RNase-free water (Ambion, Austin, TX) or the Tri Reagent (Molecular Research Center, Inc., Cincinnati, OH) using 1-bromo-3-chloropropane (BCP) as a substitute for chloroform as per manufacturer's instructions (Chomczynski and Mackey, 1995). Total RNA from seeds and siliques was isolated using the Concert Plant RNA Reagent, according to the manufacturer's instructions (Invitrogen, Carlsbad, CA) except that BCP (Molecular Research Center, Inc., Cincinnati, OH) was substituted for chloroform. Total RNA from roots, 2-day old seedlings as well as 35-day old rosette leaves was extracted with Tri Reagent (Molecular Research Center, Inc., Cincinnati, OH) as described above.

Contaminating DNA was removed using either the RNase free DNase (Qiagen, Valencia, CA) with two elutions of five minutes in 30 μL RNase-free water (Ambion, Austin, TX) or the DNA-free DNase I system (Ambion, Austin, TX). The purity of RNA was judged by the A_{260}/A_{280} ratios (1.8-2.0). RNA integrity was assessed by examining the rRNA bands on a standard agarose gel (Sambrook *et al*., 1989). In order to quantify the DNase-treated RNA, the optical density at 260 nm was determined in three different dilutions of the final RNA preparation and the concentration was then calculated.

Constant amounts of 2 μg or 500 ng RNA were reverse-transcribed to cDNA in a total volume of 100 μL and 25 μL, respectively using random hexamer primers and the

TaqMan Reverse Transcription Kit (Applied Biosystems, Foster City, CA). Each 100-μL reaction was prepared as follows: 34.75 μL RNA sample in RNase-free water (Ambion, Austin, TX), 10.0 μL 10X TaqMan RT Buffer, 22.0 μL $MgCl_2$ (5.5 mM), 20.0 μL dNTPs (500 μM each), 5.0 μL random hexamer primers (2.5 μM), 2.0 μL RNase inhibitor (0.4 U/ μL) and 6.25 μL Multiscribe Reverse Transcriptase (3.125 U/ μL). The 25-μL reaction contained 8.68 μL RNA sample in RNase-free water (Ambion, Austin, TX), 2.5 μL 10X TaqMan RT Buffer, 5.5 μL $MgCl_2$ (5.5 mM), 5.0 μL dNTPs (500 μM each) 1.25 μL random hexamer primers (2.5 μM), 0.5 μL RNase inhibitor (0.4 U/ μL) and 1.56 μL Multiscribe Reverse Transcriptase (3.125 U/ μL). After ten-minute incubation at 25^0C to increase primer-RNA template binding, reverse transcription was performed for one hour at 37^0C followed by inactivation of the reverse transcriptase at 95^0C for five minutes. The final volume of each 25-μL RT reaction was brought to 50 μL by the addition of 25 μL of RNase-free water and the cDNA was stored at -80^0C until further use. No-template controls were generated at the same time by combining 2 μg or 500 ng RNA with RNase-free water to a 100-μL or 50-μL final total volume.

The DNase I treatment carried out during the reverse transcription reaction was performed according to the method described by Huang *et al.* (1996). Briefly, 1 U of DNase I (Ambion, Austin, TX) was added to the RT reaction prior to the addition of the RT enzyme. After an incubation period of 30 min at 37^0C followed by heat denaturation of DNase I at 75^0C for 5 min and a 4^0C soak, the Multiscribe Reverse Transcriptase (Applied Biosystems, Foster City, CA) was added and the RT reactions were performed as described above.

Primer Design

All the gene-specific primers were designed using Primer Express® software v2.0 (Applied Biosystems Foster City, CA) according to the software guidelines except for the *trn* and *rps16* primers which were designed with Primer3 program (http://www.genome.wi.mit.edu/cgi-bin/primer/primer3_www.cgi) of the Whitehead Institute (Cambridge, MA, USA). The same guidelines provided by the Primer Express® software were used in the design of all the amplicons. Briefly, primers for each gene target were selected to contain minimal hairpins and primer-dimer formation as determined by the software and having compatible T_m's, each within 1^0-2^0C of the other. In addition, primers were designed to be 15-30 bases in length with a minimum and maximum amplicon size of 59 bp and 150 bp, respectively. All primers were synthesized by IDT (Integrated DNA Technologies, Inc., Coralville, IA) except for the *psbD190*, *psbD550*, *psbDLRP* and *rbcL* primers which were purchased from Applied Biosystems (Foster City, CA). The 18S rRNA primers and probe that produce a 187-bp amplicon were included in the TaqMan rRNA Control Reagents kit (Applied Biosystems, Foster City, CA). In order to verify the specificity of the primers, all primers were used as query sequences in Blast searches of the NCBI database either alone, together with the DNA segment generated by the PCR process or with Ns substituted for the sequence between the primers. A list of the primer sequences that were found to perform well in the real-time PCR reactions is given in Table 10.

Real-time PCR: SYBR Green Detection

PCR reactions were carried out in 384-well optical plates on an ABI Prism 7900HT Sequence Detection System using the 2X SYBR Green PCR Master Mix (Applied Biosystems, Foster City, CA) as recommended by the manufacturer. For each sample, a master mix was generated by combining 3.3 µL of cDNA with 29.7 µL of 2X SYBR Green PCR Master Mix (Applied Biosystems) supplemented with primers to a final concentration of 50 nM each and PCR-grade water to a 33 µL final total volume. This mixture was distributed into three replicates of 10 µL each in 384-well amplification plates and sealed with optical adhesive covers (Applied Biosystems). For each primer pair, a no-template control (NTC) was also run in triplicate. The following amplification parameters were used: 10 minutes at 95^0C for optimal AmpliTaq Gold DNA polymerase activation followed by 47 cycles of denaturation at 96^0C for 10 sec and annealing/extending at 60^0C for 1 min. A dissociation curve was generated according to the protocol present in the ABI Prism 7900HT software (SDS v2.1). Briefly, following the final cycle of the PCR, the reactions were heat denatured over a 35^0C temperature gradient from 60^0 to 95^0C.

Real-time PCR: TaqMan Detection

The master mix for the real-time PCR using TaqMan detection consisted of 3.3 µL of cDNA with 29.7 µL of 2X TaqMan Master Mix (Applied Biosystems) supplemented with primers to a final concentration of 50 nM each, VIC-labeled hybridization probe to a final concentration of 50 nM and PCR-grade water to a 33 µL final total volume. This mixture

was distributed into three replicates of 10 µL each in 384-well amplification plates and sealed with optical adhesive covers (Applied Biosystems). A no-template control (NTC) was also run in triplicate. Real-time PCR was performed identically to that described for SYBR Green detection except that the dissociation curve generation step was omitted.

Real-time PCR: Data Analysis

The data generated from both SYBR Green and TaqMan chemistries were analyzed in a similar manner. The C_T values were determined using a signal/noise ratio set to 10 standard deviations above background subtracted mean fluorescence values (ΔR_n) for a baseline value adjusted manually for each set of primers. The signals of the constitutively expressed ribosomal 18S rRNA and *Apt* (adenine phosphoribosyltrans-ferase) genes were used to normalize against differences in RNA isolation as well as against any possible efficiency difference in the reverse transcription reactions and PCRs. The real-time PCR data containing the C_T values were exported into a Microsoft® Excel spreadsheet for further analysis. The slope was calculated from the plot of log input versus C_T and exponential amplification (efficiency) was determined from the equation $E = 10^{(-1/slope)}$ (Rasmussen, 2001). The amplification efficiencies of the target genes and normalizers were compared by determining the slope from the plot of log template dilution versus $\Delta C_T = (C_{T\ sample} - C_{T\ normalizer})$ according to instructions given by Applied Biosystems (Relative quantitation of gene expression, User Bulletin # 2).

Table 10. Primer sequences.

Gene	Primer sequence[a]	Product Length (bp)
	*Plastid Genes	
rpoA	for 121: CAAGCCGACACAATAGGCATT rev 195: TGCACGTGTAATACATGTTCCTTCT	74
rpoC1	for 1187: GATTGCCTCGCGAAATAGCA rev 1271: CCTATGTTCGAAGCCAGGTGTT	84
rps14	for 201: AAGACCGAGAGCTAACTATCGAGACT rev 279: TGGCAACAAACATGCCTGAA	78
rps15	for 56: CCGTTGAATTTCAAGTATTTAGTTTCACT rev 153: TAGACCCCGCTGAGATAAATAATCTT	97
rps16	for 137: CTTTTTTAAACCTTTCTGCTATTCTCGAT rev 224: CCAGCCTTCTTTGAAATATCATGAG	87
rpl32	for 30: CTCGAAAAAGCGTATTCGTAAA rev 96: AAAAGCTTTCAACGATGTCCA	66

Table 10. (continued).

Gene	Primer sequence[a]	Product Length (bp)
rrn16	for 440: GGGAATAAGCATCGGCTAACTCT rev 509: ATTCCGGATAACGCTTGCAT	69
trnC-GCA	for 5: GCATGGCCGAGTGGTAA rev 67: GGCACCCGGATTTGAAC	62
trnE-UUC	for 3: CCCCCATCGTCtAGTGGTT rev 62: AAGTCGAATCCCCGCTG	59
trnfM-CAU	for 2: GCGGGGTAGAGCAGTTTG rev 66: ACAGGATTTGAACCCGTGAC	64
trnS-GCU	for 17: CGAACCCTCGGTACGATTA rev 88: GGAGAGATGGCTGAGTGGAC	71
trnV-GAC	for 9: AGCTCAGTTAGGTAGAGCACCTC rev 67: ATACGGACTCGAACCGTAGAC	58
trnW-CCA	for 2: CGCTCTTAGTTCAGTTCGGTAG rev 73: ACGCTCTGTAGGATTTGAACC	71

Table 10. (continued).

Gene	Primer sequence[a]	Product Length (bp)
atpA	for 583: GTTTATGTAGCTATTGGTCAAAAAGCTTCT rev 657: CATTGCCCCTCGTTCCTGTA	74
atpB	for 78: CATTGGTCCGGTACTGGATGT rev 143: ACCAGAGCATTGTAAATATTAGGCATT	65
ndhA	for 617: GGAATTTGTGGCGTCAACCTA rev 712: CTTCCGCTTCTGGTAAATCAAAC	95
ndhB	for 377: CTCATCAATGGACTCCTGACGTATA rev 461: GAAGCAGCTACTTTCGAAGTAACAGA	84
ndhF	for 714: TGCTAAATCCGCACAATTTCC rev 798: AGCATGTATAAGACCCGAAATGG	84
ndhJ	for 363: TTATGATAGCCATCCACGACTGAA rev 428: CGTAAAGGCCACCCTATCCAA	65
petA	for 761: AATCCATTAAACTCGATCAACCATTA rev 828: CGCATCCCCCTGACCAA	67

Table 10. (continued).

Gene	Primer sequence[a]	Product Length (bp)
psaA	for 729: TCGGGATCTTTTGGCTCAAC rev 811: CCGAGTATTTTGACCAATTTAAGGTAA	82
psaB	for 657: CCAAGGGTTAGGCCCACTTT rev 753: TCCGGATCCTTGGGAGGTA	96
psaJ	for 22: CTTTCCGTAGCACCGGTACTAAGT rev 116: AATGTTAATGCATCTGGAAATAAACG	94
psbA	for 99: TGGTGTTTTGATGATCCCTACCTTA rev 181: CAATATCTACTGGAGGAGCAGCAA	82
psbD190	for 62: GCGCGAGAAATTAAATCATAAACA rev 167: TCAACCATTTCCGAACACCTT	105
psbD550	for 235: TCTGAATAATGAGTCATCCGACA rev 325: ACTCAATTTGTTTCTTCCTTGCT	90
psbDLRP	for 238: GCAAAGTAATAACTAAAAGGGCGTTT rev 378: TTGATATCTGAAGCCATGATTATGATTC	140

Table 10. (continued).

Gene	Primer sequence[a]	Product Length (bp)
rbcL	for 1009: GGAGACAGGGAGTCAACTTTG rev 1083: ACCGCGGCTTCGATCTTT	74
accD	for 801: TCCGGGTACTTGGAATCCTATG rev 879: ATAAGGTTCCTCCTTCGAATGAAAT	78
clpP	for 261: GCGACCCGATGTACAGACAA rev 329: CCTCCGACTAGGATAAAGGATGCT	68

Nuclear Genes

Gene	Primer sequence[a]	Product Length (bp)
[b]*Apt*	for 305: CCATGAGGAAGCCCAAGAAG rev 382: CAATCGTATCTGTTCCATACTCCAA	77
[c]*Lhca 1*	for 135: GGCATAGCCGCCGTGTAC rev 201: GAACTCCGGCGGATACGAAT	66
[d]*Lhcb 1.2*	for 615: GGCTTTCGCGGAGTTGAAG rev 690: AACGAAGAATCCAAACATAGAGAACATA	66

Table 10. (continued).

Gene	Primer sequence[a]	Product Length (bp)
[e]*RbcS*	for 336: CACTCCCGGATACTACGATGGA rev 404: GAGTCGGTGCATCCGAACA	68
[f]*PetH*	for 1204: AGGAAGCCTCTGAGGGAGTAATTATAT rev 1334: GAATTGATGCTCTCTTTTGAATGTTT	130
[g]*RpoT;1*	for 2758: GGTGTTGACTCTAAGCCGTGAGA rev 2830: AAAATTTGGTGCAAAAGCAGTCAT	73
[h]*RpoT;2*	for 1632: TCATGGAGCCAAGCAACAAAG rev 1715: AGCGTATCCAGGGCCTCAA	83
[i]*RpoT;3*	for 3051: TAGCACCAGTGAACCATCTGAAG rev 3124: GTTATTTACAGGCCACCAAGGAA	74

[a] Primers were designed using the Primer Express® v2.0 package (Applied Biosystems, Foster City, CA, USA) except for the *trn* and *rps16* primers which were designed with the Web-based Primer3 program.(http://www.genome.wi.mit.edu/cgi-bin/primer/primer3_www.cgi). All amplicons were designed following the same guidelines provided by the Primer Express® software (T_m, 58 -60^0 C; maximum product length, 150 bp; minimum product length, 59 bp). for = forward; rev = reverse

[*] GenBank acc.no. : AP00043
[b] GenBank acc.no. : AY128377
[c] GenBank acc.no. : M85150
[d] GenBank acc.no. : X03908
[e] GenBank acc.no. : AY64686
[f] GenBank acc.no. : AJ243705
[g] GenBank acc.no. : Y08137
[h] GenBank acc.no. : AJ278248
[l] GenBank acc.no. : Y08463

CHAPTER III

REAL-TIME PCR ANALYSIS OF THE RNA LEVELS OF PLASTID-ENCODED GENES IN DIFFERENT TISSUES AND STAGES OF *Arabidopsis thaliana* DEVELOPMENT

INTRODUCTION

Plant tissues possess a set of semi-autonomous, DNA-containing organelles, collectively referred as plastids. Plastids as well as mitochondria are thought to have originated from a free-living eubacterial ancestor that entered an endosymbiotic relationship with a host cell (reviewed in Gray, 1999; McFadden, 1999). Plastids carry out a number of metabolic processes including photosynthesis as well as steps in the synthesis of compounds such as amino acids, starch, lipids, pyrimidines, terpenoids, tetrapyrroles, and plant hormones (reviewed in Beale, 1984; Gibbs, 1971; Goowin, 1971; Kirk, 1978a). Plastid-synthesized compounds are utilized by plastids during organelle development and serve critical cellular functions during embryo development, seed germination and post-germinative growth (Apuya *et al.,* 2001). In wild-type plants, nearly every cell type possesses its special type of plastid and all the plastids within a given plant contain identical genomes. These different forms of plastids include proplastids in the meristematic tissues of the shoot and root, etioplasts in etiolated seedlings, amyloplasts in the differentiated cells of the roots as well as in the cotyledons, endosperm and tubers, chloroplasts in leaves and cotyledons, and chromoplasts in fruits and flowers (Kirk, 1978b; Thomson and Whatley, 1980).

The plastid genome of higher plants, also known as plastome, is highly conserved across species and consists of multiple (22-900 copies per plastid) DNA molecules (Bendich, 1987) ranging in size from 120 to 220 kb (reviewed in Mache and Mache-L, 2001; Odintsova and Yurina, 2003). A physical feature common to almost all plastomes is the an inverted repeat (IR) region which separates the remainder of the genome into a small single copy (SSC) region and a large single copy (LSC) region. The inverted repeats contain mainly 23S and 16SrRNA genes and account for most of the size variation in plastid genomes among different plant species (reviewed in Palmer, 1985). The complete sequencing of the plastid genomes from twelve land plants has revealed that the general coding content and gene order is highly conserved among the plastid genomes (reviewed in De Las Rivas *et al.,* 2002; Odintsova and Yurina, 2003).

The plastome contains over 120 genes (reviewed in Igloi and Kössel, 1992; Gruissem and Tonkyn, 1993; Mullet, 1993) that can be classified into three major groups: (1) genes involved in transcription and translation encoding rRNAs (16S, 23S, 4.5S, 5S), tRNAs (~ 30 *trn* genes), protein subunits of the prokaryotic plastid RNA polymerase core-enzyme (*rpoA, rpoB, rpoC1, rpoC2*) and ribosomes (12 *rps* and 9 *rpl* genes); (2) genes involved in electron transport and photosynthesis encoding components of photosystem I (*psaA, B, C, I, J*), photosystem II (*psbA, B, C, D, E, F, H, I, J, k, L, M, N, T*), cytochrome b6/f complex *(petA, B, D, G*), ATP synthase (*atpA, B, E, F, H, I*), NADH oxido-reductase (ndhA, B, C, D, E, F, G, H, I, J, K), large subunit of ribulose-1,5-biphosphate carboxylase, Rubisco (*rbcL*); and (3) genes related to biosynthetic processes encoding a subunit of the prokaryotic-type acetyl-CoA carboxylase (*accD*), a subunit of an ATP-dependent protease (*clpP*) as well as several

open reading frames designated *ycf* for hypothetical chloroplast open reading frame encoding proteins with unknown function (Sugiura, 1992; Gruissem and Tonkyn, 1993).

Genetic and biochemical studies have shown that regulation of plastid gene expression is complex (reviewed in Gruissem and Tonkyn, 1993). A large number of plastid genes are organized in polycistronic transcription units. Plastid RNAs undergo extensive processing giving rise to complex mRNA patterns (Barkan, 1988; Westhoff and Herman, 1988; Mullet, 1993). RNA processing includes intron splicing, intercistronic cleavage, RNA editing, as well as 5′ and 3′ end trimming (reviewed in Monde et al., 2000). In addition, the presence of multiple transcription initiation sites within a transcription unit adds to the complexity of plastid mRNA populations and contributes to the variation in transcript ratios generated from polycistronic transcription units (Yao *et al*., 1989; Sexton *et al.,* 1990; Haley and Bogorad; 1990; Christopher *et al*., 1992; Kapoor *et al*., 1994; Hoffer and Christopher, 1997).

Regulation of plastid gene expression occurs at several levels including transcription, RNA processing, turn-over and translation. Transcription activity varies from one gene to another and in response to developmental and environmental cues such as light. The steady-state mRNA levels of different plastid genes during one stage of chloroplast development vary over 1000-fold and transcription rates for the same genes vary over 300-fold (Rapp *et al.,* 1992; Baumgartner *et al.,* 1993). Furthermore, a 30-fold variation in mRNA stability has been observed (Rapp et al., 1992). It is well established that expression of many plastid genes is regulated by light. Examples of the effects of light and the developmental state on the activity of plastid promoters include the *psbA* promoter and the blue-light regulated promoter (LRP) of the *psbD-psbC* operon (Sexton *et al.,* 1990; Kim and Mullet, 1995; Kim *et al.*, 1999; Allison and Maliga,

1995; Christopher *et al.,* 1992; Hoffer and Christopher, 1997; Satoh *et al.,* 1997; reviewed in Link, 1988; 1996; Klein and Mullet, 1990). In mature leaves, illumination increases the overall rate of chloroplast transcription and differentially activates transcription from *psbA* and *psbD* (Christopher and Mullet, 1994). The *psbD* gene, encoding the D2 reaction center protein of photosystem II, is located in a complex operon that contains two additional photosystem II protein genes, *psbC*, encoding the CP43 antenna protein and *psbZ*, encoding a 6.5 kDa protein (Vermaas and Ikeuchi, 1991; Swiatek *et al.,* 2001). Transcription from the *psbD-psbC* operon is driven from at least three different promoters (Sexton *et al.,* 1990). During chloroplast development transcription from a blue-light responsive promoter (*psbD-LRP*) is differentially activated when plants are illuminated by high-fluence blue light (Christopher and Mullet, 1994; Gamble and Mullet, 1989). As chloroplasts mature, the blue-light induced transcripts become the most abundant *psbD* transcripts (Christopher and Mullet, 1994). Plastid gene expression is also regulated through redox signals generated by plastoquinone (Pfannschmidt *et al.,* 1999), thioredoxin (Danon and Mayfield, 1994), and the cytochrome *b6/f* complex (Alfonso *et al.,* 2000; Pearson *et al*., 1993). For example, expression of the *psaA/B* genes, encoding the reaction center apoproteins of Photosystem I is transcriptionally regulated via redox signals generated through plastoquinone (Pfannschmidt *et al.,* 1999; reviewed in Surpin *et al.,* 2002). Expression of *psbA*, encoding the D1 polypeptide of Photosystem II, *psbD-LRP* encoding the D2 protein of Photosystem II, and *rbcL*, encoding the large subunit of Rubisco is also sensitive to redox signals (Pfannschmidt *et al.,* 1999; Thum, 2000). Superimposed upon the light and redox regulation of the *psbD-LRP* promoter is additional control by endogenous circadian rhythms (Nakahira, 1998) as well as by various environmental

stresses such as low temperature, high light, salt, and osmotic conditions (Nagashima *et al*., 2004).

Plant development and organ formation are connected to the transformation of proplastids found in embryonic and meristematic tissues into photosynthetically competent chloroplasts in cotyledons or leaves and into amyloplasts in roots with the other various types of specialized plastids being derived either from proplastids or from photosynthetically active chloroplasts (see Figure 4 in Chapter I). This differentiation process is accompanied by dramatic morphological and molecular changes. For instance, differentiation of proplastids or etioplasts into chloroplasts involves rapid accumulation of chlorophyll, photosynthetic membranes, and the associated photosynthetic proteins with profound changes in plastid gene expression (reviewed in Gruissem, 1989; Gruissem and Tonkyn, 1993). Overall plastid transcription rates and mRNA levels, which are low in proplastids, increase dramatically during the early stages of chloroplast development and are followed by a decline during the late stages of chloroplast maturation (Baumgartner *et al.,* 1989). In addition, plastid genes encoding the plastid transcription and translation apparatus are activated early in chloroplast development whereas genes required for photosynthesis are expressed at higher levels later in development (Baumgartner *et al.,* 1993; DuBell and Mullet, 1995). In contrast, during fruit ripening, the chloroplasts differentiate into non-photosynthetic chromoplasts with concomitant degradation of the thylakoid system and a reduction in chloroplast gene transcription (reviewed in Marano *et al*., 1993). In root amyloplasts of *Arabidopsis*, transcription of the photosynthetic genes *atpB/E*, *psbA* and *rbcL* is repressed although low levels of 16S rRNA are detected (Isono *et al.,* 1997a). Differential promoter usage has been documented for the spinach and *Arabidopsis rrn16* Pc promoter. In spinach,

this promoter is active in leaf and cotyledon plastids but not in root plastids (Iratni *et al.,* 1997) whereas in *Arabidopsis*, Pc is active in roots and leaves but not in cotyledons (Sriraman *et al.,* 1998b). In addition, *psbD-LRP* was not highly expressed in cotyledons of light-grown or etiolated wild-type *Arabidopsis* seedlings. It was proposed that a key activator of *psbD-LRP* that was present in developing leaves was absent in cotyledons of light-grown seedlings (Christopher and Hoffer, 1998).

Despite extensive studies, an understanding of the regulation of gene expression in plastids of higher plants is far from complete. Because of their role in photosynthesis, chloroplasts are by far the best studied of the various plant plastid types. Most of the previous research efforts have focused on characterizing the changes in gene expression that occur in leaves of monocotyledonous plants during leaf and chloroplasts development whereas less is known about gene expression in plastids present in other plant organs. Furthermore, only a limited number of such studies have been performed in dicotyledonous plants (Degenhardt *et al*., 1991; Harak *et al*., 1995; Isono *et al*., 1997a). Therefore, we used the model plant *Arabidopsis thaliana* to analyze plastid RNA levels in various organs and stages of development. The dicot *Arabidopsis thaliana* has become a preferred species for the study of the biology of the flowering plants mainly because of its short generation cycle, complete gene sequence and the availability of well-defined mutants (reviewed in Meyerowitz, 1989). Furthermore, the availability of a large collection of T-DNA insertion lines provides the basis for more detailed analysis of plastid development.

In the present study, we monitored the steady-state mRNA levels of twenty-eight plastid genes in different tissues and developmental stages of the dicotyledonous plant *Arabidopsis thaliana* using real-time PCR. To determine the temporal and spatial

activation of plastid gene expression as a function of developmental stage we assessed the RNA levels of genes belonging to a diverse array of plastid functions and operons in tissues containing proplastids, leucoplasts as well as chloroplasts at different stages of development.

RESULTS

Experimental Design

Plastid gene expression studies have relied heavily on measurements of mRNA steady-state levels using Northern blotting. However, this technique is laborious and requires relatively large amounts of starting RNA. In addition, its low sensitivity makes it unsuitable for detection of low abundance mRNAs. Therefore, in the present study we employed the highly sensitive method of quantitative real-time PCR. Based on the sequence of *Arabidopsis thaliana* chloroplast DNA (Sato *et al*., 1995) primer pairs were designed for twenty-eight plastid target genes using the Primer Express® software v2.0 (Applied Biosystems Foster City, CA) according to the software guidelines or the Primer3 program (http://www.genome.wi.mit.edu/cgi-bin/-primer/primer3_www.cgi) of the Whitehead Institute (Cambridge, MA, USA). The same guidelines provided by the Primer Express® software were used to design all of the amplicons. In addition, all primers were designed with a melting temperature (T_m) of 58-60^{0}C to allow the use of identical temperature cycle conditions for PCR amplification. In order to verify the specificity of the primers, the designed primer sets were used as query sequences in Blast searches of the NCBI database either alone, together with the DNA segment

generated by the PCR process or with N's substituted for the sequence between the primers. To correct for differences in input RNA, all quantifications were normalized to the amount of cytoplasmic 18S rRNA and expressed as $2^{-\Delta CT}$, where $\Delta C_T = (C_{T\ sample}-C_{T\ normalizer})$ based on the method outlined by Schmittgen and Zakrajsek (2000) and Livak and Schmittgen (2001). Real-time PCR reactions for each set of primers were performed in triplicate along with non-template control reactions and the specificity of the RT-PCR products was verified by both electorophoretic and melting curve analysis. In addition, all primer sets were tested for comparable amplification efficiencies with the endogenous reference primers by plotting the ΔC_T value against the log cDNA input. Only primer sets that showed little variation over the dilution series were employed for quantification of mRNA levels (see Table 7 and Figures 8 & 9 in Chapter II).

Quantitative analysis of RNA levels was performed on plastid genes encompassing a range of functional groups and operons (see Table 11 for a list of genes and operons analyzed in this study). These genes include: (1) four genes encoding 30s and 50s ribosomal subunits, (2) one gene encoding 16S rRNA, (3) six genes for tRNAs, (4) two genes encoding subunits of the plastid RNA polymerase, (5) two genes encoding subunits of the ATP synthase complex, (6) one gene encoding a component of the cytochrome *b6/f* complex, (7) four genes encoding components of the NADH dehydrogenase complex, (8) six genes encoding components of photosystem I, photosystem II and Rubisco, (9) one gene encoding for a protein involved in lipid biosynthesis, and (10) one gene encoding for an enzyme involved in protein degradation. Among the protein coding genes analyzed, *psbA*, encoding the D1 reaction center protein of PSII, *rbcL*, encoding the large subunit of Rubisco, *ndhF* encoding a subunit of the NADH dehydrogenase complex, *rps15* and *rps16* encoding

30s ribosomal proteins as well as *rpl32*, encoding a 50s ribosomal protein are known to be transcribed monocistronically (Matsubayashi *et al.,* 1987; Vera *et al*., 1992; reviewed in Shinozaki *et al.,* 1986; Sugiura *et al*., 1998). In addition, all the tRNAs analyzed in this study are transcribed independently except *trnE-UUC* which is transcribed as a tricistronic precursor (consisting of *trnE-UUC-trnY-GUA-trnD-GUC*) and *trnW-CCA* which is likely co-transcribed with *trnP-UGG* (Ohme *et al*., 1985; Kanno and Hirai, 1993; Sugita and Sugiura, 1996). The remaining genes belong to either heterogeneous or homogeneous gene clusters that are transcribed polycistronically and are subsequently processed to generate mature RNAs (reviewed in Gruissem and Tonkyn, 1993; Kanno and Hirai, 1993; Sugita and Sugiura, 1996; Sugiura *et al*., 1998). Except for *psbD*, the primers did not distinguish between the various transcripts generated from a given operon. The *psbD* operon, which includes the *psbD*, *psbC* and *psbZ* genes encoding PSII components, has been shown to have multiple promoter elements giving rise to a complex set of transcripts. At least four *psbD* mRNA 5′-ends, located at positions 190, 256, 550 and 950 with respect to the translation initiation site have been reported (Hoffer and Christopher, 1997; Christopher and Hoffer, 1998; Hanaoka *et a*l., 2003).

Table 11. List of plastid genes analyzed in this study (parentheses indicate well-defined transcription units)

Transcription and translation apparatus

Gene	Product	Gene Organization and Transcription Units
rpoA	β subunit of PEP	*(trnI-CAU-rpl23-rpl2-rps19-rpl22-rps3-rpl16-rpl14-rps8-rpl36-rps11-rpoA)*
rpoC1	β´ subunit of PEP	*(rpoB-rpoC1-rpoC2)*
rps14	30s ribosomal protein CS14	*(ycf3-psaA-psaB-rps14)*
rps15	30s ribosomal protein CS15	*ycf1-(rps15)*
rps16	30s ribosomal protein CS16	*trnQ-UUG(-rps16)-trnK 5´-matK-trnK 3-(psbA)-trnH-GUC*
rpl32	50S ribosomal protein CL32	*(rpl32)-trnL-UAG-ycf5*
rrn16	16S rRNA	*trnV-GAC-(rrn16-trnI-GAU-trnA-UGC-23S-4.5S-5S)*
trnC-GCA	Cys-tRNA (GCA)	*trnC-GCA-ycf6*
trnE-UUC	Glu-tRNA (UUC)	*(trnE-UUC-trnY-GUA-trnD-GUC)*
trnfM-CAU	fMet-tRNA (CAU)	*(ycf3- psaA-psaB-rps14)-trnfM-CAU*
trnS-GCU	Ser-tRNA-GCU	*trnS-GCU*
trnV-GAC	Val-tRNA (GAC)	*trnV-GAC-(rrn16-trnI-GAU-trnA-UGC-23S-4.5S-5S)*

Table 11. (continued).

Gene	Product	Gene Organization and Transcription Units
trnW-CCA	Trp-tRNA (CCA)	*trnP-UGG-trnW-CCA*
NADH dehydrogenase complex		
ndhA	NADH dehydrogenase subunit ND1	*(ndhH,A,I,G,E-psaC-ndhD)*
ndhB	NADH dehydrogenase subunit ND2	*(rps12-rps7-ndhB)*
ndhF	NADH dehydrogenase subunit ND5	*(ndhF)*
ndhJ	NADH dehydrogenase subunit 30 k-Da protein	*(atpB-atpE) -trnV-UAC-(ndhC-ndhK-ndhJ)*
ATP synthase complex		
atpA	ATP synthase complex Cf1 subunits, α	*(rps2-atpI-atpH-atpF-atpA)*
atpB	ATP synthase complex Cf1 subunits, β	*(atpB-atpE) -trnV-UAC-(ndhC-ndhK-ndhJ)*
Cytochrome *b6/f* complex		
petA	Cytochrome b_6/f complex Cytochrome f	* *((rbcL)-(accD-psaI-ycf4-cemA-petA))*
Photosystem I and II		
psaA	PSI –P700 apoprotein A1	*(ycf3-psaA-psaB-rps14)*

Table 11. (continued).

Gene	Product	Gene Organization and Transcription Units
psaB	PSI –P700 apoprotein A2	*(ycf3-psaA-psaB-rps14)*
psaJ	PSI 5-kDa protein	*(petL-petG-psaJ-rpl33-rps18)*
psbA	PSII protein D1	**trnQ-UUG-(rps16)-(trnK-UUU5´-matK trnK-UUU35´-(psbA))-trnH-GUC*
psbD190	PSII protein D2	*(psbD-psbC-psbZ)-trnG-GCC*
psbDLRP	PSII protein D2	*(psbD-psbC-psbZ)-trnG-GCC*
Rubisco		
rbcL	Rubisco large subunit	** ((rbcL)) - (accD-psaI-ycf4-cemA-petA))*
Plastid genes encoding components involved in other metabolic processes		
accD	ACCase-β carboxytransferase subunit	** ((rbcL)- (accD-psaI-ycf4-cemA-petA))*
clpP	Clp protease-ClpP1 catalytic subunit	*(clpP-rps12-rpl20)*

* Crossland *et al.,* 1984; Poulsen, 1984; Stern and Gruissem, 1987; Nickelsen and Link, 1991; Staub and Maliga; 1995; Meurer *et al.,* 1998

The best characterized of these promoters is the blue-light regulated promoter (LRP), which is located the furthest upstream of the multiple promoters and has been shown to produce an mRNA that originates at the -950 position (Hoffer and Christopher, 1997). Because *psbD* transcripts have been shown to exhibit differential patterns of accumulation, we designed one primer set that specifically detects the transcript driven by *psbD-LRP* whereas a second set of primers was used to monitor the levels of all transcripts carrying *psbD* coding sequences.

Tissues and Plastid Transcripts Analyzed

Plastid mRNA abundance from several tissues and different developmental stages was monitored by real-time PCR (Figure 10). Transcript levels for twenty-eight plastid genes (see Table 11) were quantified in dry seeds, 2-day seedlings, 5-day seedlings, 5-day roots, 40-day roots and 34-day siliques. In addition, the levels of mRNAs for a subset of plastid genes (*rpoA*, *rrn16*, *rbcL*, *psbA*, and *psbD*) were examined in 10-day, 12-day and 15-day cotyledons, as well as in 35-day rosette leaves and 35-day cauline leaves.

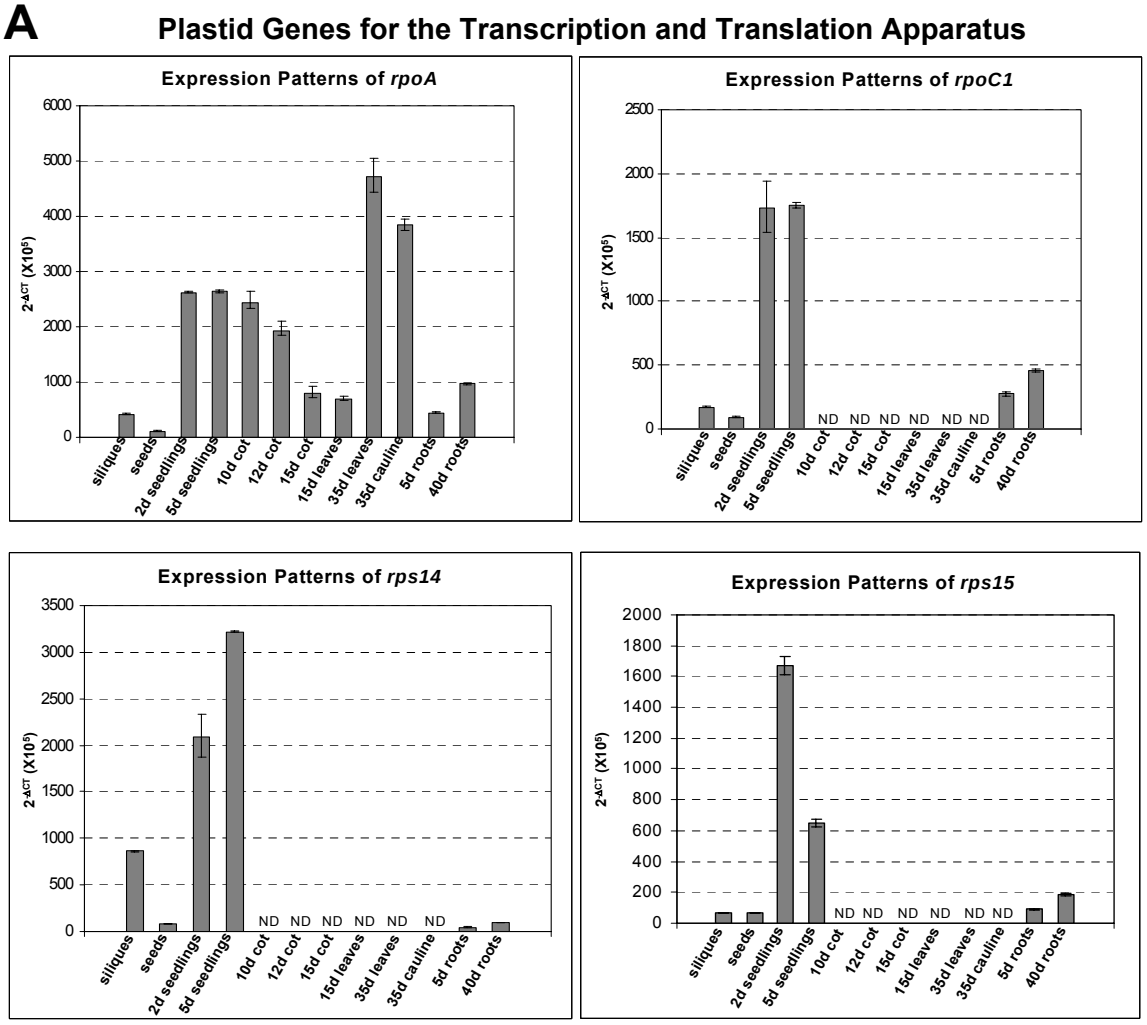

Figure 10. Abundance of plastid gene mRNA in various tissues.

Total RNA was isolated from siliques, seeds, 2-day seedlings, 5-day seedlings, 5-day roots, 40-day roots, 10-day cotyledons, 12-day cotyledons, 15-day cotyledons and 15-day rosette leaves of *A. thaliana* seedlings grown on MS medium supplemented with 1% sucrose as well as from 35-day rosette leaves and 35-day cauline leaves of *Arabidopsis* plants grown on soil after a 15-day period of growth on MS medium containing 1% sucrose. Equivalent amounts of total RNA were converted to cDNA and assayed for plastid mRNA abundance by real-time PCR. Reactions were run in triplicate and data were normalized relative to cytoplasmic 18S rRNA levels and expressed as $2^{-\Delta CT}$ X10^5, where ΔCT = ($C_{T\ sample}$-$C_{T\ normalizer}$).

(A) mRNA abundance of plastid genes encoding the transcription and translation apparatus.
(B) mRNA abundance of plastid genes encoding components of the NADH dehydrogenase complex.
(C) mRNA abundance of plastid genes encoding components of the ATP synthase and cytochrome *b6/f* complexes.
(D) mRNA abundance of plastid genes encoding components of photoststem I, photosystem II and RUBISCO.
(E) mRNA abundance of plastid genes encoding components involved in other metabolic processes.

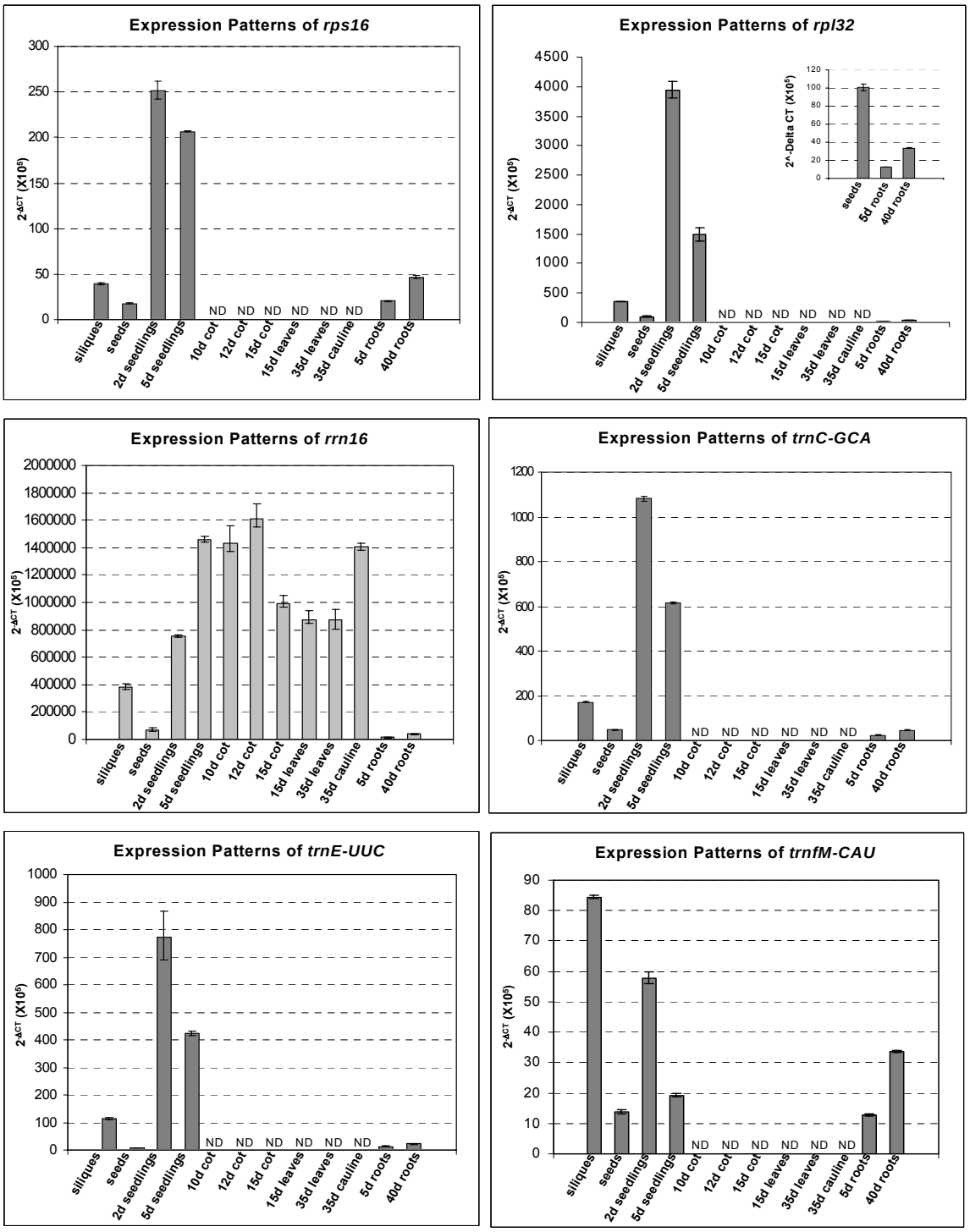

Figure 10. (continued).

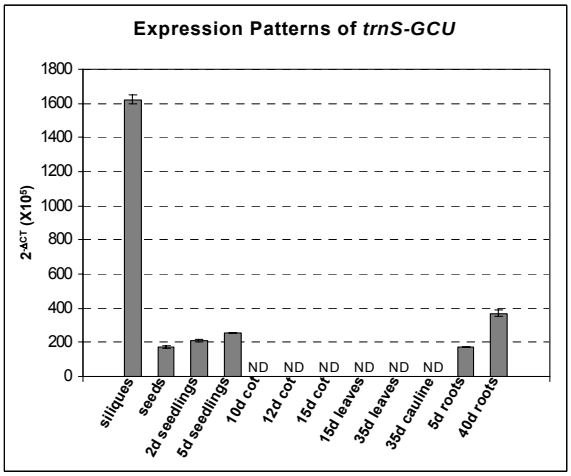

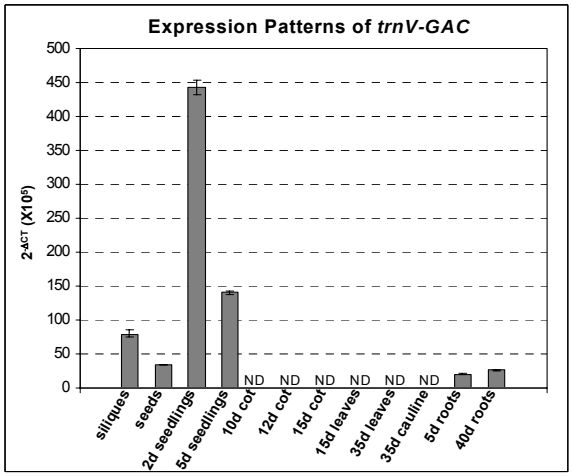

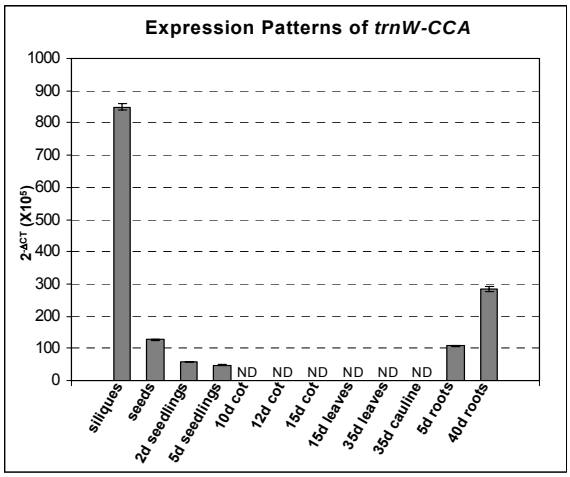

B **Plastid Genes for the NADH Dehydrogenase Complex**

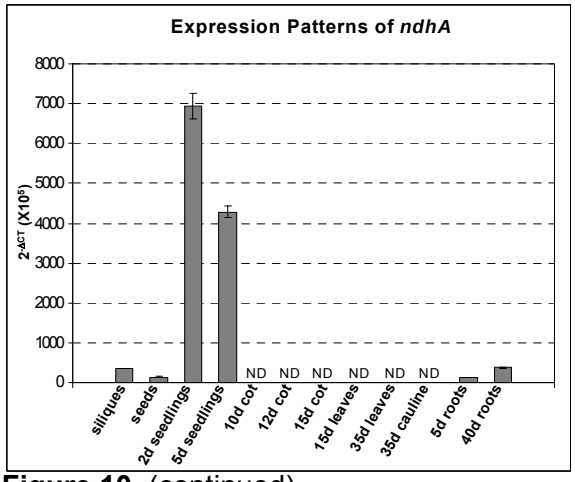

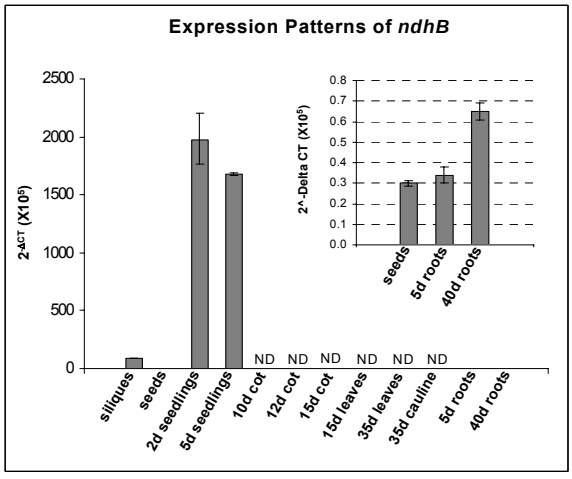

Figure 10. (continued).

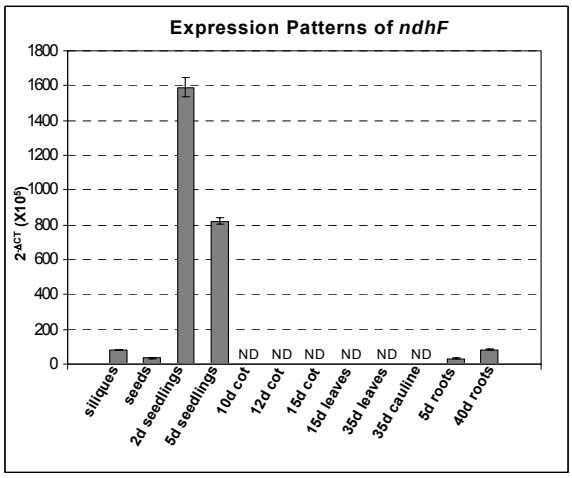

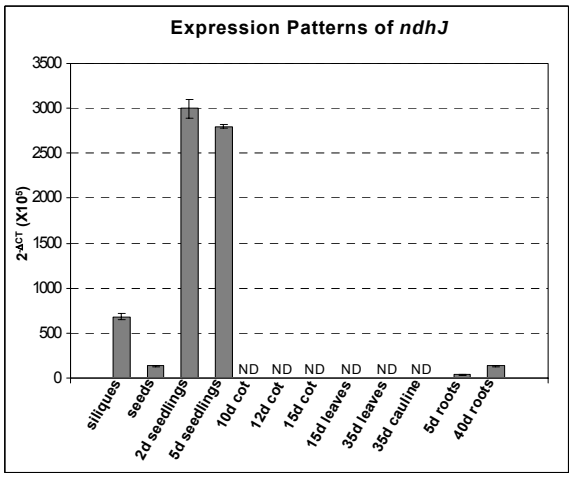

C Plastid Genes for the ATP Synthase and Cytochrome *b6/f* Complexes

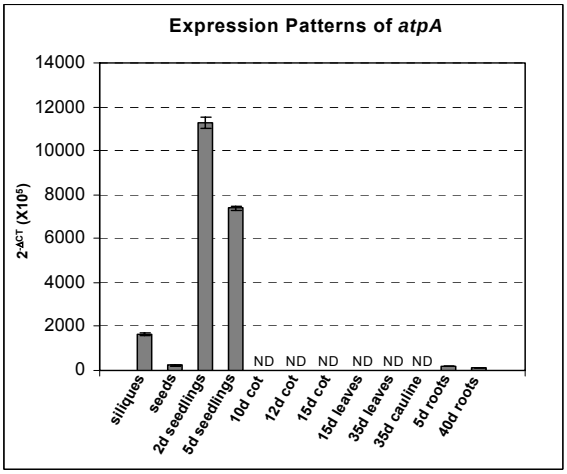

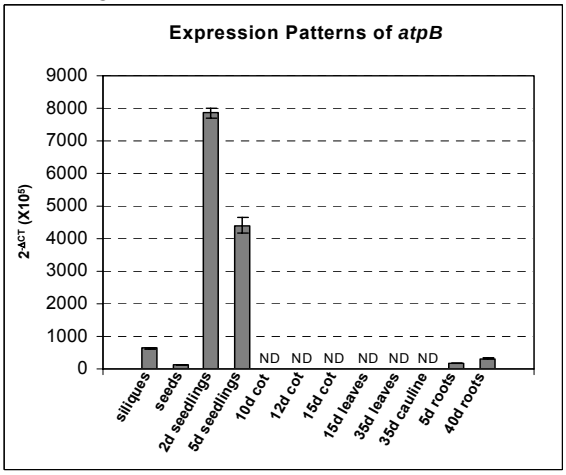

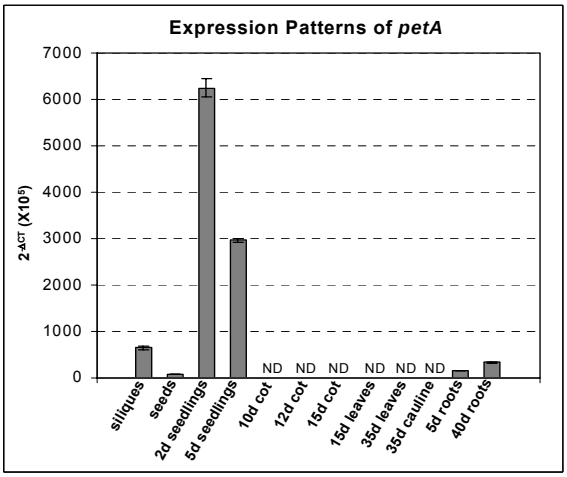

Figure 10. (continued).

D **Plastid Genes for the Photosystem I, Photosystem II and Rubisco**

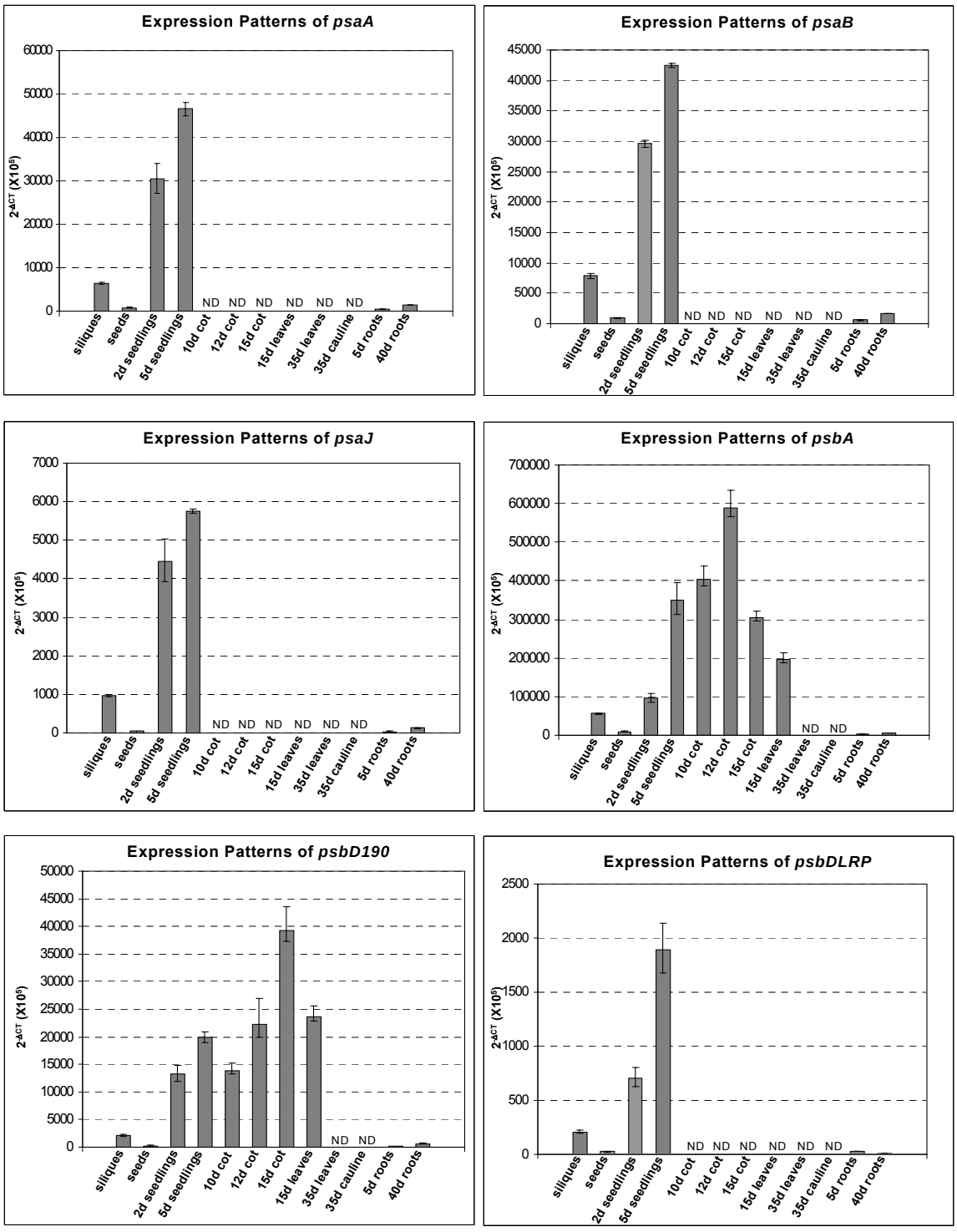

Figure 10. (continued).

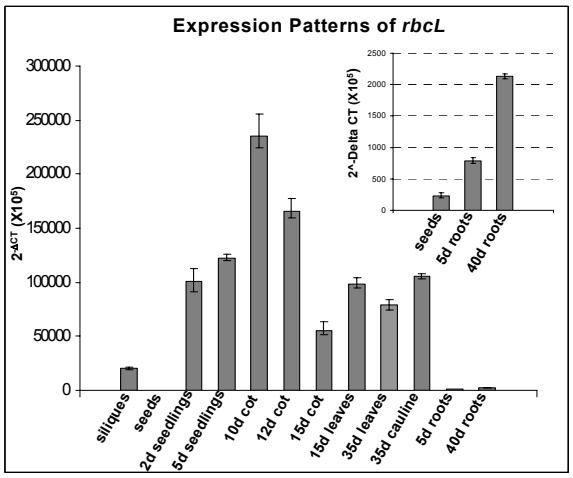

E **Plastid Genes for Other Metabolic Processes**

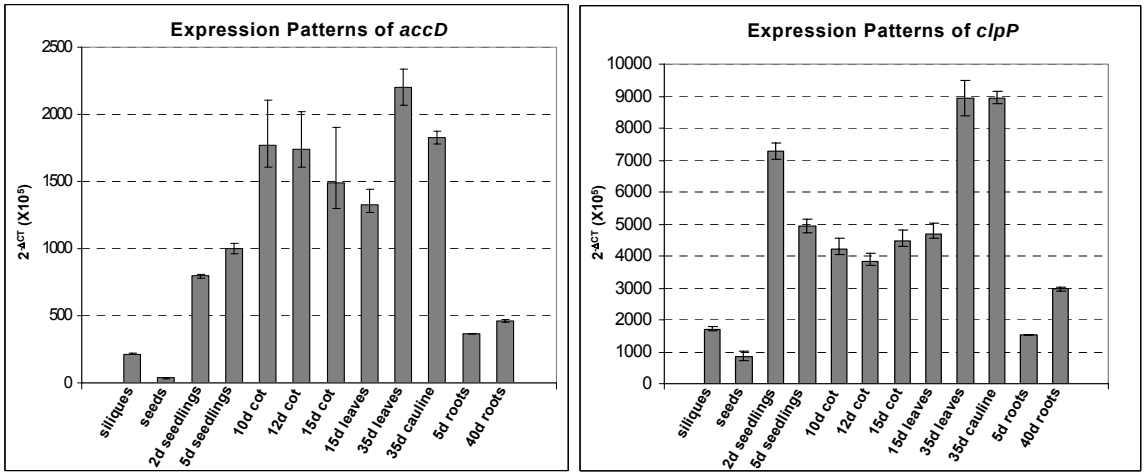

Figure 10. (continued).

Plastid Transcript Accumulation during Plant Development

We monitored the RNA levels of twenty-eight plastid gene during four key developmental stages of *Arabidopsis thaliana* by real-time PCR. The developmental stages examined constitute a developmental progression starting with seed formation

and maturation through the early stages of seedling establishment (Figure 11). To identify possible groups of co-regulated genes, we clustered the expression profiles for siliques, seeds, 2-day seedlings and 5-day seedlings based on the kinetics of transcript accumulation through the four stages of development. Based on our previous study on intra- and inter-assay precision of the real time PCR assay (see Chapter II), >1.5-fold differences in transcript abundance were considered significant. The analysis identified three main groups of co-regulated genes (Figure 12). Cluster I consists of three tRNAs (*trnfM-CAU*, *trnS-GCU* and *trnW-CCA*) that are highly expressed in siliques (~6-, 10-, and 7-fold greater than mature seeds, respectively) but are either moderately induced in 2-day and 5-day seedlings relative to seeds (*trnfM-CAU* and *trnS-GCU*) or show reduced transcript levels in 2-day and 5-day seedlings relative to seeds (*trnW-CCA*). Cluster II (A and B) includes genes encoding components of the plastid transcription and translation apparatus (*rpoA*, *rpoC*, *rps15*, *rps16*, *rpl32*, *trnC-GCA*, *trnE-UUC*, *trnV-GAC*), genes encoding for subunits of the plastid ATP synthase complex (*atpA* and *atpB*), genes encoding for subunits of the plastid NADH dehydrogenase complex (*ndhA*, *B*, *F*, *J*), one gene encoding a component of the cytochrome *b6/f* complex (*petA*), one gene encoding a subunit of the plastid acetyl-CoA carboxylase (*accD*) and one gene encoding the proteolytic subunit of an ATP-dependent plastid protease (*clpP*). Cluster II is characterized by relatively low expression in siliques and seeds, high transcript

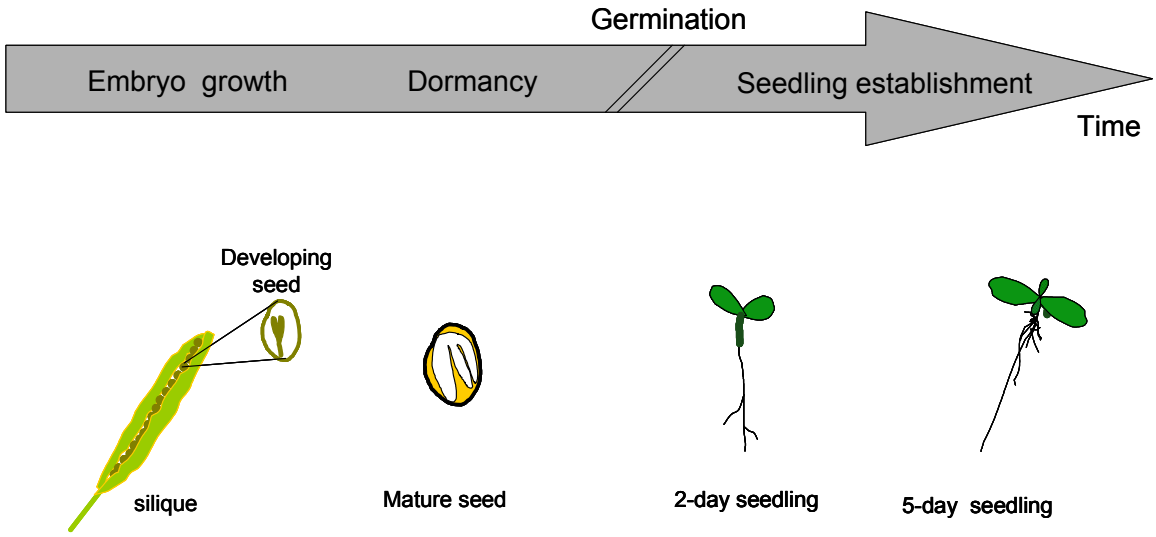

Figure 11. Schematic representation of the chronological progression of selected developmental stages in the life cycle of *Arabidopsis thaliana*

Seed development consists of the embryo development and seed maturation phases. During the growth phase, the body plan of the mature embryo is established with the axis or hypocotyl-radicle region and the cotyledons. During the seed maturation phase, the embryo growth arrests while food reserves accumulate and the seed containing a full size embryo enters a metabolically quiescent state of dormancy. Upon germination, embryo arrest is reversed while stored reserves are mobilized to provide a source of energy for the growing seedling (Bewley, 1997; Raz *et al*. 2001). Plastids play a significant role during embryo development by synthesizing products for the developing embryo and during germination when photosynthetically active chloroplasts function as an energy source for seedling establishment and development.

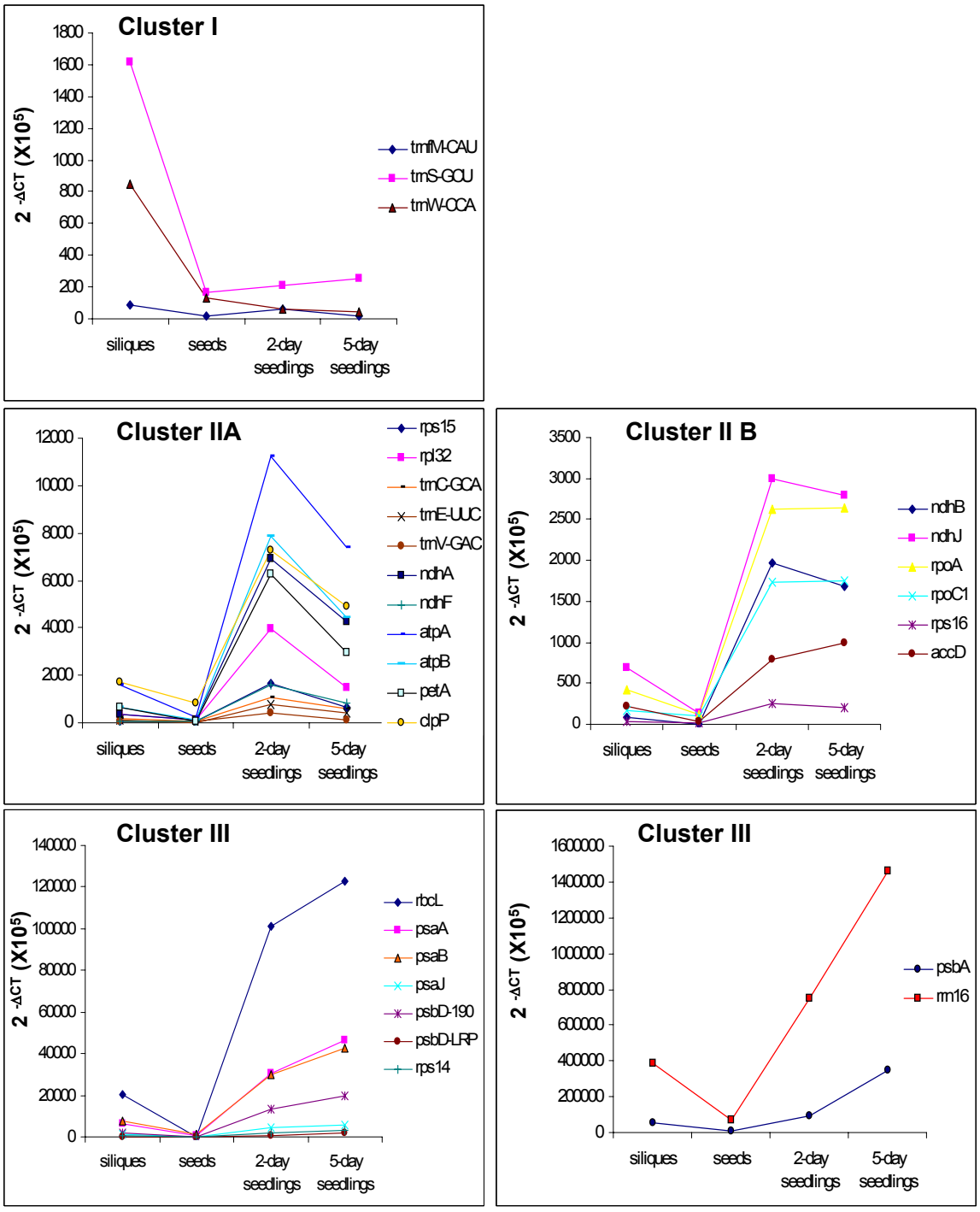

Figure 12. The three main clusters of plastid expression patterns

Arabidopsis siliques, seeds, 2-day seedlings and 5-day seedlings were assayed for plastid mRNA abundance by real-time PCR. Equivalent amounts of DNase treated total RNA from each tissue were reverse transcribed and employed as template for real-time PCR analysis. Quantitative PCRs were performed in triplicate with a cDNA input corresponding to 10 ng of reverse transcribed total RNA. Cytosolic 18S rRNA amplification levels were used for the normalization of the real-time PCR data. The normalized given values are expressed as $2^{-\Delta CT} \times 10^5$, where ΔC_T ($C_{T\ sample} - C_{T\ normalizer}$).

abundance at the 2-day seedling stage followed by either a steep (Cluster IIA) or a moderate decline/increase (Cluster IIB) in RNA levels at the 5-day seedling stage. Cluster III includes genes encoding components of photosystem I (*psaA*, *psaB* and *psaJ*), photosystem II (*psbA*, *psbD190* and *psbD LRP*), Rubisco (*rbcL*) and two genes encoding components of the translation apparatus (*rps14* and *rrn16*). The expression profile of these genes is characterized by an initial increase in transcript levels relative to seeds at the 2-day seedling stage and a further increase in RNA level in 5-day old seedlings.

Survey of Plastid Transcript Accumulation in Various Tissues and Stages of Development

A. Differential Plastid Transcript Accumulation in Dry Seeds

In general, the plastid genes examined showed the lowest level of expression relative to 18S rRNA in dry seeds. However, plastid RNA levels fluctuated to some extent with 16S rRNA being the most abundant plastid RNA species in dry seeds (Figure 10A). These results agree with previous reports indicating that *rrn16* is the most highly expressed plastid gene in proplastids and amyloplasts (Krupinska and Falk, 1994; Deng and Gruissem, 1988; Harak *et al.,* 1995).Among plastid transcripts, the mRNAs from *psaA*, *psaB*, *psbA*, encoding subunits of photosystem I and II and *clpP*, encoding a catalytic subunit of the ATP-dependent Clp protease were relatively abundant in dry seeds (Figure 10D and E). The remaining plastid transcripts were present in low amounts in dry seeds with the transcript for *ndhB*, encoding a subunit of the NADH dehydrogenase

complex exhibiting the lowest relative abundance (Figure 10B).To facilitate the detection of differential transcript accumulation, the abundance of plastid RNAs in the various tissues and developmental stages examined was expressed relative to that in seeds (Table 12). Additionally, changes in the ratio of a transcript's abundance in 5- and 40-day old roots as well as 2- and 5-day old seedlings relative to the abundance in seeds were calculated and are listed in separate columns in Table 12.

B. Differential Plastid Transcript Accumulation in Siliques Relative to Seeds

At present, there is little information on plastid RNA levels in siliques. Therefore, the steady-state mRNA levels of plastid genes were examined during silique development. For this study, whole immature siliques were collected before the completion of flower production (Boyes *et al.,* 2001). At this stage, the siliques as well as the seeds were green indicating the presence of chloroplasts. Quantitative analysis of plastid transcript accumulation revealed a general increase of RNA levels in siliques as compared to mature seeds. However, the amounts of individual RNA species for the plastid genes examined varied depending on the gene analyzed (see Figure 10 and Table 12). For instance, the largest increase in transcript abundance relative to mature seed was observed for the *ndhB* and the *rbcL* transcripts (~294- and 87-fold, respectively). In contrast, transcripts for 16S rRNA as well as RNAs for genes encoding ribosomal proteins (*rps16*, *rpl32*) and genes encoding two subunits of the plastid RNA polymerase (*rpoA*, *rpoC1*) were only ~2- to 5-fold higher in siliques as compared with mature seeds. The monocistronic *rps15* transcript accumulated to similar levels in both siliques and mature seeds whereas the *rps14* transcript was ~11-fold more abundant in siliques

relative to mature seeds. The *rps14* gene is located downstream from the *psaA* and *psaB* genes and is part of a transcription unit including these genes (see Table 11). Since our primers did not discriminate between the different transcripts containing *rps14* sequences, the *rps14* transcript abundance could reflect the accumulation of the tricistronic *psaA-psaB-rps14* message. RNA levels for three *ndh* genes (*ndhA*, *ndhF* and *ndhJ*) encoding subunits of the NADH dehydrogenase complex were also ~2- to 5-fold more abundant in siliques relative to mature seeds whereas transcripts for two ATP synthase genes (*atpA* and *atpB*) and one cytochrome b6/f gene *(petA*) showed a ~5- to 8-fold increase in siliques relative to mature seeds. A similar increase in RNA abundance was observed for *psaA*, *psaB* and *psbA* genes encoding components of the photosynthetic apparatus. The *psbD* RNAs, however, showed a much larger increase in abundance relative to other transcripts for photosynthetic genes (12- to 18-fold). Finally, changes in tRNA abundance were variable with the *trnV-GAC* exhibiting a ~4-fold increase in siliques relative to seeds whereas RNAs encoding for *trnfM-CAU*, *trnW-CCA* and *trnS-GCU* were 6-, 7- and 9-fold higher in siliques relative to seeds. Accumulation of *trnE- UUC* transcripts in siliques relative to mature seeds was the highest among the tRNA transcripts (~14-fold). The increase in *trnE-UUC* could be due to a higher demand for this tRNA which is involved in the synthesis of γ-aminolevulinic acid, a common precursor in heme and chlorophyll biosynthesis.

Table 12. Abundance of plastid genes mRNA in siliques, 2-day seedlings, 5-day seedlings, 5-day roots and 40-day roots relative to seeds[a]

Gene	Siliques	2-day seedlings	5-day seedlings	ratio 2d/5d seedlings	5-day roots	40-day roots	ratio 40d/5d roots
Plastid genes encoding the transcription apparatus							
rpoA	3.9 (3.1-4.7)	23.9 (20.0-28.4)	24.0 (20.0-28.7)	1.0 (0.7-1.4)	4.1 (3.4-4.9)	8.8 (7.3-10.5)	2.2 (1.4-3.0)
rpoC1	1.8 (1.7-2.0)	18.6 (15.7-21.7)	18.8 (17.7-20.0)	1.0 (0.8-1.2)	3.0 (2.7-3.3)	4.9 (4.6-5.3)	1.7 (1.4-2.0)
Plastid genes encoding the translation apparatus							
rps14	11.3 (11.2-11.4)	27.3 (24.3-30.7)	42.1 (41.7-42.4)	0.65 (0.57-0.74)	0.59 (0.56-0.63)	1.20 (1.18-1.22)	2.0 (1.9-2.2)
rps15	0.88 (0.82-0.93)	21.5 (20.0-23.1)	8.4 (7.8-9.0)	2.6 (2.2-3.0)	1.2 (1.1-1.3)	2.4 (2.2-2.6)	2.0 (1.7-2.4)
rps16	2.3 (2.1-2.4)	14.4 (13.3-15.5)	11.8 (11.3-12.3)	1.2 (1.1-1.4)	1.2 (1.1-1.2)	2.7 (2.5-2.9)	2.3 (2.0-2.6)
rpl32	3.6 (3.4-3.7)	39.2 (36.3-42.1)	14.9 (13.2-16.6)	2.7 (2.2-3.1)	0.90 (0.82-0.99)	2.6 (2.5-2.8)	2.9 (2.5-3.4)
rrn16	5.4 (4.1-6.9)	10.5 (8.4-12.9)	20.4 (16.3-25.1)	0.51 (0.31-0.75)	0.19 (0.13-0.27)	0.55 (0.41-0.71)	2.8 (1.2-4.8)

Table 12. (continued).

Gene	Siliques	2-day seedlings	5-day seedlings	ratio 2d/5d seedlings	5-day roots	40-day roots	ratio 40d/5d roots
trnC-GCA	3.6 (3.5-3.7)	22.6 (22.1-23.5)	12.9 (12.6-13.4)	1.8 (1.7-1.9)	0.51 (0.49-0.54)	0.95 (0.90-1.02)	1.9 (1.7-2.1)
trnE-UUC	14.4 (13.3-15.5)	98 (82-115)	53.6 (50.0-57.4)	1.8 (1.4-2.3)	1.7 (1.6-1.9)	2.8 (2.5-3.0)	1.6 (1.3-1.9)
trnfM-CAU	6.2 (5.8-6.5)	4.2 (3.9-4.6)	1.4 (1.3-1.5)	3.0 (2.5-3.5)	0.93 (0.88-0.98)	2.5 (2.3-2.6)	2.6 (2.4-3.0)
trnS-GCU	9.5 (9.1-10.5)	1.2 (1.1-1.4)	1.5 (1.5-1.6)	0.81 (0.71-0.97)	1.0 (0.96-1.1)	2.2 (2.0-2.5)	2.2 (1.9-2.6)
trnV-GAC	2.3 (2.2-2.6)	13.0 (12.6-13.5)	4.1 (4.0-4.3)	3.2 (3.0-3.4)	0.59 (0.56-0.63)	0.77 (0.72-0.82)	1.3 (1.1-1.5)
trnW-CCA	6.7 (6.5-6.9)	0.45 (0.44-0.47)	0.37 (0.35-0.39)	1.2 (1.1-1.3)	0.84 (0.82-0.87)	2.2 (2.1-2.3)	2.7 (2.5-2.8)
Plastid genes encoding components of ATP synthase, NADH dehydrogenase and cytochrome *b6/f* complexes							
atpA	7.3 (6.9-8.1)	50.6 (47.6-55.5)	33.2 (31.4-36.2)	1.5 (1.4-1.8)	0.86 (0.81-0.94)	0.53 (0.49-0.60)	0.6 (0.5-0.8)
atpB	5.1 (4.9-5.5)	62.8 (60.2-66.9)	35.3 (32.6-38.9)	1.8 (1.6-2.1)	1.4 (1.3-1.5)	2.5 (2.3-2.8)	1.8 (1.5-2.1)
ndhA	2.5 (2.4-2.6)	49.2 (45.1-53.5)	30.4 (28.3-32.6)	1.6 (1.4-1.9)	0.88 (0.82-0.95)	2.7 (2.5-2.8)	3.0 (2.6-3.4)

Table 12. (continued).

Gene	Siliques	2-day seedlings	5-day seedlings	ratio 2d/5d seedlings	5-day roots	40-day roots	ratio 40d/5d roots
ndhB	294 (271-317)	6600 (5600-7680)	5600 (5300-5920)	1.2 (0.9-1.4)	1.1 (1.0-1.3)	2.2 (1.9-2.4)	1.9 (1.4-2.5)
ndhF	2.4 (2.3-2.6)	47.2 (43.2-51.5)	24.4 (22.6-26.3)	1.9 (1.6-2.3)	0.95 (0.86-1.05)	2.5 (2.3-2.6)	2.6 (2.2-3.0)
ndhJ	5.2 (4.8-5.6)	22.8 (21.2-24.4)	21.3 (20.4-22.2)	1.1 (1.0-1.2)	0.27 (0.24-0.31)	1.0 (0.95-1.1)	3.7 (3.0-4.4)
petA	7.9 (7.5-8.3)	75.9 (70.4-81.7)	36.0 (34.1-37.9)	2.1 (1.9-2.4)	1.9 (1.7-2.0)	4.1 (3.7-4.5)	2.2 (1.8-2.6)
Plastid genes encoding photosystem I, photosystem II and Rubisco components							
psaA	8.0 (7.2-8.9)	38 (32-46)	59 (53-65)	0.7 (0.5-0.9)	0.7 (0.6-0.8)	1.8 (1.6-2.0)	2.6 (2.1-3.3)
psaB	8.1 (7.9-8.2)	30.4 (29.2-31.5)	43.5 (42.5-44.5)	0.70 (0.66-0.74)	0.64 (0.61-0.67)	1.71 (1.65-1.77)	2.7 (2.5-2.9)
psaJ	19.1 (17.8-20.5)	88 (74-104)	114 (108-121)	0.8 (0.6-1.0)	0.8 (0.7-0.9)	2.6 (2.3-2.9)	3.4 (2.6-4.1)
psbA	6.5 (5.6-7.8)	11 (9-15)	41 (32-53)	0.3 (0.2-0.4)	0.20 (0.17-0.25)	0.7 (0.6-0.9)	3.5 (2.4-5.2)
psbD190	12.2 (11.4-13.0)	76 (64-89)	113 (101-125)	0.7 (0.5-0.9)	0.83 (0.75-0.92)	3.8 (3.4-4.2)	4.6 (3.6-5.6)

Table 12. (continued).

Gene	Siliques	2-day seedlings	5-day seedlings	ratio 2d/5d seedlings	5-day roots	40-day roots	ratio 40d/5d roots
psbDLRP	18.0 (15.8-20.3)	62 (51-73)	165 (138-194)	0.37 (0.25-0.51)	0.59 (0.52-0.66)	2.7 (2.4-3.0)	4.5 (3.5-5.6)
rbcL	87 (68-108)	435 (317-569)	525 (426-640)	0.8 (0.5-1.3)	3.4 (2.6-4.2)	9.1 (7.5-11.0)	2.7 (1.6-3.9)
Plastid genes encoding components involved in other metabolic processes							
accD	6.3 (5.2-7.6)	23 (19-28)	29 (24-36)	0.8 (0.5-1.0)	10.8 (9.0-12.8)	13.6 (11.2-16.2)	1.3 (0.8-1.8)
clpP	2.0 (1.6-2.5)	8.5 (6.8-10.6)	5.8 (4.6-7.3)	1.5 (0.9-2.2)	1.8 (1.5-2.2)	3.5 (2.8-4.3)	1.9 (1.2-2.8)

[a] Seeds of *Arabidopsis thaliana* ecotype Columbia were surface-sterilized and sown in Petri dishes on MS medium containing 1% sucrose. The plates were placed at 4^0C for 5 days before being transferred to continuous white light (40 µmol m^{-2} sec^{-1}). Siliques were collected from 34-day old *Arabidopsis* plants grown on soil after a 15-day period of growth on MS medium containing 1% sucrose. Total RNA was isolated from siliques, seeds, 2-day seedlings, 5-day seedlings, 5-day roots and 40-day roots and converted to cDNA in reactions that were normalized to contain equivalent amounts of total RNA. A cDNA input corresponding to 10 ng of reverse transcribed total RNA was employed as template for real-time PCR analysis. Reactions were run in triplicate and data were normalized relative to cytoplasmic 18S rRNA levels and expressed as $2^{-\Delta CT}$ $X10^5$, where $\Delta C_T = (C_{T\ sample} - C_{T\ normalizer})$. The fold change in mRNA abundance of each gene in siliques, 2-day seedlings, 5-day seedlings, 5-day roots and 40-day roots relative to seeds was derived from the ratio of the individual $2^{-\Delta CT}$ values in each tissue to the respective $2^{-\Delta CT}$ values in seeds . The range given in parenthesis is determined by evaluating the expression $2^{-\Delta CT}$ with ΔC_T + SD and ΔC_T – SD, where SD = the standard deviation of the ΔC_T value calculated according to the formula $S = \sqrt{(S^2_{\ sample} + S^2_{\ normalizer})}$

C. Differential Plastid Transcript Accumulation in 2-day and 5-day Seedlings Relative to Seeds

The abundance of most of the plastid RNAs was higher in 2-day and 5-day old seedlings relative to seeds (see Table 11, Table 12 and Figure 10). For instance, transcripts for *rpoC1* and *rpoA*, encoding subunits of the plastid RNA polymerase (PEP) exhibited a ~19- to 24-fold increase in abundance relative to mature seeds at both the 2-day and 5-day stage whereas the 16S rRNA levels, which are relatively high in the dry seeds, increased ~10-fold in 2-day seedlings and reached a maximal difference (~20-fold higher) relative to seeds at the 5-day stage. Transcripts encoding ribosomal proteins (*rps15*, *rps16* and *rpl32*) showed a sharp increase (~21-, 14- and 39-fold, respectively) in 2-day seedlings relative to seeds then decreased 1.2- to 2.7-fold in 5-day seedlings relative to 2-day seedlings. It is noteworthy that transcript accumulation of *rps14*, which is part of the *psaA-psaB-rps14* transcription unit, showed a ~27-fold increase at the 2-day stage relative to seeds followed by a ~1.5-fold increase in 5-day seedlings relative to 2-day seedlings. The accumulation kinetics for the tRNA transcripts varied depending on the transfer RNA studied. For instance, in 2-day seedlings the sharpest increase in transcript accumulation relative to seeds was recorded for *trnE-UUC* (~98-fold) whereas *trnfM-CAU*, *trnV-GAC* and *trnC-GCA* showed an increase of ~ 4-, 13- and 23-fold, respectively. This increase in transcript accumulation was followed by a decrease in 5-day seedlings relative to 2-day seedlings of 1.8-fold (*trnE-UUC* and *trnC-GCA*) to ~3-fold (*trnfM-CAU* and *trnV-GAC*). The amount of *trnW-CCA* was lower in 2-day and 5-day seedlings relative to seeds (~0.5- and 0.4-fold, respectively) whereas the levels of *trnS-GCU* in 2-day as well as 5-day seedlings exhibited only a

slight increase relative to seeds (~1.2 and 1.5-fold, respectively). Transcript levels of the *atp* genes (*atpA* and *atpB*), encoding subunits of the plastid ATP synthase complex, *ndh* genes (*ndhA, B, F, J*), encoding subunits of the plastid NADH dehydrogenase complex and *petA*, encoding a component of the cytochrome b_6/f complex also showed a large increase at the 2-day stage relative to seeds and either decreased slightly or remained unchanged at the 5-day stage relative to 2-day seedlings (~1- to 2-fold; see also Figure 10 and Table 12). In contrast, transcript accumulation for photosystem I genes (*psaA*, *psaB* and *psaJ*), photosystem II genes (*psbA*, *psbD190* and *psbDLRP*) and for *rbcL*, encoding the large subunit of Rubisco was 41- to 435-fold higher in 2-day seedlings relative to seeds and increased further in 5-day seedlings (Figure 10 and Table 12). Finally, the levels of the *clpP* transcript increased ~9-fold in 2-day seedlings relative to seeds and decreased ~ 1.5-fold in 5-day seedlings relative to 2-day seedlings whereas the *accD* transcripts showed ~23- to 29-fold increase in accumulation relative to mature seeds at the 2-day and 5-day stage, respectively.

D. Differential Plastid Transcript Accumulation in Roots Relative to Seeds

Although the levels of mRNAs for all plastid genes investigated were relatively low in dry seeds and 5-day roots, differential plastid transcript accumulation occurs in these tissues (Table 12). For example, the 16S rRNA level in 5-day roots was 5-fold lower than that of seeds. A similar difference in mRNA abundance was observed for *psbA*. Other plastid mRNAs that showed lower abundance in 5-day roots relative to seeds include transcripts for *ndhJ, psbD*, *psaJ* as well as transcripts for the *psaA-psaB-rps14* operon. Two tRNA genes (*trnV-GAC* and *trnC-GCA*) also showed lower relative

transcript levels in 5-day roots. In contrast, *accD* transcripts were 11-fold higher in 5-day roots relative to seeds. The mRNAs levels for *rpoA*, *rpoC1* and *rbcL* were 3- to 4-fold higher in 5-day roots as compared to seeds. Additionally, the mRNA abundance of *petA*, *clpP*, as well as *trnE-UUC* was ~2-fold higher in 5-day roots relative to seeds. Transcripts for several plastid genes accumulated to similar levels in both dry seeds and 5-day roots. These include transcripts for three ribosomal protein genes (*rps15*, *rps16*, and *rpl32*), transcripts for three *ndh* genes (*ndhA*, *ndhB*, and *ndhF*) encoding NADH dehydrogenase subunits, transcripts for two *atp* genes (*atpA* and *atpB*) encoding subunits of the ATP synthase as well as transcripts for three tRNA genes (*trnfM-CAU*, *trnS-GCU*, and *trnW-CCA*).

Although most roots of soil-grown plants contain amyloplasts, which do not assemble a functional photosynthetic apparatus, when roots are exposed to light, they turn green due to the conversion of the amyloplasts into photosynthetically active chloroplasts (von Arnin and Deng, 1996; Yu and Li, 2001). Therefore, transcript levels in illuminated 40-day root tissue from *Arabidopsis* seedlings grown on the surface of agar media were quantified. Comparison of plastid RNA accumulation from 5-day and 40-day light-exposed roots (see Figure 10 and Table 12) indicated that there was a significant increase in the abundance of most plastid transcripts examined in the 40-day roots as compared to 5-day roots. For example, the abundance of transcripts from all genes encoding components of the transcription apparatus except *trnV-GAC* as well as components of ATP synthase, NADH dehydrogenase and cytochrome b_6/f complexes except *atpA* increased 1.7- to 3.7 fold in 40-day old roots relative to 5-day-old roots whereas RNA abundance for genes encoding photosynthesis electron transport/ Rubisco components increased 2.6- to 4.9-fold. An increase of 1.9-fold was also

observed in the abundance of the transcript from the *clpP* gene, encoding the ClpP1 protein of an ATP dependent plastid-localized protease (Adam *et al.,* 2001), whereas the *accD* transcript accumulated to similar levels in both 40-day and 5-day roots.

E. Differential Plastid Transcript Accumulation in 10-day, 12-day and 15-day Cotyledons Relative to Seeds

Transcript accumulation for a subset of plastid genes was analyzed in 10-day, 12-day and 15-day cotyledons. The genes examined included *rpoA* and *rrn16*, encoding components of the plastid transcription and translation apparatus *psbA*, *psbD190* and *rbcL*, encoding components of photosystem II and Rubisco, *accD*, encoding a subunit of the plastid acetyl-CoA carboxylase and *clpP*, encoding the proteolytic subunit of an ATP-dependent protease For this experiment, imbibed seeds sown on MS medium supplemented with 1% sucrose were placed at 4^0C for 48 hrs under dark conditions, and then germinated at 23^0C under continuous light. At day 2, the emerging cotyledons begin to turn green and by day six they are fully opened. Days 7 through 11 mark a period of general growth for the plant after which the cotyledons begin to senesce. Real-time PCR analysis revealed that the individual mRNAs accumulate to different levels at the developmental stages examined (see Figure 10 and Table 13). For example, transcript levels of *rpoA*, *rbcL* and *accD* peak at day 10 (~22-, 1006- and 50-fold relative to mature seeds) and then progressively decline at days 12 and 15 whereas transcript amounts of *rrn16*, and *psbA* peak at day 12 (~23-and 68-fold relative to seeds) and decline at day 15. In contrast, *psbD190* showed a progressive increase in transcript accumulation and reached its peak at day 15 (~222-fold relative to mature

Table 13. Abundance of plastid genes mRNA in 10-day, 12-day and 15-day cotyledons relative to seeds [a]

Gene	10-day cotyledons	12-day cotyledons	ratio 10d/12d cotyledons	15-day cotyledons	ratio 10d/15d cotyledons
rpoA	22 (18-28)	18 (14-22)	1.3 (0.8-2.0)	7.2 (5.5-9.7)	3.1 (1.8-5.0)
rrn16	20 (16-26)	23 (18-29)	0.9 (0.5-1.4)	14 (11-18)	1.4 (0.8-2.2)
rbcL	1006 (797-1288)	710 (569-897)	1.4 (0.8-2.2)	237 (182-316)	4.2 (2.4-6.9)
psbA	46 (41-55)	68 (60-81)	0.7 (0.5-0.9)	35 (31-42)	1.3 (1.0-1.8)
psbD190	79 (74-83)	126 (118-133)	0.63 (0.55-0.70)	222 (209-235)	0.35 (0.31-0.40)
accD	50 (40-64)	46 (37-59)	1.1 (0.72-1.7)	44 (31-64)	1.2 (0.6-2.0)
clpP	4.9 (3.9-6.4)	4.5 (3.6-5.8)	1.1 (0.7-1.8)	5.2 (4.1-6.7)	1.0 (0.6-1.5)

[a] Total RNA was isolated from seeds as well as 10-day, 12-day and 15-day cotyledons of *A. thaliana* seedlings grown on MS medium supplemented with 1% sucrose. Equivalent amounts of total RNA were converted to cDNA and assayed by real time PCR as described in Table 12.

seeds). Finally, *clpP* showed a constant level of transcript abundance at days 10, 12 and 15 (~5-fold increase relative to seeds).

F. Differential Plastid Transcript Accumulation in 15-day Rosette Leaves, 35-day Rosette Leaves and 35-day Cauline Leaves Relative to Seeds

Several reports indicate that chloroplast biogenesis in cotyledons follows a different developmental program than in true leaves (Mansfield and Briarty, 1996; Hoffer and Christopher, 1997). Therefore, we investigated transcript accumulation for a subset of plastid genes in young 15-day rosette leaves of *Arabidopsis* plants sown on MS medium containing 1% sucrose and in mature 35-day rosette leaves as well as 35-day cauline leaves of plants transferred to soil after an initial 15-day period of growth on MS medium. The results in Figure 10 and Table 14 indicate a moderate transcript accumulation in young 15-day rosette leaves relative to mature seeds for *rpoA* (~6-fold versus ~7-fold in 15-day cotyledons), *rrn16* (~12-fold versus ~14-fold in 15-day cotyledons), *psbA* (~23-fold versus ~35-fold in 15-day cotyledons), *accD* (~39-fold versus ~44-fold in 15-day cotyledons) and *clpP* (~5-fold in both 15-day rosette leaves and 15-day cotyledons). In contrast, transcript levels relative to mature seeds for *psbD190* in 15-day rosette leaves were similar to the levels in 12-day cotyledons (~134-fold versus ~126-fold in 12-day cotyledons) whereas transcript levels for *rbcL* were ~1.8-fold higher than the levels in 15-day cotyledons and ~1.7-fold lower than the levels in 12-day cotyledons. On the other hand, mature 35-day rosette and cauline leaves showed similar but enhanced levels of transcript accumulation relative to young 15-day rosette leaves for *rpoA* (~43-fold and 35-fold, respectively), *accD* (~65-fold and

Table 14. Abundance of plastid genes mRNA in 15-day rosette leaves, 35-day rosette leaves and 35-day cauline leaves relative to seeds [a]

Gene	15-day rosette leaves	35-day rosette leaves	35-day cauline leaves
rpoA	6.3 (5.0-8.0)	43 (34-54)	35 (29-42)
rrn16	12 (10-16)	12 (9-16)	21 (16-24)
rbcL	421 (337-530)	340 (264-427)	454 (368-552)
psbA	23 (20-27)	ND	ND
psbD190	134 (127-142)	ND	ND
accD	39 (32-50)	65 (51-81)	54 (44-65)
clpP	5.5 (4.4-7.1)	10.5 (8.0-13.4)	10.5 (8.5-13.0)

[a] Total RNA was isolated from 15-day rosette leaves of *A. thaliana* plants grown on MS medium supplemented with 1% sucrose, 35-day rosette leaves and 35-day cauline leaves of *A. thaliana* plants grown on soil after a 15-day period of growth on MS medium containing 1% sucrose. Equivalent amounts of total RNA were converted to cDNA and assayed by real time PCR as described in Table 12.

54-fold, respectively) and *clpP* (~11-fold in both 35-day rosette leaves and 35-day cauline leaves) whereas *rrn16* transcript levels in mature 35-day rosette leaves were identical to the levels in young 15-day rosette leaves but ~1.8-fold lower than the levels in 35-day cauline leaves.

DISCUSSION

Previous studies in monocotyledonous plants have provided insights into the transcriptional activity of a limited number of plastid genes for several developmental stages indicating that gene specific mechanisms for transcriptional regulation are associated with the various plastid differentiation processes (Deng and Gruissem, 1988; Ngernprasirtsiri *et al.*, 1988; Baumgartner *et al.*, 1989; 1993; Schrubar *et al.*, 1990; Klein and Mullet, 1990; Rapp *et al.*, 1992; Krupinska, 1992; Sakai *et al.*, 1992; Krupinska and Falk, 1994). In the present work, transcript abundance for twenty-eight plastid genes was monitored in several tissues and developmental stages by real-time PCR. The tissues examined included dry seeds, 2-day seedlings, 5-day seedlings, 10-day, 12-day and 15-day cotyledons, as well as 35-day rosette leaves, 35-day cauline leaves, 5-day roots, 40-day roots and 34-day siliques. As shown in Figure 10 and Tables 11, 12 and 13, plastid genes showed differential transcript accumulation in various tissues and developmental stages. For instance, plastid RNA levels were lowest in seeds and 5-day roots, higher in siliques as well as in 40-day roots and even higher in 2-day and 5-day seedlings followed by progressive decline in older tissues such as 12-day and 15-day cotyledons. Seeds contain non-photosynthetic leucoplasts as well as proplastids that will subsequently develop into chloroplasts in the cotyledons and leaves whereas most root tissues contain proplastids and amyloplasts rather than

chloroplasts (reviewed in Thomson and Whatley, 1980; Whatley; 1983). Our results showed that the amounts of plastid RNAs in seed as well as root plastids were the lowest among the plastid types studied consistent with earlier results indicating a low transcriptional activity in non-photosynthetic plastids such as proplastids and amyloplasts (Sakai *et al.*, 1992, Krupinska and Falk, 1994). Our data indicated higher transcript levels in the dry seeds relative to roots for several of the plastid genes studied including *rrn16*, *trnV-GAC*, *trnC-GCA*, *ndhJ*, *psbD*, *psbA*, *psaJ* as well as the *psaA-psaB-rps14* operon. It is well known that proplastids contain ribosomes necessary to start translation during the onset of chloroplast development. In addition, preformed RNAs are stored in mature and desiccated seeds and may be used during early germination until new transcripts are synthesized (reviewed in Bewley, 1997). Transcript levels of the remaining plastid genes studied were similar in both seeds and 5-day roots except *rpoA*, *rpoC1*, *trnE-UUC*, *petA*, *clpP* and *accD* transcripts which were ~2- to 11-fold higher in 5-day roots relative to seeds. The plastid *clpP* gene encodes the proteolytic subunit of the plastid-localized ATP-dependent Clp protease thought to be responsible for most protein degradation (reviewed in Callis, 1995; Shikanai, 2001). Our results showed that the *clpP* transcript was relatively abundant in dry seeds possibly reflecting the requirement for preformed *clpP* message that can be mobilized during germination to assemble the Clp protease for rapid degradation of storage proteins into amino acids that will be subsequently transported to the growing seedling (Callis, 1995). The fact that *clpP* transcript levels increase ~2-fold in roots relative to seeds may reflect a possible function of the Clp protease in the degradation of specific regulatory factors present in root amyloplasts as suggested by Shikanai *et al*., (2001). The plastid *accD* gene, which encodes a subunit of the prokaryotic-type acetyl-CoA carboxylase involved

in de novo fatty acid biosynthesis in plastids, also showed elevated transcript levels in roots relative to seeds (11-fold). This increase may reflect a higher demand for fatty acid biosynthesis in the roots compared with that in dry seeds.

The remaining tissues investigated, which include siliques, 2-day seedlings, 5-day seedlings, 10-day, 12-day and 15-day cotyledons, as well as 35-day rosette leaves and 35-day cauline leaves, contain chloroplasts in various stages of development. The silique is the long, narrow fruit of *Arabidopsis* and other members of the Brassicaceae family which protects the embryo and endosperm during seed development. As it develops, the *Arabidopsis* embryo passes through a series of distinct morphological stages which culminate with deposition of storage materials followed by desiccation and seed dormancy (Goldberg *et al.,* 1989). During this transition, proplastids contained in the zygote develop into green chloroplasts that are believed to be involved in the production of storage reserves and products required for embryo development (Schultz and Jensen, 1968; Mansfield and Briarty, 1991; Apuya *et al.,* 2001). Few studies have investigated the expression patterns of plastid genes in siliques. Ke *et al.*, (2000) investigated the spatial distribution of ACCase mRNAs during silique formation and showed that these transcripts accumulate to different levels during silique development. In the present study we quantified twenty-eight plastid transcripts at one stage of silique development. The results presented in Figure 10 and Table 12 showed a moderate increase in transcript level relative to mature seeds of 2- to 8-fold for most plastid transcripts except for *ndhB* and *rbcL* transcripts, which exhibited a ~294- and 87-fold increase, respectively as well as the *trnE-UUC* and the two *psbD* RNAs, which showed a ~ 14-, 12-, and 18-fold increase, respectively. While the increased accumulation of *trnE-UUC* relative to other tRNAs could be due to its function in both translation and

chlorophyll/heme biosynthesis, the increased levels of the *psbD* transcripts in siliques could be correlated with increased synthesis of the D2 protein to allow plants to replace damaged photosystem II subunits. Two tRNAs, *trnS-GCU* and *trnW-CCA* showed differential increase in siliques.

Light-dependent seed germination and post-germinative development are critical stages in the life cycle of *Arabidopsis* plants. During germination and initial plant growth corresponding to the radicle emergence from the seed coat, lipid and protein reserves stored in the cotyledons are mobilized to provide an energy source for the growing seedling prior to the onset of autotrophic growth (Thomas, 1993; Bewley, 1997; Eastmond and Graham, 2001). Following light-dependent seedling emergence, cotyledons begin to green and expand considerably in size becoming the first photosynthetically active organs (Mansfield and Briarty, 1996; Fridlender *et al.,* 1996; Bakalova-Stoynova *et al.,* 2004). Plastid differentiation is an early event in seed germination. During the early stages of seedling establishment, proplastids differentiate mainly into amyloplasts in roots whereas in cotyledons proplastids differentiate into photosynthetically active chloroplasts by rapidly accumulating thylakoid membranes and the associated complexes of the photosynthetic electron transport chain (Mansfield and Briarty, 1996). To investigate changes in plastid gene expression during the early stages of seedling establishment transcript levels for twenty-eight plastid genes were quantified at the 2-day and 5-day seedling stages. The results were organized into clusters of genes with similar transcript accumulation kinetics to identify groups of coordinately regulated genes. The results shown in Table 12 and Figures 10 and 12 show that genes encoding the plastid transcription and translation apparatus (*rpoA*, *rpoC1*, *rps15*, *rpl32*, rps16, *trnC-GCA*, *trnE-UUC*, *trnV-GAC*), one gene encoding a

subunit of the plastid localized protease (*clpP*), one gene encoding a component of the plastid acetyl-CoA carboxylase (*accD*) as well as genes encoding components of cytochrome b_6/f (*petA*), NADH (*ndhA, B, F, J*) and ATP synthase (*atpA, atpB*) complexes reached maximum transcript abundance in 2-day seedlings whereas genes encoding components of the photosynthetic apparatus (*psaA*, *psaB*, *psaJ*, *psbD190*, *psbDLRP*, *psbA*) and Rubisco (*rbcL*) showed maximum transcript accumulation in the later phases of chloroplast development (5-day seedlings or older). Two genes *rrn16*, encoding 16S rRNA and *rps14*, encoding a 30S ribosomal protein subunit, which are part of the transcription and translation apparatus, exhibited transcript accumulation kinetics similar to that of the photosynthetic genes. Since *rps14* is part of the *psaA-psaB-rps14* operon, which is known to be polycistronically transcribed, it is not surprising that *rps14* mRNA levels showed a pattern of accumulation similar to *psaA/psaB* transcripts. On the other hand, the accumulation kinetics of 16S rRNA probably reflect the high stability of this rRNA due to its association with ribosomes (Kim *et al*., 1993a; Baumgartner *et al*., 1993). Our results on the transcript accumulation kinetics for genes encoding components of the transcription and translation apparatus coincide with previous studies in barley and pea (Baumgartner *et al.,* 1993; DuBell and Mullet, 1995) that showed a differential transcription of genes for the transcription and translation apparatus early during chloroplast development. The finding that genes encoding the transcription and translation apparatus increase their expression in advance of the genes encoding the photosynthetic apparatus is consistent with the hypothesis that components of the plastid–encoded RNA polymerase (PEP) and ribosomes are required early in chloroplast development (Mullet, 1993). The early build-up of the transcription and translation apparatus provides capacity for rapid synthesis

and assembly of the photosynthetic apparatus. That components of cytochrome b_6/f, NADH dehydrogenase and ATP synthase complexes are also made early in chloroplast development is consistent with the concept that chlororespiration, which refers to a putative respiratory electron transport chain in the thylakoid membranes of chloroplasts (Bennoun, 1992, 2002) provides an energy-generating source to drive plastid development until the photosynthetic apparatus takes over this function.

Two genes encoding plastid components involved in other metabolic processes also showed differential expression. One gene, *clpP*, encoding the proteolytic subunit of the plastid ATP-dependent protease, reached maximal transcript accumulation in 2-day seedlings (~9-fold relative to mature seeds) followed by a slight decline in 5-day seedlings (~6-fold relative to mature seeds). Disruption of the tobacco *clpP* gene by chloroplast transformation indicated that Clp protease is involved in several stages of chloroplast development including the early developmental stage of thylakoid grana formation (Shikanai et al., 2001). Since this is a period of massive increase in protein synthesis, Shikanai *et al.,* proposed (2001) that the plastid ATP-dependent protease may function early during chloroplast development to degrade denatured or unassembled plastid proteins. Our results on differential early accumulation of the *clpP* transcripts support the hypothesis that Clp protease performs an important function during the early stages of chloroplast development. The plastid gene *accD*, encoding a subunit of the plastid acetyl-CoA carboxylase, which is involved in fatty acid biosynthesis, also showed differential early mRNA accumulation with a sharp increase relative to seeds at the 2-day stage followed by a moderate increase at the 5-day stage which may reflect the increased requirement for lipid synthesis during the assembly of the thylakoid membranes.

Interestingly, *trnW-CCA* and *trnS-GCU* do not get induced during chloroplast development. In fact, the levels of these two tRNAs are highest in siliques (~7- and 10-fold, respectively) relative to mature seeds whereas in 2-day and 5-day seedlings *trnW-CCA* levels are only 0.5- and 0.4-fold higher as compared to mature seeds while *trnS-GCU* levels do not change significantly throughout leaf development. It is well known that plants contain low levels of soluble tryptophan particularly in seeds (Radwanski and Last, 1995). In addition, previous studies in tobacco, spinach and maize leaves have shown that the amounts of $tRNA^{Trp}$ are the lowest among the tRNAs and that there is a positive correlation between plastid codon usage and tRNA concentrations *(*Pfitzinger *et al.,* 1987*).* It is notable that the accumulation of these tRNAs takes place in siliques during the phase of massive production of vegetative proteins. It is possible that high amounts of $tRNA^{Trp}$ as well as $tRNA^{Ser}$ are made and used during embryogenesis and seed formation for the synthesis of seed storage proteins. Another tRNA that exhibits significantly higher levels in siliques relative to other tissues examined is *trnfM-CAU* (~6-fold increase relative to dry seeds). However, the levels of *trnfM-CAU* exhibit another peak in 2-day seedlings (~4-fold increase relative to mature seeds) and a decline in 5-day seedlings (~1.4-fold increase relative to dry seeds) similar to the pattern exhibited by the transcript levels of genes encoding components of the transcription and translation apparatus The fact that formyl-methionyl-$tRNA^{Met}$, which initiates protein biosynthesis in plastids, exhibits one peak in siliques and a second peak in 2-day seedlings suggests that plastids have a mechanism to ensure that high levels of $tRNA_f^{Met}$ are made in order not to be a limiting factor in the initiation of translation.

The finding that transcript levels of plastid genes are coordinately expressed at different developmental stages indicates the presence of regulatory mechanisms that modulate gene transcription during chloroplast development in different plant tissues and/ or stages. Regulation of chloroplast gene expression has been demonstrated for several sets of genes (Igloi and Kössel*,* 1992; Baumgartner *et al.,* 1993). Evidence also exists suggesting that early signals for chloroplast development originate from the nucleus (Mullet, 1993; Harrak *et al.,* Mache *et al.,* 1997). In addition, transcription in plastids has been shown to be performed by two distinct groups of RNA polymerases of different phylogenetic origins: a plastid-encoded RNA polymerase (PEP) whose activity is controlled by nucleus-encoded sigma-like factors and at least two nuclear-encoded phage-type RNA polymerases (NEP) (reviewed in Allison, 2000; Hess and Börner, 1999). The molecular mechanisms underlying the changes in plastid mRNA levels during chloroplast development are not well understood. The present study revealed the presence of differential class-specific accumulation of plastid transcripts. We hypothesize that nucleus-encoded factors are involved in the regulation of plastid transcription during leaf and chloroplast development.

MATERIALS AND METHODS

Plant Growth

Arabidopsis *thaliana* Col-0 wild-type seeds were surface sterilized in 95% ethanol for one minute followed by ten minutes incubation in 100% bleach (5.25% sodium hypochlorite-LABBCO, Inc., Houston, TX) + 0.0001% Tween-20. Seeds were washed

three times in sterile water and plated on media containing 1x Murashige and Skoog salts and vitamin mixture (Gibco-BRL), 1% sucrose, 0.5 g L-1 2-[N-Morpholino] ethane-sulfonic acid (MES) and 0.8% phytagar (Gibco-BRL). The plates were placed at 4^0 C for 5 days and then transferred to continuous white light (40 μE m^{-2} s^{-1}). After fifteen days, some Arabidopsis seedlings were transferred to soil whereas others were transferred to fresh plates. For root excision, *Arabidopsis* plants were grown vertically on 1X Murashige and Skoog medium as described above. Two-day old seedlings, 5-day old seedlings, 10-day, 12-day and 15-day cotyledons as well as 5-day and 40-day old roots were harvested, frozen in liquid nitrogen and stored at 80^0 C until further use. Rosette and cauline leaves from 35-day old plants as well as siliques from 34-day old plants transferred to soil after a fifteen-day period of growth on plates were harvested, frozen in liquid nitrogen and stored at 80^0 C until further use.

RNA Isolation and Reverse Transcription

Total RNA from roots, 2-day and 5-day old seedlings as well as 10-day cotyledons, 12-day cotyledons, 15-day cotyledons, 35-day rosette and cauline leaves was extracted with Tri Reagent (Molecular Research Center, Inc., Cincinnati, OH) using 1-bromo-3-chloropropane (BCP) as a substitute for chloroform as per manufacturer's instructions (Chomczynski and Mackey, 1995). Total RNA from seeds and siliques was isolated using the Concert Plant RNA Reagent, according to the manufacturer's instructions (Invitrogen, Carlsbad, CA) except that BCP (Molecular Research Center, Inc., Cincinnati, OH) was substituted for chloroform. Contaminating DNA was removed using the RNase free DNase (Qiagen, Valencia, CA) with two elutions of five minutes in 30 μL

RNase-free water (Ambion, Austin, TX). The purity of RNA was judged by the A_{260}/A_{280} ratios (1.8-2.0) and RNA integrity was assessed by examining the rRNA bands on a standard agarose gel (Sambrook *et al*., 1989). Constant amounts of 2 μg RNA were reverse-transcribed to cDNA in a total volume of 100 μL using random hexamer primers and the TaqMan Reverse Transcription Kit (Applied Biosystems, Foster City, CA). Each 100-μL reaction was prepared as follows: 34.75 μL RNA sample in RNase-free water (Ambion, Austin, TX), 10.0 μL 10X TaqMan RT Buffer, 22.0 μL $MgCl_2$ (5.5 mM), 20.0 μL dNTPs (500 μM each) 5.0 μL random hexamer primers (2.5 μM), 2.0 μL RNase inhibitor (0.4 U/ μL) and 6.25 μL Multiscribe Reverse Transcriptase (3.125 U/ μL). After a ten-minute incubation at 25^0C to increase primer-RNA template binding, reverse transcription was performed for one hour at 37^0C followed by inactivation of the reverse transcriptase at 95^0C for five minutes. The final volume of each 100-μL RT reaction was brought to 200 μL by the addition of 100 μL of RNase-free water and the cDNA was stored at -80^0C until further use. No-template controls were generated at the same time by combining 2 μg RNA with RNase-free water to a 200-μL final total volume.

Primer Design

All the gene-specific primers were designed using Primer Express® software v2.0 (Applied Biosystems Foster City, CA) according to the software guidelines except for the *trn* and *rps16* primers which were designed with Primer3 program (http://www.genome.wi.mit.edu/cgi-bin/primer/primer3_www.cgi) of the Whitehead Institute (Cambridge, MA, USA). All amplicons were designed according to the same guidelines provided by the Primer Express® software. Briefly, primers for each gene

target were selected to contain minimal hairpins and primer-dimer formation as determined by the software and having compatible T_m's, each within 1^0-2^0C of the other. In addition, primers were designed to be 15-30 bases in length with a minimum and maximum amplicon size of 59 bp and 150 bp, respectively. All oligonucleotide primers used were synthesized by IDT (Integrated DNA Technologies, Inc., Coralville, IA) except for the *psbD190*, *psbDLRP* and *rbcL* primers which were purchased from Applied Biosystems (Foster City, CA). Oligonucleotide sequences are shown in Table 15. The 18S rRNA primers and probe that produce a 187-bp amplicon were included in the TaqMan rRNA Control Reagents kit (Applied Biosystems, Foster City, CA). In order to verify the specificity of the primers, all primers were used as query sequences in Blast searches of the NCBI database either alone, together with the DNA segment generated by the PCR process or with Ns substituted for the sequence between the primers.

Real-time PCR: SYBR Green Detection

PCR reactions were carried out in optical 384-well plates on an ABI Prism 7900HT Sequence Detection System using the 2X SYBR Green PCR Master Mix (Applied Biosystems, Foster City, CA) as recommended by the manufacturer. For each sample, a master mix was generated by combining 3.3 µL of cDNA with 29.7 µL of 2X SYBR Green PCR Master Mix (Applied Biosystems) supplemented with primers to a final concentration of 50 nM each and PCR-grade water to a 33 µL final total volume. This

Table 15. Sequences of PCR forward (for) and reverse (rev) primers for *plastid genes

Gene	Primer sequence	(bp)
rpoA	for 121: CAAGCCGACACAATAGGCATT rev 195: TGCACGTGTAATACATGTTCCTTCT	74
rpoC1	for 1187: GATTGCCTCGCGAAATAGCA rev 1271: CCTATGTTCGAAGCCAGGTGTT	84
rps14	for 201: AAGACCGAGAGCTAACTATCGAGACT rev 279: TGGCAACAAACATGCCTGAA	78
rps15	for 56: CCGTTGAATTTCAAGTATTTAGTTTCACT rev 153: TAGACCCCGCTGAGATAAATAATCTT	97
rps16	for 137: CTTTTTTAAACCTTTCTGCTATTCTCGAT rev 224: CCAGCCTTCTTTGAAATATCATGAG	87
rpl32	for 30: CTCGAAAAAGCGTATTCGTAAA rev 96: AAAAGCTTTCAACGATGTCCA	66
rrn16	for 440: GGGAATAAGCATCGGCTAACTCT rev 509: ATTCCGGATAACGCTTGCAT	69

Table 15. (continued).

Gene	Primer sequence	Product Length (bp)
trnC-GCA	for 5: GCATGGCCGAGTGGTAA rev 67: GGCACCCGGATTTGAAC	62
trnE-UUC	for 3: CCCCCATCGTCtAGTGGTT rev 62: AAGTCGAATCCCCGCTG	59
trnfM-CAU	for 2: GCGGGGTAGAGCAGTTTG rev 66: ACAGGATTTGAACCCGTGAC	64
trnS-GCU	for 17: CGAACCCTCGGTACGATTA rev 88: GGAGAGATGGCTGAGTGGAC	71
trnV-GAC	for 9: AGCTCAGTTAGGTAGAGCACCTC rev 67: ATACGGACTCGAACCGTAGAC	58
trnW-CCA	for 2: CGCTCTTAGTTCAGTTCGGTAG rev 73: ACGCTCTGTAGGATTTGAACC	71
atpA	for 583: GTTTATGTAGCTATTGGTCAAAAAGCTTCT rev 657: CATTGCCCCTCGTTCCTGTA	74

Table 15. (continued).

Gene	Primer sequence	Product Length (bp)
atpB	for 78: CATTGGTCCGGTACTGGATGT rev 143: ACCAGAGCATTGTAAATATTAGGCATT	65
ndhA	for 617: GGAATTTGTGGCGTCAACCTA rev 712: CTTCCGCTTCTGGTAAATCAAAC	95
ndhB	for 377: CTCATCAATGGACTCCTGACGTATA rev 461: GAAGCAGCTACTTTCGAAGTAACAGA	84
ndhF	for 714: TGCTAAATCCGCACAATTTCC rev 798: AGCATGTATAAGACCCGAAATGG	84
ndhJ	for 363: TTATGATAGCCATCCACGACTGAA rev 428: CGTAAAGGCCACCCTATCCAA	65
petA	for 761: AATCCATTAAACTCGATCAACCATTA rev 828: CGCATCCCCCTGACCAA	67
psaA	for 729: TCGGGATCTTTTGGCTCAAC rev 811: CCGAGTATTTTGACCAATTTAAGGTAA	82

Table 15. (continued).

Gene	Primer sequence	Product Length (bp)
psaB	for 657: CCAAGGGTTAGGCCCACTTT rev 753: TCCGGATCCTTGGGAGGTA	96
psaJ	for 22: CTTTCCGTAGCACCGGTACTAAGT rev 116: AATGTTAATGCATCTGGAAATAAACG	94
psbA	for 99: TGGTGTTTTGATGATCCCTACCTTA rev 181: CAATATCTACTGGAGGAGCAGCAA	82
psbD190	for 62: GCGCGAGAAATTAAATCATAAACA rev 167: TCAACCATTTCCGAACACCTT	105
psbDLRP	for 238: GCAAAGTAATAACTAAAAGGGCGTTT rev 378: TTGATATCTGAAGCCATGATTATGATTC	140
rbcL	for 1009: GGAGACAGGGAGTCAACTTTG rev 1083: ACCGCGGCTTCGATCTTT	74
accD	for 801: TCCGGGTACTTGGAATCCTATG rev 879: ATAAGGTTCCTCCTTCGAATGAAAT	78
clpP	for 261: GCGACCCGATGTACAGACAA rev 329: CCTCCGACTAGGATAAAGGATGCT	68

* GeneBank acc. no. AP00043

mixture was distributed into three replicates of 10 µL each in 384-well amplification plates and sealed with optical adhesive covers (Applied Biosystems). For each primer pair, a no-template control (NTC) was also run in triplicate. The following amplification parameters were used for all PCRs: 10 minutes at 95^0C for optimal AmpliTaq Gold DNA polymerase activation followed by 47 cycles of denaturation at 96^0C for 10 sec and annealing/extending at 60^0C for 1 min. A dissociation curve was generated according to the protocol present in the ABI Prism 7900HT software (SDS v2.1). Briefly, following the final cycle of the PCR, the reactions were heat denatured over a 35^0C temperature gradient from 60^0 to 95^0C.

Real-time PCR: TaqMan Detection

The master mix for the real-time PCR using TaqMan detection consisted of 3.3 µL of cDNA with 29.7 µL of 2X TaqMan Master Mix (Applied Biosystems) supplemented with primers to a final concentration of 50 nM each, VIC-labeled hybridization probe to a final concentration of 50 nM and PCR-grade water to a 33 µL final total volume. This mixture was distributed into three replicates of 10 µL each in 384-well amplification plates and sealed with optical adhesive covers (Applied Biosystems). A no-template control (NTC) was also run in triplicate. Real-time PCR was performed identically to that described for SYBR Green detection except that the dissociation curve generation step was omitted.

Real-time PCR: Data Analysis

The data generated from both SYBR Green and TaqMan chemistries were analyzed in

a similar manner. The C_T values were determined using a signal/noise ratio set to 10 standard deviations above background subtracted mean fluorescence values (ΔR_n) for a baseline value adjusted manually for each set of primers. The real-time PCR data containing the C_T values were exported into a Microsoft® Excel spreadsheet for further analysis. Plastid gene expression was normalized to that of cytoplasmic 18S rRNA and expressed as $2^{-\Delta CT}$, where $\Delta C_T = (C_{T\ sample} - C_{T\ 18S\ rRNA})$. PCR efficiency for each primer pair was determined by analyzing a series of template dilutions (see Chapter II).The slope was calculated from the plot of log input versus C_T and exponential amplification (efficiency) was determined from the equation $E = 10^{(-1/slope)}$ (Rasmussen, 2001). In addition, the amplification efficiencies of the target genes and normalizer (18S rRNA) were compared by determining the slope from the plot of log template dilution versus $\Delta C_T = (C_{T\ sample} - C_{T\ normalizer})$ according to instructions given by Applied Biosystems (Relative quantitation of gene expression, User Bulletin # 2). The fold change in plastid transcript abundance relative to seeds was obtained from the ratios of the individual $2^{-\Delta CT}$ in each tissue to the respective $2^{-\Delta CT}$ values in seeds.

CHAPTER IV

IDENTIFICATION AND ANALYSIS OF A KNOCKOUT *RpoT;3* T-DNA INSERTION MUTANT

INTRODUCTION

In higher plants, plastid transcription has evolved into a highly complex system that involves at least two different groups of RNA polymerases, namely the plastid-encoded plastid RNAP (PEP) and the nucleus-encoded plastid RNAP (NEP). PEP is a eubacterial-type enzyme whose core subunits (α, β, β' and β'') are encoded by the plastid genes *rpoA*, *rpoB, rpoC1* and *rpoC2* which have sequence homology to the *E. coli* RNA polymerase subunits (Umesono and Ozeki, 1987; Igloi and Kössel, 1992; Allison *et. al*, 1996). The plastid *rpoB, rpoC1* and *rpoC2* genes are part of one transcription unit whereas *rpoA* is located at the distal end of a complex transcription unit that contains mainly genes encoding ribosomal protein subunits (see Table 11 in Chapter III). These operons are polycistronically transcribed and processed post-transcriptionally (Ruf and Kössel, 1988). The initiation specificity of the PEP enzyme is conferred by σ-type subunits that are encoded by the nucleus and are imported into the plastid post-translationally (reviewed in Link, 1996; Allison, 2000). So far, six sigma factor genes (SIG1 through SIG6) have been identified in *Arabidopsis thaliana* and five in maize (Tanaka *et al*., 1997; Isono *et al*., 1997b; Kanamaru *et al*., 1999; reviewed in Allison, 2000). In contrast, NEPs are a single-subunit enzymes encoded by nuclear *RpoT* genes that have sequence similarity to the RNA polymerases of T3, T7 and SP6

bacteriophages (Hedke *et al.,* 1997; Hajdukiewicz *et al.,* 1997). Three members of the *RpoT* gene family have been identified in *Arabidopsis thaliana* and six in *Nicotiana tabacum* (Hedke *et al*., 1997; 2000; 2002). The *Arabidopsis RpoT;1* and *RpoT;3* genes encode phage-type enzymes that are targeted exclusively either to mitochondria or plastids, respectively, whereas the *RpoT;2* gene encodes a phage-type enzyme that is targeted to both mitochondria and plastids (Hedke *et al.,* 1999; 2000).

Many plastid gene promoters contain sequences that resemble *E. coli* -10 (TATAAT) and -35 (TTGACA) promoter sequences (Hanley-Bowdoin and Chua, 1987; Gruissem and Tonkyn, 1993; Hess and Börner, 1999). These promoters are recognized by the plastid-encoded bacterial-type RNA polymerase (PEP) and can be recognized by the *E. coli* RNA polymerase *in vitro* (Sugiura, 1992; Gruissem and Tonkyn, 1993). Analysis of transcription initiation in the plastid ribosome-deficient *albostrians* mutants of barley (Hübschmann and Börner, 1998) as well as in transplastomic tobacco plants that lack PEP activity because of targeted mutation of one of the *rpo* genes (Allison *et al.*, 1996; Serino and Maliga, 1998; DeSantis-Maciossek *et al*., 1999; Liere and Maliga, 1999) led to the identification of consensus NEP promoters that contain the core sequence YRTA [Y = (T, C), R = (A, G)] that is similar to mitochondrial promoters (Class Ia promoters) (Hess and Börner, 1999; Weihe and Börner, 1999). Examples of class Ia NEP promoters include the *Nicotiana tabacum rpoB-147*, *rpoB-345*, *accD-129*, *rps2-152* and *ycf-1577* (reviewed in Weihe and Börner, 1999). Some NEP promoters such as *atpB-289* from *Nicotiana tabacum* contain a GAA motif upstream of the YRTA motif and have been designated as class Ib NEP promoters (Kapoor and Sugiura, 1999). In addition, other non-consensus or exceptional NEP promoters have been described that do not contain a YRTA motif. Examples of non-consensus promoters are the *clpP-53*

promoter in tobacco that was found to be conserved in liverworts and conifers (Sriraman *et al.*, 1998a) and a non-consensus NEP promoter in the ribosomal RNA operon (*rrn*) of spinach (Iratni *et al*., 1994; Bligny *et al*., 2000; reviewed in Lerbs-Mache, 2000). Finally, some plastid tRNA genes (*trnS*, *trnQ* and *trnH* from mustard) contain internal sequence elements that are similar to those for nuclear tRNA genes recognized by RNA polymerase III (Galli *et al*., 1981; Stern *et al*., 1997; reviewed in Hess and Börner, 1999). At present there is no direct evidence for an RNA Pol III – type RNAP in plastids.

Analysis of transcription activity in PEP-deficient tobacco plants (Allison *et al*., 1996; Hajdukiewicz *et al*., 1997; reviewed in Hess and Börner, 1999) has led to the classification of plastid genes into three classes: (1) genes with promoters transcribed by PEP (mostly genes encoding photosynthetic proteins such as *psaA*, *psbA*, *psbC*, *psbD*, *psbE* but also *ndhA*, encoding a subunit of the NADH dehydrogenase complex and *petB*, encoding a component of the cytochrome b_6/f complex), (2) genes with promoters transcribed by both PEP and NEP (genes encoding components of the transcription and translation apparatus such as *rps16*, *rrn16*, genes encoding subunits of the ATP synthase complex (*atpB*) and NADH dehydrogenase complex (*ndhB*, *ndhF*) and one gene encoding a subunit of the Clp protease (*clpP*) and, (3) genes with promoters transcribed by NEP (genes encoding components of the transcription and translation apparatus such as *rpl33-rps18*, *rpoB* and one gene encoding a subunit of the acetyl-CoA carboxylase (*accD*). Based on these results it was proposed that NEP functions mainly in non-green tissues to initiate transcription of the *rpo* genes encoding subunits of PEP, whereas PEP transcribes genes of the photosynthetic apparatus in green tissues (Hajdukiewicz *et al*., 1997; Maliga, 1998; Hess and Börner, 1999). Run-on

transcription analysis of PEP-deficient plastids revealed that most plastid genes are transcribed to some extent in the absence of PEP (Krause *et. al*., 2000, Legen *et. al*., 2002).

To date little is known about how the relative activity of NEP and PEP modulate transcription during plastid development. The aim of the present study was to study the role of the plastid NEP enzyme encoded by *RpoT;3*. To do this we identified and characterized an *Arabidopsis thaliana* T-DNA insertion mutant that disrupts the *RpoT;3* gene. To gain further insight into the functional role of this polymerase in different tissues and stages of chloroplast development, quantitative real-time PCR was used to investigate transcript abundance for twentry-eight plastid genes in both wild-type and mutant tissues.

RESULTS

Identification of an *RpoT;3* T-DNA Insertion Mutant

We searched the sequence-indexed *Arabidopsis* T-DNA insertion database provided by the SALK Institute Genomic Analysis Laboratory (SIGnal) (http:// signal.salk.edu/cgi-bin/tdnaexpress) for an *RpoT;3* mutant. One T-DNA –tagged line was identified in which the T-DNA was inserted into the *RpoT;3* coding region (SALK_067191) of the Columbia 0 ecotype. PCR with primers designed to detect T-DNA insertions or a wild-type sequence identified several plants that were heterozygous for the T-DNA insertion and exhibited a phenotype indistinguishable from that of wild-type plants. Genomic DNA isolated from the heterozygous plants was subjected to a second round of PCR using a

second primer for the left border of the T-DNA. One heterozygous plant was allowed to self-pollinate, and its progeny were screened on agar plates for visible phenotypic alterations. Approximately 25% of the progeny (414/1089) exhibited a significantly pale green phenotype while the rest of the plants exhibited a phenotype indistinguishable from wild-type plants (Figure 13A, *rpoZ191*). The phenotypic segregation profile of the progeny is explained most easily if the original plant was hemizygous for a single T-DNA insertion and the pale *rpoZ191* plants corresponded to plants homozygous for the insertion. Therefore, green and pale green *rpoZ191* plants were screened by PCR with primers designed to amplify the wild-type or the T-DNA-tagged allele. The results indicated that all the pale green plants examined were homozygous for the *RpoT;3* disruption. The homozygous plants also displayed a delay in greening and were retarded in growth compared to wild-type. The mutant plants were viable upon transfer to soil, but the green tissues remained pale green throughout the life cycle of the plants. Additional differences in phenotype were observed including deeply serrated leaves, shorter siliques and reduced apical dominance (Figure 13A, B and C).

A DNA fragment flanking the left border of the T-DNA was isolated and its sequence was found to be identical to that of the *RpoT;3* gene of *Arabidopsis thaliana* (GenBank accession number: Y08722). The T-DNA insertion site was located in the eighteenth exon of *RpoT;3* , at position +2827 relative to the first ATG codon (Figure 14). Real-time PCR analysis of 2-day old wild-type and mutant seedlings was performed to examine the effect of T-DNA insertion on the *RpoT;3* transcript levels. No product was obtained after 47 cycles of PCR amplification with primers that flank the T-

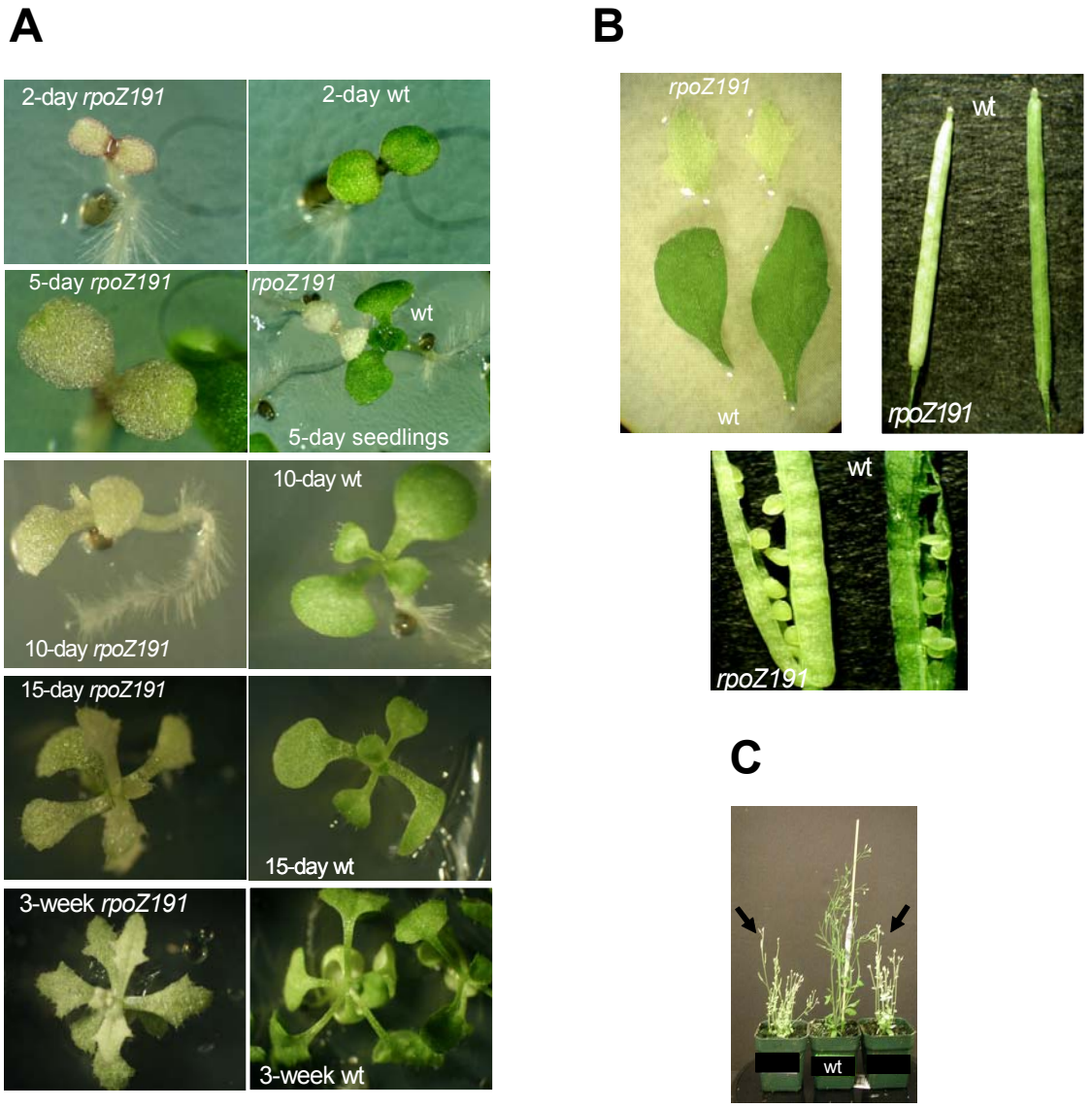

Figure 13. Phenotype of the *rpoZ191* mutant at different developmental stages.

Imbibed seeds of mutant and wild-type *A. thaliana* were sown on MS medium containing 1% sucrose. The seeds were placed at 4^0C under dark for 5 days to synchronize germination and then cultivated under continuous light (40μmol m^{-2} sec^{-2}).
After 15 days some seedlings were transferred to soil whereas others were transferred to fresh plates.

(A) Comparison of mutant and wild-type seedlings grown on plates.
(B) Comparison of mutant and wild-type leaves and siliques.
(C) Mature mutant (arrows) and wild-type plants

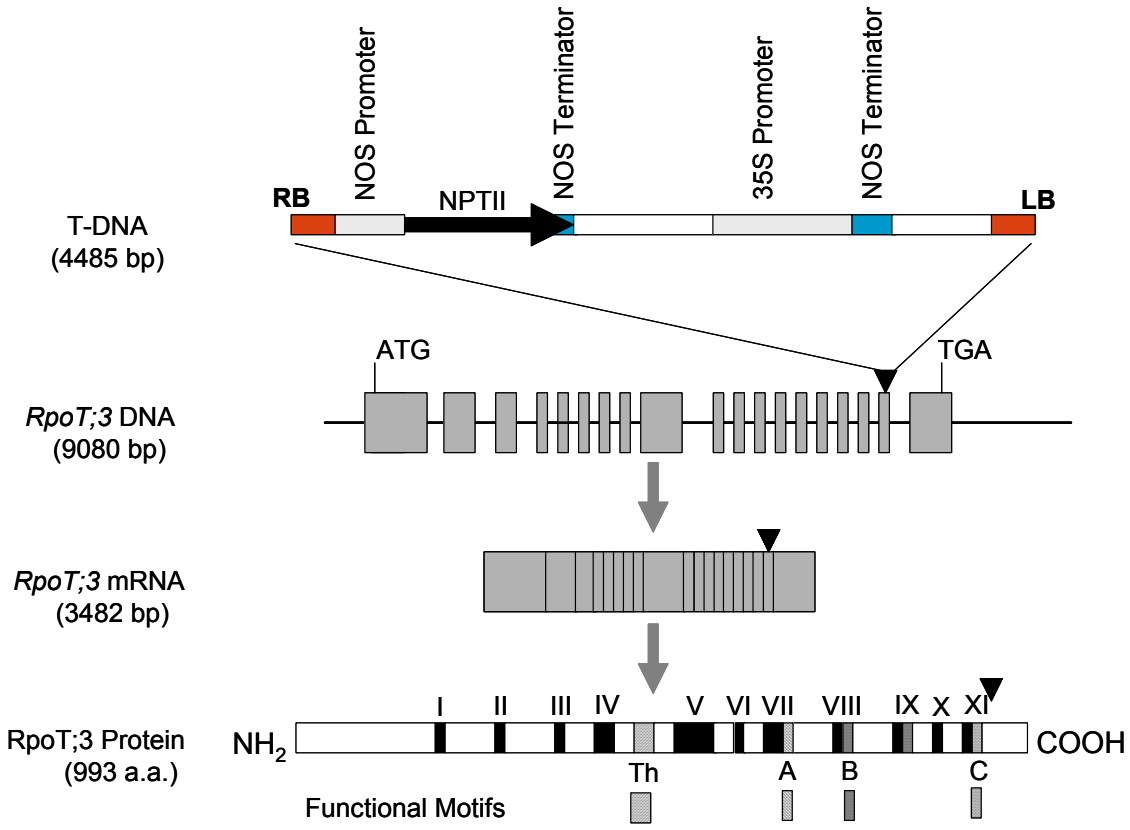

Figure 14. Insertion of T-DNA into *the RpoT;3* gene of *A.thaliana*.

The structures of T-DNA at the insertion site, of *RpoT;3* mRNA, and of the RpoT;3 protein are shown.. Roman numerals indicate conserved domains (I-XI) between RpoT;3, T7 RNA polymerase and other RNA polymerases. Motifs A, B, and C are part of the catalytic pocket (McAlister and Raskin, 1993) whereas the thumb (Th) motif is structurally similar to that of the Klenow fragment of DNA polymerase I and reverse transcriptase (Sousa et al., 1993). An arrowhead indicates the site of T-DNA insertion – exon 18 of *rpoT;3* which encodes part of domain XI including motif C. LB, left border of T-DNA; RB, right border of T-DNA.

DNA insertion site ($2^{-\Delta CT}$ (*rpoZ191*) = 0.03). Similar results were obtained with primers for the 3′ coding region flanking the T-DNA insertion ($2^{-\Delta CT}$ (*rpoZ191*) = 0.04). Real-time PCR analysis of the *RpoT;3* 5′ coding region revealed enhanced transcript

accumulation in the mutant plant (2-fold increase relative to the wild-type) indicating that the T-DNA insertion did not result in loss of the *RpoT;3* mRNA but caused accumulation of a truncated transcript. This insertion, however, would generate a truncated RpoT;3 protein lacking the conserved domain XI of the carboxy terminus which has been shown to be essential for the activity of the T7 RNA polymerase (reviewed in Hess and Börner, 1999). Because this conserved domain contains motif C which together with motifs A and B forms the catalytic pocket of T7 RNA polymerase (McAllister and Raskin, 1993), it is presumed that a truncated RpoT;3 protein expressed from *rpoZ191* is nonfunctional.

Ultrastructural Analysis

The effect of the *rpoZ191* mutation on chloroplast structure in 2-day and 7-day-old cotyledons was examined by electron microscopy (Figure 15). While wild-type 2-day-old cotyledons contained normal chloroplasts with numerous stacked grana thylakoids and evenly distributed plastoglobuli (Figure 15A), the plastids of mutant cotyledon cells at the same stage were smaller and appeared less differentiated internally (Figure 15B). The proliferation of thylakoid membranes and stacked grana thylakoids were not observed while clusters of plastoglobuli (PG) were predominant. In contrast, the chloroplasts from 7-day cotyledons of mutant plants had far more developed lamellar structure and resembled the wild-type plastids in size and shape (Figure 15C and D). These observations indicate that the *rpoZ191* mutation affects chloroplast development in the early stage of seedling growth in the light.

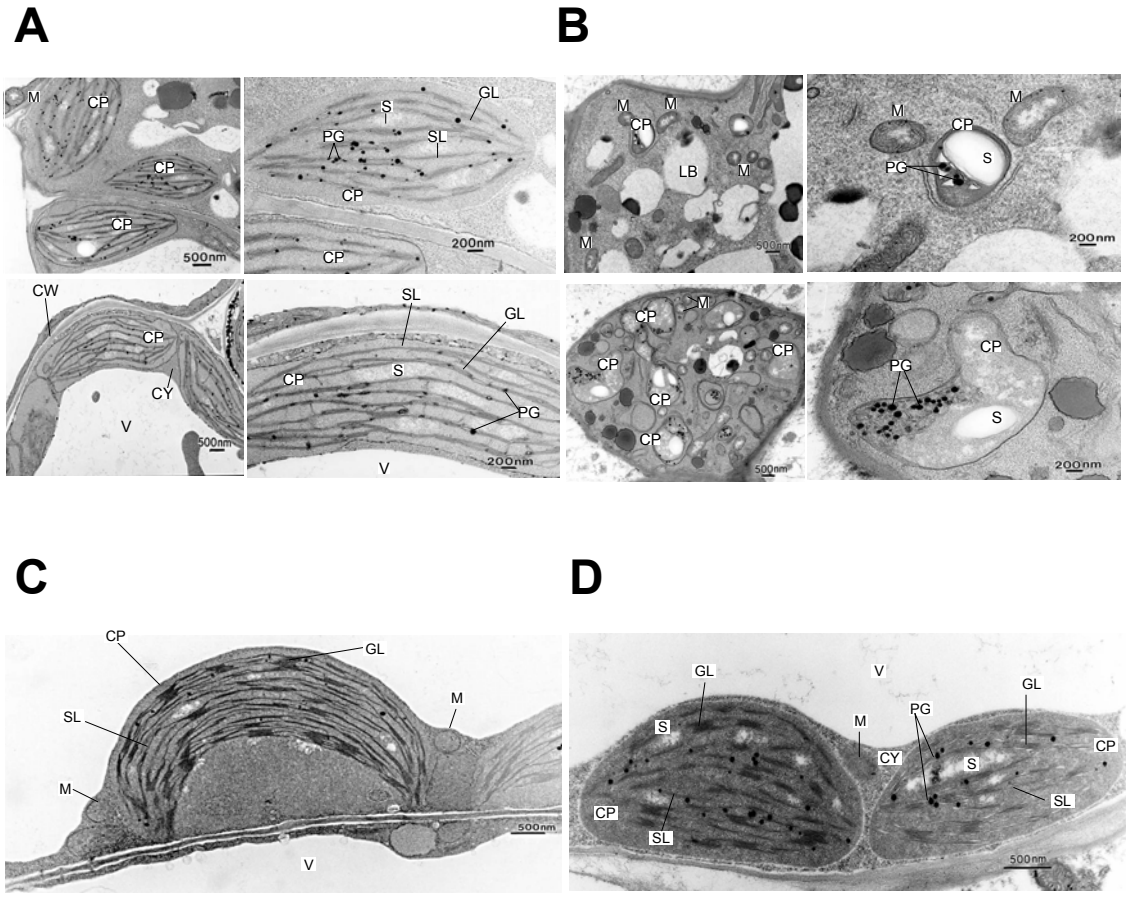

Figure 15. Transmission electron micrographs of thin sections from cotyledons of wild-type and *rpoz191 Arabidopsis* mutants.

(A) Cotyledons of 2-day-old wild-type.
(B) Cotyledon cells of 2-day-old *rpoZ191* mutant. Note the higher magnification of wild- type and *rpoZ191* mutant plastids (right panels).
(C) Cotyledons of 7-day-old wild-type.
(D) Cotyledons of 7-day-old *rpoz191* mutant. Abbreviations; CP, chloroplast; CW, cell wall; CY, cytoplasm; GL, grana lamellae; LB, lipid bodies; M, mitochondria; PG, plastoglobuli; S, starch; SL, stroma lamellae; V, vacuole.

Plastid Gene Transcript Accumulation in the *rpoZ191* Mutant

Experimental Design

Quantitative real-time PCR was used to investigate whether plastid gene transcript abundance is altered in the *RpoT;3* mutants. Primer pairs were designed for twenty-eight plastid target genes based on the sequence of *Arabidopsis thaliana* chloroplast DNA (Sato *et al*., 1995). To correct for differences in input RNA, all quantifications were normalized to the amount of cytoplasmic 18S rRNA and expressed as $2^{-\Delta CT}$, where $\Delta C_T = (C_{T\ sample}-C_{T\ normalizer})$ based on the method outlined by Schmittgen and Zakrajsek (2000) and Livak and Schmittgen (2001). Real-time PCR reactions for each set of primers were performed in triplicate along with non-template control reactions and the specificity of the RT-PCR products was verified by both electrophoretic and melting curve analysis. In addition, all primer sets were tested for comparable amplification efficiencies with the endogenous reference primers by plotting the ΔC_T value against the log cDNA input. Only primer sets that showed little variation in amplification efficiency over the dilution series were employed for quantification of mRNA levels (see Table 7 and Figures 6 & 7 in Chapter II).

Quantitative analysis of RNA levels was performed on plastid genes encompassing a range of functions and operons (see Table 11 in Chapter III for a list of genes and operons analyzed in this study). These genes include: (1) four genes encoding 30s and 50s ribosomal subunits, (2) one gene encoding 16S rRNA, (3) six genes for tRNAs, (4) two genes encoding subunits of the plastid RNA polymerase, (5) two genes encoding subunits of the ATP synthase complex, (6) one gene encoding a

component of the cytochrome b_6/f complex, (7) four genes encoding components of the NADH dehydrogenase complex, (8) six genes encoding components of photosystem I, photosystem II and Rubisco, (9) one gene encoding for a protein involved in lipid biosynthesis, and (10) one gene encoding for an enzyme involved in protein degradation. Except for *psbD*, the primers did not distinguish between the various transcripts generated from a given operon. The *psbD* operon, which includes the *psbD*, *psbC* and *psbZ* genes encoding PS II components, has been shown to have multiple promoter elements giving rise to a complex set of transcripts. At least four *psbD* mRNA 5′-ends have been reported, located at positions 190, 256, 550 and 950 with respect to the translation initiation site (Hoffer and Christopher, 1997; Christopher and Hoffer, 1998; Hanaoka *et a*l., 2003). The best characterized of these promoters is the blue-light regulated promoter (LRP), which is located the furthest upstream of the multiple promoters and has been shown to produce an mRNA that originates at the -950 position (Hoffer and Christopher, 1997). Because *psbD* transcripts have been shown to exhibit differential patterns of accumulation, we designed one primer set that specifically detects the RNA transcribed from psbD-LRP whereas a second set of primers was used to monitor the levels of all transcripts carrying *psbD* coding sequences.

Tissues and Plastid Transcripts Analyzed

Plastid mRNA abundance in several tissues and from different developmental stages was monitored in both wild-type and *rpoZ191* mutant by real-time PCR. Transcript levels for twenty-eight plastid genes were quantified in dry seeds, 2-day seedlings, 5-day seedlings, 5-day roots, 40-day roots and 34-day siliques. In addition, the levels of

mRNAs for a subset of plastid genes (*rpoA*, *rrn16*, *rbcL*, *psbA*, and *psbD*) were examined in 10-day, 12-day and 15-day cotyledons, as well as in 35-day rosette leaves and 35-day cauline leaves. The results of this study were grouped in three clusters (I, IIA/B and III) according to the pattern of transcript accumulation previously identified for the wild-type plants and are shown in Figure 16.

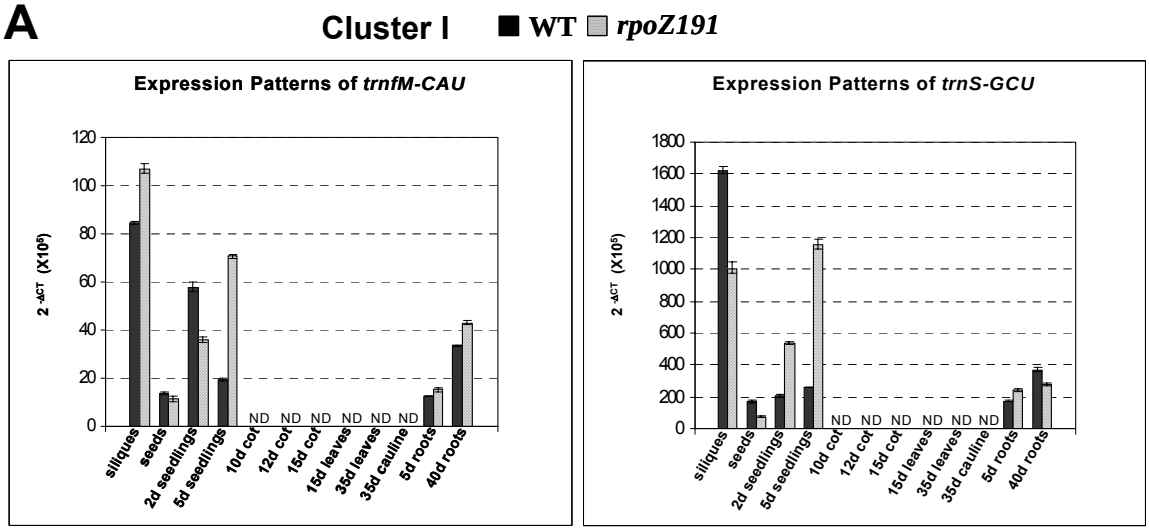

Figure 16. Expression profiles of individual plastid genes in wild-type and *rpoZ191* plants.

Total RNA was isolated from siliques, seeds, 2-day seedlings, 5-day seedlings, 5-day roots, 40-day-roots,10-day cotyledons, 12-day cotyledons, 15-day cotyledons and 15-day rosette leaves of wild-type and *rpoZ191* seedlings grown on MS medium supplemented with 1% sucrose as well as from 35-day rosette leaves and 35-day cauline leaves of wild-type and *rpoZ191* plants grown on soil after a 15-day period of growth on MS medium containing 1% sucrose. Equivalent amounts of total RNA from each tissue were converted to cDNA and employed as template for real-time PCR analysis. Reactions were run in triplicate and data were normalized relative to cytoplasmic 18S rRNA levels and expressed as $2^{-\Delta CT}$ X10^5, where $\Delta C_T = (C_{T\ sample}-C_{T\ normalizer})$. Plastid genes were grouped according to the clusters of expression patterns identified in Figure 12 (Chapter III).
(A) Expression profiles of Cluster I plastid genes
(B) Expression profiles of Cluster IIA plastid genes.
(C) Expression profiles of Cluster IIB plastid genes.
(D) Expression profiles of Cluster III plastid genes.

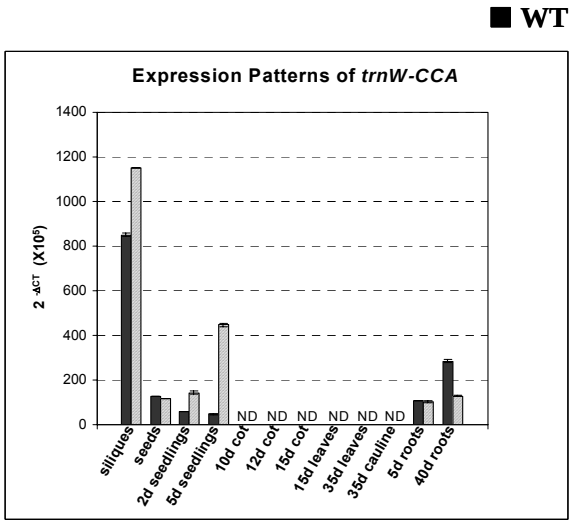

B **Cluster IIA**

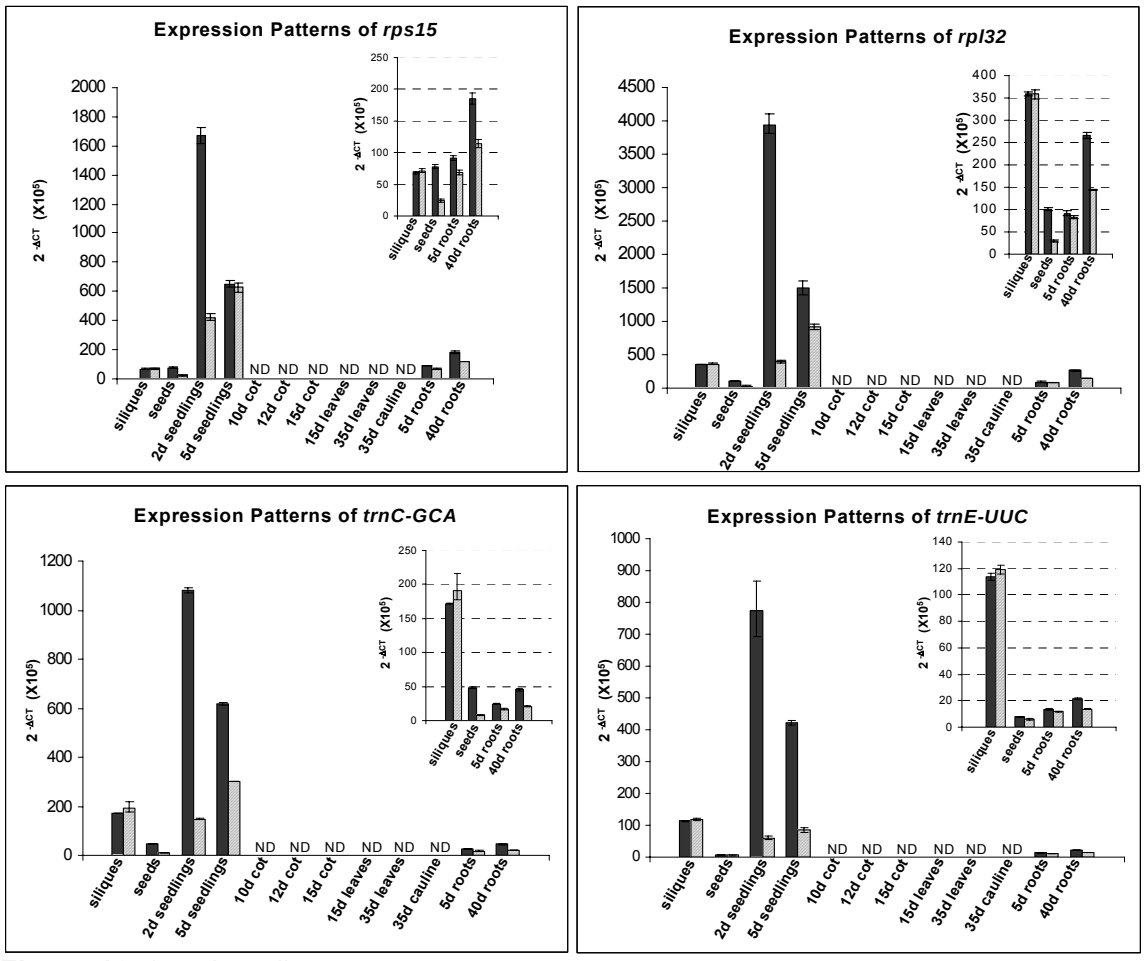

Figure 16. (continued).

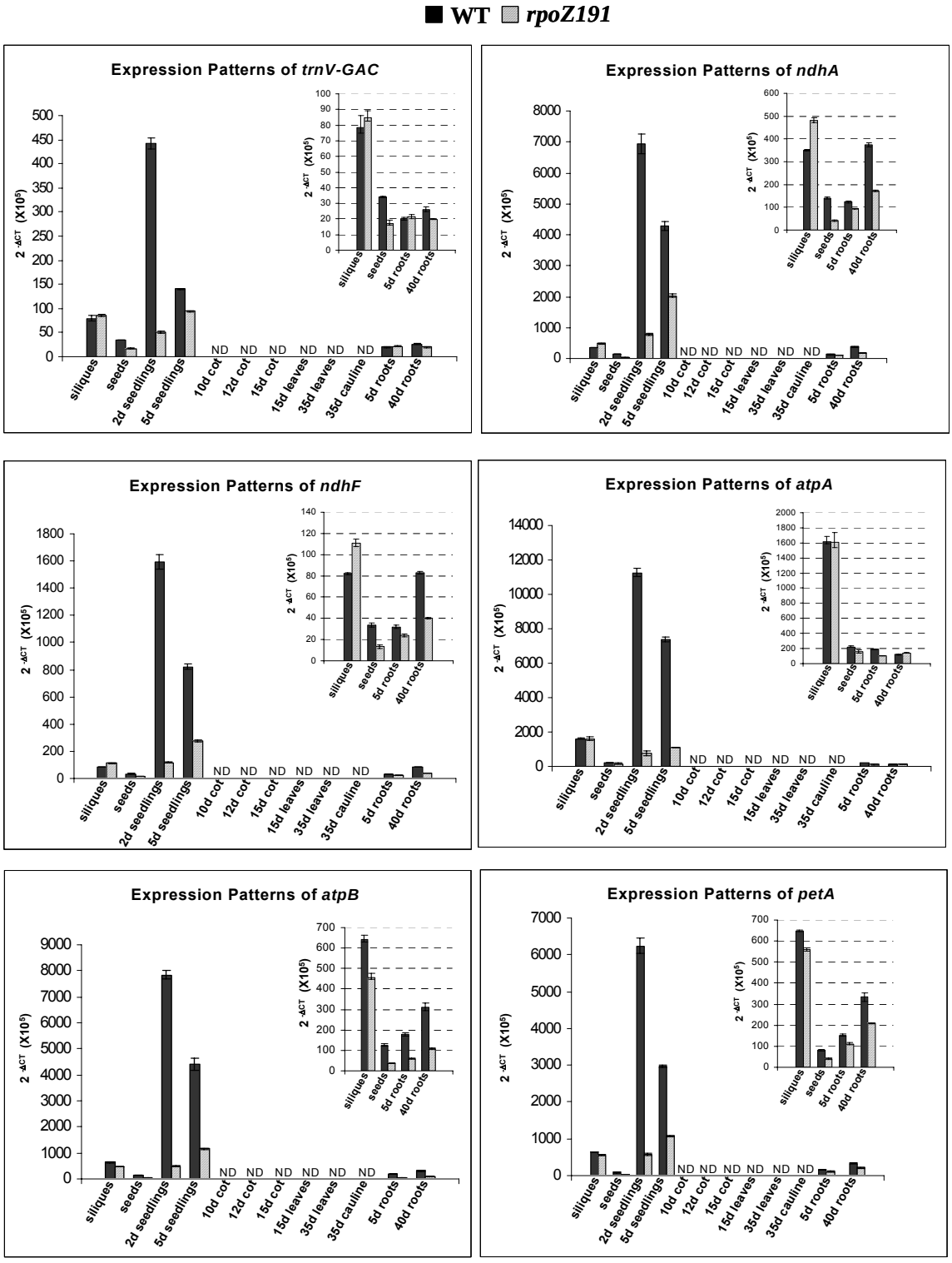

Figure 16. (continued).

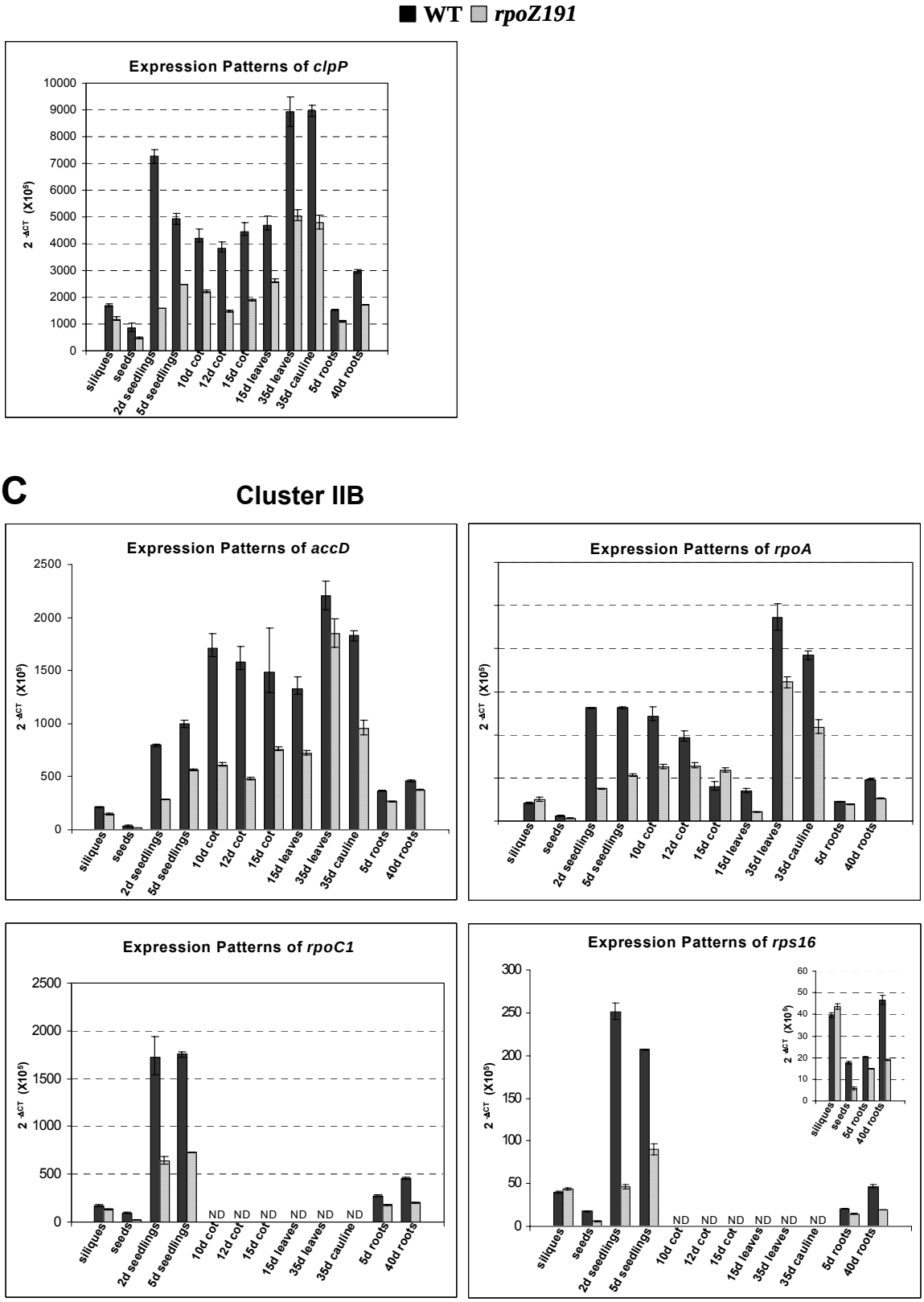

Figure 16. (continued).

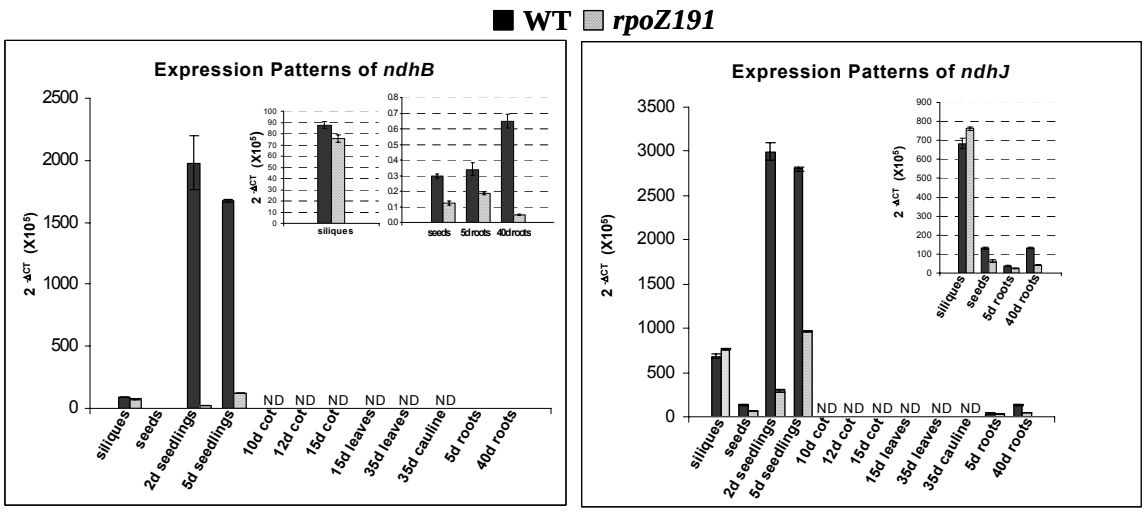

D **Cluster III**

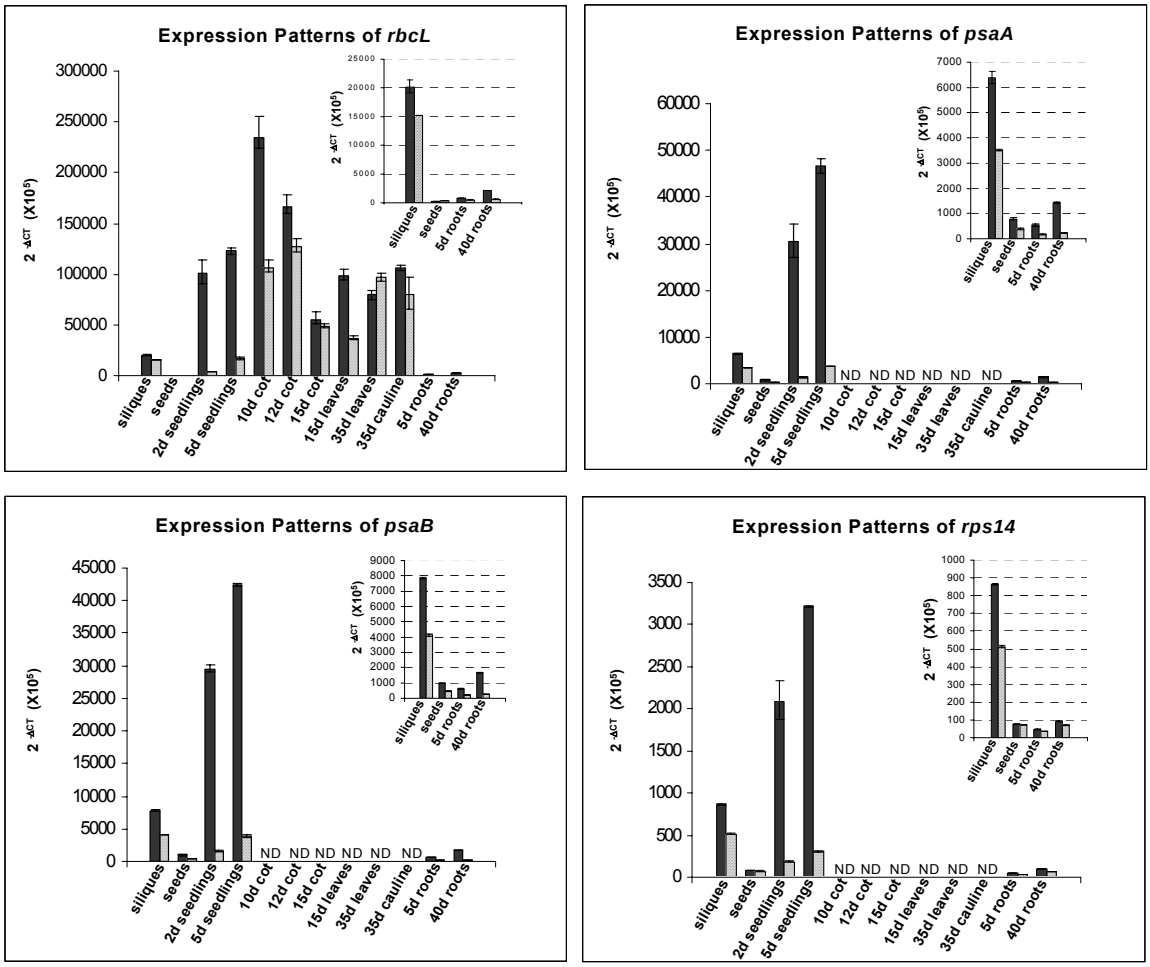

Figure 16. (continued).

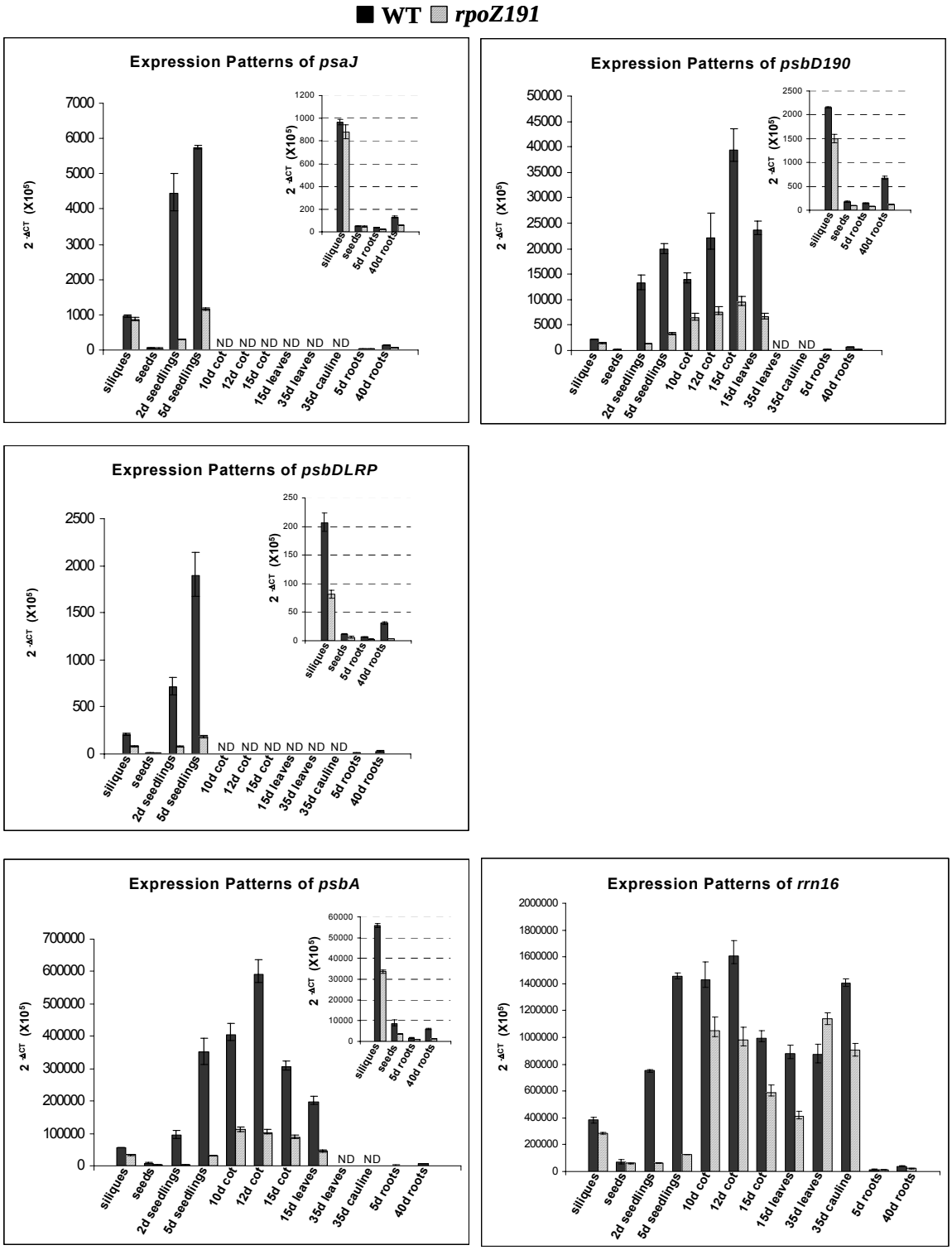

Figure 16. (continued).

Survey of Plastid Transcript Accumulation in Various Tissues and Stages of Development of the *RpoT;3* Mutant

A. Effect of RpoT;3 Mutation on Plastid Transcript Levels in Siliques, Seeds, 2-day Seedlings, 5-day Seedlings, 5-day Roots and 40-day Roots

The results of real-time PCR analysis of plastid transcripts using RNA from siliques, seeds, 2-day seedlings, 5-day seedlings, 5-day roots and 40-day roots showed distinct tissue specific effects of the *RpoT;3* mutation (Figure 17A; see also Figure 16). For example, in siliques the levels of plastid transcripts in the mutant were not significantly different from those of the wild-type (Figure 17A and B, see also Table 23 in Appendix A) except for the tricistronic *psaA-psaB-rps14*, *psbA* and *psbDLRP* transcripts which showed a moderate decrease in the mutant compared to the wild-type (from ~1.7-to 2.6-fold). A moderate reduction in the transcript levels of plastid genes (from ~1.4-fold to 5.8-fold) was also recorded in the *rpoZ191* mature seeds (Figure 17A and C, see also Table 24 in Appendix A). While the levels of most plastid transcripts in 5-day roots of wild-type and *rpoZ191* mutant plants were quite similar, transcript accumulation in 40-day light-exposed roots was moderately reduced in the mutant compared to the wild type (Figure 17A and D) with the *ndhB* transcripts exhibiting the largest reduction in abundance (~13-fold). The most dramatic effect of the *RpoT;3* mutation was seen in the 2-day seedlings (Figure 17A and E). At this stage, the abundance of plastid transcripts was significantly lower in mutant than in the wild-type. However, the reduction in transcript accumulation in the *rpoZ191* 2-day seedlings varied depending on the gene

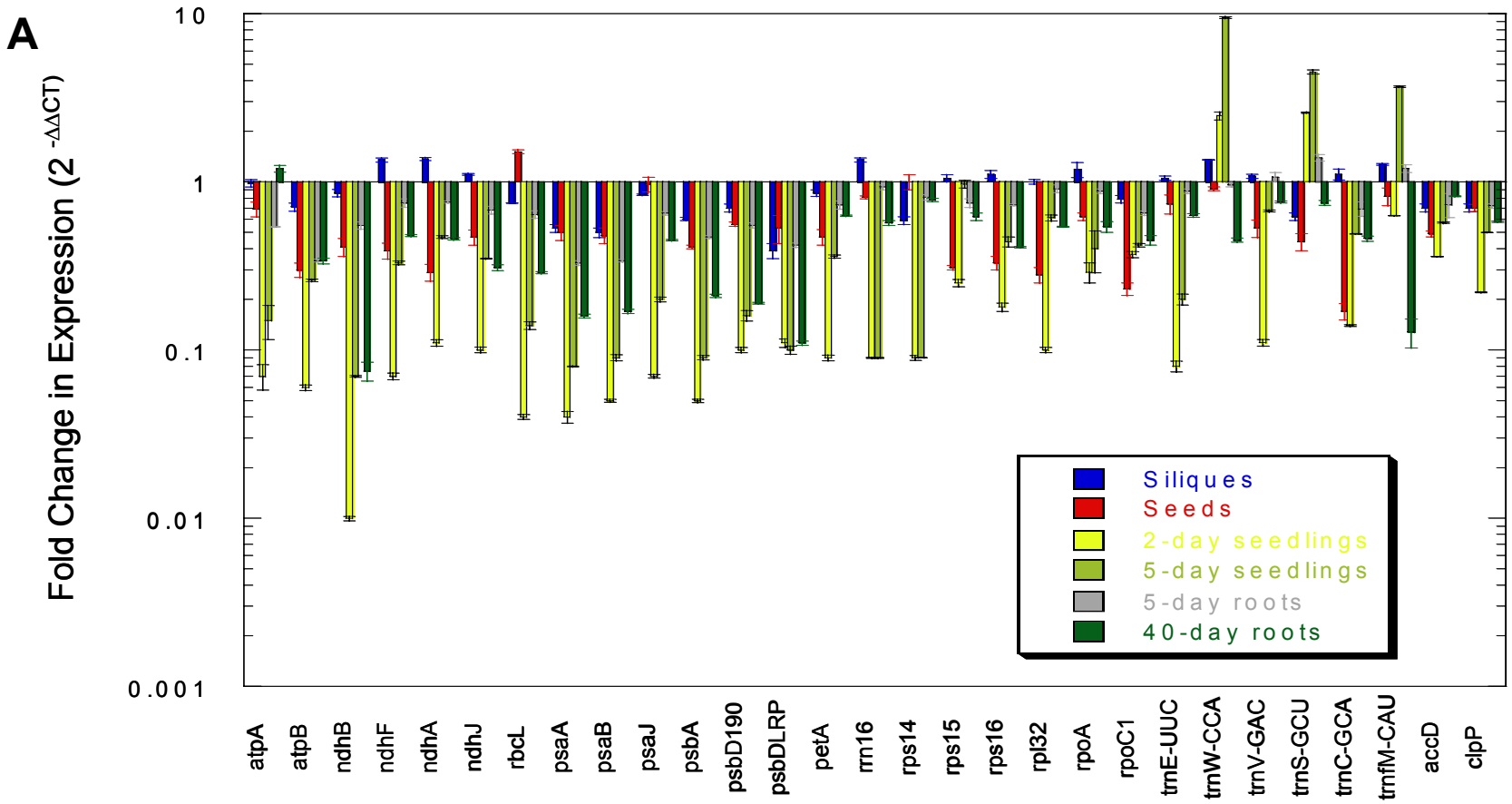

Figure 17. Relative fold changes in mRNA abundance of plastid genes in the *rpoZ191* mutant.

Total RNA was isolated from siliques, seeds, 2-day seedlings, 5-day seedlings, 5-day roots and 40-day roots of wild-type and *rpoZ191* seedlings grown on MS medium containing 1% sucrose. A cDNA input corresponding to 10 ng of reverse transcribed total RNA was used for real-time PCR analysis. The 18S rRNA normalized real-time PCR data were used to determine the relative fold change calculated using the $2^{-\Delta\Delta CT}$ method, where $\Delta\Delta C_T = \Delta C_{T\ mutant} - \Delta C_{T\ wild\text{-}type}$, and ΔC_T is the C_T of the normalizer subtracted from the C_T of the target gene. The mean of each triplicate well is plotted and the error bars represent SD calculated from the SD values of the target gene and the 18S rRNA values.

(A) Fold changes in mRNA abundance of plastid genes from siliques, seeds, 2-day seedlings, 5-day seedlings, 5-day roots and 40-day roots.

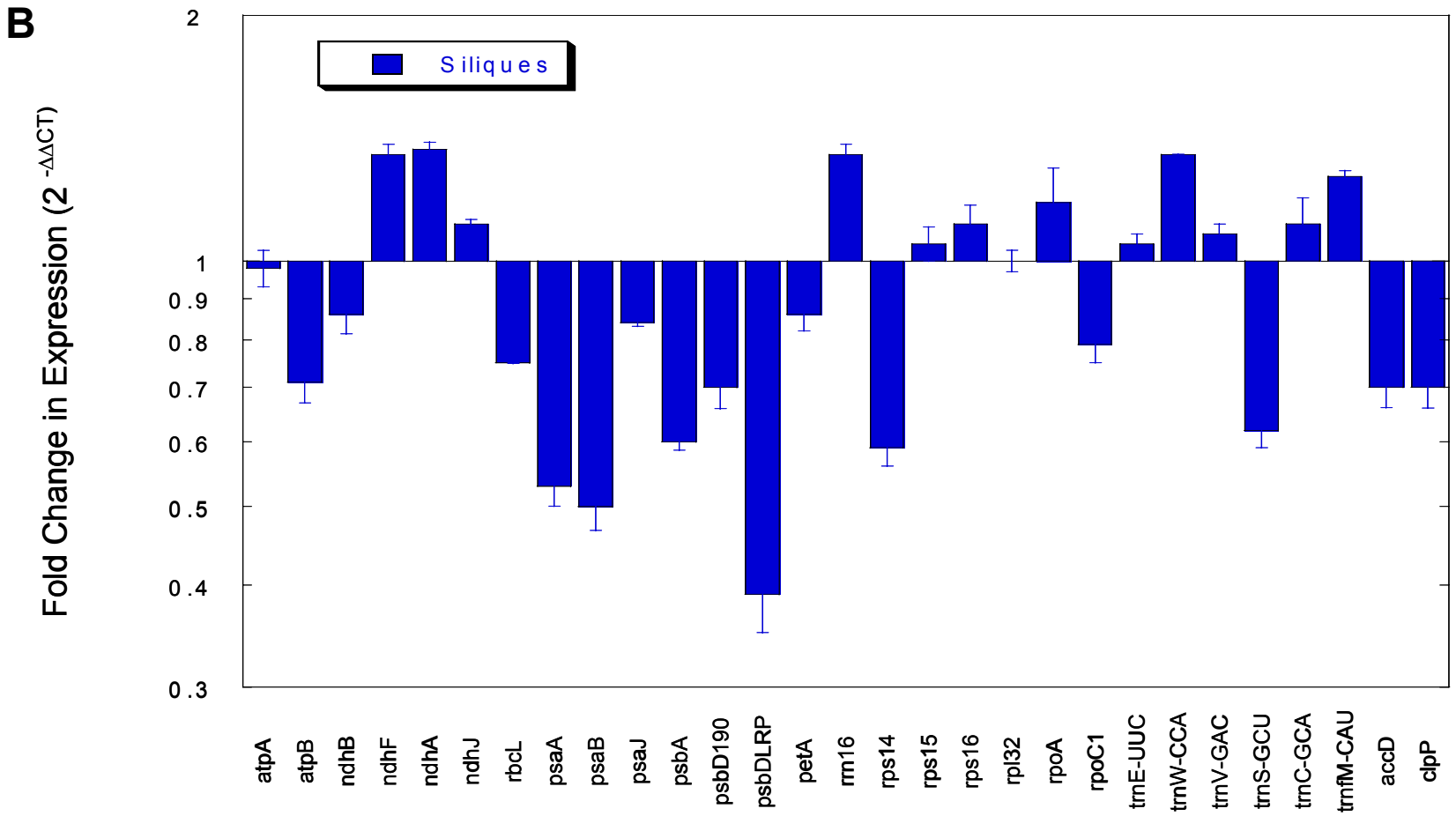

Figure 17. (continued).

(B) Fold changes in mRNA abundance of plastid genes from siliques.

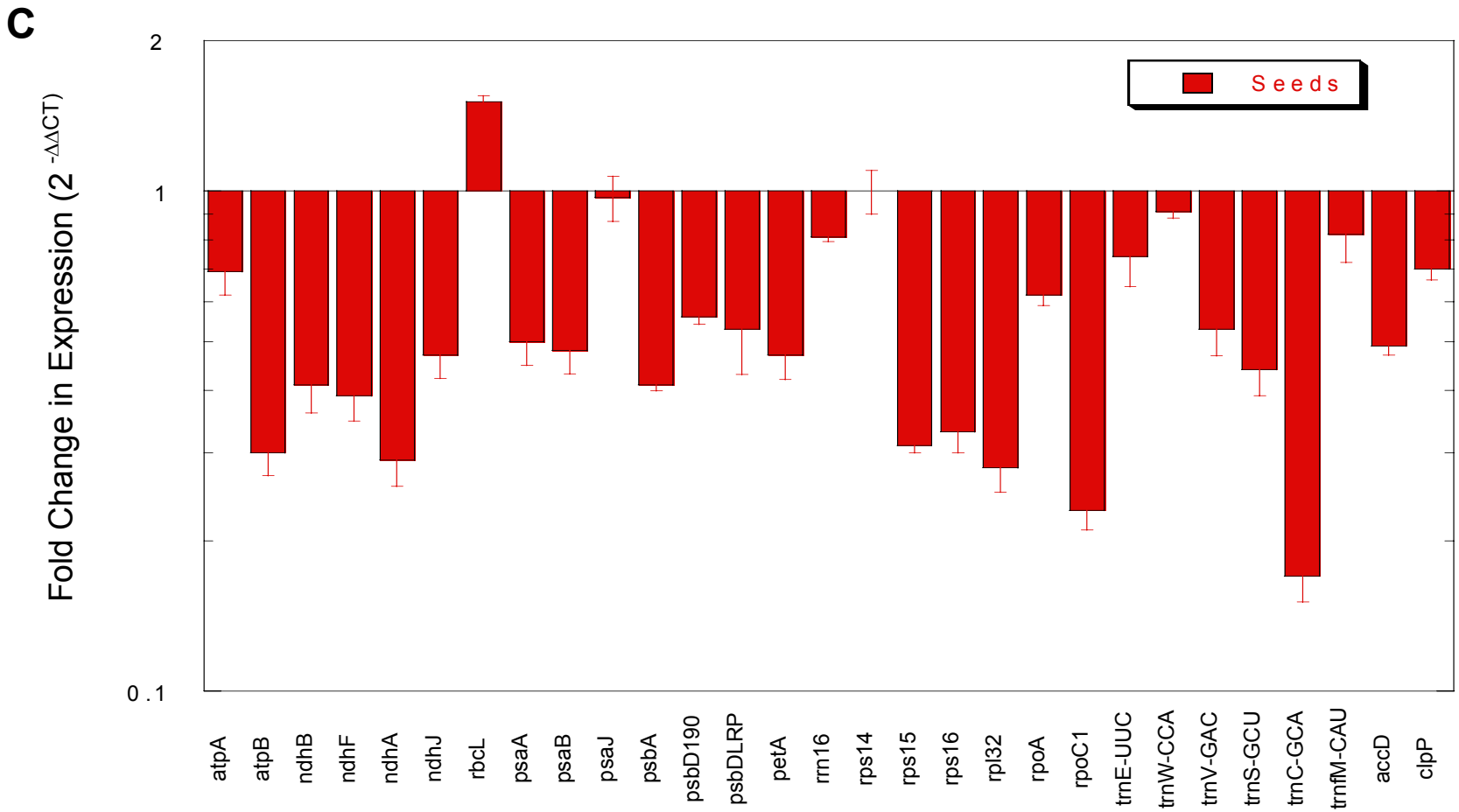

Figure 17. (continued).

(C) Fold changes in mRNA abundance of plastid genes from seeds.

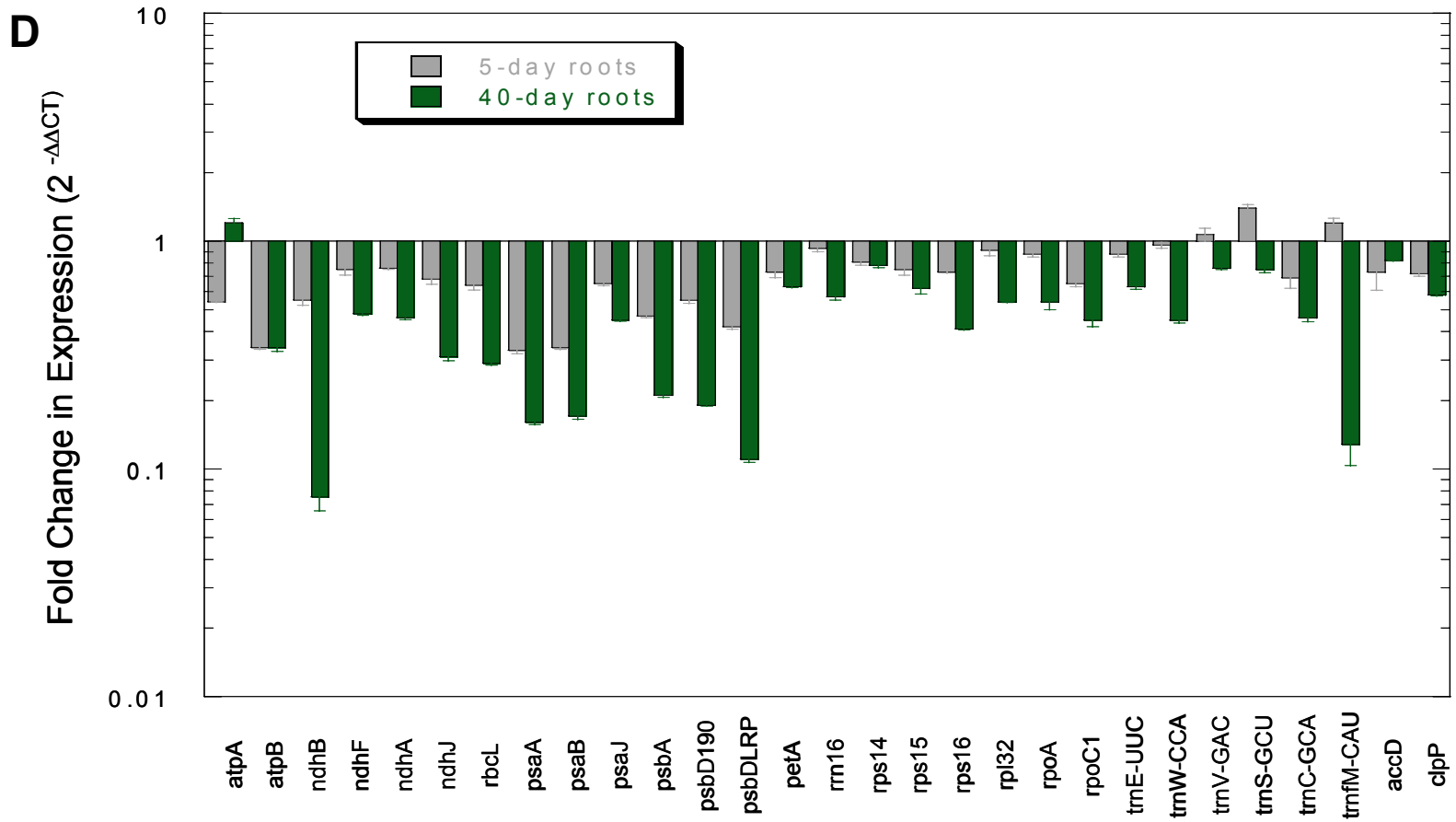

Figure 17. (continued).

(D) Fold changes in mRNA abundance of plastid genes from 5-day and 40-day roots.

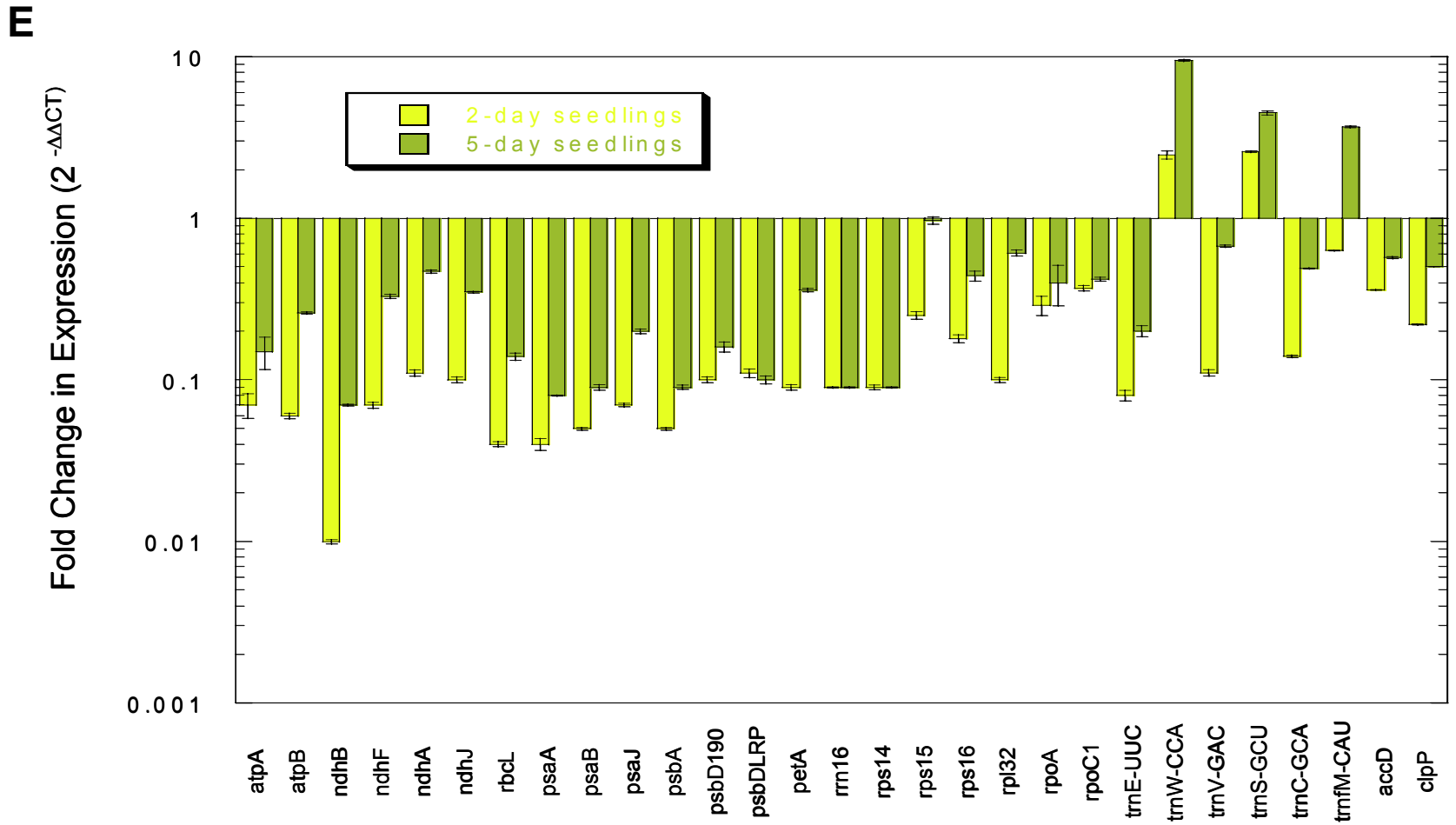

Figure 17. (continued).

(E) Fold changes in mRNA abundance of plastid genes from 2-day and 5-day seedlings.

studied. For example, transcripts for *rpoC1* and *rpoA*, encoding subunits of the plastid RNA polymerase, *rps15, rps16* and *rpl32* encoding ribosomal protein subunits, tRNAs (*trnfM-CAU*, *trnC-GCA* and *trnV-GAC*), *accD*, encoding a subunit of the plastid acetyl-CoA carboxylase, *clpP*, encoding the catalytic subunit of a plastid protease, *ndhA* and *ndhJ*, encoding subunits of the plastid NADH dehydrogenase complex *psbD190* and *psbDLRP*, encoding a photosystem II component, decreased ~1.6- to 10-fold in the mutant. In contrast, transcripts for *rps14*, *rrn16* and *trnE-UUC*, the NADH dehydrogenase complex (*ndhB* and *ndhF*), the ATP synthase complex (*atpA* and *atpB*), cytochrome b_6/f complex (*petA*) photosystem I (*psaA*, *psaB* and *psaJ*), photosystem II (*psbA*) and Rubisco (*rbcL*) exhibited significantly lower levels in the mutant than in the wild-type with the transcript for *ndhB* exhibiting the largest decrease in relative abundance (~112-fold decrease relative to the wild-type). Surprisingly, two tRNAs, *trnS-GCU* and *trnW-CCA*, exhibited higher transcript levels in the mutant compared to the wild-type (~2.5-fold).

Quantitative analysis of plastid transcript accumulation in mutant plants revealed a general increase of RNA levels in 5-day seedlings as compared to 2-day seedlings except for *rrn16*, *rps14* and *psbDLRP* transcripts that were not significantly different from those of the 2-day mutant plants (Figure 17A and E). However, most transcripts in the *rpoZ191* mutant accumulated at a lower level than in the wild-type at the 5-day stage (from ~2- to 14-fold decrease relative to wild-type plants). On the other hand, three tRNA transcripts exhibited an increase of 3.7-fold (*trnfM-CAU*), 4.5-fold (*trnS-GCU*) and 9.5-fold (*trnW-CCA*) in mutant relative to wild-type 5-day seedlings.

B. Effect of RpoT;3 Mutation on Plastid Transcript Levels in 10-day, 12-day and 15-day Cotyledons

Transcript accumulation for a subset of plastid genes was analyzed in 10-day, 12-day and 15-day cotyledons of wild-type and *rpoZ191* mutant plants (Figure 18A). The genes examined included *rpoA* and *rrn16*, encoding components of the plastid transcription and translation apparatus, *psbA*, *psbD190* and *rbcL*, encoding components of photosystem II and Rubisco, *accD*, encoding a subunit of the plastid acetyl-CoA carboxylase and *clpP*, encoding the proteolytic subunit of an ATP-dependent protease For this experiment, imbibed seeds sown on MS medium supplemented with 1% sucrose were placed at 4^0C for 48 hrs under dark conditions, and then germinated at 23^0C under continuous light. Real-time PCR analysis revealed a general reduction in the individual mRNAs levels. However, the RNA accumulation levels in the *rpoZ191* mutant varied depending on the gene and developmental stage examined. For example, transcript levels of *rpoA*, *rbcL* and a*ccD*, which in the wild-type peak at day 10 (~22-, 1006- and 50-fold relative to mature seeds; see Table 13 in Chapter III)) and then progressively decline at days 12 and 15 showed the greatest reduction in 10-day or 12-day cotyledons whereas transcript amounts of *rrn16* and *psbA*, which in the wild-type peak at day 12 (~23-and 68-fold relative to seeds) and decline at day 15, showed the greatest reduction in 12-day cotyledons. On the other hand, *psbD190*, which in the wild-type exhibits a progressive increase in transcript accumulation and reaches its peak at day 15 (~222-fold relative to mature seeds, showed the greatest reduction relative to wild type in 15-day cotyledons. Finally, *clpP*, which in the wild-type exhibits a constant

transcript level at days 10, 12 and 15 (~5-fold higher relative to seeds), showed a similar increment of transcript accumulation in the mutant for all three developmental stages examined.

C. Effect of RpoT;3 Mutation on Plastid Transcript Levels in 15-day Rosette Leaves, 35-day Rosette Leaves and 35-day Cauline l Leaves

We investigated transcript accumulation for a subset of plastid genes in young 15-day rosette leaves of wild-type and *rpoZ191* mutant plants sown on MS medium containing 1% sucrose and in mature 35-day rosette leaves as well as 35-day cauline leaves of plants transferred to soil after an initial 15-day period of growth on MS medium. The results in Figure 18B indicate a moderate reduction in the transcript levels for all genes and developmental stages examined. However, the difference in transcript levels the mutant and the wild-type was more pronounced in young 15-day leaves for the *rpoA*, *rrn16* and *rbcL* genes whereas the difference in transcript levels between the mutant and the wild-type for the *accD* and *clpP* genes was relatively constant for all stages examined.

A

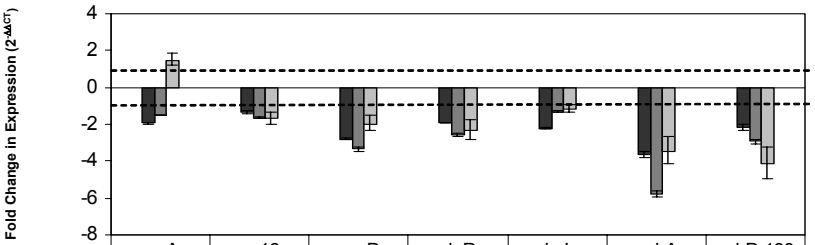

	rpoA	rrn16	accD	clpP	rbcL	psbA	psbD-190
10-day cotyledons	-1.95	-1.36	-2.80	-1.92	-2.21	-3.62	-2.16
12-day cotyledons	-1.51	-1.63	-3.32	-2.57	-1.31	-5.79	-2.93
15-day cotyledons	1.48	-1.68	-1.96	-2.36	-1.15	-3.46	-4.18

B

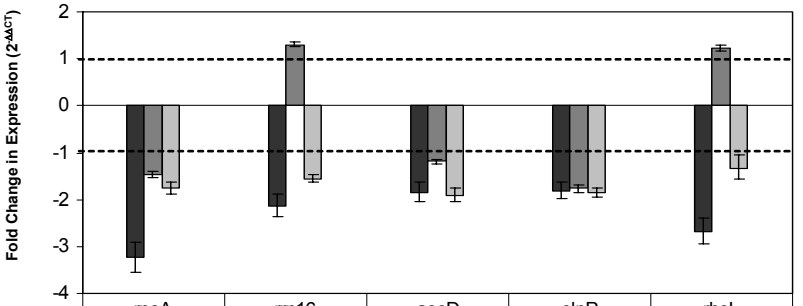

	rpoA	rrn16	accD	clpP	rbcL
15-day leaves	-3.24	-2.13	-1.85	-1.81	-2.69
35-day leaves	-1.47	1.30	-1.19	-1.77	1.23
35-day cauline leaves	-1.76	-1.55	-1.91	-1.87	-1.33

Figure 18. Relative fold changes in mRNA abundance of plastid genes in the *rpoZ191* cotyledons and leaves.

Total RNA was isolated from 10-day cotyledons, 12-day cotyledons, 15-day cotyledons and 15-day leaves of wild-type and *rpoZ191* seedlings grown on MS medium supplemented with 1% sucrose as well as from 35-day rosette leaves and 35-day cauline leaves of wild-type and *rpoZ191* plants grown on soil after a 15-day period of growth on MS medium containing 1% sucrose. A cDNA input corresponding to 10 ng of reverse transcribed total RNA was used for real-time PCR analysis as described in Figure 4.
(A) Expression changes in the *rpo191* cotyledons.
(B) Expression changes in the *rpo191* leaves.

Effect of the *RpoT;3* Mutation on the Accumulation of Plastid Transcripts during Development

To investigate whether the *RpoT;3* disruption affected the wild-type pattern of plastid transcript accumulation during development, we performed real-time PCR analysis of twenty eight plastid genes in siliques, seeds, 2-day seedlings and 5-day seedlings. The results obtained for the wild-type and the *rpoZ191* mutant were organized into clusters of genes with similar transcript accumulation kinetics in the developmental stages investigated and plotted on the same graph (Figure 19; see also Figure 16). In the wild-type, Cluster I contains three tRNAs (*trnfM-CAU*, *trnS-GCU* and *trnW-CCA*) that exhibit high transcript abundance in siliques and are either moderately induced in 2-day and 5-day seedlings relative to seeds (*trnfM-CAU* and trnS-*GCU*) or show reduced transcript levels in 2-day and 5-day seedlings relative to seeds (*trnW-CCA*). In the *rpoZ191* mutants the transcript accumulation kinetics of Cluster I genes were not significantly different from those of the wild-type although there were notable differences in transcript accumulation of each tRNA in the tissues examined (Figure 19 and Figure 16A). For instance, the transcript amounts of *trnfM-CAU* and *trnW-CCA* in siliques as well as seeds were not significantly different from the wild-type (~1.3- fold in siliques and ~0.9-fold in seeds) whereas the levels of *trnS-GCU* were reduced in the mutant (~0.6- and 0.4-fold, respectively). In 2-day seedlings the amounts of *trnW-CCA* and *trnS-GCU* were enhanced in the mutant (~2.5-fold) while *trnfM-CAU* levels were reduced in the mutant (~0.6-fold). Finally, in 5-day seedlings transcript levels of all three tRNAs were increased in the *rpoZ191* plants (3.7-fold for *trnfM-CAU*, 9.5-fold for *trnW-CCA* and 4.5-fold for *trnS-GCU*). In contrast, the accumulation kinetics of Cluster IIA and Cluster IIB

genes (*rpoA*, *rpoC1*, *rps15*, *rps16, rpl32, trnC-GCA, trnE-UUC, trnV-GAC, atpA, atpB, ndhA, B, F, J, petA, accD* and *clpP)* were significantly different from those of the wild-type (Figure19 and Figure16B &C). For example, in the wild-type the accumulation of RNAs associated with Cluster IIA and Cluster IIB genes exhibit a sharp increase relative to seeds at the 2-day stage followed by either a steep (Cluster IIA) or a moderate (Cluster IIB) decline/increase at the 5-day seedling stage. In the *rpoZ191* mutant, on the other hand, the levels of Cluster IIA and Cluster IIB transcripts exhibit a moderate increase relative to seeds and are reduced relative to wild-type at the 2-day stage (from ~2.7- to 112-fold). In contrast to the situation in the wild-type, the levels of these transcripts did not decline at the 5-day stage but continued to increase. However, the levels of most transcripts in the *rpoZ191* mutant were still considerable lower than in the wild-type (from ~2.4- to 13.8-fold) except the *rps15* and *rpl32* transcripts that accumulated to similar levels in the mutant and wild-type seedlings (see Figure 19 and Figure16B). Finally, the accumulation kinetics of Cluster III gene transcripts (*psaA*, *psaB*, *psaJ*, *psbA*, *psbD190*, *psbD LRP*, *rbcL*, *rps14*, and *rrn16*) were similar to those in the wild-type and exhibited an initial increase at the 2-day stage followed by a maximum at the 5-day stage (see Figure 19 and Figure 16C). The levels of Cluster III transcripts at the 2-day and 5-day stage, however, were much lower in the *rpoZ191* mutant compared to the wild-type (from ~2.8- to 26.5-fold in 2-day seedlings and from ~1.8- to 12.1-fold in 5-day seedlings). In the mutant seedlings most of the Cluster III transcripts examined showed an increase in abundance at the 5-day stage relative to the 2-day stage except *rps14*, *rrn16* and *psbD LRP* transcripts which did not increase in abundance at the 5-day stage.

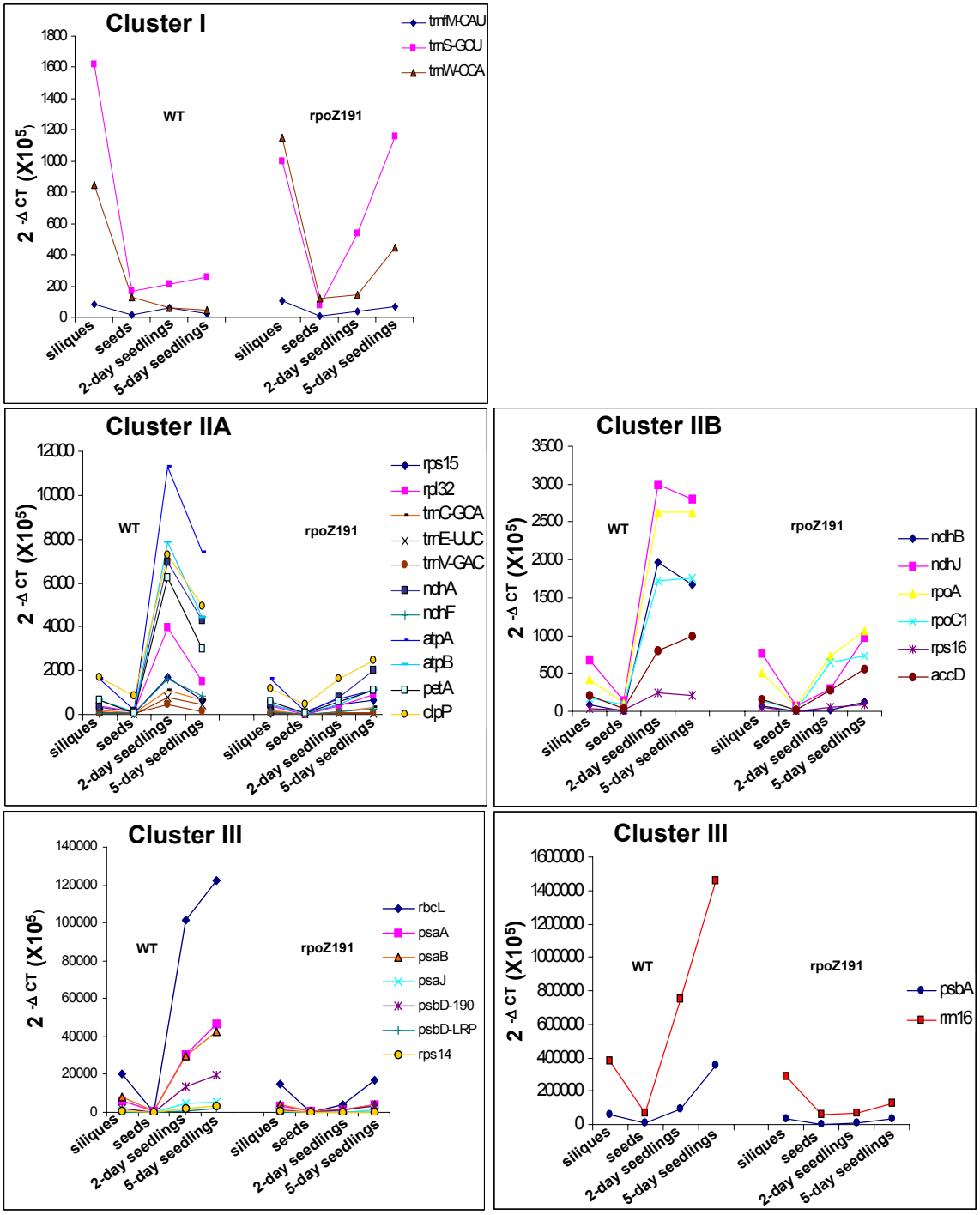

Figure 19. Changes of plastid expression patterns in the *rpoZ191* mutants.

Expression levels of plastid genes in siliques, seeds, 2-day seedlings and 5-day seedlings of wild-type and *rpoZ191* were monitored by real-time PCR. Quantitative PCRs were performed in triplicate with a cDNA input corresponding to 10 ng of reverse transcribed total RNA and expressed relative to cytosolic 18SrRNA amplification levels. The normalized given values are expressed as $2^{-\Delta CT}$ X 10^5, where ΔC_T ($C_{T\ sample} - C_{T\ normalizer}$).

DISCUSSION

Transcription in higher plant plastids is known to operate with at least two types of RNA polymerases (RNAPs): the plastid encoded eubacteria-type RNAP (PEP) and the nucleus-encoded phage-type RNAP (NEP) (reviewed in Hess and Börner, 1999). Recently, a number of nucleus-encoded phage-type RNA polymerase (*RpoT*) genes have been identified in a wide variety of flowering plants (Hedke *et al*., 1997; Weihe e*t al*., 1997; Chang *et al.*, 1999; Ikeda and Gray, 1999; Hedke *et al.,* 2002). In dicots, the *RpoT* genes consist of three members (Hedke *et al.,* 1997; 2000) encoding: a mitochondria-targeted NEP (*RpoT;1*), a plastid-targeted NEP (*RpoT;3*) and a dual-targeted NEP (*RpoT;2*). Analysis of an *Arabidopsis RpoT;2* mutant, which exhibited reduced root length and a moderate delay in greening, revealed that the mutation resulted in a decrease in transcript accumulation of NEP-, NEP + PEP- as well as many PEP-dependent genes after 1-day illumination whereas after 6-day illumination only the levels of NEP- and NEP + PEP-dependent genes exhibited a reduction in transcript levels while a significant effect on PEP-transcribed genes was not observed at this stage (Baba *et al.*, 2004).

To gain insight into the function and physiological significance of the different organellar RNAPs, we have investigated the effects of *RpoT;3* mutation on plastid transcript levels in a range of tissues and developmental stages. The *rpoZ191* mutant we characterized carries a T-DNA insertion in the eighteenth exon of the *RpoT;3* gene that encodes the plastid-targeted phage-type RNAP. Since the position of the T-DNA insertion corresponded to the carboxy terminal part of conserved domain XI, which has been shown to be important for the function of the T7 RNA Polymerase (Patra *et al.*,

1992; McAllister and Raskin, 1993; reviewed in Hess and Börner, 1999), it is unlikely that a truncated protein produced in the *rpoZ191* mutant is functional. The pale green and retarded growth phenotype as well as the slower chloroplast differentiation in the *rpoZ191* mutants suggest that RpoT*;3* plays an important role in the early steps of plant development and chloroplast differentiation. However, while the green tissues remain pale, the mutant plants can complete their life cycle photoautotrophically, indicating that RpoT;3 is not essential for the survival of the plant.

The elimination of PEP activity in *Δrpo* plants showed that despite a decrease in the transcript levels of PEP-dependent genes and an increase in the transcript levels of NEP-dependent genes, all plastid genes are transcribed to some extent in the *rpo*-deficient plastids (Allison *et al*., 1996; Hajdukiewicz *et al.,* 1997; Krause *et al*., 2000; Legen *et al*., 2002). However, until now there was no clear distinction between the roles of the different NEP enzymes in plastid transcription. Our analysis of plastid RNA accumulation in various tissues and stages of development revealed that the primary defect in the *rpoZ191* mutant is a general decrease in the accumulation of plastid transcripts during the early stages of chloroplast development, which causes a slow greening phenotype of the mutant plants.

The largest decrease in plastid transcript accumulation was recorded at the 2-day stage followed by a smaller reduction in transcript levels at the 5-day stage and even smaller reduction at later stages indicating that during the early stage of plastid development, RpoT;3 plays a key role in plastid gene transcription. In the wild-type, plastid mRNA levels, which are low in proplastids, increase dramatically during the early stages of chloroplast development, followed by a decline during the late stages of chloroplast maturation (Baumgartner *et al.*, 1989). Since in the wild-type this early stage

of leaf and chloroplast development is characterized by a massive increase in plastid expression associated with the greening and the conversion of plastids into photosynthetically active chloroplasts, plastid RNAP activity should be significantly increased. In fact, our results indicate that RpoT;3 represents a critical NEP activity that drives the transcription of plastid genes during the early stages of plastid development. In addition, our results indicate that the *RpoT;3* mutation has tissue specific effects. In the wild-type, plastid genes show differential transcript accumulation in various tissues and developmental stages with the lowest RNA levels in seeds and 5-day roots, higher in siliques as well as 40-day roots and even higher in 2-day and 5-day seedlings followed by a progressive decline in older tissues such as 12-day and 15-day cotyledons (see Chapter III). In the *rpoZ191* mutant the levels of plastid transcripts in tissues with the lowest RNA levels such as seeds and 5-day roots were not significantly different from the wild-type suggesting that RpoT;3 does not play a major role in the transcription of the plastid genes in the non-photosynthetic plastids of seeds and roots. Furthermore, the lack of RpoT;3 did not cause reduction of any of the plastid transcripts analyzed in the mutant siliques indicating that the RpoT;3 activity is not essential at this stage of development and that PEP and RpoT;2 or another NEP might be responsible for the transcription of plastid genes in wild-type siliques.

Although, the 2-day seedlings were characterized by a general decrease in plastid transcript accumulation, the amount of RNA reduction in the *rpoZ191* mutant varied depending on the gene examined. For example, at the 2-day stage, genes in Cluster IIA and IIB (Figure 19) encoding components of the plastid transcription and translation apparatus (*rpoA*, *rpoC1*, *rps15*, *rps16*, *rpl32*, *trnC-GCA*, *trnE-UUC*, *trnV-GAC*), the plastid ATP synthase complex (*atpA* and *atpB*), the plastid NADH

dehydrogenase complex (*ndhA*, *B*, *F*, *J*), the cytochrome b_6/f complex (*petA*), the plastid acetyl-CoA carboxylase (*accD*), and an ATP-dependent plastid protease (*clpP*) showed a decrease in transcript abundance between 2.8- and 16.3-fold except for the *ndhB* transcripts that exhibited the largest decrease relative to wild-type 2-day seedlings (~112-fold). Most of these genes are either NEP- or NEP + PEP-dependent genes (*rpoA*, *rpoC1, rps15*, *rpl32*, *ndhB*, *ndhF, ndhJ*, *rps16, atpA, atpB, accD, clpP)* with only *trnE-UUC*, *ndhA* and *petA* assumed to be transcribed by PEP while the promoters of *trnC-GCA* and *trnV-GAC* have not been investigated to date (Hess *et al.,* 1993; Hajdukiewicz *et a*l., 1997; Kanamaru et al., 2001). Surprisingly, the mRNAs for the *ndh* genes, which are assumed to encode components of the same complex, also showed differential accumulation in the 2-day *rpoZ191* mutant. For instance, the *ndhA* gene, which has been assumed to be a PEP-dependent gene, *ndhJ* and *ndhF*, which are assumed to be NEP+PEP transcribed genes showed a reduction of ~9- to 14-fold relative to 2-day wild-type seedlings whereas *ndhB*, also a NEP+PEP-dependent gene, exhibited a ~112-fold reduction relative to wild-type plants. The observed differential accumulation may indicate a strong dependence of the *ndhB* promoter on the *RpoT;3*-encoded NEP enzyme at the 2-day stage.

In contrast, Cluster III contains mostly PEP-transcribed genes encoding components of photosystem I (*psaA*, *psaB* and *psaJ*), photosystem II (*psbA*, *psbD190* and *psbD LRP*), Rubisco (*rbcL*), the translation apparatus (*rps14*) and one–gene (*rrn16*) transcribed by NEP + PEP. These genes showed a ~10- to 26-fold decrease in transcript accumulation relative to wild-type 2-day seedlings. Notably, even though the transcript levels of *rpoA* and *rpoC1*, encoding PEP subunits, exhibited a moderate reduction of ~3.5- and 2.6-fold, respectively, the levels of many PEP-dependent

transcripts showed a larger decrease relative to NEP- and NEP+PEP- transcribed genes. One possible explanation for the greater reduction in levels of PEP-dependent transcripts in the *rpoZ191* mutant could be due to a compound effect of the overall reduction in the transcript levels of genes encoding components of the transcription and translation apparatus resulting in decreased translation of *RpoA* and *RpoB/C1/C2* transcripts. It is also possible that the *RpoT;3* mutation could have an indirect effect on the transcript levels of the nucleus-encoded sigma factors resulting in reduced levels of active PEP enzyme.

At the 5-day stage most of the Cluster IIA, IIB and III transcripts showed an increase in abundance relative to the 2-day stage except for *rps14*, *rrn16*, and *psbDLRP* transcripts which did not increase in abundance. Possible explanations for the lack of increase in the transcript levels of these three genes are the inability of RpoT;2 to replace the levels of these transcripts transcribed predominantly by RpoT;3 in the chloroplasts of wild-type plants and/or altered stability of the transcripts. Two Cluster IIA transcripts (*rps15* and *rpl32*) showed almost similar quantities in both wild-type and *rpoZ191* mutant at the 5-day stage (Figure 16B). The tobacco *rpl32* is known to be transcribed from one type Ib NEP promoter and one internal divergent PEP promoter that lacks the typical -35 promoter element (Vera *et. al.,* 1992; Vera *et al.,* 1996) and *rps15* is transcribed from one uncharacterized NEP promoter (Hess *et al.,* 1993). The observed transcript accumulation indicates a stronger dependence of the *rps15 and rpl32* NEP promoters on the *RpoT;2*-encoded NEP enzyme at the 5-day stage. Interestingly, Cluster I genes, (*trnfM-CAU, trnS-CCA* and *trnW-CCA*), exhibited higher transcript levels in the *rpoZ191* 2-day and/or 5-day mutants compared to that in the wild-type. For instance, in the 2-day seedlings *trnS-GCU* and *trnW-CCA* transcripts

accumulated at a higher level in the mutant than in the wild-type (~2.5-fold) and even higher level in the 5-day seedlings (~4.5-and 9.5-fold, respectively). In addition, the *trnfM-CAU* transcripts accumulated to lower levels in the mutant than in the wild-type at the 2-day stage (~1.6-fold) but were enhanced in the mutant at the 5-day stage (~3.7-fold).These results indicate that in absence of RpoT;3, a compensatory increase in the levels or activity of RpoT;2 or some other nucleus-encoded polymerase might result in an increase levels of these transcripts. This is the first report indicating that expression of *trnS-GCU*, *trnW-CCA* and *trnfM-CAU* depends on NEP.

Particularly interesting is the differential accumulation in the *rpoZ191* plants of the mRNAs for genes harboring either NEP or both NEP+ PEP promoter sequences. For instance, the *atpA* and *atpB* genes, which are transcribed by NEP + PEP and are components of the same complex, show a larger reduction in transcript level (~15- and 16-fold respectively) in the *rpoZ191* mutants relative to the 2-day wild-type seedlings than the NEP + PEP-dependent *clpP* gene (~4.6-fold reduction), the NEP-dependent *accD* gene (~2.8-fold reduction) and the NEP- and/or NEP + PEP-dependent genes encoding components of the transcription and translation apparatus such as *rpoA*, *rpoC1*, *rps14*, *rps15*, *rps16*, *rpl32*, and *rrn16* which decrease from 2.7- to 11.4-fold. It is well known that most of the plastid genes are organized in polycistronic transcription units (see Table 11 in Chapter III) that are subsequently processed to generate a complex set of overlapping plastid transcripts with different stabilities (Monde *et al*., 2000). Moreover, multiple sites of transcription initiation add to the complexity of plastid transcript patterns (Christopher *et al.,* 1992; Kapoor et al., 1994). Consequently, the differential transcript accumulation seen in the *rpoZ191* mutant could be due to a difference in the stability of the various transcripts perhaps due to altered redox state as

seen in *Chlamydomonas reinhardtii* (Salvador and Klein, 1999). The simplest explanation for the differential accumulation of plastid transcripts could be a result of different promoter preferences of the two NEP polymerases (RpoT;2 and RpoT;3). In higher plants, three different types of NEP promoters have been identified: type Ia (*rpoB-147*, *rpoB-345*, *accD-129*, *clpP-511*), type Ib (rps16-*107*, *rrn16-64*, *rpl32-1018*, *atpB-290*, *clpP-173*) and type II (*clpP-53*) or exceptional NEP promoters (reviewed in Weihe and Börner, 1999). In addition, transcription of plastid genes and operons from multiple promoters is common. Examples are the tobacco *atpB* gene that is transcribed from three PEP promoters and one type Ib NEP promoter, the *rrn16* gene of tobacco that is transcribed from one PEP promoter one type Ia promoter and one type Ib NEP promoter and the tobacco *clpP* gene that is transcribed from one PEP promoter and three NEP promoters: one type Ia, one type Ib and one exceptional or type II NEP promoter (Liere *et al.,* 2004; Sriraman *et al*., 1998a; reviewed in Weihe and Börner, 1999). Several hypotheses can be advanced to explain the differential accumulation of plastid transcripts in the 2-day and 5-day mutant plants. One possibility is that the different NEPs (*RpoT;2* and *RpoT;3*) recognize the different promoters with different efficiencies. For example, overexpression of the *Arabidopsis* and tobacco *RpoT;3* revealed that transcription from the type I NEP promoters such as *atpB-289*, *accD-129* and *clpP- 511* was enhanced in comparison with the wild-type whereas no influence on the transcript levels of the type II *clpP-53* promoter was detected in tobacco plants overexpressing T3-NEP (Liere *et al*., 2004). Another possibility is that recognition of NEP promoters by RpoT;3 is facilitated by specificity factors present in plastids. The fact that the specificity loop amino acid residues that confer promoter specificity for the T7RNAP are not conserved in the maize NEP enzyme (Chang *et al.,* 1999) suggests

that the RpoT enzymes might require promoter-specific transcription factors. One such specificity factor, MTF1, has been shown to be required for the yeast mitochondrial phage-like RNAP in order to activate transcription (Jang and Jaehning, 1991). In plants, the p63 protein from wheat mitochondria has been shown to interact with a mitochondrial promoter and stimulate specific transcription *in vitro* (Ikeda and Gray, 1999). In addition, the spinach CDF2 protein has been shown to confer promoter recognition properties to a NEP enzyme (Bligny *et al.,* 2000). Furthermore, a ribosomal protein (RLP4) was found to be associated with a T7-like NEP suggesting that it may be involved in the regulation of plastid transcription (Trifa *et al.,* 1998).

Based on the effects of the *RpoT;3* mutation on plastid RNA accumulation in various tissues and stages of development of *Arabidopsis* plants, the plastid genes analyzed in this studies can be assigned to four classes (Figure 20): genes with uncharacterized promoters that are not affected by the *RpoT;3* mutation (Class I), genes with NEP or PEP + NEP promoters that are somewhat affected by the *RpoT;3* mutation (Class II), genes with NEP or mixed PEP + NEP promoters that are strongly affected by the *RpoT;3* mutation (Class III) and genes with PEP promoters only that are strongly affected by the *RpoT;3* mutation. (Class IV). Class I includes three tRNAs (*trnS-GCU*, *trnW-CCA* and *trnfM-CAU*) whose RNA steady-state levels are enhanced in the *rpoZ191* mutant siliques, 2-day and 5-day seedlings (Figure 20A).The expression of these plastid-encoded tRNAs is likely driven by RpoT;2 or another NEP. Class II includes genes with type Ia NEP promoters (e. g. *accD*, *rpoC1*), undefined NEP promoters (e.g. *rpoA*) and mixed PEP + NEP (Ia, Ib, II) promoters (e. g. *clpP*). In the *RpoT;3* mutant, the transcript levels of these genes showed a uniform decrease of 2- to 4-fold across development (Figure 20B). This suggests that RpoT;3, RpoT;2 or another

NEP may recognize these promoters with similar efficiencies. Class III includes genes with type Ib NEP promoters (e.g. *rps16*, *rpl32*) and *ndhB*, a NEP+PEP-dependent gene, which exhibited significantly lower transcript levels in the 2-day *RpoT;3* mutant plants than in the wild-type plants (Figure 20C). The expression of these genes at the 2-day stage is likely driven by RpoT;3 in association perhaps with a specificity factor. Finally, Class IV includes plastid genes (e.g. *rbcL*, psaA, psaB, *psaJ*, *psbA*, *psbD*, *trnE- UUC*) transcribed mostly from PEP promoters (Allison *et al.,* 1996; Hajdukiewicz *et al.,* 1997; Krause *et al.,* 2000; Kanamaru *et al.,* 2001) that showed a strong inhibition in the 2-day *RpoT;3* mutant plants followed by a partial recovery at the 5-day stage (Figure 20D). The transcript levels of two tRNAs (*trnC-GCA* and *trnV-GAC*) whose promoters have not been investigated yet displayed a pattern of accumulation similar to that of PEP-transcribed genes. The fact that the *RpoT;3* mutation had such a profound effect on PEP-transcribed genes may be due to reduced levels of the PEP enzyme and/or reduced levels of nucleus-encoded sigma factors that are known to confer PEP promoter selectivity (Allison, 2000; Mullet, 1993). This could, in turn affect PEP activity due to a downstream cascade effect. Thus in the absence of RpoT;3, slower chloroplast differentiation is signaled to the nucleus resulting in reduced expression of nucleus-encoded sigma factors, which in turn leads to reduced levels of the active form of PEP. Recent published studies have shown that an *Arabidopsis* SIG2 mutant exhibited elevated levels of NEP transcripts in the absence of SIG2 (Kanamaru *et al.,* 2001; see also Table 5 in Chapter I). This suggests a complex interaction between PEP and NEP during chloroplast development.

Previous studies have concluded that one function of the NEP polymerase is to activate synthesis of the PEP enzyme during the early phases of plant and plastid

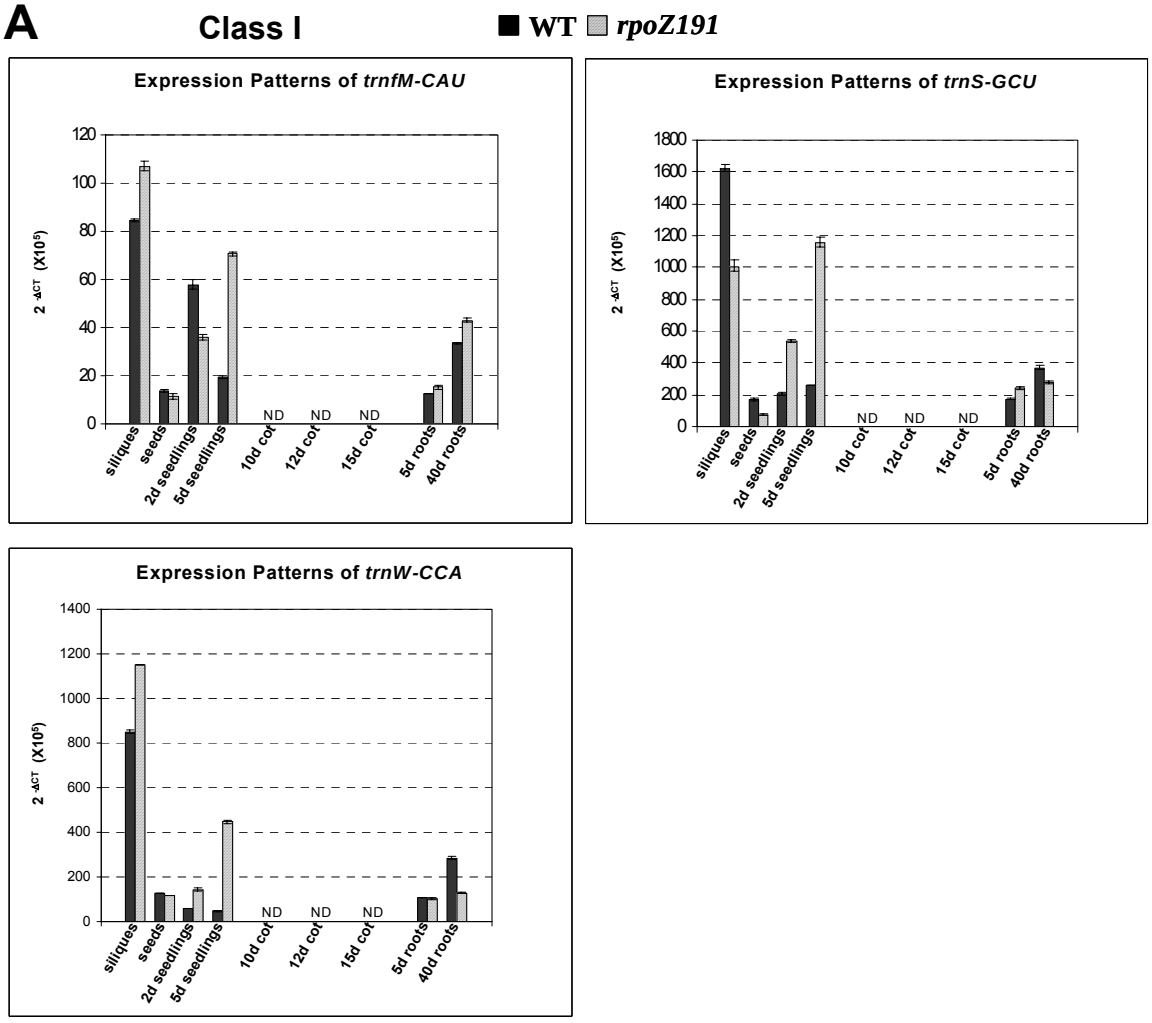

Figure 20. Expression profiles of representative classes of plastid genes in wild-type and *rpoz191* plants.

Total RNA was isolated from siliques, seeds, 2-day seedlings, 5-day seedlings, 10-day cotyledons, 12-day cotyledons 15-day cotyledons, 5-day roots and 40-day roots of *A. thaliana* seedlings grown on MS medium supplemented with 1% sucrose. Equivalent amounts of total RNA from each tissue were converted to cDNA and employed as template for real-time PCR analysis. Reactions were run in triplicate and data were normalized relative to cytoplasmic 18S rRNA levels and expressed as $2^{-\Delta CT}$ X10^5, where $\Delta C_T = (C_{T\ sample}-C_{T\ normalizer})$.
(A) Expression profiles of Class I plastid genes
(B) Expression profiles of Class II plastid genes.
(C) Expression profiles of Class III plastid genes.
(D) Expression profiles of Class IV plastid genes.

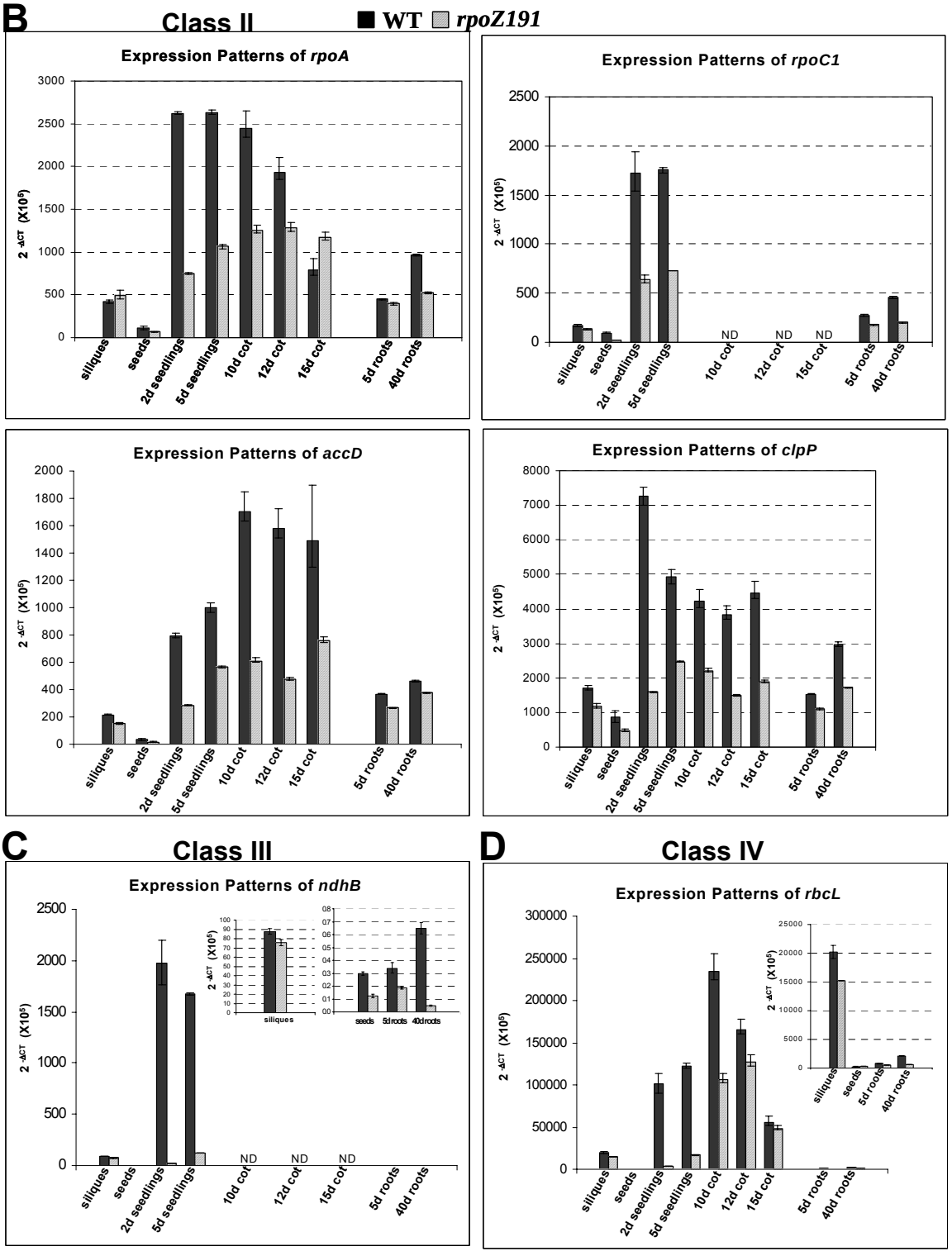

Figure 20. (continued).

development and to ensure transcription of non-photosynthetic genes such as *accD* and *clpP* whose functions in fatty acid metabolism and protein degradation, respectively would be expected to be required irrespective of developmental status (Lerbs-Mache, 1993; Mullet, 1993; Silhavy and Maliga, 1998a). Analysis of plastid transcript accumulation during the early stages of seedling establishment in the wild-type (see Chapter III) showed that maximal expression of plastid genes encoding components of the transcription/translation apparatus, ATP synthase, NADH dehydrogenase and cytochrome b_6/f complexes (Clusters IIA and IIB in Figure 12, Chapter III) precedes maximal expression of plastid genes encoding components of the photosynthetic apparatus (Cluster III in Figure 12). The phenotype of the r*poZ191* mutant indicates that RpoT;3 is limiting during the early steps of chloroplast differentiation perhaps because it is required in the wild-type in order to enhance transcription of the *rpo* genes and other genes encoding components of the transcription and translation apparatus. However, during the later stages of development, when plants and plastid transcript levels recover, the lack of RpoT;3 is compensated for by an increase in the steady-state levels of RpoT;2 or another NEP enzyme, which is then able to transcribe the whole plastid genome.

MATERIALS AND METHODS

Plant Growth

Arabidopsis *thaliana* (Col-0) wild-type and *rpoZ191* mutant seeds were surface sterilized in 95% ethanol for one minute followed by ten minutes incubation in 100% bleach (5.25% sodium hypochlorite-LABBCO, Inc., Houston, TX) + 0.0001% Tween-20. Seeds were washed three times in sterile water and plated on media containing 1x Murashige and Skoog salts and vitamin mixture (Gibco-BRL), 1% sucrose, 0.5 g L-1 2-[N-Morpholino]ethanesulfonic acid (MES) and 0.8% phytagar (Gibco-BRL). The plates were placed at 4^0 C for 5 days and then transferred to continuous white light (40 μE m^{-2} s^{-1}). For root excision, *Arabidopsis* plants were grown vertically on 1X Murashige and Skoog medium as described above. After fifteen days, some *Arabidopsis* seedlings were transferred to soil whereas others were transferred to fresh plates. Two-day old seedlings, 5-day old seedlings, 10-day, 12-day and 15-day cotyledons as well as 5-day and 40-day old roots were harvested, frozen in liquid nitrogen and stored at 80^0 C until further use. Rosette and cauline leaves from 35-day old plants as well as siliques from 34-day old plants transferred to soil after a fifteen-day period of growth on plates were harvested, frozen in liquid nitrogen and stored at 80^0 C until further use.

Identification of the *rpoZ191* Mutant

Identification of the *RpoT;3* T-DNA insertion mutant plants was done by screening the sequence-indexed *Arabidopsis* T-DNA insertion library provided by the SALK Institute

Genomic Analysis Laboratory (SIGnAL) available for screening at (http:// signal. salk. edu/cgi–bin/tdnaexpress). Seeds from a knockout line identified (SALK_067191) were obtained from the Arabidopsis Biological Resource Center (ABRC--Ohio State University, Columbus, OH) and renamed *rpoZ191* plants. The presence of the T-DNA insertion was verified by PCR using the primers RpoT;3-forward and RpoT-;3 –reverse flanking the T-DNA insertion (5´-AAA TCA TCT CTC TGC GAG CCA ATA AT-3´ and 5´-GCG AGC CAA TAA TTT TGA CTT TGT AAT C-3´) and the T-DNA left-border primers LBa1 (5´-TGG TTC ACG TAG TGG GCC ATC G -3´) and LBb1 (5´-GCG TGG ACC GCT TGC TGC AAC T -3´) designed using Primer3 program (http:// www.genome wi.mit.edu/cgi-bin/primer/primer3_www.cgi) of the Whitehead Institute (Cambridge, MA, USA). Genomic DNA was extracted in urea lysis buffer (Cocciolone and Cone, 1993) from the first inflorescence of both wild-type and *rpoZ191* plants transferred to soil after a fifteen-day period of growth on plates. PCR was performed in a Perkin Elmer Thermal Cycler using 50-µL reactions containing 0.2 ng/µL of genomic DNA, 2.5 units of Ex-Taq polymerase (Takara), 20 mM dNTPs and 12 pmol/µL of each primer. PCR conditions were 5 min at 96^{o}C, followed by 36 cycles (94^{o}C, 15 sec; 65^{o}C 30 sec; 72^{o}C 2 min) and a final extension at 72^{o}C for 4 min. A 854 bp product was generated from the wild-type allele and a 642 bp (LBa1) or a 432 bp (LBb1) product from the disrupted allele. The presence of the T-DNA insertion was confirmed by sequencing the PCR products from *rpoZ191* genomic DNA generated by the *RpoT;3* reverse gene specific primer and the T-DNA left border primers LBa1 or LBb1.

Microscopy

The transmission electron microscopy examination of the ultrastuctural features of plastids from both wild-type and *rpoZ191* mutant tissues were performed by E. Ann Ellis of the Microscopy and Imaging Center, Texas A&M University. Briefly, cotyledons of wild-type and *rpoZ191* plants were fixed in 2.5% glutaraldehyde-1.0% acrolein (vol/vol) in 0.1M PIPES buffer, pH 6.8 for 1 hr at room temperature with intermittent vacuum. Specimens were then washed 4X15 minutes with 0.1 M PIPES buffer, pH 6.8 followed by post fixation in 1% osmium tetroxide-1.5 % potassium ferricyanide (wt/vol) in PIPES buffer, pH 6.8, overnight in the cold. Specimens were then dehydrated in an ethanol series to propy- lene oxide and infiltrated and embedded in epoxy resin. Blocks of tissue were thin sectioned at 80-100 nm and grids were post stained with 2% aqueous uranyl acetate followed by Reynolds lead citrate (Reynolds, 1963). Grids were examined and photographed in A JEOL 1200EX transmission electron microscope at an accelerating voltage of 100kV.

RNA Isolation and Reverse Transcription

Total RNA from roots, 2-day and 5-day old seedlings as well as 10-day cotyledons, 12-day cotyledons, 15-day cotyledons, 35-day rosette and cauline leaves was extracted with Tri Reagent (Molecular Research Center, Inc., Cincinnati, OH) using 1-bromo-3-chloropropane (BCP) as a substitute for chloroform as per manufacturer's instructions (Chomczynski and Mackey, 1995). Total RNA from seeds and siliques was isolated using the Concert Plant RNA Reagent, according to the manufacturer's instructions

(Invitrogen, Carlsbad, CA) except that BCP (Molecular Research Center, Inc., Cincinnati, OH) was substituted for chloroform. Contaminating DNA was removed using the RNase free Dnase (Qiagen, Valencia, CA) with two elutions of five minutes in 30 μL RNase-free water (Ambion, Austin, TX). The purity of RNA was judged by the A_{260}/A_{280} ratios (1.8-2.0) and RNA integrity was assessed by examining the rRNA bands on a standard agarose gel (Sambrook *et al*., 1989). Constant amounts of 2 μg RNA were reverse-transcribed to cDNA in a total volume of 100 μL using random hexamer primers and the TaqMan Reverse Transcription Kit (Applied Biosystems, Foster City, CA). Each 100-μL reaction was prepared as follows: 34.75 μL RNA sample in RNase-free water (Ambion, Austin, TX), 10.0 μL 10X TaqMan RT Buffer, 22.0 μL $MgCl_2$ (5.5 mM), 20.0 μL dNTPs (500 μM each) 5.0 μL random hexamer primers (2.5 μM), 2.0 μL RNase inhibitor (0.4 U/ μL) and 6.25 μL Multiscribe Reverse Transcriptase (3.125 U/ μL). After a ten-minute incubation at 25^0C to increase primer-RNA template binding, reverse transcription was performed for one hour at 37^0C followed by inactivation of the reverse transcriptase at 95^0C for five minutes. The final volume of each 100-μL RT reaction was brought to 200 μL by the addition of 100 μL of RNase-free water and the cDNA was stored at -80^0C until further use. No-template controls were generated at the same time by combining 2 μg RNA with RNase-free water to a 200-μL final total volume.

Primer Design

All the gene-specific primers were designed using Primer Express® software v2.0 (Applied Biosystems Foster City, CA) according to the software guidelines except for the *trn* and *rps16* primers which were designed with Primer3 program

(http://www.genome.wi.mit.edu/cgi-bin/primer/primer3_www.cgi) of the Whitehead Institute (Cambridge, MA, USA). All amplicons were designed according to the same guidelines provided by the Primer Express® software. Briefly, primers for each gene target were selected to contain minimal hairpins and primer-dimer formation as determined by the software and having compatible T_m's, each within 1^0-2^0C of the other. In addition, primers were designed to be 15-30 bases in length with a minimum and maximum amplicon size of 59 bp and 150 bp, respectively. All oligonucleotide primers used were synthesized by IDT (Integrated DNA Technologies, Inc., Coralville, IA) except for the *psbD190*, *psbDLRP* and *rbcL* primers which were purchased from Applied Biosystems (Foster City, CA). Oligonucleotide sequences are shown in Table 16. The 18S rRNA primers and probe that produce a 187-bp amplicon were included in the TaqMan rRNA Control Reagents kit (Applied Biosystems, Foster City, CA). In order to verify the specificity of the primers, all primers were used as query sequences in Blast searches of the NCBI database either alone, together with the DNA segment generated by the PCR process or with Ns substituted for the sequence between the primers.

Real-time PCR: SYBR Green Detection

PCR reactions were carried out in optical 384-well plates on an ABI Prism 7900HT Sequence Detection System using the 2X SYBR Green PCR Master Mix (Applied Biosystems, Foster City, CA) as recommended by the manufacturer. For each sample, a master mix was generated by combining 3.3 µL of cDNA with 29.7 µL of 2X SYBR Green PCR Master Mix (Applied Biosystems) supplemented with primers to a final

concentration of 50 nM each and PCR-grade water to a 33 µL final total volume. This mixture was distributed into three replicates of 10 µL each in 384-well amplification plates and sealed with optical adhesive covers (Applied Biosystems). For each primer pair, a no-template control (NTC) was also run in triplicate. The following amplification parameters were used for all PCRs: 10 minutes at 95^0C for optimal AmpliTaq Gold DNA polymerase activation followed by 47 cycles of denaturation at 96^0C for 10 sec and annealing/extending at 60^0C for 1 min. A dissociation curve was generated according to the protocol present in the ABI Prism 7900HT software (SDS v2.1). Briefly, following the final cycle of the PCR, the reactions were heat denatured over a 35^0C temperature gradient from 60^0 to 95^0C.

Real-time PCR: TaqMan Detection

The master mix for the real-time PCR using TaqMan detection consisted of 3.3 µL of cDNA with 29.7 µL of 2X TaqMan Master Mix (Applied Biosystems) supplemented with primers to a final concentration of 50 nM each, VIC-labeled hybridization probe to a final concentration of 50 nM and PCR-grade water to a 33 µL final total volume. This mixture was distributed into three replicates of 10 µL each in 384-well amplification plates and sealed with optical adhesive covers (Applied Biosystems). A no-template control (NTC) was also run in triplicate. Real-time PCR was performed identically to that described for SYBR Green detection except that the dissociation curve generation step was omitted.

Table 16. PCR forward (for) and reverse (rev) primer sequences for *plastid-encoded genes

Gene	Primer sequence	(bp)
rpoA	for 121: CAAGCCGACACAATAGGCATT rev 195: TGCACGTGTAATACATGTTCCTTCT	74
rpoC1	for 1187: GATTGCCTCGCGAAATAGCA rev 1271: CCTATGTTCGAAGCCAGGTGTT	84
rps14	for 201: AAGACCGAGAGCTAACTATCGAGACT rev 279: TGGCAACAAACATGCCTGAA	78
rps15	for 56: CCGTTGAATTTCAAGTATTTAGTTTCACT rev 153: TAGACCCCGCTGAGATAAATAATCTT	97
rps16	for 137: CTTTTTTAAACCTTTCTGCTATTCTCGAT rev 224: CCAGCCTTCTTTGAAATATCATGAG	87
rpl32	for 30: CTCGAAAAAGCGTATTCGTAAA rev 96: AAAAGCTTTCAACGATGTCCA	66
rrn16	for 440: GGGAATAAGCATCGGCTAACTCT rev 509: ATTCCGGATAACGCTTGCAT	69

Table 16. (continued.)

Gene	Primer sequence	Product Length (bp)
trnC-GCA	for 5: GCATGGCCGAGTGGTAA rev 67: GGCACCCGGATTTGAAC	62
trnE-UUC	for 3: CCCCCATCGTCtAGTGGTT rev 62: AAGTCGAATCCCCGCTG	59
trnfM-CAU	for 2: GCGGGGTAGAGCAGTTTG rev 66: ACAGGATTTGAACCCGTGAC	64
trnS-GCU	for 17: CGAACCCTCGGTACGATTA rev 88: GGAGAGATGGCTGAGTGGAC	71
trnV-GAC	for 9: AGCTCAGTTAGGTAGAGCACCTC rev 67: ATACGGACTCGAACCGTAGAC	58
trnW-CCA	for 2: CGCTCTTAGTTCAGTTCGGTAG rev 73: ACGCTCTGTAGGATTTGAACC	71
atpA	for 583: GTTTATGTAGCTATTGGTCAAAAAGCTTCT rev 657: CATTGCCCCTCGTTCCTGTA	74

Table 16. (continued).

Gene	Primer sequence	Product Length (bp)
atpB	for 78: CATTGGTCCGGTACTGGATGT rev 143: ACCAGAGCATTGTAAATATTAGGCATT	65
ndhA	for 617: GGAATTTGTGGCGTCAACCTA rev 712: CTTCCGCTTCTGGTAAATCAAAC	95
ndhB	for 377: CTCATCAATGGACTCCTGACGTATA rev 461: GAAGCAGCTACTTTCGAAGTAACAGA	84
ndhF	for 714: TGCTAAATCCGCACAATTTCC rev 798: AGCATGTATAAGACCCGAAATGG	84
ndhJ	for 363: TTATGATAGCCATCCACGACTGAA rev 428: CGTAAAGGCCACCCTATCCAA	65
petA	for 761: AATCCATTAAACTCGATCAACCATTA rev 828: CGCATCCCCCTGACCAA	67
psaA	for 729: TCGGGATCTTTTGGCTCAAC rev 811: CCGAGTATTTTGACCAATTTAAGGTAA	82

Table 16. (continued).

Gene	Primer sequence	Product Length (bp)
psaB	for 657: CCAAGGGTTAGGCCCACTTT rev 753: TCCGGATCCTTGGGAGGTA	96
psaJ	for 22: CTTTCCGTAGCACCGGTACTAAGT rev 116: AATGTTAATGCATCTGGAAATAAACG	94
psbA	for 99: TGGTGTTTTGATGATCCCTACCTTA rev 181: CAATATCTACTGGAGGAGCAGCAA	82
psbD190	for 62: GCGCGAGAAATTAAATCATAAACA rev 167: TCAACCATTTCCGAACACCTT	105
psbDLRP	for 238: GCAAAGTAATAACTAAAAGGGCGTTT rev 378: TTGATATCTGAAGCCATGATTATGATTC	140
rbcL	for 1009: GGAGACAGGGAGTCAACTTTG rev 1083: ACCGCGGCTTCGATCTTT	74
accD	for 801: TCCGGGTACTTGGAATCCTATG rev 879: ATAAGGTTCCTCCTTCGAATGAAAT	78
clpP	for 261: GCGACCCGATGTACAGACAA rev 329: CCTCCGACTAGGATAAAGGATGCT	68

* GeneBank acc. No. AP00043

Real-time PCR: Data Analysis

The data generated from both SYBR Green and TaqMan chemistries were analyzed in a similar manner. The C_T values were determined using a signal/noise ratio set to 10 standard deviations above background subtracted mean fluorescence values (ΔR_n) for a baseline value adjusted manually for each set of primers. The real-time PCR data containing the C_T values were exported into a Microsoft® Excel spreadsheet for further analysis. Plastid gene expression was normalized to that of cytoplasmic 18S rRNA and expressed as $2^{-\Delta CT}$, where $\Delta C_T = (C_{T\ sample} - C_{T\ 18S\ rRNA})$. PCR efficiency for each primer pair was determined by analyzing a series of template dilutions (see Chapter II).The slope was calculated from the plot of log input versus C_T and exponential amplification (efficiency) was determined from the equation $E = 10^{(-1/slope)}$ (Rasmussen, 2001). In addition, the amplification efficiencies of the target genes and normalizers were compared by determining the slope from the plot of log template dilution versus $\Delta C_T = (C_{T\ sample} - C_{T\ normalizer})$ according to instructions given by Applied Biosystems (Relative quantitation of gene expression, User Bulletin # 2). The fold change in plastid transcript abundance relative to wild-type was determined by the $2^{-\Delta\Delta CT}$ method (Livak, 1997; 2001), where $\Delta\Delta C_T = (\Delta C_{T\ mutant} - \Delta C_{T\ wild\text{-}typer})$.

CHAPTER V

EFFECT OF THE *RpoT;3* MUTATION ON NUCLEAR GENES ENCODING CHLOROPLAST PROTEINS

INTRODUCTION

Current estimates suggest that the chloroplast proteome consists of 2500-5000 different proteins with the nuclear genome encoding more than 90% of the proteins present in chloroplasts (Martin and Herrmann, 1998; Abdallah *et al.,* 2000). Nuclear genes encode many structural components of the photosynthetic apparatus, the plastid genetic system as well as a large number of factors that are involved in regulating the co-ordinated expression of plastid and nuclear genes encoding plastid proteins (Somanchi and Mayfield, 1999; Barkan and Goldschmidt-Clermont, 2000). For instance, photosystem I and photosystem II are complex structures that contain protein subunits encoded by both the nuclear and the plastid genome (see Table 3 Chapter I). In addition each photosystem has light harvesting antennae (LHC I and LHC II) composed of a set of light-harvesting chlorophyll a/b-binding proteins encoded by the *Lhca* and *Lhcb* nuclear gene families (Jansson, 1999; Frisco *et al.,* 2004). Evidence suggests that the development of a fully functional chloroplast as well as the ability of the plant cell to adapt to environmental fluctuation depend on the exchange of information between the nucleus and chloroplast (reviewed in Somanchi and Mayfield, 1999). The biosynthesis of Rubisco constitutes a classic example of integrated nucleus and plastid gene expression. Rubisco, which catalyzes both the carboxylation and oxygenation of RuBP, is composed of eight small subunits (SS), encoded by a nuclear multigene family

(*RbcS*), and eight large subunits, encoded by a single gene (*rbcL*) located on the plastid genome (reviewed in Hartman and Harpel, 1994; Gutteridge and Gatenby; 1995; Rodermel, 2001). Previous research has shown that the expression of *RbcS* and *rbcL* is coordinated at several levels to maintain the stoichiometry of the subunits in the holoenzyme. In the case of limiting SS accumulation, for example, LS accumulation is controlled at the level of *rbcL* mRNA translation initiation whereas in the case of LS limiting accumulation, SS accumulation is controlled at the level of protein degradation (Rodermel, 1999). In addition, SS and LS accumulation is regulated at a number of other steps. For instance, SS accumulation is regulated at the level of *RbcS* transcription in response to light, hormones and chloroplast development whereas LS accumulation is regulated at several levels including transcription and transcript stability (reviewed in Rodermel, 1999).

Genetic analysis of mutants has identified a series of nuclear genes that encode products involved in chloroplast development (reviewed in Somanchi and Mayfield, 1999; Papenbrock and Grimm; 2001). For example, the nuclear DET and COP proteins repress nuclear and chloroplast gene expression in the dark (reviewed in von Arnim and Deng, 1996) whereas the PAC and IM proteins are believed to be involved in chloroplast mRNA processing and prevention of photo-oxidative damage during the early phase of chloroplast development, respectively (Meurer *et al.,* 1998; Carol *et al.,* 1999). Although the nucleus has a major role in controlling plastid differentiation, a considerable body of evidence indicates that signals from the developing plastid, coupled to complex light signal transduction pathways mediated by phytochrome and cryptochrome photoreceptors modulate the expression of nuclear genes involved in plastidogenesis (Oelmüller, 1989; Papenbrock and Grimm; 2001; Quail, 2002; Taylor,

1989). Several distinct plastid–to-nucleus signaling pathways have been identified. Tetrapyrrole biosynthetic intermediates and carotenoids have been associated with the generation of a plastid-derived signal that transmits information to the nucleus concerning the metabolic and/or developmental state of the plastids (reviewed in Rodermel. 2001; Gray et al., 2003; Surpin *et al.,* 2002). In addition, several plastid processes such as transcription, translation and photosynthesis have been shown to be involved in signaling to the nucleus (reviewed in Gray et al., 2003; Surpin *et al.,* 2002). Analysis of barley *albostrian* mutants, which are deficient in plastid ribosomes (Bradbeer *et al.,* 1979; Hess *et al.,* 1991, 1994), as well as treatment of barley and/or tobacco plants with plastid transcription inhibitors such as tagetitoxin or nalidixic acid (Rapp and Mullett, 1991; Gray *et al.,* 1995) or plastid translation inhibitors such as lincomycin (Gray *et al.,* 1995) showed a decrease in transcripts of a subset of nuclear genes (*Lhcb1*, *RbcS*, *PetH*) for plastid proteins. The rice temperature conditional *viriscent-2* mutant, which is deficient in plastid translation during the early stages of leaf development, showed a similar decrease in the *RbcS* and *Lhcb* transcript levels (Sugimoto *et al.,* 2004). These results suggest that plastid gene expression during early development might be involved in generation of plastid-to-nucleus signals that modulate the transcription of nucleus-encoded plastid proteins. Finally, signals derived from the plastid photosynthetic electron transport (redox signals) have been shown to control the expression of plastid genes as well as nuclear genes. However, the redox control of nuclear gene expression, which has been shown to operate later during development, is believed to be an adaptational process that allows plants to acclimatize to changes in light quality (reviewed in Gray *et al.,* 2003; Surpin *et al.,* 2002).

Several lines of evidence suggest that the early activation a nucleus-encoded RNA polymerase (NEP) is responsible for the build-up of the plastid transcriptional and translational apparatus, including the plastid-encoded RNA polymerase (PEP), which, in turn, activates a plastid-to-nucleus signaling pathway that leads to enhanced expression of nuclear and plastid genes encoding components of the photosynthetic apparatus (Mullet, 1993; Allison *et., al.,* 1996; Hajdukiewicz *et al.,* 1997; Kusumi *et al.,* 1997, Sugimoto *et al.,* 2004). To date, a number of nucleus-encoded phage-type RNA polymerase (*RpoT*) genes have been identified in a wide variety of flowering plants (Hedke *et al*., 1997; Weihe e*t al*., 1997; Chang *et al*., 1999; Ikeda and Gray, 1999; Hedke *et al.,* 2002). In dicots, the *RpoT* genes consist of three members: a mitochondria-targeted *RpoT;1*, a plastid-targeted *RpoT;3* and a dual-targeted *RpoT;2* (Hedke *et al.,* 1997; 2000).

Recently, we isolated a *RpoT;*3 mutant, *rpoz191*, in which a T-DNA was inserted into the exon 18 of the the *RpoT;3* gene corresponding to the conserved region IX (see Chapter IV). This mutant shows a pronounced pale green phenotype and displays a general reduction in growth as well as a delay in greening (Figure 13 in Chapter IV). Additionally, during the early stages of seedling growth, the mutant plants develop small chloroplasts that appear to be less differentiated internally as compared to the wild type chloroplasts (see Figure 15 in Chapter IV). Real-time PCR analysis showed that plastid transcript accumulation in this mutant was drastically reduced at the 2-day as well as 5-day stage indicating that during the early stages of chloroplast differentiation, RpoT;3 plays a key role in transcribing plastid genes. Because plastid gene expression during early development is thought to be involved in generation of a plastid-to-nucleus signal that modulates the transcription of nucleus-encoded plastid proteins, the *rpoZ191*

mutation may affect the expression of nuclear genes encoding products needed for chloroplast function. To investigate this possibility, we performed quantitative real-time PCR analysis of nuclear gene transcript abundance in different tisssues of mutant and wild-type seedlings.

RESULTS

Tissues and Transcripts Analyzed

To investigate RNA abundance of nuclear genes in several tissues and different developmental stages of the wild type as well as the *RpoT;3 Arabidopsis* mutants, we employed the highly sensitive method of quantitative real-time PCR. Transcript levels for four nuclear genes were quantified in dry seeds, 2-day seedlings, 5-day seedlings, 5-day roots, 40-day roots and 34-day siliques (Figure 21). The nuclear genes analyzed include *Lhca 1* (Acc.No.M85150), encoding a polypeptide of light-harvesting complex I (LHC I) associated with photosystem I, *Lhcb 1.2* (Acc.No. X03908), encoding a polypeptide of light-harvesting complex II (LHC II) associated with photosystem I and II, *RbcS* (Acc.No.AY64686), encoding the large subunit of Rubisco and *PetH* (AJ243705), encoding ferredoxin-$NADP^+$-oxidoreductase.

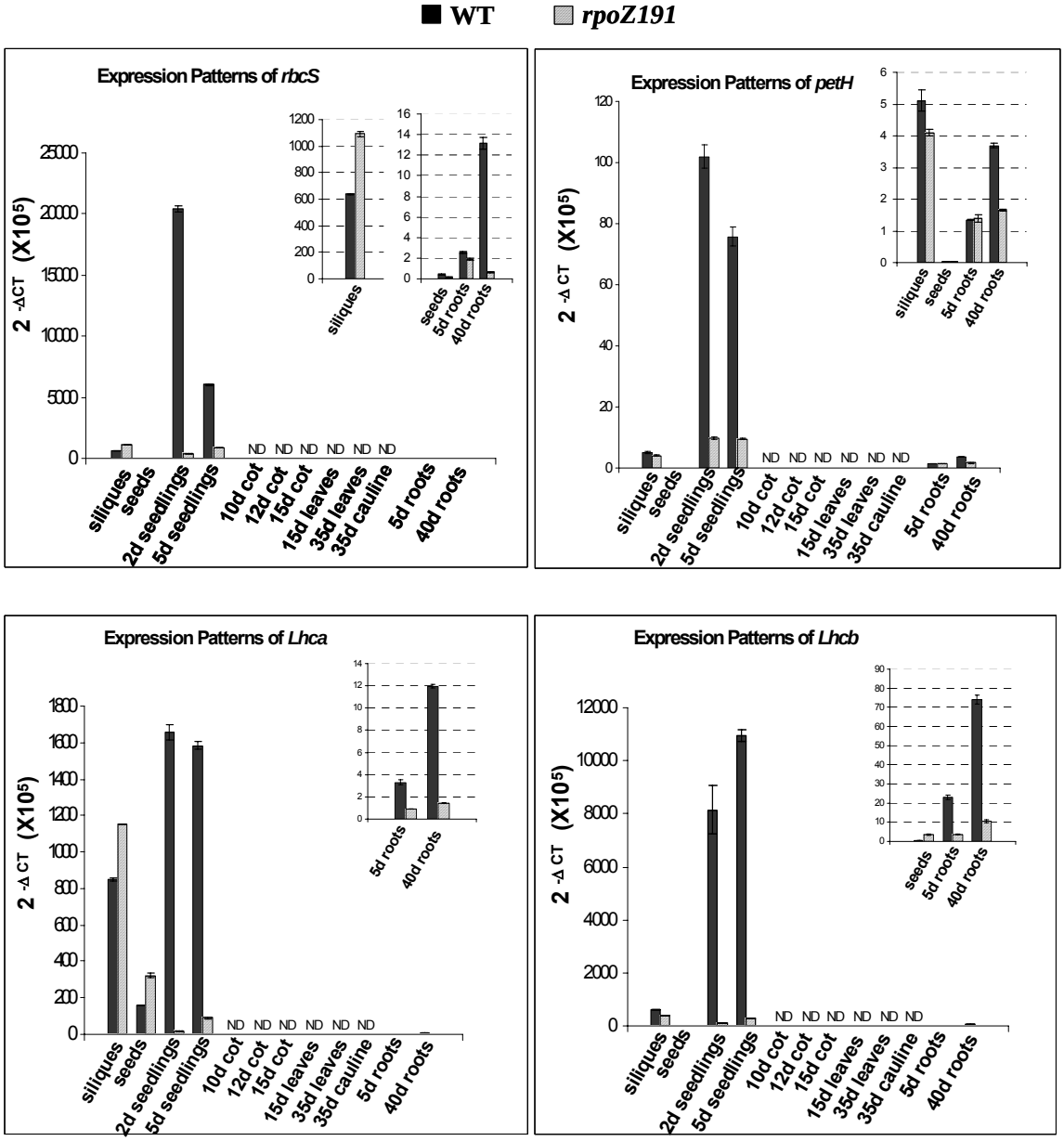

Figure 21. Transcript accumulation of nuclear genes encoding plastid proteins in the wild-type and *rpoZ191* mutant.

Total RNA was isolated from siliques, seeds, 2-day seedlings, 5-day seedlings, 5-day roots and 40-day roots of wild-type and *rpoZ191* seedlings grown on MS medium supplemented with 1% sucrose. Equivalent amounts of total RNA were converted to cDNA and assayed for mRNA abundance by real-time PCR. Real-time data were normalized relative to cytoplasmic 18S rRNA levels and expressed as $2^{-\Delta CT}$ X10^5, where ΔCT = ($C_{T\ sample}$-$C_{T\ normalizer}$). The given values represent the mean of triplicate measurements.

Accumulation of Transcripts for Nucleus-Encoded Chloroplast Proteins in Various Tissues and Stages of Plant Development

The nuclear genes examined showed the lowest levels of expression relative to 18S rRNA in dry seeds. To facilitate the detection of differential transcript accumulation, RNA abundance in the various tissues and developmental stages examined was expressed relative to that in seeds. In addition, changes in the ratio of transcript abundance in 2- and 5-day old seedlings as well as 5- and 40-day old roots relative to the abundance in seeds were calculated and are listed in separate columns in Table 17. Quantitative analysis of *Lhca 1*, *Lhcb 1.2*, *RbcS* and *PetH* transcript levels revealed a general increase of RNA levels in siliques relative to mature seeds. The smallest increase in transcript abundance relative to mature seeds was observed for the *PetH* and *Lhca 1* transcripts (~214- and 344-fold, respectively). In contrast, transcripts for *RbcS* and *Lhcb 1.2* increased ~1,600- to 2,000-fold in siliques as compared with mature seeds. The most significant increase in transcript abundance relative to seeds was recorded at the 2-day as well as 5-day seedling stage. The results shown in Figure 21 and Table 17 indicate that nuclear genes encoding proteins associated with the plastid photosynthetic apparatus (*Lhca 1* and *Lhcb 1.2*) showed a pattern of accumulation similar to that of plastid genes encoding components of photosystem I and II (see also Figure 12, Cluster III in Chapter III) whereas *PetH*, encoding ferredoxin NADP-oxidoreductase, showed a time course of mRNA accumulation similar to that of plastid genes encoding components of cytochrome b_6/f, NADH dehydrogenase and ATP synthase complexes (see also Figure 12, Clusters IIA and IIB in Chapter III). On the

Table 17. Abundance of nuclear genes mRNA in siliques, 2-day seedlings, 5-day seedlings, 5-day roots and 40-day roots relative to seeds[a]

Gene	Siliques	2-day seedlings	5-day seedlings	ratio 2d/5d seedlings	5-day roots	40-day roots	ratio 40d/5d roots
RbcS	1640 (1410-1900)	52300 (44600-61000)	15400 (13100-18000)	3.4 (2.4-4.5)	6.6 (5.4-7.9)	34 (28-40)	5.1 (3.3-7.1)
PetH	214 (192-237)	4260 (3940-4590)	3170 (2920-3430)	1.3 (1.1-1.6)	56 (53-59)	154 (145-163)	2.8 (2.5-3.1)
Lhca 1	344 (343-346)	8504 (8497-8512)	8630 (7660-9710)	1.0 (0.8-1.2)	17 (16-18)	69 (67-70)	3.9 (3.6-4.3)
Lhcb 1.2	2110 (2080-2140)	28417 (28412-28423)	38300 (35200-41700)	0.74 (0.65-0.82)	80 (77-84)	259 (251-267)	3.2 (2.9-3.5)

[a] Seeds of *Arabidopsis thaliana* ecotype Columbia were surface-sterilized and sown in Petri dishes on MS medium containing 1% sucrose. The plates were placed at 4^0C for 5 days before being transferred to continuous white light (40 µmol m^{-2} sec^{-1}). Siliques were collected from 34-day old *Arabidopsis* plants grown on soil after a 15-day period of growth on MS medium containing 1% sucrose. Total RNA was isolated from siliques, seeds, 2-day seedlings, 5-day seedlings, 5-day roots and 40-day roots and converted to cDNA in reactions that were normalized to contain equivalent amounts of total RNA. A cDNA input corresponding to 10 ng of reverse transcribed total RNA was employed as template for real-time PCR analysis. Reactions were run in triplicate and data were normalized relative to cytoplasmic 18S rRNA levels and expressed as $2^{-\Delta CT}$ $X10^5$, where $\Delta C_T = (C_{T\ sample} - C_{T\ normalizer})$. The fold change in mRNA abundance of each gene in siliques, 2-day seedlings, 5-day seedlings, 5-day roots and 40-day roots relative to seeds was derived from the ratio of the individual $2^{-\Delta CT}$ values in each tissue to the respective $2^{-\Delta CT}$ values in seeds. The range given in parenthesis is determined by evaluating the expression $2^{-\Delta CT}$ with ΔC_T + SD and ΔC_T – SD, where SD = the standard deviation of the ΔC_T value calculated according to the formula $S = \sqrt{(S^2_{\ sample} + S^2_{\ normalizer})}$.

other hand, *RbcS*, encoding the small subunit of ribulose 1,5-biphosphate carboxylase/oxygenase (Rubisco), did not show a similar pattern of transcript accumulation as that of *rbcL*, encoding the large subunit of Rubisco. Instead, the *RbcS* transcripts showed a pattern of early accumulation that resembled that of plastid genes in Clusters IIA (see Figures 12 and 21). Finally, analysis of nuclear transcript accumulation in 5-day and 40-day light-exposed roots revealed a general increase of RNA levels relative to dry seeds. In addition, comparison of transcript accumulation from 5-day and 40-day roots (see Figure 21 and Table 15) indicated that there was a ~3- to 5-fold increase in the abundance of nuclear transcripts examined in the 40-day roots as compared to 5-day roots.

Effect of *RpoT;3* Mutation on Transcript Levels for Nucleus-Encoded Chloroplast Proteins in Siliques, Seeds, 2-day Seedlings, 5-day Seedlings, 5-day Roots and 40-day Roots

The low levels of plastid mRNAs in the *rpoZ191* mutant prompted us to investigate whether expression of nuclear genes encoding plastid proteins is altered in the mutant. The results of real-time PCR analysis of selected nuclear transcripts using wild-type and mutant RNA from siliques, seeds, 2-day seedlings, 5-day seedlings, 5-day roots and 40-day roots shown in Figures 21 and 22 indicate that the *RpoT;3* mutation, had tissue and developmental specific effects (see also Figure 17A in Chapter IV). For instance, accumulation of *PetH*, *RbcS*, *Lhca 1* and *Lhcb 1.2* was significantly reduced in the mutant 2-day seedlings (from ~10- to 90-fold decrease relative to the wild-type plants),

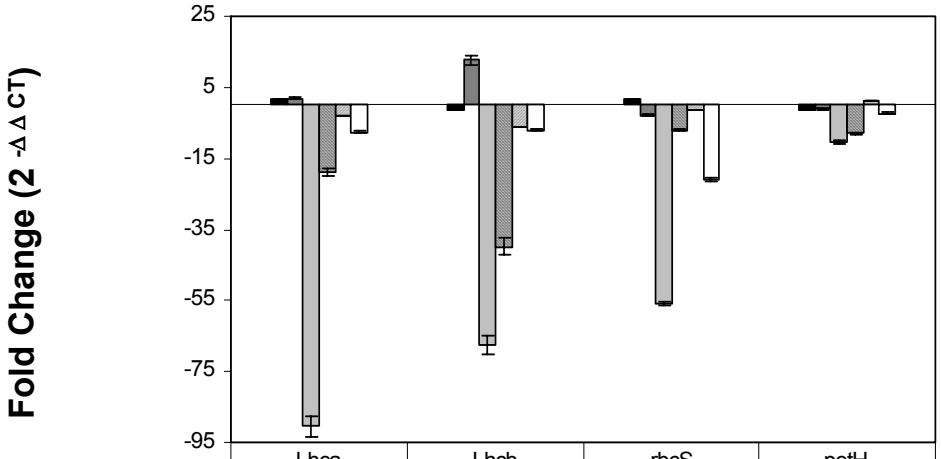

	Lhca	Lhcb	rbcS	petH
Siliques	1.9	-1.6	1.7	-1.2
Seeds	2.0	13	-2.8	-1.1
2-day seedlings	-90	-68	-56	-10
5-day seedlings	-19	-40	-7.0	-7.9
5-day Roots	-3.0	-6.3	-1.4	1.0
40-day Roots	-7.5	-7.0	-21	-2.2

Figure 22. Relative fold changes in mRNA abundance of nuclear genes encoding plastid proteins in the *rpoZ191* mutant.

Total RNA was isolated from siliques, seeds, 2-day seedlings, 5-day seedlings, 5-day roots and 40-day roots of wild-type and *rpoZ191* seedlings grown on MS medium supplemented with 1% sucrose A cDNA input corresponding to 10 ng of reverse transcribed total RNA was used for real-time PCR analysis as described in Figure 17 (Chapter IV).

and at the 5-day seedling stage (from ~8- to 40-fold decrease relative to the wild-type plants). However, the levels of nuclear transcripts in mutant siliques were not significantly different from those of the wild-type (see also Table 23 in Appendix A). Furthermore, accumulation of *Lhca 1* and *Lhcb 1.2* transcripts in 5-day roots was moderately reduced in the mutant compared to the wild-type while *PetH* and *RbcS* transcript levels were unaffected. A moderate reduction in the transcript levels of nuclear genes was also recorded in the 40-day light-exposed mutant roots with the *RbcS* transcripts exhibiting the greatest decrease (~21-fold). Finally, the effect of the *RpoT;3* mutation on the nuclear transcript levels in the *rpoZ191* mature seeds varied depending on the gene studied. For example, *PetH* transcripts, which are barely detectable in wild-type seeds (see Figure 21, see also Table 24 in Appendix A), accumulated to normal levels in the mutant seeds while *RbcS* transcripts were ~3-fold lower in the mutant as compared with wild-type seeds. Interestingly, *Lhca 1* and *Lhcb 1.2* exhibited slightly enhanced transcript levels in the mutant compared to the wild-type seeds (~2- and 12-fold, respectively).

DISCUSSION

An impressive body of biochemical and genetic evidence points to the existence of plastid-derived signaling pathways that affect the transcription or mRNA accumulation of a subset of nuclear genes. Although the exact nature of the signals is not known, at least five different plastid-derived signaling pathways have been identified to date including ROS (reactive oxygen species), redox signaling through plastoquinone or thioredoxin, tetrapyrrole biosynthesis and plastid gene expression (Rodermel, 2001;

Surpin *et al.,* 2002; *Gray et al.,* 2003). Furthermore, previous studies have indicated that plastid signals are generated during early plastid development and are required continuously for the proper expression of nuclear genes encoding chloroplast proteins (Oelmüller *et al.,* 1986; Burgess and Taylor, 1988; Gray *et al.,* 1995).

In the present study we have analyzed the accumulation of transcripts from four nuclear genes (*PetH*, *RbcS*, *Lhca 1* and *Lhcb 1.2*) in both wild-type and *rpoZ191* mutant *Arabidopsis* plants in order to obtain information on the possible role of RpoT;3 in the plastid-to-nucleus signaling pathway. Analysis of *PetH*, *RbcS*, *Lhca 1* and *Lhcb 1*.2 RNA accumulation showed differential transcript accumulation in various tissues and stages of development of wild-type *Arabidopsis* plants with the lowest RNA levels in seeds and 5-day roots, higher in siliques as well as 40-day roots and even higher in 2-day and 5-day seedlings (Figure 21 and Table 15). This pattern of expression resembles the pattern of plastid gene expression (see Figures 10 and 12 in Chapter III) and is in agreement with previous findings that expression of plastid and nuclear genes encoding plastid proteins is coordinated during chloroplast development (reviewed in Simpson and Herrera-Estrella, 1990; Mullet, 1993). Quantitative analysis of *PetH*, *RbcS*, *Lhca 1* and *Lhcb 1.2* RNA levels in the *rpoZ191* mutant showed that the accumulation of these nuclear transcripts was significantly reduced at the 2-day and 5-day stage relative to wild-type plants. In contrast, the steady-state RNA levels produced by the four nuclear genes in the mutant siliques were not significantly affected by the *RpoT;*3 mutation.

RpoT;3 is a nuclear gene and its protein product, (NEP), is responsible for the transcription of many plastid genes including the *rpo* genes encoding subunits of the plastid-encoded RNA polymerase (PEP). The *rpoz191* mutant phenotype demonstrates

that RpoT;3 is required for normal chloroplast biogenesis. In the absence of RpoT;3, plants display a slow greening phenotype where chloroplast biogenesis is perturbed to the greatest extend early in development. At the 2-day seedling stage, for instance, mutant chloroplasts are small and fail to develop normal membrane structures (see Figure 15A in Chapter IV). At the 7-day stage, however, the mutant chloroplasts contain internal membranes and resemble the wild-type plastids in size and shape (see Figure 15B in Chapter IV). Notably, mRNA accumulation of many plastid genes was severely reduced in the mutant 2-day seedlings followed by a partial recovery in transcript levels at the 5-day stage (see Figure 16 and Figure 17A in Chapter IV). The same pattern was observed for the nuclear gene transcripts examined. This suggests that the *rpoZ191* mutation creates a general defect that affects accumulation of plastid and nuclear transcripts during early chloroplast differentiation. However, plastid-encoded as well as nucleus-encoded transcripts are less affected in the *rpoZ191* mutant siliques and roots (Figure 22; see also Figure 17A in Chapter IV). This suggests that the general defect caused by the lack of RpoT;3 has its greatest effect on the early phase of plant development and chloroplast differentiation.

Earlier studies have shown that transcription of nuclear genes encoding products localized in the chloroplasts depends on chloroplast development and gene expression (Oelmüller *et al.,* 1986; Sullivan and Gray, 1999). In addition, plants coordinately regulate the expression of plastid and nuclear genes coding for chloroplast-destined proteins (Taylor, 1989). Since the *RpoT;3* mutation affects both the rate of chloroplast development as well as the expression of plastid and nuclear genes, it seems likely that a plastid-to-nucleus signaling pathway is disrupted in the mutant. The defects caused by the *RpoT;3* mutation are pleiotropic and transcript levels

of many chloroplast genes are drastically reduced including genes encoding components of the transcription and translation apparatus (*rpoA*, *rpoC*, *rps14, rps15*, *rps16*, *rpl32*, *rrn16, trnC-GCA*, *trnV-GAC*), genes encoding subunits of the plastid ATP synthase complex (*atpA* and *atpB*), genes encoding subunits of the plastid NADH dehydrogenase complex (*ndhA*, *B*, *F*, *J*), one gene encoding a component of the cytochrome b_6/f complex (*petA*), one gene encoding a subunit of the plastid acetyl-CoA carboxylase (*accD*), one gene encoding the proteolytic subunit of an ATP-dependent plastid protease (*clpP*) as well as genes encoding components of photosystem I (*psaA*, *psaB* and *psaJ*), photosystem II (*psbA*, *psbD190* and *psbD LRP*) and Rubisco (*rbcL*). It is, therefore, difficult to define a specific signaling pathway responsive to RpoT;3 activity. Homozygous *rpoZ191* mutants are pale-green to yellow-green in color indicating a deficiency in chlorophyll accumulation. It is well established that defects in chlorophyll biosynthesis have a profound effect on the structure of the plastids (von Wettsein *et al.,* 1971; Mascia and Robertson, 1978). In addition, intermediates in chlorophyll biosynthesis have been shown to be involved in plastid-to-nucleus signaling (reviewed in Rodermel, 2001; Surpin *et al.,* 2002). Therefore, it is likely that the slow-greening phenotype displayed by the *rpoz191* mutant plants is due in part to a delay in chlorophyll synthesis. In fact, our results indicate that the transcript levels of *trnE-UUC*, which is involved in the initiation of 5-aminolevulinc (ALA) synthesis, a key precursor for chlorophyll/heme biosynthesis (reviewed in von Wettstein *et al.,* 1995; Kumar *et al.,* 1996), are reduced ~13-fold relative to wild-type at the 2-day stage of seedling development. This plastid-encoded tRNA functions in both chlorophyll/heme biosynthesis and plastid protein synthesis. Since the expression of the plastid translation machinery is also involved in plastid-to nucleus signaling, it is conceivable

that the decreased levels of *trnE-UUC* impair the plastid signals responsive to plastid translation as well as the plastid signals derived from the tetrapyrrole biosynthetic pathway.

Many studies have provided evidence that plastid redox signals regulate the transcription of plastid genes encoding componenets of Photosystem I and Photosystem II (Pfannschmidt *et al.,* 1999). In addition, studies have shown that photosynthetic electron transport is involved in the regulation of nuclear gene expression. In particular, transcription of *Lhcb* and *RbcS* has been shown to be very sensitive to changes in plastid redox state (reviewed in Rodermel, 2001; Pfannschmidt *et al.,* 2003). Because *rpoz191* inhibits RNA accumulation from plastid genes encoding subunits of the plastid ATP synthase complex, NADH dehydrogenase complex, cytochrome b_6/f complex, photosystem I and photosystem II, it is likely that electron transport activity is reduced in the mutant. This, in turn, could disrupt the plastid-to-nucleus redox signals resulting in decreased transcript levels for nuclear genes encoding chloroplast proteins. Each nuclear gene probably responds to one or more different plastid signals. For instance, in higher plants, transcription of *Lhcb* and *RbcS* responds to the redox status of thioredoxin or glutathionine whereas the *PetH* gene, encoding ferredoxin:NADP:oxidoreductase (FNR) does not respond to the same redox signals (reviewed in Rodermel, 2001; Pfannschmidt *et al.,* 2003).

In summary, the data indicate that RpoT;3 plays an important role in the development of functional chloroplasts especially during the early phases of tissue differentiation. The late greening phenotype of *rpoZ191* is probably caused by the overall decrease in the transcription of plastid genes, which also causes a disruption of the plastid-to-nucleus signals. These observations are consistent with the hypothesis

that NEP plays a key role in activation of the chloroplast transcriptional and translational machinery during the early phases of chloroplast differentiation, which, in turn, leads to a build-up of the photosynthetic apparatus and enhanced transcription of the nuclear genes coding for chloroplast proteins (Mullet, 1993; Allison *et al.,* 1996; Hajdukiewicz *et al.,* 1997).

MATERIALS AND METHODS

Plant Growth

Arabidopsis thaliana wild-type (Col-0) and *rpoZ191* mutant seeds were surface sterilized in 95% ethanol for one minute followed by ten minutes incubation in 100% bleach (5.25% sodium hypochlorite-LABBCO, Inc., Houston, TX) + 0.0001% Tween-20. Seeds were washed three times in sterile water and plated on media containing 1x Murashige and Skoog salts and vitamin mixture (Gibco-BRL), 1% sucrose, 0.5 g L-1 2-[N-Morpholino]ethanesulfonic acid (MES) and 0.8% phytagar (Gibco-BRL). The plates were placed at 4^0 C for 5 days and then transferred to continuous white light (40 μE m^{-2} s^{-1}). For root excision, *Arabidopsis* plants were grown vertically on 1X Murashige and Skoog medium as described above. After fifteen days, some Arabidopsis seedlings were transferred to soil whereas others were transferred to fresh plates. Two-day old seedlings, 5-day old seedlings, as well as 5-day and 40-day old roots were harvested, frozen in liquid nitrogen and stored at 80^0 C until further use. Siliques from 34-day old plants transferred to soil after a fifteen-day period of growth on plates were harvested, frozen in liquid nitrogen and stored at 80^0 C until further use.

RNA Isolation and Reverse Transcription

Total RNA from roots, 2-day and 5-day old seedlings was extracted with Tri Reagent (Molecular Research Center, Inc., Cincinnati, OH) using 1-bromo-3-chloropropane (BCP) as a substitute for chloroform as per manufacturer's instructions (Chomczynski and Mackey, 1995). Total RNA from seeds and siliques was isolated using the Concert Plant RNA Reagent, according to the manufacturer's instructions (Invitrogen, Carlsbad, CA) except that BCP (Molecular Research Center, Inc., Cincinnati, OH) was substituted for chloroform. Contaminating DNA was removed using the RNase free DNase (Qiagen, Valencia, CA) with two elutions of five minutes in 30 μL RNase-free water (Ambion, Austin, TX). The purity of RNA was judged by the A_{260}/A_{280} ratios (1.8-2.0) and RNA integrity was assessed by examining the rRNA bands on a standard agarose gel (Sambrook *et al*., 1989). Constant amounts of 2 μg RNA were reverse-transcribed to cDNA in a total volume of 100 μL using random hexamer primers and the TaqMan Reverse Transcription Kit (Applied Biosystems, Foster City, CA). Each 100-μL reaction was prepared as follows: 34.75 μL RNA sample in RNase-free water (Ambion, Austin, TX), 10.0 μL 10X TaqMan RT Buffer, 22.0 μL $MgCl_2$ (5.5 mM), 20.0 μL dNTPs (500 μM each) 5.0 μL random hexamer primers (2.5 μM), 2.0 μL RNase inhibitor (0.4 U/ μL) and 6.25 μL Multiscribe Reverse Transcriptase (3.125 U/ μL). After a ten-minute incubation at 25^0C to increase primer-RNA template binding, reverse transcription was performed for one hour at 37^0C followed by inactivation of the reverse transcriptase at 95^0C for five minutes. The final volume of each 100-μL RT reaction was brought to 200 μL by the addition of 100 μL of RNase-free water and the cDNA was stored at -80^0C until further

use. No-template controls were generated at the same time by combining 2 μg RNA with RNase-free water to a 200-μL final total volume.

Primer Design

Primer pairs were designed for four nuclear target genes using the Primer Express® software v2.0 (Applied Biosystems Foster City, CA) according to the software guidelines The same guidelines provided by the Primer Express® software were used to design all of the amplicons. Briefly, primers for each gene target were selected to contain minimal hairpins and primer-dimer formation as determined by the software and having compatible T_m's, each within 1^0-2^0C of the other (T_m of 58-60^0C) to allow the use of identical temperature cycle conditions for PCR amplification. In addition, primers were designed to be 18-28 bases in length with a minimum and maximum amplicon size of 66 bp and 130 bp, respectively. All oligonucleotide primers used were synthesized by IDT (Integrated DNA Technologies, Inc., Coralville, IA). The sequences of the RT-PCR primers sets are as follows: 5′-GGC ATA GCC GCC GTG TAC-3′and 5′-GAA CTC CGG CGA TAC GAA T-3′ for *Lhca 1*, 5′-GGC TTT CGC GGA GTT GAA G-3′ and 5′-AAC GAA GAA TCC AAA CAT AGA GAA CAT A-3′ for *Lhcb 1.2*, 5′-CAC TCC CGG ATA CTA CGA TGG A-3′ and 5′-GAG TCG GTG CAT CCG AAC A-3′ for *RbcS*, 5′-AGG CCT CTG AGG GAG TAA TTA TAT-3′ and 5′-GAA TTG ATG CTC TCT TTT GAA TGT TT-3′ for *PetH*. In order to verify the specificity of the primers, the designed primer sets were used as query sequences in Blast searches of the NCBI database either alone, together with the DNA segment generated by the PCR process or with N's substituted for the sequence between the primers. The 18S rRNA primers and probe

that produce a 187-bp amplicon were included in the TaqMan rRNA Control Reagents kit (Applied Biosystems, Foster City, CA). Real-time PCR reactions for each set of primers were performed in triplicate along with non-template control reactions and the specificity of the RT-PCR products was verified by both electrophoretic and melting curve analysis. In addition, all primer sets were tested for comparable amplification efficiencies with the endogenous reference primers by plotting the ΔC_T value against the log cDNA input. Only primer sets that showed little variation in amplification efficiency over the dilution series were employed for quantification of mRNA levels (see Table 7 and Figures 6 & 7 in Chapter II).

Real-time PCR: SYBR Green Detection

PCR reactions were carried out in optical 384-well plates on an ABI Prism 7900HT Sequence Detection System using the 2X SYBR Green PCR Master Mix (Applied Biosystems, Foster City, CA) as recommended by the manufacturer. For each sample, a master mix was generated by combining 3.3 µL of cDNA with 29.7 µL of 2X SYBR Green PCR Master Mix (Applied Biosystems) supplemented with primers to a final concentration of 50 nM each and PCR-grade water to a 33 µL final total volume. This mixture was distributed into three replicates of 10 µL each in 384-well amplification plates and sealed with optical adhesive covers (Applied Biosystems). For each primer pair, a no-template control (NTC) was also run in triplicate. The following amplification parameters were used for all PCRs: 10 minutes at 95^0C for optimal AmpliTaq Gold DNA polymerase activation followed by 47 cycles of denaturation at 96^0C for 10 sec and annealing/extending at 60^0C for 1 min. A dissociation curve was generated according to

the protocol present in the ABI Prism 7900HT software (SDS v2.1). Briefly, following the final cycle of the PCR, the reactions were heat denatured over a 35^0C temperature gradient from 60^0 to 95^0C.

Real-time PCR: TaqMan Detection

The master mix for the real-time PCR using TaqMan detection consisted of 3.3 µL of cDNA with 29.7 µL of 2X TaqMan Master Mix (Applied Biosystems) supplemented with primers to a final concentration of 50 nM each, VIC-labeled hybridization probe to a final concentration of 50 nM and PCR-grade water to a 33 µL final total volume. This mixture was distributed into three replicates of 10 µL each in 384-well amplification plates and sealed with optical adhesive covers (Applied Biosystems). A no-template control (NTC) was also run in triplicate. Real-time PCR was performed identically to that described for SYBR Green detection except that the dissociation curve generation step was omitted.

Real-time PCR: Data Analysis

The data generated from both SYBR Green and TaqMan chemistries were analyzed in a similar manner. The C_T values were determined using a signal/noise ratio set to 10 standard deviations above background subtracted mean fluorescence values (ΔR_n) for a baseline value adjusted manually for each set of primers. To correct for differences in input RNA, all quantifications were normalized to the amount of cytoplasmic 18S rRNA and expressed as $2^{-\Delta CT}$, where $\Delta C_T = (C_{T\ sample} - C_{T\ 18S\ rRNA})$ based on the method outlined by Schmittgen and Zakrajsek (2000) and Livak and Schmittgen (2001). PCR

efficiency for each primer pair was determined by analyzing a series of template dilutions (see Chapter II).The slope was calculated from the plot of log input versus C_T and exponential amplification (efficiency) was determined from the equation $E = 10^{(-1/slope)}$ (Rasmussen, 2001). In addition, the amplification efficiencies of the target genes and normalizer (18S rRNA) were compared by determining the slope from the plot of log template dilution versus $\Delta C_T = (C_{T\ sample} - C_{T\ normalizer})$ according to instructions given by Applied Biosystems (Relative quantitation of gene expression, User Bulletin # 2). The fold change in transcript abundance relative to seeds was obtained from the ratios of the individual $2^{-\Delta CT}$ in each tissue to the respective $2^{-\Delta CT}$ values in seeds. The relative fold changes in nucleat transcript abundance in the *rpoZ191* mutant were obtained by the $2^{-\Delta\Delta CT}$ method (Livak, 1997; 2001), where $\Delta\Delta C_T = (\Delta C_{T\ mutant} - \Delta C_{T\ wil\text{-}type})$.

CHAPTER VI

ANALYSIS OF *RpoT* TRANSCRIPT ACCUMULATION IN DIFFERENT TISSUES AND STAGES OF *Arabidopsis thaliana* DEVELOPMENT

INTRODUCTION

RNA polymerase enzymes (NEPs) related to T7 and T3 RNA polymerases are widely found in eukaryotes (Cermakian *et al.,* 1996), including plants such as *Arabidopsis thaliana* (Hedke *et al.,* 1997; 2000), *Chenopodium album* (Weihe *et al.,* 1997), *Triticum aestivum* (Ikeda and Gray, 1999), *Zea mays* (Young *et al.,* 1998; Chang *et al.,* 1999), *Nicotiana tabacum* (Hedke *et al.,* 2002) and *Hordeum vulgare* (Emanuel *et al.,* 2004). Recent data indicate that, in higher plants, a small family of *RpoT* genes encodes mitochondrial as well as plastid RNA polymerases resembling the bacteriophage T7 RNA polymerase. For instance, the *Arabidopsis* genome contains three such genes, *RpoT;1*, *RpoT;2* and *RpoT;3*. While RpoT;2 has been shown to be directed to both mitochondria and plastids, the RpoT;1 and RpoT;2 enzymes are targeted exclusively to mitochondria and plastids, respectively (Hedke *et al.,* 1997; 1999; 2000). Plastids have in addition retained their bacterial type transcription system, including the *rpo* genes encoding the core subunits of the eubacterial RNA polymerase (PEP).

Early evidence for the existence of NEP has come from studies of mutant plants lacking plastid ribosomes. Though unable to synthesize plastid-encoded proteins, including PEP subunits, these plants are still able to synthesize plastid RNAs. Similar results were obtained in transgenic tobacco plants in which the individual *rpo* genes have been deleted (reviewed in Hess and Börner, 1999). Furthermore, studies of these

plants have allowed the identification of the promoter elements recognized by the PEP and NEP enzymes. This led to the hypothesis that NEP is responsible for the transcription of housekeeping genes including the *rpo* genes during the early steps of plastid development while PEP is involved in transcribing photosynthesis-related genes as well as housekeeping genes during the later stages of chloroplast development (Hess and Börner, 1999; Maliga, 1998). Subsequent detailed studies of the transgenic tobacco plants lacking the *rpo* genes have revealed that plastid genes reported to have only PEP promoters are transcribed at low levels in these plants (Krause *et al.,* 2000; Legen *et al.,* 2002). In addition, quantitative analysis of mRNA accumulation from the mitochondrial and plastid-targeted *RpoT* genes (*RpoTm* and *RpoTp*, respectively) in different tissues of maize revealed that *RpoTm* transcripts were more abundant in nonphotosynthetic tissues such as silks and roots whereas *RpoTp* transcripts were more abundant in phototosynthetic tissues such as leaves. However, both genes were expressed to some extent in all tissues examined indicating that their products are required for basal mitochondrial and plastid functions (Chang *et al.,* 1999). Similarly, analysis of *RpoTm* and *RpoTp* transcript abundance in barley indicated differential mRNA accumulation for both transcripts in roots and over the developmental leaf gradient examined with *RpoTm* transcripts being more prevalent in roots while *RpoTp* transcripts were more abundant throughout leaf development (Emanuel *et al.*, 2004). Finally, a similar pattern of mRNA accumulation was also observed for the *Arabidopsis RpoT;1* and *RpoT;3* genes encoding a mitochondrial-directed and a plastid–directed RNAP, respectively (Baba *et al.,* 2004).

Our previous studies documented differential plastid transcript accumulation in various tissues and developmental stages of *Arabidopsis thaliana* with the lowest

transcript levels observed in seeds and 5-day roots. In contrast, mRNA accumulation of plastid genes in siliques as well as in 40-day roots was higher and reached a peak in 2-day and 5-day seedlings followed by progressive decline in older tissues such as 12-day and 15-day cotyledons (see Figure 10 and Figure 12 in Chapter III). Moreover, real-time PCR analysis of plastid RNA accumulation in the *Arabidopsis RpoT;3* mutant (*rpoZ191*) indicated that the *RpoT;3* mutation had a differential effect early in leaf development (see Figure 17 in Chapter IV). This suggests that the different NEPs might have distinct roles in organellar gene transcription. To gain further insight into the functional role of *RpoT;1*, *RpoT;2* and *RpoT;3*, quantitative real-time PCR was used to investigate the tissue specific expression of all three NEPs. In addition, our previous studies have indicated that plastid transcript accumulation during the transition from seed to 2-day and 5-day seedlings is strongly dependent on RpoT;3 (see Chapter IV). Therefore, in the present study we wanted to examine if the increase in RpoT;3-dependent plastid mRNA accumulation was paralleled by an increase in *RpoT;3* mRNA level.

RESULTS

Tissues and Transcripts Analyzed

Previous studies have shown that transcript accumulation from the *RpoT* genes was low (Hedke *et al.,* 1997; Weihe *et al.,* 1997). Therefore, in the present study, we employed quantitative real-time PCR to measure the steady state mRNA levels of the three *RpoT* genes in several tissues and different developmental stages of the wild type

as well as the RpoT*;3 Arabidopsis* mutants. Transcript levels for the three *RpoT* genes were quantified in dry seeds, 2-day seedlings, 5-day seedlings, 5-day roots, 40-day roots and 34-day siliques (Figure 23A). In addition, the mRNA levels of *RpoT;2* and *RpoT;3* were examined in 10-day cotyledons, 12-day cotyledons, 15-day cotyledons (Figure 23B), 15-day and 35-day rosette leaves as well as 35-day cauline leaves. The *RpoT* genes analyzed include *RpoT;1* (Acc.No.Y08137), encoding a phage-type RNA polymerase targeted to mitochondria, *RpoT;2* (Acc.No. AJ278248), encoding a phage-type RNA polymerase targeted to both mitochondria and plastids and *RpoT;3* (Y08463), encoding a plastid-targeted phage-type RNA polymerase.

Differential *RpoT* Transcript Accumulation in Various Tissues and Stages of Development of Arabidopsis *thaliana*

The results of quantitative real-time PCR of *RpoT;1*, *RpoT;2*, *RpoT;3* transcripts revealed differential expression of *RpoT* genes in wild-type tissues with the *RpoT;3* being the most abundant *RpoT* transcript in all tissues examined except in siliques where the levels of *RpoT;2* showed a ~2-fold increase relative to the *RpoT;3* levels (see Figure 23). To facilitate the detection of differential transcript accumulation, RNA abundance in the various tissues and developmental stages examined was expressed relative to that in seeds. In addition, changes in the ratio of transcript abundance in 2- and 5-day old seedlings, 5- and 40-day old roots,10-day and 12-day cotyledons as well as 10-day and 15-day cotyledons relative to the abundance in seeds were calculated and listed in columns in Tables 18 &19.

Quantitative real-time PCR showed a differential expression of *RpoT* genes in dry seeds (Figure 23). For instance, the relative amounts of *RpoT;3* and *RpoT;2* normalized to those of 18S rRNA were 3.8 and 2.4, respectively, whereas the relative amount of *RpoT;*1 to 18S rRNA was 0.9. In siliques, however, the transcript levels of *RpoT;3* and *RpoT;1* were lower relative to mature seeds whereas the *RpoT;2* transcripts accumulated to similar levels in both siliques and mature seeds (Table 18). To study the changes in steady-state levels of the *RpoT* RNAs during the early stages of seedling establishment, we performed real-time PCR analysis on RNA from 2-day and 5-day seedlings. At the 2-day stage, our data show a moderate increase in transcript abundance relative to seeds only for the *RpoT;1* mRNA whereas the transcript levels of *RpoT;3* and *RpoT;2* were not significantly different in 2-day seedlings compared with mature seeds. At the 5-day stage, we observed a ~2- to 2.5-fold increase in transcript abundance relative to seeds for all three *RpoT* RNAs analyzed (see Table 18). Analysis of *RpoT* transcript accumulation in 5-day and 40-day light-exposed roots revealed a ~2-fold increase of *RpoT;1* and *RpoT;2* RNA levels relative to dry seeds. In contrast, the mRNA abundance of *RpoT;3* was lower in 5-day roots relative to dry seeds. In addition, comparison of *RpoT* transcript accumulation from 5-day and 40-day roots (see Table 18) indicated that there was an increase in the abundance of *RpoT;1* and *RpoT;2* transcripts as compared to 5-day roots (~4- to 5-fold) while *RpoT;3* transcript levels remained unchanged.

Transcript accumulation for the *RpoT;2* and *RpoT;3* genes was analyzed in 10-day, 12-day and 15-day cotyledons (see Figure 23B). When *RpoT* RNA abundance is expressed relative to that in seeds (Table 19), it can be seen that *RpoT;2* transcripts

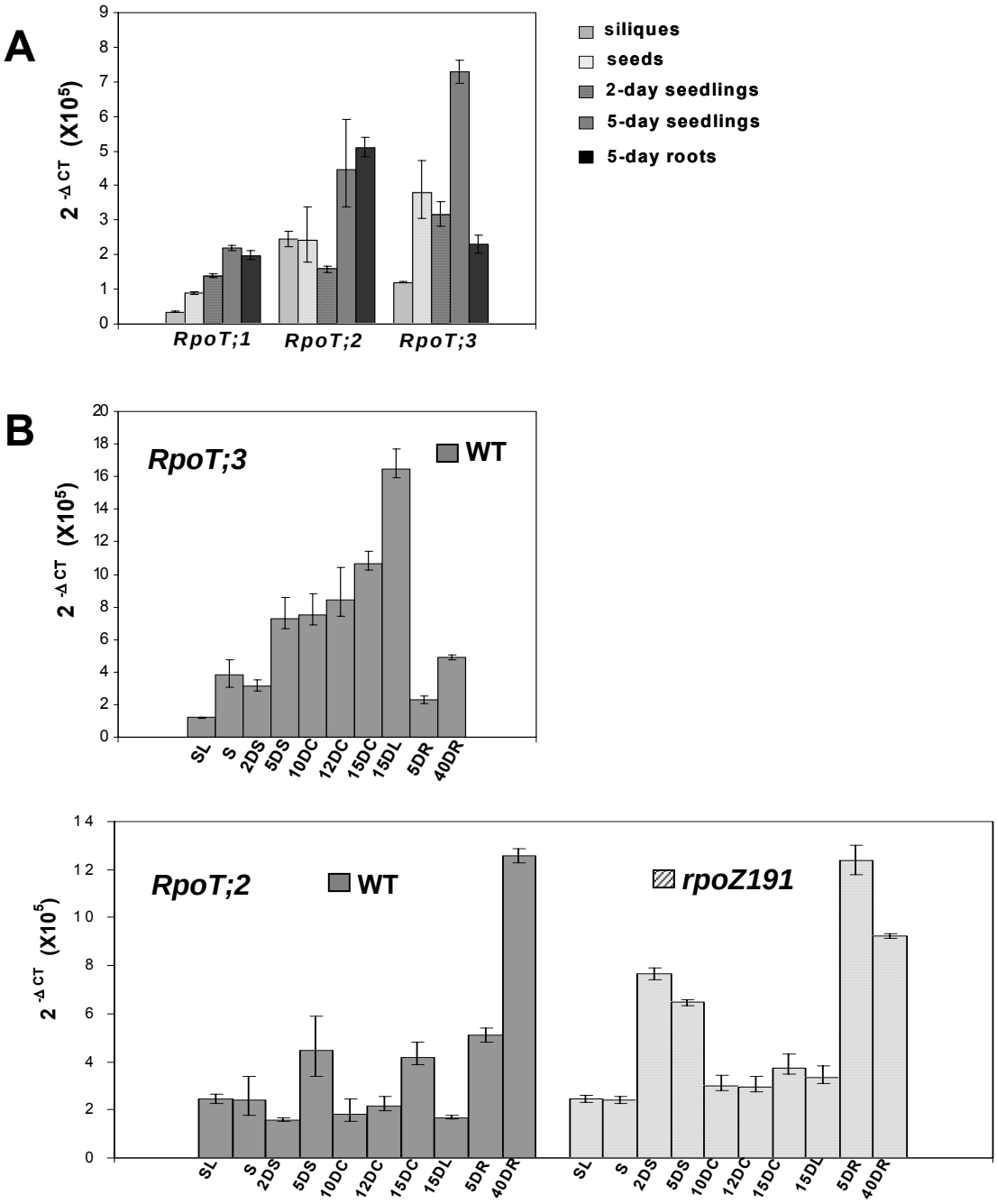

Figure 23. Real-time PCR analysis of *RpoT;1*, *RpoT;2*,and *RpoT;3* transcript abundance in various tissues.

Total RNA was isolated from siliques (SL), seeds (S), 2-day seedlings (2DS), 5-day seedlings (5DS), 10-day cotyledons (10DC), 12-day cotyledons (12DC),15-day cotyledons (15DC), 15-day leaves (15DL), 5-day roots (5DR) and 40-day roots (40DR) of wild-type and *rpoZ191* seedlings grown on MS medium supplemented with 1% sucrose. A cDNA input corresponding to 10 ng of total RNA was used for real-time PCR analysis. The bar graphs represent the amounts of *RpoT* transcripts from the mean of three trials relative to cytoplasmic 18S rRNA levels, with the standard deviation indicated. The given data are expressed as $2^{-\Delta CT}$ X10^5, where $\Delta C_T = (C_{T\ sample}-C_{T\ normalizer})$.
(A) Transcript accumulation of *RpoT;1*, *RpoT;2* and *RpoT;3* in wild-type.
(B) Transcript accumulati on of *RpoT;3* and *RpoT;2* in wild-type and *rpoZ191* mutant.

Table 18. Abundance of *RpoT* mRNA in siliques, 2-day seedlings, 5-day seedlings, 5-day roots and 40-day roots relative to seeds[a]

Gene	Siliques	2-day seedlings	5-day seedlings	ratio 2d/5d seedlings	5-day roots	40-day roots	ratio 40d/5d roots
RpoT;1	0.40 (0.36-0.44)	1.6 (1.5-1.7)	2.5 (2.3-2.7)	0.6 (0.5-0.7)	2.3 (2.0-2.5)	3.9 (3.6-4.2)	1.7 (1.4-2.0)
RpoT;2	1.0 (0.7-1.5)	0.8 (0.5-1.1)	1.9 (0.9-3.2)	0.4 (0.1-0.8)	2.1 (1.4-3.1)	5.2 (3.6-7.4)	2.5 (1.0-4.6)
RpoT;3	0.32 (0.25-0.40)	0.8 (0.6-1.1)	1.9 (1.5-2.5)	0.4 (0.2-0.7)	0.6 (0.4-0.8)	1.3 (1.0-1.7)	2.1 (1.0-3.5)

[a] Seeds of *Arabidopsis thaliana* ecotype Columbia were surface-sterilized and sown in Petri dishes on MS medium containing 1% sucrose. The plates were placed at 4^0C for 5 days before being transferred to continuous white light (40 µmol m^{-2} sec^{-1}). Siliques were collected from 34-day old *Arabidopsis* plants grown on soil after a 15-day period of growth on MS medium containing 1% sucrose. Total RNA was isolated from siliques, seeds, 2-day seedlings, 5-day seedlings, 5-day roots and 40-day roots and converted to cDNA in reactions that were normalized to contain equivalent amounts of total RNA. A cDNA input corresponding to 10 ng of reverse transcribed total RNA was employed as template for real-time PCR analysis. Reactions were run in triplicate and data were normalized relative to cytoplasmic 18S rRNA levels and expressed as $2^{-\Delta CT}$ $X10^5$, where $\Delta C_T = (C_{T\ sample} - C_{T\ normalizer})$. The fold change in mRNA abundance of each gene in siliques, 2-day seedlings, 5-day seedlings, 5-day roots and 40-day roots relative to seeds was derived from the ratio of the individual $2^{-\Delta CT}$ values in each tissue to the respective $2^{-\Delta CT}$ values in seeds . The range given in parenthesis is determined by evaluating the expression $2^{-\Delta CT}$ with ΔC_T + SD and ΔC_T – SD, where SD = the standard deviation of the ΔC_T value calculated according to the formula $S = \sqrt{(S^2_{\ sample} + S^2_{\ normalizer})}$

Table 19. Abundance of *RpoT; 2* and *RpoT; 3* mRNA in 10-day, 12-day and 15-day cotyledons relative to seeds [a]

Gene	10-day cotyledons	12-day cotyledons	ratio 10d/12d cotyledons	15-day cotyledons	ratio 10d/15d cotyledons
RpoT;2	0.8 (0.4-1.3)	0.9 (0.6-1.4)	0.8 (0.6-1.3)	1.7 (1.1-2.7)	0.4 (0.3-0.7)
RpoT;3	2.0 (1.4-2.8)	2.2 (1.5-3.3)	0.9 (0.4-1.7)	2.8 (2.2-3.7)	0.7 (0.3-1.2)

[a] Total RNA was isolated from seeds as well as 10-day, 12-day and 15-day cotyledons of *A. thaliana* seedlings grown on MS medium supplemented with 1% sucrose. Equivalent amounts of total RNA were converted to cDNA and assayed by real- time PCR as described in Table 18.

accumulate in 10-day and 12-day cotyledons at a constant level and increase in 15-day cotyledons (~1.7- fold increase relative to mature seeds). In contrast, *RpoT;3* showed a progressive increase in transcript accumulation from ~2- to 2.8-fold relative to mature seeds. We also investigated transcript accumulation for the *RpoT;2* and *RpoT;3* genes in young 15-day rosette leaves of *Arabidopsis* plants sown on MS medium containing 1% sucrose and in mature 35-day rosette leaves as well as 35-day cauline leaves of plants transferred to soil after an initial 15-day period of growth on MS medium. The results shown in Table 20 indicate limited transcript accumulation in young 15-day rosette leaves similar to the levels seen in dry seeds for *RpoT;2*. In contrast, transcript levels relative to mature seeds for *RpoT;3* in 15-day rosette leaves were ~4-fold higher. On the other hand, in mature 35-day rosette and cauline leaves *RpoT;2* and *RpoT;3* showed similar but enhanced levels of transcript accumulation relative to mature seeds (~3- to 4-fold increase relative to dry seeds).

Effect of *RpoT;3* Mutation on *RpoT;2* Transcript Levels

To investigate whether *RpoT;2* transcript abundance is affected in the *RpoT;3* mutants, *RpoT;2* mRNA abundance in several tissues and from different developmental stages was monitored in both wild-type and *rpoZ191* mutant by real-time PCR. Transcript levels for the *RpoT;2* gene were quantified in dry seeds, 2-day seedlings, 5-day seedlings, 10-day cotyledons, 12-day cotyledons, 15-day cotyledons,15-day rosette leaves, 35-day rosette leaves, 35-day cauline leaves, 5-day roots, 40-day roots as well

Table 20. Abundance of *RpoT;2* and *RpoT;3* mRNA in 15-day rosette leaves, 35-day rosette leaves and 35-day cauline leaves relative to seeds [a]

Gene	15-day rosette leaves	35-day rosette leaves	35-day cauline leaves
RpoT;2	0.7 (0.5-1.0)	3.8 (2.5-5.5)	3.6 (2.6-5.1)
RpoT;3	4.3 (3.3-5.7)	3.2 (2.3-4.3)	3.8 (3.0-4.9)

[a] Total RNA was isolated from 15-day rosette leaves of *A. thaliana* plants grown on MS medium supplemented with 1% sucrose, 35-day rosette leaves and 35-day cauline leaves of *A. thaliana* plants grown on soil after a 15-day period of growth on MS medium containing 1% sucrose. Equivalent amounts of total RNA were converted to cDNA and assayed by real-time PCR as described in Table 18.

as 34-day siliques (Figure 23B). The results in Table 21 showed distinct tissue specific effects of the *RpoT;3* mutation on the *RpoT;2* transcript accumulation. For instance, in siliques, seeds, 12-day cotyledons, 15-day cotyledons, 35-day rosette leaves, 35-day cauline leaves as well as 40-day roots the *RpoT;2* transcipts in the mutant were not significantly different from those of the wid-type. However, the transcript level of *RpoT;2* in the mutant was higher compared to that in the wild-type in young photosynthetic tissues such as 5-day seedlings, 10-day cotyledons as well as 15-day rosette leaves (~1.5-, 1.7- and 2.0-fold, respectively). Interestingly, the largest increase in the *RpoT;2* trancript levels was observed at the 2-day stage (~4-fold increase relative to the wild-type plants).

DISCUSSION

In higher plants, the small nuclear *RpoT* gene family encodes organellar destined RNA polymerases resembling the bacteriophage T7 RNA polymerase. Recent evidence has shown that *RpoT;1* and *RpoT;3* are targeted exclusively either to mitochondria or plastids whereas *RpoT;2* is targeted to both mitochondria and plastids (Hedke *et al.,* 1997; 1999; 2000). Additionally, our previous results have indicated that in the *RpoT;3* mutant, the levels of plastid transcripts in tissues such as seeds and 5-day roots were not significantly different from the wild-type suggesting that RpoT;3 does not play a major role in the transcription of the plastid genes in the non-photosynthetic plastids of seeds and roots. Furthermore, the lack of RpoT;3 did not have any effect on plastid transcript abundance in the siliques indicating that the RpoT;3 activity is not

Table 21. Relative fold changes in *RpoT;2* mRNA abundance in the *rpoZ191* mutant[a]

Tissue	Fold Change
Siliques	1.0 (0.9-1.2)
Seeds	1.0 (0.9-1.1)
2-day seedlings	4.2 (3.9-4.6)
5-day seedlings	1. 5 (1.1-1.9)
10-day cotyledons	1. 7 (1.5-1.8)
12-day cotyledons	1.4 (1.3-1.5)
15-day cotyledons	0.9 (0.8-1.2)
15-day rosette leaves	2.0 (1.7-2.3)
35-day rosette leaves	0.8 (0.7-0.9)
35-day cauline leaves	0.8 (0.7-0.9)
5-day roots	2.4 (2.2-2.7)
40-day roots	0.73 (0.71-0.76)

[a] Total RNA was isolated from wild-type and *rpoZ191* mutant as described in Table 16, Table 17 and Table 18. The 18S rRNA normalized real-time PCR data were used to determine the relative fold change calculated using the $2^{-\Delta\Delta CT}$ method, where $\Delta\Delta C_T = \Delta C_{T\ mutant} - \Delta C_{T\ wild\text{-}type}$, and ΔC_T is the C_T of the normalizer subtracted from the C_T of the target gene. The range given in parenthesis is determined by evaluating the expression $2^{-\Delta\Delta CT}$ with $\Delta\Delta C_T$ + SD and $\Delta\Delta C_T$ – SD, where SD = the standard deviation of the $\Delta\Delta C_T$ value calculated according to the formula $S = \sqrt{(S^2_{\ sample} + S^2_{\ normalizer})}$

essential at this stage of development and that RpoT;2 or another NEP might be responsible for the transcription of plastid genes in wild-type siliques (see Chapter IV).

To gain further insight into the function of the different organellar RNA polymerases, we have examined the patterns of expression of the three *RpoT* genes, *RpoT;1*, *RpoT;2* and *RpoT;3*, in various tissues and developmental stages of *Arabidopsis* wild-type and *RpoT;3* mutant plants. Our data indicate that *RpoT* gene expression in the wild-type varies among plant tissues with the *RpoT;3* being the most abundant *RpoT* transcript in all tissues examined except in siliques where *RpoT;2* was found to be the most abundant *RpoT* transcript. In addition, the transcript levels of *RpoT;2* as well as *RpoT;1* were ~2.1- and 2.3-fold higher in 5-day roots relative to dry seeds whereas *RpoT;3* transcripts accumulated to similar levels in both mature seeds and 5-day roots (see Figure 23A). Our results on the transcript accumulation kinetics of the *RpoT* genes during plant development coincide with previous studies obtained with tobacco and *Arabidopsis* (Hedke *et al.,* 2002; Baba *et al.,* 2004) indicating a differential transcription of the *RpoT* genes in various plant tissues.To facilitate the detection of differential transcript accumulation, changes in the ratio of *RpoT;3* transcript abundance in siliques, seeds, 2- and 5-day old seedlings, 10- day,12-day, 10-day and 15-day cotyledons, 15-day and 35-day rosette leaves, 35-day cauline leaves as well as 5- and 40-day old roots, relative to the *RpoT;2* abundance were calculated and are listed in Table 22. In general, the relative ratio of *RpoT;3* to *RpoT;2* transcripts varied according to the tissue or stage of development examined. For instance, *RpoT;3* transcripts accumulated to higher levels relative to *RpoT;2* transcripts in young photosynthetic tissues such as 2-day and 5-day seedlings, 10-day, 12-day and 15-day cotyledons as well as 15-day rosette leaves. In older photosynthetic tissues such as 35-day rosette

Table 22. Ratios of *RpoT;3* relative to *RpoT;2* mRNA abundance in various tissues of *A.thaliana*.

Tissue	*RpoT;3 / RpoT;2*
Siliques	0.49 (0.44-0.54)
Seeds	1.6 (0.8-2.6)
2-day seedlings	1.7 (1.6-2.0)
5-day seedlings	1.6 (1.2-2.2)
10-day cotyledons	4.1 (3.1-6.4)
12-day cotyledons	3.9 (3.1-5.6)
15-day cotyledons	2.6 (2.3-3.1)
15-day rosette leaves	9.9 (9.2-11.4)
35-day rosette leaves	1.4 (1.1-1.6)
35-day cauline leaves	1.7 (1.6-1.7)
5-day roots	0.45 (0.38-0.53)
40-day roots	0.39 (0.37-0.41)

[a]The ratio of *RpoT;3* relative to *RpoT;2* mRNA abundance was derived from the data in Table 25 (see Appendix A). The range given in parenthesis is determined by evaluating the expression $2^{-\Delta CT}$ with ΔC_T + SD and ΔC_T – SD, where SD = the standard deviation of the ΔC_T value calculated according to the formula $S = \sqrt{(S^2_{sample} + S^2_{normalizer})}$.

and cauline leaves as well as in the non-photosynthetic plastids of seeds *RpoT;2* and *RpoT;3* accumulated to similar levels. On the other hand, *RpoT;3* transcripts accumulated to lower levels relative to *RpoT;2* in siliques (~0.5-fold) as well as in light grown 5-day and 40-day old roots (~0.5- and 0.4-fold, respectively).These results suggest that there is division of labor between the two NEPs with RpoT;3 being the dominant NEP in young photosynthetic tissues whereas RpoT;2 activity is more important in siliques as well as roots. These findings are consistent with our previous results (see Capter IV) indicating the *RpoT;3* mutation has tissue specific effects.

In the wild-type the early stage of plant and chloroplast development is characterized by a massive increase in plastid expression associated with the greening and the conversion of plastids into photosynthetically active chloroplasts. Plastid mRNA levels, which are low in proplastids, increase dramatically during the early stages of chloroplast development and are followed by a decline during the later stages of chloroplast maturation (Baumgartner *et al.*, 1989). Thus, one would expect a significant increase in plastid RNAP activity during the early stages of chloroplast differentiation. One of the most interesting findings of this study is that mRNA levels of *RpoT;2* as well as *RpoT;3* do not increase significantly during development. In fact, *RpoT;2* transcript levels did not increase from seeds to 2-day seedlings, 10-day cotyledons and 12-day cotyledons and were slightly enhanced in 5-day seedlings as well as in 15-day cotyledons. In contrast, *RpoT;3* showed a progressive but small increase in transcript accumulation (see Figure 23B) and reached its peak at day 15 (~2.8-fold increase relative to mature seeds). Our previous studies indicated that in the absence of *RpoT;3*, plants display a delay in greening and in chloroplast development (see Figures 13 &15 in Chapter IV). Additionally, mRNA accumulation of many plastid and nuclear genes

encoding plastid localized components was drastically reduced in the mutant 2-day seedlings, followed by a partial recovery in transcript levels at the 5-day stage (see Figure 16 and Figure 17A in Chapter IV) indicating that in the plastids of young seedlings the RpoT;3 deficiency was not compensated for by RpoT;2 even though *RpoT;2* showed an enhanced level of transcript accumulation in the *rpoZ191* mutant plants at the 2-day stage (~4-fold increase compared to the wild-type plants). These observations clearly suggest that *RpoT;2* does not represent the critical NEP activity that drives the transcription of plastid genes during the early stages of plastid development. Instead, our results are consistent with *RpoT;3*, playing a differential important role in transcribing plastid genes during the early stages of plastid development. However, although the largest effect of the *RpoT;3* mutation was recorded at the 2-day stage, we did not observe a substantial increase in the *RpoT;3* RNA at this stage (see Figure 23A). We, therefore, concluded that the increase in *RpoT;3* activity during the early phases of chloroplast development is not due to an increase in mRNA steady state levels. This, in turn, implies the existence of post-transcriptional mechanisms of activation. In this scenario, activation of RpoT;3 could be mediated by increased synthesis of nucleus encoded plastid localized specificity factors and/or reversible phosphorylation.

Protein phosphorylation is a very important post-translational modification involved in signal transduction and metabolic pathways and chloroplasts contain a series of protein kinases that are known to phosphorylate several organellar proteins including components of the photosynthetic apparatus (Bennett, 1991; Gal *et al.,* 1990; Race and Hind, 1996). Regulation of plastid transcription through reversible phosphorylation has been shown in mustard where purified σ-like factors were found to

be phosphorylated in the dark and de-phosphorylated in the light (Tiller and Link 1993a; 1993b). In addition, a serine-specific protein kinase, PTK, has been found to associate with the plastid-encoded RNA polymerase (PEP). Recognition of promoters and initiation of transcription by PEP require sigma factors, which are encoded in the nuclear genome. This polymerase-associated kinase phosphorylates chloroplast σ-factors *in vitro* and is itself regulated by reversible phosphorylation (Baginski *et al*., 1997; González-Baena *et al.,* 2001).

RpoT;3 is a nucleus-encoded plastid localized RNAP (NEP) related to the RNA polymerases of T7 and T3 bacteriophages. In contrast to the T7 polymerase, the NEP enzymes lack the specificity loop amino acid residues that confer promoter specificity for the T7 RNA polymerase (Chang *et al*, 1999) and cannot initiate transcription from their cognate promoters *in vitro* (Bligny *et al.,* 2000; Cahoon and Stern*,* 2001). It is, therefore, conceivable that during the early stages of chloroplast differentiation, which are characterized by a burst in transcription of many plastid genes, RpoT;3-dependent transcription of plastid genes requires the presence of specificity factors. In plants, the RNAP-associated p63 protein from wheat mitochondria has been shown to interact with a mitochondrial promoter and stimulate transcription *in vitro* (Ikeda and Gray, 1999). Additionally, the spinach CDF2 protein has been shown to confer promoter recognition properties to a NEP enzyme while a different version of this factor was found to interact with PEP (Bligny et al., 2000). Finaly, the dual-targeted maize ZmSig2B sigma factor which was shown to confer promoter specicifity to PEP was also found to co-purify with the mitochondrial RpoT enzyme suggesting that ZmSig2B could act as an RpoT specificity factor (Beardslee *et al., 2002)*.

MATERIALS AND METHODS

Plant Growth

Arabidopsis thaliana wild-type (Col-0) and *rpoZ191* mutant seeds were surface sterilized in 95% ethanol for one minute followed by ten minutes incubation in 100% bleach (5.25% sodium hypochlorite-LABBCO, Inc., Houston, TX) + 0.0001% Tween-20. Seeds were washed three times in sterile water and plated on media containing 1x Murashige and Skoog salts and vitamin mixture (Gibco-BRL), 1% sucrose, 0.5 g L-1 2-[N-Morpholino]ethanesulfonic acid (MES) and 0.8% phytagar (Gibco-BRL). The plates were placed at 4^0 C for 5 days and then transferred to continuous white light (40 μE m^{-2} s^{-1}). For root excision, *Arabidopsis* plants were grown vertically on 1X Murashige and Skoog medium as described above. After fifteen days, some Arabidopsis seedlings were transferred to soil whereas others were transferred to fresh plates. Two-day old seedlings, 5-day old seedlings, as well as 5-day and 40-day old roots were harvested, frozen in liquid nitrogen and stored at 80^0 C until further use. Siliques from 34-day old plants transferred to soil after a fifteen-day period of growth on plates were harvested, frozen in liquid nitrogen and stored at 80^0 C until further use.

RNA Isolation and Reverse Transcription

Total RNA from 5-day and 40-day roots, 2-day old seedlings, 5-day old seedlings, 10-day, 12-day and 15-day cotyledons, as well as 35-day rosette and cauline leaves was extracted with Tri Reagent (Molecular Research Center, Inc., Cincinnati, OH) using 1-

bromo-3-chloropropane (BCP) as a substitute for chloroform as per manufacturer's instructions (Chomczynski and Mackey, 1995). Total RNA from seeds and siliques was isolated using the Concert Plant RNA Reagent, according to the manufacturer's instructions (Invitrogen, Carlsbad, CA) except that BCP (Molecular Research Center, Inc., Cincinnati, OH) was substituted for chloroform. Contaminating DNA was removed using the RNase free DNase (Qiagen, Valencia, CA) with two elutions of five minutes in 30 μL RNase-free water (Ambion, Austin, TX). The purity of RNA was judged by the A_{260}/A_{280} ratios (1.8-2.0) and RNA integrity was assessed by examining the rRNA bands on a standard agarose gel (Sambrook *et al*., 1989). Constant amounts of 2 μg RNA were reverse-transcribed to cDNA in a total volume of 100 μL using random hexamer primers and the TaqMan Reverse Transcription Kit (Applied Biosystems, Foster City, CA). Each 100-μL reaction was prepared as follows: 34.75 μL RNA sample in RNase-free water (Ambion, Austin, TX), 10.0 μL 10X TaqMan RT Buffer, 22.0 μL $MgCl_2$ (5.5 mM), 20.0 μL dNTPs (500 μM each) 5.0 μL random hexamer primers (2.5 μM), 2.0 μL RNase inhibitor (0.4 U/ μL) and 6.25 μL Multiscribe Reverse Transcriptase (3.125 U/ μL). After a ten-minute incubation at 25^0C to increase primer-RNA template binding, reverse transcription was performed for one hour at 37^0C followed by inactivation of the reverse transcriptase at 95^0C for five minutes. The final volume of each 100-μL RT reaction was brought to 200 μL by the addition of 100 μL of RNase-free water and the cDNA was stored at -80^0C until further use. No-template controls were generated at the same time by combining 2 μg RNA with RNase-free water to a 200-μL final total volume.

Primer Design

Primer pairs were designed for three *RpoT* target genes using the Primer Express® software v2.0 (Applied Biosystems Foster City, CA) according to the software guidelines The same guidelines provided by the Primer Express® software were used to design all of the amplicons. Briefly, primers for each gene target were selected to contain minimal hairpins and primer-dimer formation as determined by the software and having compatible T_m's, each within 1^0-2^0C of the other (T_m of 58-60^0C) to allow the use of identical temperature cycle conditions for PCR amplification. In addition, primers were designed to be 19-24 bases in length with a minimum and maximum amplicon size of 73 bp and 83 bp, respectively. All oligonucleotide primers used were synthesized by IDT (Integrated DNA Technologies, Inc., Coralville, IA). The sequences of the RT-PCR primers sets are as follows: 5´- GGT GTT GAC TCT AAG CCG TGA GA -3´and 5´- AAA ATT TGG TGC AAA AGC AGT CAT-3´ for *RpoT;1* (GenBank acc.no. Y08137), 5´- TCA TGG AGC CAA GCA ACA AAG -3´ and 5´- AGC GTA TCC AGG GCC TCA A -3´ for *RpoT;2* (GenBank acc.no. AJ278248), 5´- TAG CAC CAG TGA ACC ATC TGA AG -3´ and 5´- GTT ATT TAC AGG CCA CCA AGG AA -3´ for *RpoT;3* (GenBank acc.no. Y08463). In order to verify the specificity of the primers, the designed primer sets were used as query sequences in Blast searches of the NCBI database either alone, together with the DNA segment generated by the PCR process or with N's substituted for the sequence between the primers. The 18S rRNA primers and probe that produce a 187-bp amplicon were included in the TaqMan rRNA Control Reagents kit (Applied Biosystems, Foster City, CA). Real-time PCR reactions for each set of primers were performed in triplicate along with non-template control reactions and the specificity of

the RT-PCR products was verified by both electrophoretic and melting curve analysis. In addition, all primer sets were tested for comparable amplification efficiencies with the endogenous reference primers by plotting the ΔC_T value against the log cDNA input. Only primer sets that showed little variation in amplification efficiency over the dilution series were employed for quantification of mRNA levels (see Table 7 and Figures 6 & 7 in Chapter II).

Real-time PCR: SYBR Green Detection

PCR reactions were carried out in optical 384-well plates on an ABI Prism 7900HT Sequence Detection System using the 2X SYBR Green PCR Master Mix (Applied Biosystems, Foster City, CA) as recommended by the manufacturer. For each sample, a master mix was generated by combining 3.3 µL of cDNA with 29.7 µL of 2X SYBR Green PCR Master Mix (Applied Biosystems) supplemented with primers to a final concentration of 50 nM each and PCR-grade water to a 33 µL final total volume. This mixture was distributed into three replicates of 10 µL each in 384-well amplification plates and sealed with optical adhesive covers (Applied Biosystems). For each primer pair, a no-template control (NTC) was also run in triplicate. The following amplification parameters were used for all PCRs: 10 minutes at 95^0C for optimal AmpliTaq Gold DNA polymerase activation followed by 47 cycles of denaturation at 96^0C for 10 sec and annealing/extending at 60^0C for 1 min. A dissociation curve was generated according to the protocol present in the ABI Prism 7900HT software (SDS v2.1). Briefly, following the final cycle of the PCR, the reactions were heat denatured over a 35^0C temperature gradient from 60^0 to 95^0C.

Real-time PCR: TaqMan Detection

The master mix for the real-time PCR using TaqMan detection consisted of 3.3 µL of cDNA with 29.7 µL of 2X TaqMan Master Mix (Applied Biosystems) supplemented with primers to a final concentration of 50 nM each, VIC-labeled hybridization probe to a final concentration of 50 nM and PCR-grade water to a 33 µL final total volume. This mixture was distributed into three replicates of 10 µL each in 384-well amplification plates and sealed with optical adhesive covers (Applied Biosystems). A no-template control (NTC) was also run in triplicate. Real-time PCR was performed identically to that described for SYBR Green detection except that the dissociation curve generation step was omitted.

Real-time PCR: Data Analysis

The data generated from both SYBR Green and TaqMan chemistries were analyzed in a similar manner. The C_T values were determined using a signal/noise ratio set to 10 standard deviations above background subtracted mean fluorescence values (ΔR_n) for a baseline value adjusted manually for each set of primers. To correct for differences in input RNA, all quantifications were normalized to the amount of cytoplasmic 18S rRNA and expressed as $2^{-\Delta CT}$, where $\Delta C_T = (C_{T\ sample} - C_{T\ 18S\ rRNA})$ based on the method outlined by Schmittgen and Zakrajsek (2000) and Livak and Schmittgen (2001). PCR efficiency for each primer pair was determined by analyzing a series of template dilutions (see Chapter II).The slope was calculated from the plot of log input versus C_T and exponential amplification (efficiency) was determined from the equation $E = 10^{(-1/slope)}$ (Rasmussen, 2001). In addition, the amplification efficiencies of the target genes

and normalizer (18S rRNA) were compared by determining the slope from the plot of log template dilution versus $\Delta C_T = (C_{T\ sample} - C_{T\ normalizer})$ according to instructions given by Applied Biosystems (Relative quantitation of gene expression, User Bulletin # 2). The fold change in transcript abundance relative to seeds was obtained from the ratios of the individual $2^{-\Delta CT}$ in each tissue to the respective $2^{-\Delta CT}$ values in seeds. The relative fold changes in *RpoT;2* transcript abundance in the *rpoZ191* mutant were obtained by the $2^{-\Delta\Delta CT}$ method (Livak, 1997; 2001), where $\Delta\Delta C_T = (\Delta C_{T\ mutant} - \Delta C_{T\ wil\text{-}type})$. *RpoT;3*/*RpoT;2* ratios were derived from the individual $2^{-\Delta CT}$ values obtained for *RpoT;3* and *RpoT;2*, where $\Delta C_T = (C_{T\ sample} - C_{T\ 18S\ rRNA})$.

CHAPTER VII

SUMMARY

Plastids are essential organelles of the plant cell that vary in their morphology and function and contain their own transcriptional and translational apparatus. Plastid gene expression, however, is controlled by a complex mechanism involving two different types of RNA polymerases. One polymerase is encoded by the plastid genome and is termed PEP, for plastid-encoded plastid RNA polymerase. PEP is a multisubunit enzyme similar to the eubacterial RNA polymerase. The core subunits of PEP are encoded by the plastid genes *rpoA*, *rpoB*, *rpoC1* and rpoC2 whereas its accessory sigma factors are encoded by the nucleus (reviewed in Allison, 2000). Organellar RNA polymerases whose catalytic subunits are encoded in the nuclear genome are termed NEP, for nucleus-encoded plastid RNA polymerase. NEP subunits show sequence similarity to the T3/T7 single-subunit phage polymerases (Hajdukiewicz *et al.,* 1997; Hess and Börner, 1999). The nuclear genome of *Arabidopsis thaliana* encodes three organellar phage-like NEPs, RpoT;1 (T1-NEP), RpoT;2 (T2-NEP) and RpoT;3 (T3-NEP) thought to have arisen through gene duplication events. Studies have demonstrated that T1-NEP and T3-NEP are present exclusively either in mitochondria or plastids, respectively, whereas T2-NEP is present in both mitochondria and plastids (Hedke *et al.,* 1997; 1999; 2000). One overall goal of this research was to further clarify the role of T3-NEP in plastid gene expression.

The first objective of this work was to develop a cost-effective, real-time PCR assay using SYBR Green and the comparative C_T ($2^{-\Delta\Delta CT}$) method suitable for high-

throughput quantitative gene expression studies This required the development of a rapid and cost- effective method for isolating high-quality RNA from the siliques, seeds, seedlings, rosette leaves and roots of *Arabidopsis thaliana*, selection of an appropriate housekeeping gene that could be used to correct for experimental variations across all tissues and target genes investigated, selection of primers with high amplification efficiencies for thirty-six plastid- and nucleus-encoded mRNAs, and determination of the precision and the reproducibility of the RT-PCR assays. Comparison of three commercial RNA extraction kits showed that the Rneasy Plant Mini Kit (Qiagen, Valencia, CA) and the Tri Reagent (Molecular Research Center, Inc., Cincinnati, OH) yielded high quality RNA from seedlings, rosette leaves and roots whereas only the Concert Plant RNA Reagent (Invitrogen, Carlsbad, CA) yielded undegraded RNA from siliques and seeds. Examination of 18S rRNA and adenine phosphoribosyltransferase (*Apt*) mRNA levels in various tissues of *Arabidopsis thaliana* indicated that the levels of 18S rRNA were relatively constant across the tissues analyzed whereas *Apt* mRNA levels were lower in seeds relative to the rest of the tissues. In addition, ΔC_T slope analysis revealed that the the amplification efficiencies of the target genes and 18S rRNA were similar. Thus, 18S rRNA was identified as the most suitable internal control for the quantitative real-time PCR assay. Investigations of accuracy, sensitivity and intra-as well as inter-assay variation indicated that the $2^{-\Delta\Delta CT}$ method yielded highly reproducible results for the target genes examined in this study ($CV_{(2^{-\Delta CT})} = \leq 30\%$, which translates into a difference in expression of less than 2 fold).

The second objective of this research was to quantify the transcript abundance of twenty-eight plastid genes in a range of tissues and developmental stages in the dicotyledonous plant *Arabidopsis thaliana* by real-time PCR. The tissues and

developmental stages examined included dry seeds, 2-day seedlings, 5-day seedlings, 10-day, 12-day and 15-day cotyledons as well as 35-day rosette leaves, 35-day cauline leaves, 5-day roots, 40-day roots and 34-day siliques. Quantitative analysis of RNA levels was performed on a large number of plastid genes belonging to a diverse array of plastid functions and operons. The data showed differential plastid transcript accumulation in various tissues and developmental stages with the lowest overall RNA levels in the non-photosynthetic plastids of dry seeds and 5-day roots, higher levels in green siliques and in light-exposed 40-day roots and even higher levels in the chloroplasts of 2-day and 5-day seedlings followed by a progressive decline in older tissues such as 12-day and 15-day cotyledons. Analysis of the expression profiles obtained from siliques, dry seeds, 2-day seedlings and 5-day seedlings identified three main groups of co-regulated genes. Cluster I included three tRNAs that showed high levels in siliques and were either moderately induced in 2-day and 5-day seedlings compared to dry seeds (*trnfM-CAU* and *trnS-GCU*) or showed reduced transcript levels in 2-day and 5-day seedlings relative to seeds (*trnW-CCA*). This is the first documented case of differential plastid expression in siliques. Genes in Cluster IIA and IIB reached maximum transcript abundance in the early phases of chloroplast development (2-day through 5-day stage) and included genes encoding components of the transcription and translation apparatus, genes encoding subunits of the plastid ATP synthase, NADH dehydrogenase and the cytochrome b_6/f complex as well as two genes encoding subunits of the plastid acetyl-CoA carboxylase and ATP-dependent protease. Cluster III included genes encoding components of the photosynthetic apparatus. This group of genes showed maximum transcript accumulation at later stages of chloroplast development (5-day through 12-day stage). Our results on the transcript accumulation

kinetics for plastid genes are consistent with and extend previous studies in barley and pea (Baumgartner et al., 1993; DuBell and Mullet, 1995) that showed differential transcription of genes for the transcription and translation apparatus early during chloroplast development. Moreover, these results are consistent with the observation that the build-up of the transcription and translation apparatus is initiated in a phase that preceeds maximum synthesis of the photosynthetic apparatus (Mullet, 1993).

The third objective of this research was to determine the role of phage-type RNA polymerase T3-NEP, which is encoded by *RpoT;3*, in the transcription of plastid genes in various tissues and stages of development of *Arabidopsis thaliana*. In this study, we identified and characterized an *Arabidopsis* T-DNA insertion mutant (*rpoZ191*) in which the T-DNA was inserted into the *RpoT;3* gene. We found that the *RpoT;3* mutation affects light-induced chloroplast development during the early stages of seedling growth resulting in a slow greening phenotype compared to wild-type plants. Plastid mRNA abundance in the mutant was quantified by real-time PCR. The results of this analysis showed distinct tissue specific effects of the *RpoT;3* mutation together with a general decrease in the accumulation of plastid transcripts during the early stages of chloroplast development. For instance, in the *rpoZ191* mutant, the levels of plastid transcripts in seeds and 5-day roots were not significantly different from the wild-type. In addition, the lack of *RpoT;3* had little effect on the transcript abundance of most plastid genes in the mutant siliques except for *trnfM-CAU* and *trnW-CCA*, which exhibited enhanced transcript levels. The most pronounced effect of the *RpoT;3* mutation was seen at the 2-day seedling stage when a large decrease in plastid transcript accumulation was recorded followed by a smaller effect at the 5-day stage and even smaller effect at later stages. This suggests that RpoT;3 is especially important for the transcription of plastid

genes during the early steps of chloroplast differentiation whereas during the later stages of development T3-NEP is less important. In addition, our study demonstrates that RpoT;3 does not play a major role in the accumulation of plastid RNAs present in dry seeds, roots or siliques. Based on the effects of the *RpoT;3* mutation on plastid transcript accumulation in the various tissues and stages of development of *Arabidopsis* plants, we assigned the plastid genes examined in this study to four classes. Class I includes genes with uncharacterized promoters whose RNA levels are enhanced in the *rpoZ191* mutant siliques (*trnfM-CAU* and *trnW-CCA*), 2-day and 5-day seedlings (*trnfM-CAU*, *trnS-GCU* and *trnW-CCA*) and are probably transcribed by another NEP. Class II includes genes with type Ia NEP promoters (e.g. *accD*, *rpoC1*), genes with undefined promoters (e.g. *rpoA*) and genes with mixed PEP+NEP promoters (e.g. *clpP*) whose transcript levels showed a uniform small decrease across development in the *rpoz191* mutant and are probably equally transcribed by different NEPs including RpoT;3. Class III includes genes with type Ib NEP promoters (e. g. *rps16*, *rpl32*) and a PEP+NEP-dependent gene (*ndhB*) whose transcript levels were strongly affected in the 2-day *rpoz191* mutant and are probably transcribed by RpoT;3 at this stage. Finally, Class IV includes mostly PEP-dependent genes (e.g. *rbcL*, *psaA/B*, *psaJ*, *psbA*, *psbD*, *trnE-UUC*) as well as genes with uncharacterized promoters (*trnC-GCA* and *trnV-GAC*) whose transcript levels were significantly reduced in the 2-day as well as 5-day *rpoZ191* mutant due in part to an indirect effect of the *rpoz191* mutation resulting in reduced levels of the active form of PEP. Taken together, these data suggest that there is a division of labor among the multiple NEPs, with RpoT;3 playing a major role in plastid gene expression during the early stages of chloroplast differentiation.

A fourth objective of this research was to determine whether the *rpoZ191* mutation affects the expression of nuclear genes encoding plastid proteins. In this study, the accumulation of transcripts from four nuclear genes (*PetH*, *RbcS*, *Lhca 1* and *Lhcb 1.2*) was analyzed by real-time PCR in both wild-type and *rpoZ19*1 mutant *Arabidopsis* plants. The accumulation of these nuclear transcripts was greatly reduced at the 2-day as well as 5-day stage whereas in siliques, the levels of all four nuclear transcripts were largely unaffected. The same pattern was observed for the plastid gene transcripts examined in the previous study. This suggests that the pleiotropic defects caused by the *RpoT;3* mutation during the early phase of plant development and chloroplast differentiation cause the disruption of plastid-derived signaling pathways that affect mRNA accumulation for a subset of nuclear genes encoding plastid components. This study emphasizes the key role played by RpoT;3 in the concerted expression of organelle and nucleus-encoded plastid-localized components that leads to the development of functional chloroplasts, which, in turn, influences plant development.

The final objective of this research was to analyze the expression of RpoT;1, RpoT;2 and RpoT;3. Transcript levels for all three NEPs were quantified in several tissues and different developmental stages of both wild-type and *rpoZ191* mutant by real-time PCR. The results showed a differential expression of *RpoT* genes in wild-type tissues with *RpoT;3* transcripts accumulating to higher levels in seeds and young photosynthetic tissues such as 2-day and 5-day seedlings, 10-day, 12-day and 15-day cotyledons as well as 15-day rosette leaves whereas *RpoT;2* transcripts accumulated to higher levels in seeds, siliques as well as in light-grown 5-day and 40-day roots. *RpoT;1* transcripts were also significantly higher in 5-day and 40-day roots compared with siliques (~5.7- and 9.7-fold, respectively) and seeds (~2.3- and 3.9-fold,

respectively). Most models invoke NEP as having its highest activity during the early stages of chloroplast differentiation (reviewed in Hess and Börner, 1999). However, it is not clear which NEP is responsible for this activity. Our results indicate that in the absence of T3-NEP, mRNA accumulation of many plastid and nuclear genes encoding chloroplast localized components was drastically reduced in young seedlings but not in siliques and roots. Furthermore, the results of this study indicated that even though *RpoT;2* transcript levels showed a ~4-fold increase in the *rpoZ191* mutant plants at the 2-day stage, the RpoT;3 deficiency was not compensated for by RpoT;2 at this stage. Taken together, these results suggest a division of labor among the NEP enzymes with RpoT;3 being more active in young photosynthetic tissues while RpoT;2 is more active in siliques as well as roots. Another interesting finding of this study was that at the 2-day seedling stage *RpoT;2* as well as *RpoT;3* transcripts did not increase significantly in abundance relative to seeds indicating that the enhanced RpoT;3 activity during the early stages of seedling development is not caused by an increase in *RpoT;3* mRNA abundance. We hypothesize that activation of RpoT;3 during the early stage of chloroplast differentiation is due to modification of the enzyme (i. e., phosporylation) or to the increased activity of a specificity factor.

In conclusion, this body of work has contributed substantially to the state of knowledge regarding the mechanism of plastid transcription regulation by the NEP enzymes in relation to plant and plastid development and has provided important information on the role of RpoT;3 in plastid gene expression during plant development. However, our understanding of the regulation of gene expression in plastids of higher plants is far from complete. Plastids as well as mitochondria are essential organelles of the plant cell that are endosymbiotic remnants of free-living prokaryotes (Gray, 1999).

Despite their eubacterial origin, plastids and mitochondria differ in the regulatory control exerted by the nucleus over the organelle genomes and their expression. While transcription of the mitochondrial genome is under the exclusive control of the nucleus-encoded phage-type NEP enzymes, transcription of plastid genes is much more complex and requires the contribution of multiple nucleus-encoded NEP enzymes as well as various forms of the eubacterial-type PEP enzyme. Furthermore, RpoT-dependent transcription of organellar genes likely requires modulation of the transcriptional activities of the various NEP enzymes during different developmental and environmental conditions. Data presented here add new insight to the complex mechanism of plastid transcription and demonstrate that during the functional integration of the RpoT genes thought to have arisen by duplication of the pre-existing gene encoding the mitochondrial NEP (Hedke *et al.,* 1997; Gray and Lang, 1998), RpoT;3 has acquired a key role in the transcription of plastid chromosome during the early stages of chloroplast development.

REFERENCES

Abdallah, F., Salamini, F., and Leister, D. (2000). A prediction of the size and evolutionary origin of the proteome of chloroplasts of *Arabidopsis*. Trends Plant Sci. **5,** 141-142.

Adam, Z., Adamska, I., Nakabayashi, K., Ostersetzer, O., Haussuhl, K., Manuell, A., Zheng, B., Vallon, O., Rodermel, S. R., and Shinozaki, K. *et al.* (2001). Chloroplast and mitochondrial proteases in *Arabidopsis*. A proposed nomenclature. Plant Physiol. **125,** 1912-1918.

Aguettaz, P., Seyer, P., Pesey, H., and Lescure, A-M. (1987). Relations between the plastid gene dosage and the levels of 16SrRNA and *rbcL* gene transcripts during amyloplast to chloroplast change in mixotrophic spinach cell. Plant Mol. Biol. **8,** 169-177.

Ahmad, M., and Cashmore, A. R. (1993). Hy4 gene of *A. thaliana* encodes a protein with characteristics of a blue-light photoreceptor. Nature **366,** 162-166.

Alfonso, M. Perewoska, I., and Kirilovski, D. (2000). Redox control of *psbA* gene expression in the cyanobacterium *Synechosystis* PCC 6803. Involvement of cytochrome *b6/f* complex. Plant Physiol. **122,** 155-515.

Allison, L.A. (2000). The role of sigma factors in plastid transcription. Biochimie **82,** 537-548.

Allison , L. A., and Maliga, P. (1995). Light-responsive and transcription-enhancing elements regulate the plastid *psbD* core promoter. EMBO J. **14,** 3721-3730.

Allison, L. A. Simon, and L. D., Maliga, P. (1996). Deletion of *rpoB* reveals a second distinct transcription system in plastids of higher plants. EMBO J. **15,** 2802-2809.

Allred, D. R., and Staehelin, L. A. (1985). Lateral distribution of the cytochrome b_6/f and coupling factor ATP synthase complexes of chloroplast thylakoid membranes. Plant Physiol. **78,** 199-202.

Anderson, B., and Anderson, J. M. (1980). Lateral heterogeneity in the distribution of chlorophyll-protein complexes of the thylakoid membranes of spinach chloroplasts. Biochem. Biophys. Acta **593,** 427-440.

Anderson. M., and Wilson, F. (2000). Growth, maintenance, and use of *Arabidopsis* genetic resources. In *Arabidopsis* A Practical Approach, Z. A. Wilson ed, (NewYork, Oxford University Press) pp. 1-28.

Apuya, N.R., Yadegari, R., Fischer, R. L., Harada, J.J., Zimmerman, J. L., and

Goldberg, R. B. (2001). The Arabidopsis embryo mutant *schlepperless* has a defect in *chaperonin-60-α* gene. Plant Physiol. **126,** 717-730.

Arezi, B. A., Xing, W., Sorge, J. A., and Hogrefe, H. H. (2003). Amplification efficiency of thermostable DNA polymerases. Anal. Biochem. **321,** 226-235.

Asada, K. Heber, U., and Schreiber, U. (1992). Pool size of electrons that can be donated to P700+, as determined in intact leaves: donation to P700+ from stromal components via the intersystem chain. Plant Cell Physiol. **34,** 39-50.

Baba, K., Schmidt, J., Espinoza-Ruiz, A., Villareho, A., Shiina, T., Gardeström, P., Sane, A. P., and Bhalerao, R. P. (2004). Organellar gene transcription and early seedling development are affected in the *rpoT;2* mutant of *Arabidopsis*. Plant Journal **38,** 38-48.

Backert, S., Dorfel, P., and Borner, T. (1995). Investigation of plant organellar DNA by pulse-field gel electrophoresis. Curr. Genet. **28,** 390-399.

Baginski, S. Tiller, K., and Link, G. (1997). Transcription factor phosphorylation by a protein kinase associated with chloroplast RNa polymerase from mustard (*Sinapsis alba*). Plant Mol. Biol. **34,** 181-189.

Bakalova-Stoynova, E., Karanov, E., Petrov, P., and Hall, M. A. (2004). Cell division and cell expansion in cotyledons of *Arabidopsis* seedlings. New Phytol.

162, 471-479.

Barber, J., Nield, J., Morris, E. P. Zheleva, D., and Hankamer, B. (1997). The structure, function and dynamics of photosystem two. Physiol. Plant. **100,** 817-827.

Barkan, A. (1988). Proteins encoded by a complex chloroplast transcription unit are each translated from both monocistronic and polycistronic RNAs. EMBO J. **7,** 2637-2644.

Barkan, A., and Goldschmidt-Clermont, M. (2000). Participation of nuclear genes in chloroplast gene expression. Biochimie **82,** 559-572.

Barne, K. A., Bown, J. A., Busby, S. J. W., and Minchin, S. D. (1997). Region 2.5 of the *Escherichia coli* RNA polymerase σ70 subunit is responsible for the recognition of the 'extended –10' motif at promoters. EMBO J. **16,** 4034-4040.

Baumgartner, B. J., Rapp, J. C., and Mullet, J.E. (1989). Plastid transcription activity and DNA copy number increase early in barley chloroplast development. Plant Physiol. **89,** 1011-1018.

Baumgartner, B. J., Rapp, J. C., and Mullet, J.E. (1993). Plastid genes encoding the transcription/translation apparatus are differentially transcribed early in barley

(*Hordeum vulgare*) chloroplast development. Plant Physiol. **101,** 781-791).

Beale, S. I. (1984). Biosynthesis of photosynthetic pigments. In Chloroplast Biogenesis, Volume 5, N. R. Baker and J. Barber eds, (Amsterdam: Elsevier Science Publishers, B.V.) pp. 133-205.

Beardslee, T. A., Chowdhury-Roy, S., Jaiswal, P., Buhot, L., Lerbs-Mache, S., Stern, D. B., and Allison, A. (2002). A nucleus-encoded maize protein with sigma factor activity accumulates in mitochondria and chloroplasts. Plant J. **31,** 199-209.

Becker-André, M., and Hahlbbrock, K. (1989). Absolute mRNA quantification using the polymerase chain reaction (PCR). A novel approach by a PCR aided transcript titration assays (PATTY). Nucleic Acids Res. **17,** 9437-9446.

Bedbrook, J. R., and Bogorad, L. (1976). Endonuclease recognition sites mapped on *Zea mays* chloroplast DNA. Proc Natl Acad Sci USA **73,**4309-4319.

Bedbrook, J. R., Kolodner, R., and Bogorad, L. (1977). *Zea mays* chloroplast ribosomal RNA genes are part of a 22,000 base pair inverted repeat. Cell **11,**739-749.

Bedbrook, J.R., Coen, D.M., Beaton, A.R., Bogorad. L., and Rich, A. (1979). Location of the single gene for the large subunit of ribulosebisphosphate

carboxylase on the maize chloroplast chromosome. J. Biol Chem. **254,** 905-910.

Bendall, D. S., and Manasse, R. S. (1995). Cyclic phosphorylation and electron transport. Biochim. Biophys. Acta **1229,** 23-38.

Bendich, A. J. (1987). Why do chloroplasts and mitochondria contain so many copies of their genome? BioEssays **6,** 279-282.

Bendich, A. J., and Smith, S. B. (1990). Structure of chloroplast and mitochondrial DNAs. Curr. Genet.**17,** 421-425.

Bennett, J. (1991). Protein phosphorylation in green plant chloroplasts. Annu. Rev. Plant Physiol. Plant Mol. Biol. **42,** 281-311.

Bennoun, P. (1982). Evidence for a respiratory chain in chloroplast. Proc. Natl. Acad. Sci. USA **79,** 4352-4356.

Bennoun, P. (2002). The present model for chlororespiration. Photosynthesis Res. **73,** 273-277.

Berends, T., Gamble, P. E., and Mullet, J. E. (1987). Characterization of the barley chloroplast transcription units containing *psaA-psaB* and *psbD-psbC*. Nucleic Acids Res. **15,** 5217-5240.

Bewley, J. D. (1997). Seed germination and dormancy. Plant Cell **9,** 1055-1066.

Bligny, M., Courtois, F., Thaminy, S., Chang, C. C., Langrange, T., Baruah-Wolff, J., Stern, D. B., and Lerbs-Mache, S. (2000). Regulation of plastid rDNA transcription by interaction of CDF2 with two different RNA polymerases. EMBO J. **19,** 1851-1860.

Bogorad, L. (1967). The role of cytoplasmic units: control mechanisms in plastid development. In Control Mechanisms in Developmental Processes: 26th symposium of the Society of Developmental Biology, (San Diego, Academic Press) pp. 1-31.

Bown, J, Barne, K., Minchin, S., and Busby, S. (1997). Extended –10 promoters. Nucleic Acids Res. **11,** 41-52.

Bowsher, C. G., and Tobin, A. K. (2001). Compartmentation of metabolism within mitochondria and plastids. J. Exp. Bot. **52,** 513-527.

Boyer, S. K., and Mullet, J. (1986). Characterization of *Pisum sativum* chloroplast *psbA* transcript produced *in vivo, in vitro,* and in *E. coli*. Plant Mol. Biol. **6,** 229-243.

Boyes, D. C., Zayed, A. M., Ascenzi, R., McCaskill, A. J., Hoffman, N. E., Davis,

K. R., and Görlach, J. (2001). Growth stage-based phenotypic analysis of *Arabidopsis*: A model for high throughput functional genomics in plants. Plant Cell **13,** 1499-1510.

Bradbeer, J. W., Atkinson, Y. E., Börner, T., and Hagermann, R. (1979). Cytoplasmic synthesis of plastid polypeptides may be controlled by plastid-synthesized RNA. Nature **279,** 816-817.

Bradley, D., and Gatenby, A. A. (1985). Mutational analysis of the maize chloroplast ATPase-beta subunit gene promoter: The isolation of promoter mutants in *E. coli* and their characterization in a chloroplast *in vitro* transcription system. EMBO J. **4,** 3641-3648.

Brown, E. C., Somachi, A., and Mayfield, S. P. (2001). Interorganellar crosstalk: new perspectives on signaling from the chloroplast to the nucleus. Genome Biology **2,** 1021.1-1021.4.

Burgess, D. G., and Taylor, W. C. (1988). The chloroplast affects the transcription of a nuclear gene family. Mol. Gen. Genet. **214,** 89-96.

Burleigh, S. H. (2001). Relative quantitative RT-PCR to study the expression of plant nutrient transporters in arbuscular mycorrhizas. Plant Sci. **160,** 899-904.

Burrows, P. A., Sazanov, L. A., Svab, Z., Maliga, P., and Nixon, P. J. (1998).

Identification of a functional respiratory complex in chloroplasts through analysis of tobacco mutants containing disrupted plastid *ndh* genes. EMBO J. **17,** 868-876.

Bustin, S. A. (2000). Absolute quantification of mRNA using real-time reverse transcription polymerase chain reaction assays. J. Mol. Endocrinol. **25,** 169-193.

Bustin, S. A. (2002). Quantification of mRNA using real-time reverse transcription PCR (RT-PCR); trends and problems. J. Mol. Endocrinol. **29,** 23-39.

Butler, R. D. (1967). The effect of light intensity on stem and leaf growth in broad bean seedlings. J. Expt. Bot. **14,** 142-152.

Cahoon, A. B., and Stern, D. B. (2001). Plastid transcription: a menage à trois? Trends Plant Sci. **6,** 45-46.

Callis, J. (1995). Regulation of protein degradation. Plant Cell **7,** 845-857.

Cardullo, R. A., Agrawal, S., Flores, C., Zamecnik, P. C., and Wolf, D. E. (1988). Detection of nucleic acid hybridization by nonradiative fluorescence resonance energy transfer. Proc. Natl. Acad. Sci. USA **85,** 8790-8794.

Carol, P., Stevenson, D., Bisanz, C., Beitenbach, J., Sandman, H., Mache, R., Coupland, G., and Kuntz, M. (1999). Mutations in the *Arabidopsis* gene

IMMUTANS cause a variegated phenotype by inactivating a chloroplast terminal oxidase associated with phytoene desaturation. Plant Cell **11,** 57-68.

Carpentier, R., LaRue, B., and Leblanc, R. M. (1984). Photoacoustic spectroscopy of *Anacystis nidulans*: III. Detection of photosynthetic activities. Arch. Biochem. Biophys. **228,** 534-543.

Catalá, R., Sabater, B., and Guera, A. (1997). Expression of the plastid *ndhF* gene product in photosynthetic and non-photosynthetic tissues of developing barley seedlings. Plant Cell Physiol. **38,** 1382-1388.

Cermakian,N., Ikeda,T.M., Cedergren,R., and Gray,M.W. (1996). Structural-functional analysis of bacteriophage T7 RNA Polymerase. *Nucleic Acids Res*., **24**, 648-654.

Chan, C. L., Lonetto, M. A., and Gross, C. A. (1996). Sigma domain structure: one down, one to go. Structure **4,** 1235-1238.

Chang, C., Sheen, J., Bligny, M., Niwa, Y., Lerbs-Mache, S., and Stern, D. B. (1999). Functional analysis of two maize cDNA encoding T7-like RNA polymerases. Plant Cell **11,** 911-926.

Chen, M. C., Cheng, M. C., and Chen, S. C. G. (1993). Characterization of the promoter of the rice plastid *psaA-psaB-rps14* operon and the DNA-specific

binding proteins. Plant Cell Physiol. **34,** 577-584.

Chomczynski, P. and Mackey, K. (1995). Substitution of chloroform by bromochloropropane in the single-step method for RNA isolation. Anal. Biochem. **225,** 163-164.

Chory, J. (1992). A genetic model for light-regulated seedling development in *Arabidopsis*. Development **115,** 337-354.

Christopher, D.A., and Hoffer, P. (1998). DET1 represses a chloroplast blue light-activated promoter in developmental and tissue-specific manner in *Arabidopsis thaliana*. Plant J. **14,** 1-11.

Christopher, D.A., Kim, M., and Mullet, J. E. (1992). A novel light-regulated promoter is conserved in cereal and dicot chloroplasts. Plant Cell **4,** 785-798.

Christopher, D.A., and Mullet, J. E. (1994). Separate photosensory pathways co-regulate blue light/ultraviolet-A-activated *psbD-psbC* transcription and light-induced D2 and CP43 degradation in barley (*Hordeum vulgare*) chloroplasts. Plant Physiol. **104,** 119-1129.

Chung, H. C., Kwon, O, H., Lee, Y. M., and Lee, S. Y. (1995). An improved method for isolating high-quality polysaccharide free RNA from tenacious plant tissues. Mol. Cell **6,** 108-111.

Cocciolone, S. M., and Cone, K. C. (1993). Pl-Bh, an anthocyanin regulatory gene of maize that leads to variegated pigmentation. Genetics **135,** 575-588.

Cogdell, R., and Frank, H. A. (1987). How carotenoids function in photosynthetic bacteria. Biochim. Biophys. Acta **895,** 63-79.

Collado-Vides, J., Magasanik, B., and Gralla, J. (1991). Control site location and transcriptional regulation in *Escherichia coli*. Microbiol. Rev. **55,** 371-394.

Connett, M. B. (1987). Mechanisms of maternal inheritance of plastids and mitochondria: developmental and ultrastructural evidence. Plant Mol. Biol. Rep. **4,** 103-205.

Cran, D. G., and Possingham, J. V. (1972). Variation of plastid types in spinach. Protoplasma **74,** 345-356.

Crossland, L. D., Rodermel, S. R., and Bogorad, L. (1984). Single gene for the large subunit of ribulosebiphosphate carboxylase in maize yields two differentially regulated mRNAs. Proc. Natl. Acad. Sci. USA **81,** 4060-4064.

Czechowski, T., Bari, R. P., Stitt, M., Scheible, R-W., and Udvardi, M. (2004). Real-time RT-PCR profiling of over 1400 Arabidopsis transcription factors: unprecedented sensitivity reveals novel root- and shoot-specific genes. Plant J. **38,** 366-379.

Danon, A., and Mayfield, S. P. (1994). Light-regulated translation of chloroplast messenger RNAs through redox potential. Science **266,** 1717-1719.

Dean, J. D., Goodwin, P. H., and Hsiang, T. (2002). Comparison of relative RT-PCR and Northern blot analysis to measure expression of β-1,3- glucanase in *Nicotiana benthamiana* infected with *Colltotrichum destructivum*. Plant Mol. Biol. Reptr. **20,** 347-356.

Degenhardt, J., Fiebig, C., and Link, G. (1991). Chloroplast and Nuclear transcripts for plastid proteins in *Arabidopsis thaliana*: tissue distribution in mature plants and during seedling development and embryogenesis. Bot. Acta **104,** 455-463.

De Las Rivas, J., Lozano, J. J., and Ortiz, A. R. (2002). Comparative analysis of chloroplast genomes: functional annotation, genome-based phylogeny, and deduced evolutionary patterns. Genome Res. **12,** 567-583.

Demmig-Adams, B. (1990). Carotenoids and photoprotection in plants – a role for the xanthophylls zeaxanthin. Biochim. Biophys. Acta **1020,** 1-24.

Deng, X-W., and Gruissem, W. (1988). Constitutive transcription and regulation of gene expression in non-photosynthetic plastids of higher plants. EMBO J. **7,** 3301-3308.

Deng, X-W., Wing, R. A., and Gruissem, W.(1989). The chloroplast genome exists in multimeric forms. Proc. Natl. Acad.Sci. USA **86,** 4256-4160.

De Santis-Maciossek, G., Kofer, W., Bock, A., Schoch, S., Maier, R. M., Wanner, G., Rüdiger, W., Koop, H. U., and Hermann, R. G. (1999). Targeted disruption of the plastid RNA polymerase genes *rpoA*, *B* and *C1*: molecular biology, biochemistry and ultrastructure. Plant J. **18,** 477-489.

Dozois, C. M., Oswald, E., Gautier, N., Serthelon, J. P.., Fairbrother, J. M., and Oswald, I. P. (1997). A reverse transcription-polymerase chain reaction method to analyze porcine cytokine gene expression. Vet. Immunol. Immunopathol. **58,** 287-300.

DuBell, A. N., and Mullet, J. E. (1995). Differential transcription of pea chloroplast genes during light-induced leaf development. Plant Physiol. **109,** 105-112.

Eastmond P. J., and Graham, I. A. (2001). Re-examining the role of the glyoxylate cycle in oilseeds. Trends in Plant Sci. **6,** 72-77.

Emanuel, C., Weihe, A., Graner, A., Hess, W. R., and Börner, T. (2004). Chloroplast development affects expression of phage-type polymerases in barley. Plant J. **38,** 460-472.

Endo, T., Mi, H., Shikanai, T., and Asada, K. (1997). Donation of electrons to

plastoquinone by NAD(P)H dehydrogenase and by ferredoxin-quinone reductase in spinach chloroplasts. Plant Cell Physiol. **38,** 1272-1277.

Endo, T., Shikanai, T., Sato, F., and Asada, K. (1998).NAD(P)H dehydrogenase-dependent, antimycin A-sensitive electron donation to plastoquinone in tobacco chloroplasts. Plant Cell Physiol. **39,** 1226-1231.

Fassler, J. S., and Gussin, G. N. (1996). Promoters and basal transcription machinery in eubacteria and eukaryotes: concepts, definitions and analogies. Meth. Enzymol. **273,** 3-29.

Fish, L. E., Kück, U., and Bogorad, L. (1985). Two partially homologous adjacent light-inducible maize chloroplast genes encoding polypeptides of the P700 chlorophyll a-protein complex of photosystem I. J. Biol. Chem. **260,** 1413-1421.

Freeman, W. M., Walker, S. J., and Vrana, K.E. (1999). Quantitative RT-PCR: pitfalls and potential. BioTechniques **26,** 112-125.

Friedrich, T., and Scheide, D. (2000). The respiratory complex I of bacteria, archaea and eukarya and its module common with membrane-bound multisubunit hydrogenases. FEBS Lett. **479,** 1-5.

Fridlender, M., Lev-Yadun, S., Baburek, I., Angelis, K., and Levy, A. A. (1996). Cell divisions in cotyledons after germination: localization, time-course and

utilization for a mutagenesis assay. Planta **199,** 307-313.

Frisco, G., Giacomelli, L., Ytterberg, A. J., Peltier, J-B., Rudella, A., Sun, Q., and van Wijk, K.J. (2004). In-depth analysis of the thylakoid membrane proteome of *Arabidopsis* thaliana chloroplasts: new proteins, new functions, and a plastid proteome database. Plant Cell **16,** 478-499.

Fujie, M., Kuroiwa, H., Kawano, S., Mutoh, S., and Kuroiwa, T. (1994). Behavior of organelles and their nucleoids in the shoot apical meristem during leaf development in *Arabidopsis thaliana* L. Planta **194,** 395-405.

Gal, A., Hauska, G., Herrmann, R., and Ohad, I. (1990). Interaction between light harvesting chlorophyll-*a/b* protein (LHCII) kinase and cytochrome b_6/f complex. *In vitro* control of kinase activity. J. Biol. Chem. **265,** 19742-19749.

Galli, G., Hofstetter, H., and Birnstiel, M. L. (1981). Two conserved sequence blocks within eukaryotic tRNA genes are major promoter elements. Nature **294,** 626-631.

Gamble, P. E., and Mullet, J. E. (1989). Blue light regulates the accumulation of two *psbD-psbC* transcripts in barley chloroplasts. EMBO J. **8,** 2785-2794.

Gandar, P. W., and Hall, A. J. (1998). Estimating position-time relationship in steady-state, one-dimensional growth zone. Planta **175,** 121-129.

Gatenby, A. A., Castleton, J. A., and Saul, M. W. (1981). Expression in *E. coli* of *Z. mays* and wheat chloroplast genes for large subunit of ribulose biphosphate carboxylase. Nature **291,** 117-121.

Gerard, C. J., Olsson, K., Ramanathan, R., Reading, C., and Hanania, E. G. (1998). Improved quantitation of minimal residual disease in multiple myeloma using real-time polymerase chain reaction and plasmid-DNA complementarity determining region III strands. Cancer Res. **58,** 3957-3964.

Gibbs, M. (1971). Carbohydrate metabolism by chloroplasts. In Structure and Function of Chloroplast, M. Gibbs ed, (Berlin: Springer-Verlag). pp. 169-214.

Gillham, N. W. (1991). Transmission of plastid genes. In The Molecular Biology of Plastids, L. Bogorad and I. K. Vasil eds, (San Diego, Academic Press). pp. 54-92.

Gilliland, G., Perrin, S., Blanchard, K., and Bunn, H. F. (1990). Analysis of cytokine mRNA and DNA: detection and quantitation by competitive polymerase chain reaction. Proc. Natl. Acad. Sci. USA **87,** 2725-2729.

Giulietti, A., Overberg, L., Valckx, D., Decallonne, B., Bouillon, R., and Mathieu, C. (2001). An overview of real-time quantitative PCR: applications to quantify cytokine gene expression. Methods **25,** 386-401.

Goldberg, R. B., Barker, S. J., and Grau-Perez, L. (1989). Regulation of gene

expression during plant embryogenesis. Cell **56,** 149-160.

Goldberg, R. B., de Paiva, G., and Yadegari, R. (1994). Plant embryogenesis: Zygote to seed. Science **266,** 605-614.

González-Baena, E., Baginski, S., Mulo, P., Aro, E-M., and Link, G. (2001). Chloroplast transcription at different light intensities. Glutathionine-Mediated phosphorylation of the major RNA polymerase involved in redox-regulated organellar gene expression. Plant Physiol. **127,** 1044-1052.

Goodchild, D. J., Anderson, B., and Anderson, J. M. (1985). Immunocytochemical localization of polypeptides associated with the oxygen evolving system of photosynthesis. Eur. J. Cell Biol. **36,** 294-298.

Goodwin, T. W. (1971). Biosynthesis by chloroplasts. In Structure and Function of Chloroplast, M. Gibbs ed, (Berlin, Springer-Verlag). pp. 215-276.

Gray, M. W. (1999). Evolution of organellar genomes. Current Opinion in Genetics & Development **9,** 678-687.

Gray, M. W., and Lang, B. F. (1998). Transcription in chloroplasts and mitochondria: a tale of two polymerases. Trends in Microbiol. **6,** 1-3.

Gray, J. C., Sornarajah, R., Zabron, A. A., Duckett, C. M., and Khan, M. S.

(1995). Chloroplast control of nuclear gene expression. In Photosynthesis, from Light to Biosphere, Volume 3, P. Mathis, ed, (Dordrecht, The Netherlands: Kluwer) pp. 543-550.

Gray, J. C., Sullivan, J. A., Wang, J. H., Jerome, C. A., and MacLean, D. (2003). Coordination of plastid and nuclear gene expression. Philos. Trans. R. Soc. Lond. B. Biol. Sci. **358,** 135-145.

Gruber, T. M., and Bryant, D. A. (1997). Molecular systematic studies of eubacteria, using σ^{70} –type sigma factors of group I and group II. J. Bacteriol. **179,** 1734-1747.

Gruissem, W., and Tonkyn, J. C. (1993). Control mechanisms of plastid gene expression. Crit. Rev. Plant Sci. **12,** 19-55.

Gruissem, W., and Zurawski, G. (1985). Analysis of promoter regions for the spinach chloroplast *rbc*L, *atpB*, and *psbA* genes. EMBO J. **4,** 3375-3383.

Guera, A. De Nova, P. G., and Sabater, B. (2000). Identification of the Ndh (NAD(P)H-plastoquinone- oxidoreductase) complex in etioplast memembranes nof barley: Changes during photomorphogenesis of chloroplasts. Plant Cell Physiol. **41,** 49-59.

Gutteridge, S., and Gatenby, A. A. (1995). Rubisco synthesis, assembly,

mechanism, and regulation. Plant Cell **7,** 809-819.

Hajdukiewicz, P. T. J., Allison, L.A., and Maliga, P. (1997). The two RNA polymerases encoded by the nuclear and the plastid compartments transcribe distinct groups of genes in tobacco plastids. EMBO J. **13,** 4041-4048.

Hakimi, M. A., Privat, J., Valay, J. G., and Lerbs-Mache, S. (2000). Evolutionary conservation of C-terminal domain of primary sigma-70 type transcription factors between plants and bacteria. J. Biol. Chem. **275,** 9215-9221.

Haley, J., and Bogorad, L. (1990). Alternative promoters are used for genes within maize chloroplast polycistronic transcription units. Plant Cell **2,** 323-333.

Hall, D. O., and Rao, K. K. (1994). Photosynthesis. (Cambridge, Cambridge University Press).

Hanaoka, M., Kanamaru, K., Takahashi, H., and Tanaka, K. (2003). Molecular genetic analysis of chloroplast gene promoters dependent on SIG2, a nucleus-encoded sigma factor for the plastid-encoded RNA polymerase, in *Arabidopsis thaliana*. Nucleic Acids Res. **31,** 7090-7098.

Hanley-Bowdoin, L., and Chua, N.H. (1987). Chloroplast promoters. Trends Bioch. Sci. **12,** 67-70.

Hanson, M.S., Cetkovic-Cvrlje, M., Ramiya, V. K., Atkinson, M.A., Maclaren, N. K., Singh, B., Elliott, J. F., Serreze, D. V., and Leiter, E. H. (1996). Quantitative thresholds of MHC class II I-E expressed on hemopoietically derived antigen presenting cells in transgenic NOD/Lt mice determine level of diabetes resistance and indicate mechanism of protection. J. Immunol. **157,** 1279-1287.

Harrak, H., lagrange, T., Seyer-Bisanz, C., Mache-Lerbs, S., and Mache, R. (1995). The expression of nuclear genes encoding plastid ribosomal proteins precedes the expression of chloroplast genes during early phases of chloroplast development. Plant Physiol. **108,** 685-692.

Hartman, F. C., and Harpel, M. R. (1994). Structure, function, regulation, and assembly of D-ribulose-1, 5-biphosphate carboxylase/oxygenase. Annu. Rev. Biochem. **63,** 197-234.

Havaux, M., and Niyogi, K. K. (1999). The violaxanthin cycle protects plants from photooxidative damage by more than one mechanism. Proc. Natl. Acad. Sci. USA **96,** 8762-8767.

Hawley, D., and McClure, W. R. (1983). Compilation and analysis of *Escherichia coli* promoter DNA sequences. Nucleic Acids Res. **11,** 2237-2255.

Hayward, A. L., Oefner, P. J., Sabatini, S., Kainer, D. B., and Hinojos, C. A. (1998). Modeling and analysis of competitive RT-PCR. Nucleic Acids Res. **26,**

2511-2518.

Hedtke, B., Börner, T., and Weihe, A. (1997). Mitochondrial and chloroplast phage-type RNA polymerases in *Arabidopsis*. Science **277,** 809-811.

Hedtke, B., Börner, T., and Weihe, A. (2000). One RNA polymerase serving two genomes. EMBO Reports **1,** 435-440.

Hedtke, B., Legen, J., Weihe, A., Hermann, R. G., and Börner, T. (2002). Six active phage-type RNA polymerase genes in *Nicotiana tabacum*. Plant J. **30,** 625-637.

Hedtke, B., Meixner, M., Gillandt, S., Richter, E., Börner, T., and Weihe, A. (1999). Green fluorescent protein as a marker to investigate targeting of organellar RNA polymerases of higher plants *in vivo*. Plant J. **17,** 557-561.

Heid, C. A., Stevens, J., Livak, K., and Williams, P. M. (1996). Real-time quantitative PCR. Genome Res. **6,** 986-994.

Heil, S. G., Kluijtmans, L. A. J., Spiegelstein, O., Finnel, R. H., and Blom, H. J. (2003). Gene-specific monitoring of T7-based RNA amplification by real-time quantitative PCR. BioTechniques **35,** 502-508.

Helmann, J. D., and Chamberlin, M. J. (1988). Structure and function of bacteria

L sigma factors. Annu. Rev. Biochem. **57,** 839-872.

Herbert, S. K., Fork, D. C., and Malkin, S. (1990). Photoacoustic measurements *in vivo* of energy storage by cyclic electron flow in algae and higher plants. Plant Physiol. **94,** 926-934.

Hess, W. R., and Börner, T. (1999). Organellar RNA polymerases of higher plants. Int. Rev. Cytol. **190,** 1-59.

Hess, W. R., Müller, A., Nagy, F., and Börner, T. (1994). Ribosome-deficient plastids affect transcription of light-induced nuclear genes: genetic evidence for a plastid-derived signal. Mol. Gen. Genet. **242,** 505-512.

Hess, W. R., Prombona, A., Fielder, B., Subramanian, A.R., and Börner, T. (1993). Chloroplast *rps15* and *rpoB/C1/C2* gene cluster are strongly transcribed in ribosome-deficient plastids: evidence for a functioning non-chloroplast-encoded RNA polymerase. EMBO J. **12,** 563-571.

Hess, W. R., Schendel, R., Börner, T., and Rüdiger, W. (1991). Reduction of mRNA levels for two nuclear encoded light regulated genes in the barley mutant *albostrians* is not correlated with phytochrome content activity. J. Plant Physiol. **138,** 292-298.

Higuchi, R., Dollinger, G., Walsh, P. S., and Griffith, R. (1992). Simultaneous

amplification and detection of specific DNA sequences. Nat. Biotechnol. **10,** 413-417.

Higuchi, R., Fockler, C., Dollinger, G., and Watson, R. (1993). Kinetic PCR analysis: real-time monitoring of DNA amplification reactions. Bio/Technology **11,** 1026-1030.

Hiratsuka, J., Shimada, H., Whittier, R.F., Ishibashi, T., Sakamoto, M., Mori, M., Kondo, C., Honji, Y., Sun, C.R., Meng, B.Y., Li, Y., Kanno, A., Nishizawa, Y., Hirai, A., Shinozaki, K., and Sugiura, M. (1989). The complete sequence of the rice (*Oryza sativa*) chloroplast genome: intermolecular recombination between distinct tRNA genes accounts for a major plastid DNA inversion during the evolution of the cereals. Mol. Gen. Genet. **217,**185-194.

Hoffer, P. H., and Christopher, D. A. (1997). Structure and blue-light-responsive transcription of a chloroplast *psbD* promoter from *Arabidopsis thaliana*. Plant Physiol. **115,** 213-222.

Holland, P. M., Abramson, R. D., Watson, R., and Gelfand, D. H. (1991). Detection of specific polymerase chain reaction product by utilizing the 5′→ 3′ exonuclease activity of *Thermus aquaticus* DNA polymerase. Proc. Natl. Acad. Sci. USA **88,** 7276-7280

Horikoshi, T., Danenberg, K. D., Stadlbauer, T. H., Volkenandt, M., Shea, L. C.,

Aigner, K., Gustavsson, B., Leichman, L., Frosing, R., and Ray, M. *et al.* (1992). Quantitation of thymidilate synthase, dihydrofolate reductase, and DT-diaphorase gene expression in human tumors using the polymerase chain reaction. Cancer Res. **52,** 108-116.

Huang, Z., Fasco, M. J., and Kaminsky, L. S. (1996). Optimization of DNase I removal of contaminating DNA from RNA for use in quantitative RNA-PCR. BioTechniques **20,** 1012-1020.

Hübschmann, T., and Börner T. (1998). Characterization of transcript initiation sites in ribosom-deficient barley plastids. Plant Mol. Biol. **36,** 493-496.

Igloi, R., and Kössel, H. (1992). The transcriptional apparatus of chloroplasts. Crit. Rev. Plant Sci. **10,** 525-558.

Ikeda, T. M., and Gray, M.W. (1999). Identification and characterization of T3/T7 bacteriophage-like RNA polymerase sequences in wheat. Plant Mol. Biol. **40,** 567-578.

Ingham, D. J., Beer, S., Money, S., and Hansen, G. (2001) Quantitative real-time PCR assay for determining transgene copy number in transformed plants. BioTechniques **31,** 132-140.

Iratni, R., Baeza, L., Andreeva, A., Mache, R., and Lerbs - Mache, S. (1994).

Regulation of rDNA transcription in chloroplasts: promoter exclusion by constitutive repression. Genes Dev. **8,** 2928-2938.

Iratni, R., Diederich, L., Harrak, H., Bligny, M., and Lerbs - Mache, S. (1997). Organ-specific transcription of the *rrn* operon in spinach plastids. J. Biol. Chem. **272,** 13676-13682.

Isono, K., Niwa, Y., Satoh, K., and Kobayashi, H. (1997a). Evidence for transcriptional regulation of plastid photosynthesis genes in *Arabidopsis thaliana* roots. Plant Physiol. **114,** 623-630.

Isono, K., Shimizu, M., Yoshimoto, K., Niwa, Y., Satoh, K., and Yokota, A., Kobayashi, H. (1997b). Leaf-specifically expressed genes for polypeptides destined for chloroplasts with domaims of σ^{70} factors of bacterial RNA polymerases in *Arabidopsis thaliana* . Proc. Natl. Acad. Sci. USA **94,** 14948-14953.

Ito, M. K., Tsunoyama, Y., Makahira, Y., Shiina, T., and Toyoshima, Y. (1999). Circadian regulated expression of nuclear-encoded plastid σ factor gene (sig A) in wheat seedlings. FEBS Lett. **451,** 275-278.

Jahn, D., Verkamp, E., and Söll, D. (1992). Glutamyl-transfer RNA: A precursor of heme and chlorophyll biosynthesis. Trends Biochem. Sci. **17,** 215-218.

Jang, S. H., and Jaehning, J. A. (1991). The yeast mitochondrial RNA polymerase specificity factor, MTF1 is similar to bacterial σ factors. J. Biol. Chem. **25,** 22671-22677.

Jansson, S. (1999). A guide to the *Lhc* genes and their relatives in *Arabidopsis*. Trends Plant Sci. **4,** 236-240.

Jones, L. J., Yuc, S. T., Chcung, C. Y., and Singer, V. L. (1998). RNA quantitation by fluorescence-based solution assay RiboGreen reagent characterization. Anal. Biochem. **265,** 368-374.

Juniper, B. E., and Clowes, F. A. L. (1965). Cytoplasmic organelles and cell growth in root caps. Nature **208,** 864-865.

Kanamaru, K., Fujiwara, M., Seki, M., Katagiti, T., Nakamaru, M., Mochizuki, N., Nagatani, A., Shinozaki, K., Tanaka, K., and Takahashi, H. (1999). Plastidic RNA polymerase σ factors in *Arabidopsis*. Plant Cell Physiol. **40,** 832-842.

Kanamaru, K., Nagashima, A., Fujiwara, M., Shimada, H., Shirano, Y., Nakabayashi, K., Shibata, D., Tanaka, K., and Takahashi, H. (2001). An *Arabidopsis* sigma factor (SIG2)- dependent expression of plastid-encode tRNAs in chloroplasts. Plant Cell Physiol. **42,** 1034-1043.

Kanno, A., and Hirai, A. (1993). A transcription map of the chloroplast genome from rice (*Oryza sativa*). Curr. Genet. **23,** 166-174.

Kapoor, S., and Sugiura, M. (1999). Identification of two essential sequence elements in the nonconsensus type II *PatpB-290* plastid promoter by using plastid transcription extracts from cultured tobacco BY-2 cells. Plant Cell **11,** 1799-1810.

Kapoor, S., Suzuki, J. Y., and Sugiura, M. (1997). Identification and functional significance of a new class of non-consensus-type plastid promoters. Plant J. **11,** 327-337.

Kapoor, S., Wakasugi, T., Deno, H., and Sugiura, M. (1994). An *atpE*-specific promoter within the coding region of the *atpB* gene in tobacco chloroplast DNA. Curr. Genet. **26,** 263-268.

Karsai, A., Müller, S., Platz, S., and Hauser, M-T. (2002). Evaluation of home-made SYBR ® Green I reaction mixture for real-time PCR quantification of gene expression. Biotechniques **32,** 790-796.

Kaufman, L. S. (1993). Transduction of blue-light signals. Plant Physiol. **102,** 333-337.

Ke, J., Wen, T-N., Nikolau, B. J., and Wurtele, E. S. (2000). Coordinate regulation

of the nuclear and plastidic genes coding for the subunits of the heteromeric acetyl-Coenzyme A carboxylase. Plant Physiol. **122,** 1057-1071.

Kesterman, M., Neukirchen, S., Kloppstech, K., and Link, G. (1998). Sequence and expression characteristics of a nuclear-encoded chloroplast sigma factor from mustard (*Sinapsis alba*). Nucleic Acids Res. **26,** 2747-2753.

Kim, L. H., Glick, R. E., and Melis, A. (1993b). Dynamics of photosystem stoichiometry adjustment by light quality in chloroplasts. Plant Physiol. **102,** 181-190.

Kim, M., Christopher, D. A., and Mullet, J. E. (1993a). Direct evidence for selective modulation of *psbA, rpoA*, *rbc*L, and *16SRNA* stability during barley chloroplast development. Plant Mol. Biol. **22,** 447-463.

Kim, M, and Mullet, J.E. (1995). Identification of a sequence-specific DNA binding factor required for transcription of the barley chloroplast blue light-responsive *psbD-psbC* promoter. Plant Cell, **7,** 1445-1457.

Kim, M., Thum, K. E., Morishige, D. T., and Mullet, J. E. (1999). Detailed architecture of the barley chloroplast *psbD-psbC* blue light-responsive promoter. J. Biol. Chem. **274,** 4684-4692.

Kirk, J. T. O. (1978a). The biosynthetic capabilities of plastids-part I: synthesis

of pigments and lipids. In The Plastids: Their Chemistry, Structure, Growth and Inheritance, 2nd ed., J.T.O Kirk and R. A. E Tilney-Bassett eds, (Amsterdam, Elsevier Biomedical Press). pp. 615-675.

Kirk, J. T. O. (1978b). The nature of plastids. In The Plastids: Their Chemistry, Structure, Growth and Inheritance. 2nd ed., J.T.O.Kirk and R. A. E. Tilney-Bassett eds, (Amsterdam, Elsevier Biomedical Press). pp. 1-250.

Klein, D. (2002). Quantification using real-time PCR technology: applications and limitations. Trends Mol. Med. **8,** 257-260.

Klein, R. R., and Mullet, J. E. (1990). Light-induced transcription of chloroplast genes. *psbA* transcription is differentially enhanced in illuminated barley. J. Biol. Chem. **265,** 1895-1902.

Kobayashi, H., Ngernprasirtsiri, J., and Akazawa, T. (1990). Transcriptional regulation and DNA methylation in plastids during transitional conversion of chloroplasts to chromoplasts. ENBO J. **9,** 307-313.

Kofer, W., Koop, H. U., Wanner, G., and Steinmuller, K. (1998). Mutagenesis of the genes encoding subunits A, C, H, I, J and K of the plastid NAD(P)H-plastoquinone-oxidoreductase in tobacco by polyethylene glycol-mediated plastome transformation. Mol. Gen. Genet. **258,** 166-173.

Krause, K., Maier, R. M., Kofer, W., Krupinska, K., and Herrmann, R. G. (2000). Disruption of plastid-encoded RNA polymerase genes in tobacco: expression of only a distinct set of genes is not based on selective transcription of the plastid chromosome. Mol. Gen. Genet. **263,** 1022-1030.

Krupinska, K. (1992). Transcriptional control of plastid gene expression during development of primary foliage leaves of barley grown under a daily light-dark regime. Planta **186,** 294-303.

Krupinska, K., and Falk, J. (1994). Changes in RNA-polymerase activity during biogenesis, maturation and senescence of barley chloroplasts. Comparative analysis of transcripts synthesized either in run-on assays or by transcriptionally active chromosomes. J. Plant Physiol. **143,** 298-305.

Kubicki, A., Funk, E., Westhoff, P., and Steinmüller, K. (1996). Differential expression of plastome-encoded *ndh* genes in mesophyll and bundle-sheath chloroplasts of the C_4 plant *Shorgum bicolor* indicates that complex I-homologous NAD(P)H plastoquinone oxidoreductase is involved in cyclic electron transport. Planta **199,** 276-281.

Kuldell, N., and Hochschild, A. (1994). Amino acid substitutions in the –35 recognition motif of sigma 70 that result in defects in phage lambda repressor stimulated transcription. J. Bacteriol. **176,** 2991-2998.

Kumar, A. M., Csankovski, G., and Söll, D. (1996). A second and differentially expressed glutamyl-tRNA reductase gene from *Arabidopsis thaliana*. Plant Mol. Biol. **30,** 419-426.

Kuroiwa, T. (1991). The replication, differentiation, and inheritance of plastids with emphasis on the concept of organelle nuclei. Int. Rev. Cytol. **128,** 1-61.

Kustu, S., Santero, E., Keener, J., Popham, D., and Weiss, D. (1989). Expression of σ^{54} (*ntrA*)-dependent genes is probably united by a common mechanism Microbiol. Rev. **53,** 367-376.

Kusumi, K., Yara, A., Mitsui, N., Tozawa, Y., and Iba, K. (2004). Characterization of a rice nuclear-encoded plastid RNA polymerase Gene *OsRpoTp*. Plant Cell Physiol. **45,** 1194-1201.

Lahiri, S. D., and Allison, L. A. (2000). Complementary expression of two plastid-localized σ-like factors in maize. Plant Physiol. **123,** 883-894.

Lam, E., and Chua, N-H. (1987). Chloroplast DNA gyrase and *in vitro* regulation of transcription by template topology and novobiocin. Plant Mol. Biol. **8,** 415-424.

Larzul, D., Guigue, F., Snisky, J. J., Mack, D. H., Brechot, C., and Guesdon, J.L. Detection of hepatitis B virus sequences in serum by using *in vitro* enzymatic

amplification. (1988). J. Virol. Methods **20,** 227-237.

Lawlor, D. W., (1993). Photosynthesis: Molecular, Physiological, and Environmental Processes. (Essex, U.K., Longman Scientific and Technical).

Lebedev, N., and Timko, M. P. (1998). Photoclorophyllide photoreduction. Photosyn. Res. **58,** 5-23.

Legen, J., Kemp, S., Krause, K., Profanter, B., Hermann, R. G., and Maier, R. M. (2002). Comparative analysis of plastid transcription profiles of entire plastid chromosomes from tobacco attributed to wild-type and PEP-deficient transcription machineries. Plant Journal **31,** 171-188.

Lennon, A. M., Prommeenate, P., and Nixon, P. J. (2003). Location, expression and orientation of the putative chlororespirartory enzymes, Ndh, and IMMUTANS, in higher-plant plastids. Planta **218,** 254-260.

Lerbs-Mache, S. (1993). The 110-kDa polypeptide of spinach plastid DNA-dependent RNA polymerase: single-subunit enzyme or catalytic core of multimeric enzyme complexes? Proc. Natl. Acad. Sci. USA **90,** 5509-5513.

Lerbs-Mache, S. (2000). Regulation of rDNA transcription in plastids of higher plants. Biochimie **82,** 525-535.

Li, H. –M., Culligan, K. Dixon, R. A., and Chory, J. (1995). CUE1: a mesophyll cell-specific positive regulator of light-controlled gene expression in *Arabidopsis*. Plant Cell **7,** 1599-1610.

Li, M., Moyle and H., and Susskind, M. M. (1994). Target of the transcriptional activation function of phage lambda cI protein. Science **263,** 75-77.

Liere, K., Kaden, D., Maliga, P., and Börner, T. (2004). Overexpression of phage-type RNA polymerase RpoTp in tobacco demonstrates its role in chloroplast transcription by recognizing a distinct promoter type. Nucleic. Acids Res. **32,** 1159-1165.

Liere, K., and Maliga, P. (1999). *In vitro* characterization of the tobacco *rpoB* promoter reveals a core sequence motif conserved between phage-type plastid and mitochondrial promoters. EMBO J. **18,** 249-257.

Lilly, J. W., Havey, M. J., Jackson, S. A., and Jiang, J. (2001). Cytogenomic analysis reveals the structural plasticity of chloroplast genome in higher plants. Plant Cell **13,** 245-254.

Link, G. (1988). Photocontrol of plastid gene expression. Plant, Cell and Environment **11,** 329-338.

Link, G. (1996). Green life: Control of chloroplast gene transcription. BioEssays

18, 465-471.

Liu, W., and Saint, D. A. (2002). A new quantitative method of real time reverse transcription polymerase chain reaction assay based on simulation of polymerase chain reaction kinetics. Anal. Biochem. **302,** 52-59.

Livak, K. J. (1997). ABI Prism sequence detection system. User Bulletin no. 2. PE Applied Biosystems, AB Website, Bulletin Reference: 4303859B 777802-002. http://docs.appliedbiosystems.com.pebiodocs/04303859.pdf

Livak, K. J., Flood, S. J. A., Marmaro, J., Giusti, W., and Deetz, K. (1995). Oligonucleotides with fluorescent dyes at opposite ends provide a quenched probe system useful for detecting PCR product and nucleic acid hybridization. PCR Methods Appl. **4,** 357-362.

Livak, K. J., and Schmittgen, T. W. (2001). Analysis of relative gene expression data using real-time quantitative PCR and the $2^{-\Delta\Delta C}{}_T$ method. Methods **25,** 402-408.

Lonetto, M., Gribskov, M., and Gross, C. A. (1992). The σ^{70} family: sequence conservation and evolutionary relationships. J. Bacteriol. **174,** 3843-3839.

Lovel. P. H., and Moore, K. G. (1970). A comparative study of cotyledons as assimilatory organs. J. Exp. Bot. **21,** 1017-1030.

Lu, C., Lu, Q., Zhang, J., and Kuang, T. (2001). Characterization of photosynthetic pigment composition, photosystem II photochemistry and thermal energy dissipation during leaf senescence of wheat plants grown in the fields. J. Expt. Bot. **52,** 1805-1810.

Lyndon, R. F., and Robertson, E. S. (1976). The quantitative ultrastructure of the pea shoot apex in relation to leaf initiation. Protoplasma **87,** 387-402.

Mache, R., and Lerbs-Mache, S. (2001). Chloroplast genetic system of higher plants: chromosome replication, chloroplast division and elements of the transcription apparatus. Current Science **80,** 217-224.

Mache, R., Zhou, D.-X., Lerbs-Mache, S., Harrak, H., Villain, P., and Gauvin, S. (1997). Nuclear control of early plastid differentiation. Plant Physiol. Biochem. **35,** 199-203.

Maier, R.M., Neckerman, K., Igloi, G.I., and Kassel, H. (1995). Complete sequence of the maize chloroplast genome: gene content, hot spots of divergence and fine tuning of genetic information by transcript editing. J. Mol. Biol. **251,**614--628.

Malhotra, A., Severinove, E., and Darst, S. A. (1996). Crystal structure of a σ^{70} subunit fragment from *E. coli* RNA polymerase. Cell **87,** 127-136.

Maliga, P. (1998). Two plastid RNA polymerases of higher plants: an evolving story. Trends in Plant Science **3**, 4-6.

Maliga, P. (2004). Plastid Transformation in higher plants. Annu. Rev. Plant Biol. **55,** 289-313.

Mancera-Z, H. A., Thomas, B. J., Thomas, H., and Scott, I. M. (1999). Regreening of senescent *Nicotiana* leaves. II. Redifferentiation of plastids. J. Exp. Bot. **50,** 1683-1689.

Mansfield, S. G., and Briarty, L. G. (1996). The dynamics of seedling and cotyledon cell development in *Arabidopsis thaliana* during reserve mobilization. Int. J. Plant Sci. **157,** 280-295.

Marano, M, r., Serra, E. C., Orellano, E. G., and Carrilo, N. (1993). The path of chromoplast development in fruits and flowers. Plant Sci. **94,** 1-17.

Martín, M., Casano, L. M., and Sabater, B. (1996). Identification of the product of *ndhA* gene as a thylakoid protein synthesized in response to photooxidative treatment. Plant Cell Physiol. **37,** 293-298.

Martin, W., and Herrmann, R. G. (1998). Gene transfer from organelles to the nucleus: How much, what happens, and why? Plant Physiol. **118,** 9-17.

Mascia, P. N., and Robertson, D. S. (1978). Studies of chloroplast development in four maize mutants defective in chlorophyll biosynthesis. Planta **143,** 207-211.

Matsubayashi, T., Wakasugi, T., Shinozaki, K., Shinozaki-Yamaguchi, K., Zaita, N., Hidaka, T., Meng, B. Y., Ohto, C., Tanaka, M., Kato, A., Maruyama, T., and Sugiura, M. (1987). Six chloroplast genes (*ndhA-F*) homologous to human mitochondrial genes encoding components of the respiratory chain NADH dehydrogenase are actively expressed: determination of the splice sites in *ndhA* and *ndhB* pre-mRNAs. Mol. Gen. Genet. **210,** 385-393.

Maxwell, P. C., and Biggins, J. (1976). Role of cyclic electron transport in photosynthesis as measured by the photoinduced turnover of P_{700} *in vivo*, Biochemistry **15,** 3975-3981.

Mayfield, S. P. (1990). Chloroplast gene regulation: interaction of the nuclear and chloroplast genomes in the expression of photosynthetic proteins. Current Opinion in Cell Biology **2,** 509-513.

Mayfield, S.P., and Taylor, W.C. (1984). Carotenoid-deficient seedlings fail to accumulate light harvesting chlorophyll a/b binding protein (LHCP) mRNA. Eur. J. Biochem. **144,** 79-84.

McAlister, W.T., and Raskin, C. A. (1993) The phage RNA polymerases are related to DNA polymerases and reverse trancriptases. Mol. Microbiol. **10,** 1-6.

McClure, W. R. (1985). Mechanisn and control of transcription initiation in prokaryotes. Ann. Rev. Biochem. **54,** 171-204.

McFadden, G. I. (1999). Endosymbiosis and evolution of the plant cell. Current Opinion in Plant Biology **2,** 513-519.

Meijerink, J., Mandigers, C., van De Locht, L., Tonnissen, E., Goodsaid, F., and Raemaekers, J. (2001). A novel method to compensate for different amplification efficiencies between patient DNA samples in quantitative real-time PCR. J. Mol. Diagn. **3,** 55-61.

Meurer, J., Berger, A., and Westhoff, P. (1996). A nuclear mutant of *Arabidopsis* with impaired stability on distinct transcripts of the plastid *psbB*, *psbD/C*, *ndhH*, and *ndhC* operons. Plant Cell **8,** 1193-1207.

Meurer, J., Grevelding, C., Westhoff, P. and Reiss, B. (1998).The PAC protein affects the maturation of specific chloroplast mRNAs in *Arabidopsis thaliana*. Mol. Gen. Genet. **258,** 342-351.

Meyerowitz, E. M. (1989). *Arabidopsis*, a useful weed. Cell **56,** 263-269.

Miller, K. R., and Staehelin, L. A. (1976). Analysis of the thylakoid outer surface coupling factor is limited to unstacked membrane regions. J. Cell Biol. **68,** 30-47.

Miyagi, T., Kapoor, S., and Sugiura, M. (1998). Transcript analysis of the tobacco

plastid operon *rps2/atpI/H/F/A* reveals the existence of a non-consensus type II (NCII) promoter upstream of the *atpI* coding sequence. Mol. Gen. Genet. **257,** 99-307.

Mochizuki, N., Brusslan, J. A., Larkin, R., Nagatani, A., and Chory, J. (2001). *Arabidopsis* genomes uncoupled 5 (GUN%) mutant reveals the involvment of Mg-chelatase H subunit in plastid-to-nucleus signal transduction. Proc. Natl. Acad. Sci. USA **98,** 2053-2058.

Mochizuki, N., Susek, R. E., and Chory, J. (1996). An intracellular signal transduction pathway between the chloroplast and nucleus is involved in de-etiolation. Plant Physiol. **112,** 1465-1469.

Mochizuki, T., Onda, Y., Fujiwara, E., Wada, M., and Toyoshima, Y. (2004). Two independent light signals cooperate in the activation of the plastid *psbD* blue light-responsive promoter in *Arabidopsis*. FEBS Lett. **571,** 26-30.

Moffatt, B. A., McWhinnie, E. A., Agarwal, S. K., and Schaff, D. A. (1994). The adenine phosphoribosyltransferase-encoding gene of *Arabidopsis thaliana*. Gene **143,** 211-216.

Monde, R. A., Schuster, G., and Stern, D. B. (2000). Processing and degradation of chloroplast RNA. Biochimie **82,** 573-582.

Morikawa, K., Ito, S., Tsunoyama, Y., Nakahira, Y., Shiina, T., and Toyoshima, Y. (1999). Circadian-regulated expression of nuclear-encoded plastid σ factor gene (*sigA*) in wheat seedlings. FEBS Lett. **451,** 275-278.

Morrison, T. B., Weis, J. J., and Wittwer, C. T. (1998). Quantification of low-copy transcripts by continuous SYBR Green I monitoring during amplification. Biotechniques **24,** 954-962.

Mühlethaler, K. (1971). The ultrastracture of plastids. In Structure and Function of Chloroplast, M. Gibbs ed, (Berlin: Springer-Verlag). pp. 7-34.

Mullet, J. E. (1988). Chloroplast development and gene expression. Ann Rev Plant Physiol Plant Mol Biol **39,** 475-502

Mullet, J. E. (1993). Dynamic regulation of chloroplast transcription. Plant Physiol **103,** 309-313.

Nagashima, A., Hanaoka, M., Shikanai, T., Fujiwara, M., kanamaru, K., Takahashi, H., and Tanaka, K. (2004). The multiple-stress responsive plastid sigma factor, SIG5, directs activation of the *psbD* blue light-responsive promoter (BLRP) in *Arabidopsis thaliana*. Plant Cell Physiol. **45,** 357-368.

Nakahira, Y., Baba, K., Yoneda, A., Shiina, T., and Toyoshima, Y. (1998). Circadian clock-regulated transcription of the *psbD* light-responsive promoter

(*psbD* LRP) in wheat chloroplasts. Plant Physiol. **118,** 1079-1088.

Nakayama, H., Yokoi, H., Fujita, J. (1992). Quantification of mRNA by non-radioactive RT-PCR and CCD imaging system. Nucleic Acids Res. **20,** 4939.

Neuhaus, H., Scholtz, A., and Link, G. (1989). Structure and expression of a split chloroplast gene from mustard (*Sinapsis alba*): ribosomal protein gene *rps16* reveals unusual transcription features and complex RNA maturation. Curr. Genet. **15,** 63-70.

Neuhaus, H. E., and Emes, M. J. (2000). Non-photosynthetic metabolism in plastids. Annu. Rev. Plant Physiol. Plant Mol. Biol. **51,** 111-134.

Ngernprasirtsiri, J, Kobayashi, H., and Akazawa, T. (1988). DNA methylation as a mechanism of transcriptional regulation in nonphotosynthetic plastids in plant cells. Proc. Natl. Acad. Sci. USA **85,** 4750-4754.

Nickelsen, J., and Link, G. (1991). RNA-protein interactions at transcript 3′ ends and evidence for *trnK-psbA* cotranscription in mustard chloroplasts. Mol. Gen. Genet. **228,** 89-96.

Nixon, P. J. (2000). Chlororespiration. Phil. Trans. R. Soc. Lond. B. **355,** 1541-1547.

Odintsova, M. S., and Yurina, N. P. (2003). Plastid genomes of higher plants and algae: structure and function. Mol. Biol. **37,** 768-783.

Oelmüller, R. (1989). Photo-oxidative destruction of chloroplasts and its effect on nuclear gene expression and extraplastidic enzyme levels. Photochem. Photobiol. **49,** 229-239.

Oelmüller, R., Levitan, I., Bergfeld, R., Rajasekhar, V.K., and Mohr, H. (1986). Expression of nuclear genes as affected by treatments acting on the plastids. Planta **168,**482-492.

Oelmüller, R., and Mohr, H. (1986). Photooxidative destruction of chloroplasts and its consequences for expression of nuclear genes. Planta **167,**106-113.

Ohme, M., Kamogashira, T., Shinozaki, K., and Sugiura, M. (1985). Structure and cotranscription of tobacco genes for $tRNA^{Glu}$(UUC), $tRNA^{Tyr}$(GUA) and $tRNA^{Asp}$(GUA). Nucleic Acids Res. **13,** 1045-1056.

Ohyama, K., Fukuzawa, H., Kohchi, T., Shirai, H., Sano, T., Shiki, Y., Takeuchi, M., Chang, Z., Aota, S., Inokuchi, H., and Ozeki, H. (1986). Chloroplast gene organization deduced from complete sequence of liverwort *Marchantia polymorhpa* chloroplast DNA. Nature **322,**572-574.

Oldenburg, D. J., and Bendich, A. J. (2004). Most chloroplast DNA of maize

seedlings in linear molecules with defined ends and branched forms. J. Mol. Biol.**335,** 953-970.

Palmer, J. D. (1985). Comparative organization of chloroplast genomes. Annu. Rev. Genet. **19,** 325-354.

Palmer, J.D. (1991). Plastid chromosomes: structure and evolution In The Molecular Biology of Plastids, L. Bogorad, and I.K. Vasil eds, (San Diego, Academic Press) pp. 5-53.

Papenbrock, J., and Grimm, B. (2001). Regulatory network of tetrapyrrole biosynthesis-studies of intracellular signaling involved in metabolic and developmental control of plastids. Planta **213,** 667-681.

Patra, D., Lafer, E. M., and Sousa, R. (1992). Isolation and characterization of mutant bacteriophage-T7 RNA polymerases. J. Mol. Biol. **224,** 307-318.

Pearson, C. K., Wilson, S. B., Schaffer, R., and Ross, A. W. (1993). NAD turnover and utilization of metabolites for RNA synthesis in a reaction sensing the redox state of cytochrome b_6/f complex in isolated chloroplasts. Eur. J. Biochem. **218,** 397-404.

Peccoud, J., and Jacob, C. (1998). Statistical estimations of PCR amplification rates. In Gene Quantitation, F. Ferré eds, (Boston, Birkhäuser) pp. 1-17.

Peltier, G., and Cournac, L. (2002). Chlororespiration. Annu. Rev. Plant Biol. **53,** 523-550.

Pesares, P., Varotto, C., Richly, E., Kurth, J., Salamini, F., and Leister, D. (2001). Functional genomics of *Arabidopsis* photosynthesis. Plant Physiol. Biochem. **39,** 285-294.

Pfannschmidt, T., and Link, G. (1994). Separation of two classes of plastid DNA-dependent RNA polymerase that are differentially expressed in mustard (*Sinapsis alba*) seedlings. Plant Mol. Biol. **25,** 69-81.

Pfannschmidt, T., and Link, G. (1997). The A and B forms of plastid DNA-dependent RNA polymerase from mustard (*Sinapsis alba L.*) transcribe the same genes in a different developmental context. Mol. Gen. Genet. **257,** 35-44.

Pfannschmidt, T., Nillson, A., and Allen, J. (1999). Photosynthetic control of chloroplast gene expression. Nature **397.** 625-628.

Pfannschmidt, T., Orgzewalla, K., Baginski, S., Sickmann, A., Meyer, H.E., and Link, G. (2000). The multisubunit chloroplast RNA polymerase A from mustard (*Sinapsis alba L.*): Integration of a prokaryotic core into a larger complex with organelle-specific functions. Eur. J. Biochem. **267,** 253-261.

Pfannschmidt, T. Schütze, K., Fey, V., Sherameti, I., and Oelmüller, R. (2003). Chloroplast redox control of nuclear gene expression – A new class of plastid signals in interorganellar communication. Antioxidants & Redox Signaling **5,** 95-101.

Pfitzinger, H., Guillemaut, P., Weil, J-H., and Pillay, D. T.N. (1987). Adjustment of tRNA population to the codon usage in chloroplasts. Nucleic Acids Res. **15,** 1377-1386.

Possingham, J. V. (1980). Plastid replication and development in the life cycle of higher plants. Annu. Rev. Plant Physiol. **31,** 113-129.

Poulsen, C. (1984). Two mRNA species differing by 258 nucleotides at the 5′ end are formed from the barley chloroplast *rbcL* gene. Carlsberg Res. Commun. **49,** 89-104.

Pyke, K. A., and Page, A. M. (1998). Plastid ontogeny during petal development in *Arabidopsis*. Plant Physiol. **116,** 797-803.

Quail, P. (1991). Phytochrome: a light-activated switch that regulates plant gene expression. Ann. Rev. Genet. **25,** 389-409.

Quail, P. (2002). Photosensory perception and signaling in plant cells: new paradigms? Curr. Opin. Cell Biol. **14,** 180-188.

Race, H. L., and Hind, G. (1996). A protein kinase in the core of photosystem II. Biochemistry **35,** 13006-13010.

Radwanski, E. R., and Last, R. L. (1995). Tryptophan biosynthesis and metabolism: biochemical and molecular genetics. Plant Cell **7,** 921-934.

Rajeevan, M. S., Ranamukhaarachchi, D. G., Vernon, S., and Unger, E. (2001). Use of real-time PCR to validate the results of cDNA Array and differential display PCR technologies. Methods **25,** 443-451.

Ramakers, C., Ruijter, J. M., Lekanne, R. H., and Moorman, A. F. M. (2003). Assumption-free analysis of quantitative real-time polymerase chain reaction (PCR) data. Neuroscience Letters **339,** 62-66.

Rapp, J. C., Baumgartner, B. J., and Mullet, J. (1992). Quantitative analysis of transcription and RNA levels of 15 barley chloroplast genes. J. Biol. Chem. **267,** 21404-21411.

Rapp, J. C., and Mullet, J. (1991). Chloroplast transcription is required to express the nuclear genes *rbcS* and *cab*. Plastid DNA copy number is regulated independently. Plant Mol. Biol. **17,** 813-823.

Rasmussen, R. (2001). Quantification on the LightCycler. In Rapid Cycle Real-time PCR, Methods and Applications, S. Meuer, C. Wittwer and K. Nakagawara eds,

(Springer Press, Heidelberg) pp. 21-34.

Ravenel, J., Peltier, G., and Havaux, M. (1994). The cyclic electron pathways around photosystem I in *Chlamydomonas reinhardtii* as determined in vivo by photoacoustic measurements of energy storage. Planta **193,** 251-259.

Raz, V., Bergervoet, J. H. W., and Koornneef, M. (2001). Sequential steps for developmental arrest in *Arabidopsis* seeds. Development **128,** 243-252.

Reynolds, E. S. (1963). The use of lead citrate at high pH as an electron-opaque stain in electron microscopy. J. Cell Biol. **17,** 208-212.

Ririe, K. M., Rasmussen, R. P., and Witwer, C. T. (1997). Product differentiation by analysis of DNA melting curves during the polymerase chain reaction. Anal. Biochem. **245,** 154-160.

Robertson, D., and Laetsch, W. M. (1974). Structure and function of developing barley plastids. Plant Physiol. **54,** 148-159.

Rochaix, J. D. (1992). Post-transcriptional steps in the expression of chloroplast genes. Ann. Rev. Cell Biol. **8,** 1-28.

Rodermel, S. (1999). Subunit control of Rubisco biosynthesis-a relic of an endosymbiotic past? Photosynthesis Res. **59,** 105-123.

Rodermel, S. (2001). Pathways of plastid-to-nucleus signaling. Trends in Plant Sci. **6,** 471-478.

Rozen, S., and Skaletsky, H. J. (2000). Primer3 on the WWW for general users and for biologist programmers. In Bioinformatics Methods and Protocols: Methods in Molecular Biology, S. Krawetz and S. Misener ed, (Humana Press, Totowa, NJ) pp.365-386.

Ruf, M., and Kössel, H. (1988). Structure and expression of the gene coding for the α-subunit of DNA-dependent RNA-polymerase from the chloroplast genome of *Zea mays*. Nucleic Acids Res. **16,** 5741-5754.

Rutlledge, R. G., and Côté, C. (2003). Mathematics of quantitative kinetics PCR and the application of standard curves. Nucleic Acids Res. **31,** E93**.**

Ruuska, S. A., and Ohlrogge, J. B. (2001). Protocol for small-scale RNA isolation and transcriptional profiling of developing *Arabidopsis* seeds. BioTechniques **31,** 752-758.

Sakai, A., Kawano, S., and Kuroiwa, T. (1992). Conversion of proplastids to amyloplasts in tobacco cultured cells is accompanied by changes in the transcriptional activities of plastid genes. Plant Physiol. **100,** 1062-1066.

Salvador, M. L., and Klein, U. (1999). The redox state regulates RNA degradation

in the chloroplast of *Chlamydomonas rheinhardtii*. Plant Physiol. **121,** 1367-1374.

Sambrook, J., Fritsch, E.F., and Maniatis, T. (1989). Molecular Cloning: A Laboratory Manual, 2nd ed. (Cold Spring Harbour, NY: Cold Spring. Harbour Laboratory Press).

Sato, N., Rolland, N., Block, M. A., and Joyard, J. (1999b). Do plastid envelope membranes play a role in the expression of the plastid genome? Biochimie **81,** 619-29.

Sato, S., Nakamura, Y., Kaneko, T., Asamizu, E., and Tabata, S. (1999a). Complete structure of the chloroplast genome of *Arabidopsis thaliana*. DNA Res. **6,** 283-290.

Satoh, J., Baba, K., Nakahira, Y., Shiina, T., and Toyoshima, Y. (1997). Characterization of the *psbD* light-induced transcription in mature wheat chloroplasts. Plant Mol. Biol. **33,** 267-278.

Satoh, J., Baba, K., Nakahira, Y., Tsunoyama, Y., Shiina, T., and Toyoshima, Y. (1999). Developmental stage-specific multi-subunit plastid RNA polymerase (PEP) in wheat. Plant J. **18,** 407-415.

Sazanov, L. A., Burrows, P. A., and Nixon, P. J. (1998). The plastid *ndh* genes

code for an NADH-specific dehydrogenase: isolation of a complex **I** analog from pea thylakoid membranes. Proc. Natl. Acad. Sci. USA **95,** 1319-1324.

Schmidt, M. A., and Parrott, W. A. (2001). Quantitative detection of transgenes in soybean [*Glycine max* (L) Merrill] and peanut (*Arachis hypogaea* L.) by real-time polymerase chain reaction. Plant Cell Rep. **20,** 422-428.

Schmittgen, T. D., and Zakrajsek, B. (2000). Effect of experimental treatment on housekeeping gene expression: validation by real-time, quantitative RT-PCR. J. Biochem. Biophys. Methods **46,** 69-81.

Schmittgen, T. D., Zakrajsek, B. A., Mills, A. G., Gorn, V., and Singer, M. J. (2000). Quantitative reverse transcription-polymerase chain reaction to study mRNA decay: comparison of endpoint and real-time methods. Anal. Biochem. **285,** 194-204.

Schneeberger, C., Speiser, P., Kury, F., and Zeillinger, R. (1995). Quantitative detection of reverse transcriptase-PCR products by means of a novel and sensitive DNA stain. PCR Methods Appl. **4,** 234-238.

Schrubar. H., Wanner, G., and Westhoff, P. (1990). Transcriptional control of plastid gene expression in greening Sorghum seedlings. Planta **183,** 101-111.

Schultz, P., and Jensen, W. A. (1968). Capsella embryogenesis: the early embryo.

J. Ultrastruct. Res. **22,** 376-392.

Serino, G., and Maliga, P. (1998). RNA polymerase subunits encoded by the plastid *rpo* genes are not shared with the nucleus–encoded plastid enzyme. Plant Physiol. **117,** 1165-1170.

Sexton, T. B., Christopher, D. A., and Mullet, J. E. (1990). Light-induced switch in barley psbD-psbC promoter utilization: a novel mechanism regulating chloroplast gene expression. EMBO J. **9,** 4485-4495.

Shikanai, T., Endo, T., Hashimoto, T., Yamada, Y., Asada, K., and Yokota, A. (1998). Directed disruption of the tobacco *ndhB* gene impairs cyclic electro flow around photosystem I. Proc Natl. Acad. Sci USA **95,** 9705-9709.

Shikanai, T., Shimizu, K., Ueda, K., Nishimura, Y., Kuroiwa, T., and Hashimoto, T. (2001). The chloroplast *clpP* gene, encoding a proteolytic subunit of ATP-dependent protease, is indispensable for chloroplast development in tobacco. Plant Cell Physiol. **42,** 264-273.

Shinozaki, K., Ohme, M., Tanaka, M., Wakazuki, T., Hayashida, N., Matsubayasbi, T., Zaita, N., Chunwongse, J., Obokata, J., Shinozaki, K. Y., Ohto, C., Torazawa, K., Meng, B. Y., Sugita, M., Deno, H., Kamogashira, T., Yamada, K., Kusuda, J., Takaiwa, F., Kato ,A., Tohdoh, N., Shimada, H, and Sugiura, M. (1986). The complete nucleotide sequence of the tobacco

chloroplast genome: its gene organization and expression. EMBO J. **5,** 2043-2049.

Short, T. W., and Briggs, W. R. (1994). The transduction of blue-light signals in higher plants. Annu. Rev. Plant Physiol. Plant Mol. Biol. **45,** 143-171.

Silhavy, D., and Maliga, P. (1998a) Mapping of promoters for the nucleus-encoded plastid RNA polymerase (NEP) in the *jojap* maize mutant. Curr. Genet. **33,** 340-344.

Silhavy, D., and Maliga, P. (1998b). Plastid promoter utilization in a rice embryogenic cell culture. Curr. Genet. **34,** 67-70.

Simpson, J., and Herrera-Estrella, L. (1990). Light-regulated gene expression. Critical Reviews in Plant Sciences **9,** 95-108.

Smith, H. (1995). Physiological and ecological function within the phytochrome family. Annu. Rev. Plant Physiol. Plant Mol. Biol. **45,** 289-315.

Somachi, A., and Mayfield, S. P. (1999). Nuclear-chloroplast signaling. Curr. Opin. Plant Biol. **2,** 404-409.

Sousa, R., Chung, Y. J., Rose, J.P., and Wang, B. –C. (1993). Crystal structure of bacteriophage T7 RNA polymerase at 3.3 Å resolution. Nature **364,** 593-599.

Sriraman, P., Silhavy, D., and Maliga, P. (1998a). The phage-type PclpP-53 plastid promoter comprises sequences downstreem of the transcription initiation site. Nucleic Acids Res. **26,** 4874-4879.

Staehelin, L. A. (2003). Chloroplast structure: from chlorophyll granules to supra-molecular architecture of thylakoid membranes. Photosynthesis Res. **76,** 185-196.

Staehelin, L. A., and Newcomb, E. H. (2000). Membrane structure and membranous organelles. In Biochemistry and Molecular Biology of Plants, R. B. Buchanan, W. Gruissem and R. L. Jones eds, (Rockville, MD, American Society of Plant Biology) pp. 2-50.

Staub, J. M., and Maliga, P. (1995). Expression of a chimeric uidA gene indicates that polycistronic mRNAs are efficiently translated in tobacco plastids. Plant J. **7,** 845-848.

Stern, D. B., and Gruissem, W. (1987). Control of plastid gene expression: 3′ inverted repeats act as mRNA processing and stabilizing element, but do not terminate transcription. Cell **51,** 1145-1157.

Stern, D. B., Higgs, D., and Yang, J. (1997). Transcription and translation in chloroplasts. Trends Plant Sci. **2,** 308-315.

Stirdivant, S. M., Crossland, L. D., and Bogorad, L. (1985). DNA supercoiling affects *in vitro* transcription of two maize chloroplast genes differently. Proc. Natl. Acad. Sci. USA **82,** 4886-4890.

Stryer, L. (1978). Fluorescence energy transfer as spectroscopic ruler. Annu. Rev. Biochem. **47,** 819-846.

Subramarian, A. R., Stahl, D, and Prombona, A. (1991). Ribosomal proteins, ribosomes, and translation in plastids In The Molecular Biology of Plastids L. Bogorad and I. K. Vasil eds, (San Diego, Academic Press). pp. 191-215.

Sugimoto, H., Kusumi, K., Tozawa, Y., Yazaki, J., Kishimoto, N., Kikichi, S., and Iba, K. (2004). The viriscent-2 mutation inhibits translation of plastid transcripts for the plastid genetic system at an early stage of chloroplast differentiation. Plant Cell Physiol. **45,** 985-996.

Sugita, M., and Sugiura, M. (1996). Regulation of gene expression in chloroplasts of higher plants. Plant Mol. Biol. **32,** 315-326.

Sugiura, M. (1992). The chloroplast genome. Plant Mol Bio **19,**149-168.

Sugiura, M., Hirose, T., and Sugiura, M. (1998). Evolution and mechanism of translation in chloroplasts. Annu. Rev. Genet. **32,** 437-459.

Sullivan, J. A., and Gray, J. C. (1999). Plastid translation is required for the expression of nuclear photosynthesis genes in the dark and in roots of the pea *lip1* mutant. Plant Cell **11,** 901-910.

Summer, H., Pfannschmidt, T., and Link, G. (2000). Transcripts and sequence elements suggest differential promoter usage within the *ycf3-psaAB* gene cluster on mustard (*Sinapsis alba*) chloroplast DNA. Curr. Genet. **37,** 45-52.

Surpin, M., Larkin, R. M., and Chory, J. (2002). Signal transduction between the chloroplast and the nucleus. Plant Cell S327-S338.

Susek, R. E., Auseubel, F. M., and Chory, J. (1993). Signal transduction mutants of *Arabidopsis* uncouple nuclear *CAB* and *RBCS* gene expression from chloroplast development. Cell **74,** 787-799.

Susek, R. E., and Chory, J. (1992). A tale of two genomes: Role of chloroplast signal in coordinating nuclear and plastid genome expression. Aust. J. Plant Physiol. **19,** 387-399.

Suzuki, T., Higgins, P. J., and Crawford, D. R. (2000). Control selection for RNA quantitation. BioTechniques **29,** 332-337.

Swiatek, M., Kuras, R., Sokolenko, A., Higgs, D., Olive, J., Cinque, G., Muller, B., Eichacker, L. A., Stern, D. B., Bassi, R., Herrmann, R. G., and Wollman, F.

A. (2001). The chloroplast gene ycf9 encodes a photosystem II (PSII) coresubunit, PsbZ, that participates in PSII supramolecular architecture. Plant Cell **13,** 1347-1367.

Tan, S., and Troxler, R. F. (1999). Characterization of two chloroplast polymerase σ factors from *Zea mays*: photoregulation and differential expression. Proc. Natl. Acad. Sci. USA **96,** 5316-5321.

Tanaka, K. Tozawa, Y., Mochizuki, N., Shinozaki, K., Nagatani, A., Wakasa, K., and Takahashi, H. (1997). Characterization of three cDNA species encoding plastid RNA polymerase sigma factors in *Arabidopsis thaliana*: evidence for the sigma factor heterogeneity in higher plants. FEBS Lett. **413,** 309-313.

Taylor, W.C. (1989). Regulatory interactions between nuclear and plastid genomes. Annu. Rev. Plant Phsiol. Plant Mol. Biol. **40,**211-233.

Tesniere, C., and Vayda, M. E. (1991). Method for the isolation of high-quality RNA from grape berry tissue without contaminating tannins or carbohydrates. Plant Mol. Biol. Reptr. **9,** 242-251.

Thomas, M. R., and Rose, R. J. (1983). Plastid number and plastid ultrastructural changes associated with tobacco mesophyll protoplast culture and plant regeneration. Planta **158,** 329-338.

Thomas, T. L. (1993). Gene expression during plant embryogenesis and germination: an overview. Plant Cell **5,** 1401-1410.

Thompson, R. J., and Mosig, G. (1987). Stimulation of a *Chlamydomonas* chloroplast promoter by novobiocin *in situ* and *E. coli* implies regulation by torsional stress in the chloroplast DNA. Cell **48,** 281-287.

Thompson, W. F., Everett, M., Polans, N. O., Jorgansen, R. A., and Palmer, J.D. (1983). Phytochrome control of RNA levels in developing pea and mung-bean leaves. Planta, **158,** 487-500.

Thompson, W. F., and White MJ (1991) Physiological and molecular studies of light-regulated nuclear genes in higher plants. Annu. Rev. Plant Physiol. Plant. Mol. Biol. **42,** 423-466.

Thomson, W, W., and Whatley, J. M. (1980). Development of non-green plastids. Annu. Rev. Plant Physiol. **31,** 375-394.

Thum, K. (2000). Mechanisms regulating *psbD* expression from a plastid blue light-responsive promoter: a glimpse of regulated plastid gene expression. Ph.D. Dissertation, Texas A&M University, College Station. pp. 108 – 111.

Tiller, K., and Link, G. (1993a). Sigma-like transcription factors from mustard (*Sinapsis alba*) etioplast are similar in size to, but functionally distinct from their

chloroplast counterparts. Plant Mol. Biol. **21,** 503-513.

Tiller, K., and Link, G. (1993b). Phosphorylation and dephosphorylation affect functional characteristics of chloroplast and etioplast transcription systems from mustard (*Sinapsis alba*). EMBO J. **12,** 1745-1753.

Tilney-Bassett, R. A. E. (1978). The inheritance and genetic behaviour of plastids. In The Plastids: Their Chemistry, Structure, Growth and Inheritance. 2nd ed., J.T.O. Kirk and R. A. E Tilney-Bassett eds, (Amsterdam, Elsevier Biomedical Press). pp. 251-524.

To, K. Y., Cheng, M. C., Suen, D. F., Mon, D. P., Chen, L. F. O., and Chen, S. C. G. (1996). Characterization of the light-responsive promoter of rice *psbD-C* operon and the sequence-specific DNA binding factor. Plant Cell Physiol. **37,** 660-666.

Töpfer, R., Matzeit, V., Gronenborn, B., Schell, J., and Steinbiss, H.-H. (1987). A set of plant expression vectors for transcriptional and translational fusions. Nucl. Acids Res. **15**, 5890.

Toyoshima, Y Onda, Y., Shiina, T., and Nakahira, Y. (2005). Plastid transcription in higher plants. Critical Reviews in Plant Sciences **24,** 59-81.

Tozawa, Y., Tanaka, K., Takahashi, H, and Wakasa, K. (1998). Nuclear encoding

of a plastid σ factor in rice and its tissue- and light-dependent expression. Nucleic Acids Res. **26,** 415-419.

Trifa, Y., Privat, I., Gagnon, J., Baeza, L., and Lerbs-Mache, S. (1998). The nuclear *RPL4* gene encodes a chloroplast protein that co-purifies with the T7-like transcription complex as well as plastid ribosomes. J. Biol. Chem. **273,** 3980-3985.

Tsunoyama, Y., Ishizaki, Y., Morikawa, K., Kobori, M., Nakahira, Y., Takeba, G., Toyoshima, Y., and Shiina, T. (2004). Blue light-induced transcription of plastid-encoded *psbD* gene is mediated by a nuclear-encoded transcription factor, AtSig5. Proc. Natl. Acad. Sci. USA **101,** 3304-3309.

Umesono, K., and Ozeki, H. (1987). Chloroplast gene organization in plants. Trends Genet. **3,** 281-287.

Vallon, O., Wollman, F. A., and Olive, J. (1985). Distribution of intrinsic and extrinsic subunits of the SPS11 protein complex between appressed and nonappressed region of the thylakoid membrane: An immunocytochemical study. FEBS Lett. **183,** 245-250.

Vaughn, K., Vierling, E., Duke, S., and Alberte, R. S. (1983). Immunocytochemical and cytochemical localization of photosystem I and II. Plant Physiol. **73,** 203-207.

Vera, A., and Sugiura, M. (1992). Combination of *in vitro* capping and ribonuclease protection improves the detection of transcription start sites in chloroplasts. Plant Mol. Biol. **19,** 309-311.

Vera, A., and Sugiura, M. (1995). Chloroplast rRNA transcription from structurally different tandem promoters: an additional novel-type promoter. Curr. Genet. **27,** 280-284.

Vera, A., Hirose, T., and Sugiura, M. (1996). A ribosomal protein (rpl32) from tobacco chloroplast DNA is transcribed from alternative promoters: similarities in promoter region organization in plastid housekeeping genes. Mol. Gen. Genet. **251,** 518-525.

Vera, A., Matsubayashi T., and Sugiura, M. (1992). Active transcription from a promoter positioned within the coding region of a divergently oriented gene: the tobacco chloroplast *rpl32* gene. Mol. Gen. Genet. **233,** 151-156.

Vermaas, W. F. J., and Ikeuchi, M. (1991). Photosystem II. In The Photosynthetic Apparatus: Molecular Biology and Operation, L. Bogorad and I. K. Vasil eds, (San Diego, Academic Press) pp. 25-111.

von Arnim, A. G., and Deng, X.–W. (1996). Light control of seedling development. Annu. Rev. Plant Physiol. Plant Mol. Biol. **47,** 215-243.

von Wettsein, D., Gough, S., and Kannangara, C. G. (1995). Chlorophyll biosynthesis. Plant Cell **7,** 1039-1057.

von Wettsein, D., Henningsen, K. W., Boynton, J. E., Kannangara, C. G., and Nielsen, O. F. (1971). The genic control of chloroplast development. In Autonomy and Biogenesis of Mitochondria and Chloroplasts, N. K. Boardman, A. W. Linnane and R. M. Smillie eds, (Amsterdam, North Holland) pp. 205-223.

Voskuil, M. I., Voeper, K., and Chambliss, G. H. (1995). The –16 region, a vital sequence for the utilization of a promoter in ***Bacillus subtilis*** and *Escherichia coli*. Mol. Microbiol. **17,** 271-279.

Wakasugi, T. Tsudzuki, J., Ito, S., Shibata, M., and Sugiura, M. (1994). A physical map and clone bank of the black pine (*Pinus thunbergii*) chloroplast genome. Plant Mol. Biol. Rep. **12,** 227-241.

Wakasugi, T. Tsudzuki, T., and Sugiura, M. (2001). The genomics of land plant chloroplasts: gene content and alteration of geneomic information by RNA editing. Photosynthesis Res. **70,** 107-118.

Wang, A. M., Doyle, M. V., and Mark, D. F. (1989). Quantitation of mRNA by the polymerase chain reaction. Proc. Natl. Acad. Sci. USA. **86,** 9717-9721.

Wang, Z.–Y., Kenigsbuch, D., Sun, L., Harel, E., Ong, M.S., and Tobin,

E.M.(1997). A Myb-related transcription factor is involved in the phytochrome regulation of an *Arabidopsis Lhcb* gene. Plant Cell **9,** 491-507.

Weihe A., and Börner, T. (1999). Transcription and the architecture of promoters in chloroplasts. Trends Plant Sci. **4,** 169-170.

Weihe, A., Hedtke, B., and Börner, T. (1997). Cloning and characterization of a cDNA encoding abacteriophage-type RNA polymerase from the higher plant *Chenopodium album*. Nucleic Acids Res. **25,** 2319-2325.

Westhoff, P., and Hermann, R. G. (1988). Complex RNA maturation in chloroplast: the *psbB* operon from spinach. Eur. J. Biochem. **171,** 551-564.

Whatley, J. M. (1983). The ultrastructure of plastids in roots. Int. Rev. Cytol. **85,** 175-220.

Whitelegge, J. P., Zhang, H., Aguilera, R., Taylor, R. M., and Cramer, W. A. (2002). Full subunit coverage liquid chromatography electrospray ionization mass spectrometry (LCMS+) of an oligomeric membrane protein. Molecular & Cellular Proteomics **1,** 816-827.

Whitmarsh, J. (1998). Electron transport and energy transduction. In Photosynthesis: A Comprehensive Treatise, A. S. Raghavendra ed, (Cambridge, Cambridge University Press) pp. 87-107.

Wiesner, R. J. (1992). Direct quantification of picomolar concentrations of mRNAs by mathematical analysis of a reverse transcription/exponential polymerase chain reaction assay. Nucleic Acids Res. **20,** 5863-5864.

Wilson, C., and Dombroski, A. J. (1997). Region 1 of σ^{70} is required for efficient isomerization and initiation of transcription by *Escherichia coli* RNA polymerase. J. Mol. Biol. **267,** 60-74.

Winner, J., Jung, C. K., Shackle, I., and Williams, P. M. (1999). Development and validation of real-time quantitative reverse transcriptase-polymerase chain reaction for monitoring gene expression in cardiac myocytes *in vitro*. Anal. Biochem. **270,** 41-49.

Wittwer, C. T., Hermann, M. G., Moss, A. A., and Rasmussen, R. P. (1997). Continuous fluorescence monitoring of rapid cycle DNA amplification. BioTechniques **22,** 130-138.

Wollman, F. A., Minai, L., and Nechushtai, R. (1999). The biogenesis and assembly of photosynthetic proteins in thylakoid membranes. Biochim. Biophys. Acta **1411,** 21-85.

Woodhead, M. Taylor, M. A., Davies, H. V., Brennan, R. M., and Mcnicol, R. J. (1997). Isolation of RNA from blackcurrant (*Ribes nigrum*) fruit. Mol. Biotechnol. **7,**1-4.

Wösten, M. M. S. M. (1998). Eubacterial sigma-factors. FEMS Microbiology Reviews. **22,** 127-150.

Wu, D. Y., Wright, D. A., Wetzel, C., Voytas, D. F., and Rodermel, S. (1999). The *immutans* variegation locus of *Arabidopsis* defines a mitochondrial alternative oxidase homolog that functions during early chloroplast biogenesis. Plant Cell **11,** 43-55.

Yao, W. B., Meng, B. Y. Tanaka, M., and Sugiura, M. (1989). An additional promoter within the protein-coding region of the *psbD-psbC* gene cluster in tobacco chloroplast DNA. Nucleic Acids Res. **17,** 9583-9591.

Yeung, A. T., Holloway, B. P., Adams, P. S., and Shipley, G. L. (2004). Evaluation of dual-labeled fluorescent DNA probe purity versus performance in real-time PCR. BioTechniques **36,** 266-275.

Young, D. A., Allen, R. L., Harvey, A. J., and Lonsdale, D. M. (1998). Characterization of a gene encoding a single-subunit bacteriophage-type RNA polymerase from maize which is alternatively spliced. Mol. Gen. Genet. **260,** 30-37.

Yu, T-S., and Li, H-m. (2001). Chloroplast protein translocon components atToc159 and atTocc33 are not essential for chloroplast biogenesis in guard cells and root cells. Plant Physiol. **127,** 90-96.

APPENDIX A

The following pages contain the real-time PCR data used to calculate the $2^{-\Delta CT}$ and $2^{-\Delta\Delta CT}$ values for plastid and nuclear genes in seeds and siliques of wild-type and *rpoZ191* mutant plants as well as the real-time PCR data used to calculate the $2^{-\Delta CT}$ values for the *RpoT* genes in siliques, seeds, 2-day seedlings, 5-day seedlings, 10-day cotyledons, 12-day cotyledons, 15-day cotyledons, 15 days rosette leaves, 35-day rosette leaves, 35-day cauline leaves, 5-day roots and 40-day roots.

Table 23. Real-time PCR values in the siliques of wild-type and *rpoZ19*1 mutant

Plastid Genes

Gene	Sample	C_T	*Avg C_T	[a]ΔC_T	[b]$\Delta\Delta C_T$	$2^{-\Delta\Delta CT}$	$2^{-\Delta CT}$ ($X10^5$)
†*rpoA*	*rpoZ191*	18.53 18.58 18.51	18.54 ± 0.04	7.65 ± 0.07	-0.24 ± 0.07	1.2 (1.1-1.2)	498 (474-524)
	wt	18.75 18.72 18.78	18.75 ± 0.03	7.89 ± 0.011	0.00 ± 0. 11	1.00 (0.93-1.08)	423 (392-456)
†*rpoC1*	*rpoZ191*	20.47 20.43 20.38	20.43 ± 0.05	9.54 ± 0.08	0.35 ± 0.08	1.27 (1.20-1.34)	134 (127-142
	wt	20.01 20.12 20.04	20.06 ± 0.06	9.20 ± 0.12	0.00 ± 0.12	1.0 (0.9-1.1)	171 (157-185
†*rps14*	*rpoZ191*	18.48 18.49 18.51	18.49 ± 0.02	7.61± 0.06	0.75 ± 0.06	1.7 (1.6-1.8)	514 (491-537)
	wt	17.84 17.72 17.71	17.72 ± 0.07	6.85 ± 0.13	0.00 ± 0.13	1.0 (0.9-1.1)	865 (791-945)
¥*rps15*	*rpoZ191*	20.99 21.09 20.96	21.01 ± 0.07	10.45 ± 0.08	-0.07 ± 0.08	1.05 (0.99-1.1)1	71 (67-76)
	wt	21.07 21.06 21.01	21.05 ± 0.03	10.52 ± 0.04	0.00 ± 0.04	1.00 (0.97-1.03)	68 (66-70)
†*rps16*	*rpoZ191*	22.09 22.05 22.01	22.05 ± 0.04	11.16 ± 0.07	-0.14 ± 0.07	1.11 (1.05-1.16)	44 (41-46)
	wt	22.22 22.15 22.14	22.17 ± 0.04	11.31± 0.11	0.00 ± 0.11	1.0 (0.9-1.1)	39 (37-43)

Table 23. (continued).

Gene	Sample	C_T	*Avg C_T	[a]ΔC_T	[b]$\Delta\Delta C_T$	$2^{-\Delta\Delta CT}$	$2^{-\Delta CT}$ ($X10^5$)
†*rpl32*	*rpoZ191*	19.05 19.01 18.97	19.01 ± 0.04	8.12 ± 0.07	-0.0007± 0.07	1.00 (0.95-1.05)	358 (340-377)
	wt	18.99 19.00 18.97	18.99 ± 0.02	8.13 ± 0.11	0.00 ± 0.11	1.00 (0.93-1.08)	358 (333-386)
¥*rrn16*	*rpoZ191*	9.02 9.06 9.10	9.06 ± 0.04	-1.50 ± 0.07	-0.43 ± 0.07	1.35 (1.29-1.41)	283000 (271000-297000)
	wt	8.67 8.49 8.60	8.59 ± 0.09	-1.94 ± 0.09	0.00 ± 0.09	1.0 (0.9-1.1)	383000 (360000-408000)
†*trnC-GCA*	*rpoZ191*	19.98 19.99 19.82	19.93 ± 0.10	9.04 ± 0.11	-0.15 ± 0.11	1.1 (1.0-1.2)	190 (176-206)
	wt	20.05 20.05 20.04	20.05 ± 0.01	9.19 ± 0.11	0.00 ± 0.11	1.0 (0.9-1.1)	172 (160-185)
†*trnE-UUC*	*rpoZ191*	20.63 20.57 20.61	20.60 ± 0.04	9.71 ± 0.07	-0.07 ± 0.07	1.05 (1.00-1.10)	119 (113-125)
	wt	20.68 20.61 20.65	20.64 ± 0.03	9.78 ± 0.11	0.00 ± 0.11	1.0 (0.9-1.1)	114 (105-123)
†*trnfM-CAU*	*rpoZ191*	20.76 20.73 20.78	20.76 ± 0.03	9.87± 0.07	-0.34 ± 0.07	1.3 (1.2-1.3)	107 (1-2-112)
	wt	21.07 21.08 21.06	21.07 ± 0.01	10.21 ± 0.11	0.00 ± 0.11	1.0 (0.9-1.1)	84 (78-91)
†*trnS-GCU*	*rpoZ191*	18.23 17.56 17.51	17.53 ± 0.04	6.64 ± 0.07	0.69 ± 0.07	1.6 (1.5-1.7)	1000 (951-1051)
	wt	16.80 16.83 16.80	16.81 ± 0.02	5.95± 0.11	0.00 ± 0.11	1.0 (0.9-1.1)	1617 (1502-1741)

Table 23. (continued.

Gene	Sample	C_T	*Avg C_T	[a]ΔC_T	[b]$\Delta\Delta C_T$	$2^{-\Delta\Delta CT}$	$2^{-\Delta CT}$ ($X10^5$)
†*trnV-GAC*	*rpoZ191*	21.12 21.05 21.11	21.09 ± 0.04	10.20± 0.07	-0.11 ± 0.07	1.08 (1.03-1.13)	85 (81-89)
	wt	21.26 21.14 21.13	21.18 ± 0.07	10.31± 0.13	0.00 ± 0.13	1.0 (0.9-1.1)	79 (72-860
†*trnW-CCA*	*rpoZ191*	17.328 17.331	17.330 ± 0.002	6.44 ± 0.06	-0.44 ± 0.06	1.35 (1.30-1.41)	1151 (1102-1202)
	wt	17.73 17.75	17.87 ± 0.01	6.88± 0.11	0.00 ± 0.11	1.0 (0.9-1.1)	850 (790-915)
†*atpA*	*rpoZ191*	16.88 16.81 16.89	16.86 ± 0.05	5.97± 0.08	0.02 ± 0.08	1.01 (0.96-1.07)	1593 (1510-1681)
	wt	16.85 16.79 16.80	16.81 ± 0.03	5.95 ± 0.11	0.00 ± 0.11	1.00 (0.93-1.08)	1618 (1500-1746)
†*atpB*	*rpoZ191*	18.74 18.64 18.69	18.69 ± 0.05	7.80 ± 0.08	0.50 ± 0.08	1.4 (1.3-1.5)	448 (424-474)
	wt	18.19 18.17 18.13	18.16 ± 0.03	7.30± 0.11	0.00 ± 0.11	1.0 (0.9-1.1)	635 (589-685)
†*ndhA*	*rpoZ191*	18.62 18.56 18.58	18.59 ± 0.03	7.70 ± 0.07	-0.53 ± 0.07	1.37 (1.31-1.44)	482 (460-506)
	wt	19.24 19.01 19.02	19.09 ± 0.13	8.23 ± 0.17	0.00 ± 0.17	1.0 (0.9-1.1)	351 (312-394)
†*ndhB*	*rpoZ191*	21.24 21.22 21.30	21.25 ± 0.05	10.36 ± 0.08	0.21 ± 0.08	1.16 (1.10-1.22)	76 (72-80)
	wt	21.07 20.97 21.01	21.02 ± 0.05	10.15± 0.11	0.00 ± 0.11	1.0 (0.9-1.1)	88 (81-95)

Table 23. (continued).

Gene	Sample	C_T	*Avg C_T	[a]ΔC_T	[b]$\Delta\Delta C_T$	$2^{-\Delta\Delta CT}$	$2^{-\Delta CT}$ ($X10^5$)
†*ndhF*	*rpoZ191*	20.72 20.73 20.67	20.71 ± 0.03	9.82 ± 0.07	-0.43 ± 0.07	1.35 (1.28-1.42)	111 (105-116)
	wt	21.13 21.10 21.11	21.11 ± 0.01	10.25 ± 0.11	0.00 ± 0.11	1.0 (0.9-1.1)	82 (76-88)
†*ndhJ*	*rpoZ191*	17.91 17.95 17.92	17.92 ± 0.02	7.04± 0.07	-0.16 ± 0.07	1.11 (1.07-1.17)	762 (729-798)
	wt	18.12 18.04 18.00	18.05 ± 0.06	19± 0.12	.00 ± 0.12	1.0 (0.9-1.1)	684 (629-744)
†*petA*	*rpoZ191*	18.35 18.39 18.38	18.37 0.02	7.48 ± 0.06	0.22 ± 0.06	1.16 (1.11-1.22)	558 (534-584)
	wt	18.14 18.13 18.12	18.13 0.01	7.27± 0.11	0.00 ± 0.11	1.0 (0.9-1.1)	650 (604-699)
†*psaA*	*rpoZ191*	15.72 15.73 15.71	15.72 ± 0.01	4.83 ± 0.06	0.86 ± 0.06	1.8 (1.7-1.9)	3516 (3367-3672)
	wt	14.79 14.81 14.89	14.83 ± 0.05	3.97 ± 0.12	0.00 ± 0.12	1.0 (0.9-1.1)	6394 (5894-6936)
†*psaB*	*rpoZ191*	15.51 15.48 15.48	15.49 ± 0.02	4.60 ± 0.07	0.93 ± 0.07	1.9 (1.8-2.0)	4121 (3937-4313)
	wt	14.57 14.53 14.54	14.53± 0.01	3.67 ± 0.11	0.00 ± 0.11	1.0 (0.9-1.1)	7845 (7292-8440)
†*psaJ*	*rpoZ191*	17.74 17.61 17.80	17.72 ± 0.10	6.83 ± 0.12	0.13 ± 0.12	1.1 (1.0-1.2)	878 (810-952)
	wt	17.53 17.55 17.60	17.56 ± 0.03	6.70 ± 0.11	0.00 ± 0.11	1.0 (0.9-1.1)	963 (892-1040)

Table 23. (continued).

Gene	Sample	C_T	*Avg C_T	[a]ΔC_T	[b]$\Delta\Delta C_T$	$2^{-\Delta\Delta CT}$	$2^{-\Delta CT}$ ($X10^5$)
¥*psbA*	*rpoZ191*	12.09 12.16 12.14	12.13 ± 0.03	1.57 ± 0.06	0.74 ± 0.06	1.66 (1.60-1.74)	33640 (32230-35110)
	wt	11.36 11.35 11.38	11.36 ± 0.02	0.84 ± 0.03	0.00 ± 0.03	1.00 (0.98-1.02)	56030 (54980-57090)
¥*psbD190*	*rpoZ191*	16.62 16.68 16.56	16.62 ± 0.06	6.06 ± 0.08	0.52 ± 0.08	1.44 (1.36-1.52)	1501 (1420-1586)
	wt	16.07 16.07 16.05	16.06 ± 0.01	5.54 ± 0.02	0.00 ± 0.02	1.00 (0.98-1.02)	2155 (2121-2189)
†*psbDLRP*	*rpoZ191*	21.24 21.07 20.70	21.16 ± 0.12	10.27 ± 0.14	1.35 ± 0.14	2.5 (2.3-2.8)	81 (74-89)
	wt	20.01 19.86 19.70	19.78 ± 0.11	8.92 ± 0.15	0.00 ± 0.15	1.0 (0.9-1.1)	207 (186-230)
¥*rbcL*	*rpoZ191*	13.24 13.28 13.28	13.26 ± 0.02	2.71 ± 0.06	0.40 ± 0.06	1.33 (1.27-1.37)	15330 (14750-15930)
	wt	12.85 12.90 12.74	12.83 ± 0.08	2.31 ± 0.08	0.00 ± 0.08	1.0 (0.9-1.1)	20210 (19070-21420)
¥*accD*	*rpoZ191*	20.02 19.86 19.94	19.94 ± 0.08	9.38 ± 0.10	0.52 ± 0.10	1.4 (1.3-1.5)	150 (140-160)
	wt	19.41 19.40 19.35	19.39 ± 0.03	8.86 ± 0.04	0.00 ± 0.04	1.00 (0.98-1.03)	215 (209-220)
†*clpP*	*rpoZ191*	17.36 17.25 17.27	17.30 ± 0.06	6.41± 0.08	0.52 ± 0.08	1.44 (1.36-1.52)	1179 (1113-1249)
	wt	16.78 16.71 16.75	16.74 ± 0.03	5.88 ± 0.11	0.00 ± 0.11	1.0 (0.9-1.1)	1696 (1571-1831)

Table 23. (continued).

Gene	Sample	C_T	*Avg C_T	[a]ΔC_T	[b]$\Delta\Delta C_T$	$2^{-\Delta\Delta CT}$	$2^{-\Delta CT}$ ($X10^5$)
Nuclear Genes							
¥*Lhca 1*	*rpoZ191*	19.82 19.78 19.79	19.80 ± 0.02	9.24 ± 0.06	-0.93 ± 0.06	1.9 (1.8-2.0)	166 (159-172)
	wt	20.69 20.69 20.70	20.70 ± 0.01	10.17 ± 0.02	0.00 ± 0.02	1.00 (0.99-1.01)	87 (86-88)
†*Lhcb 1.2*	*rpoZ191*	19.00 18.96 18.99	18.98 ± 0.02	8.09 ± 0.06	0.72 ± 0.06	1.64 (1.57-1.72)	366 (350-383)
	wt	18.24 18.22 18.25	18.24 ± 0.02	7.38 ± 0.11	0.00 ± 0.11	1.0 (0.9-1.1)	602 (559-648)
†*RbcS*	*rpoZ191*	17.42 17.38 17.42	17.41 ± 0.02	6.52 ± 0.07	-0.77 ± 0.07	1.7 (1.6-1.8)	1091 (1042-1143)
	wt	18.16 18.15 18.15	18.15 ± 0.01	7.29 ± 0.11	0.00 ± 0.11	1.0 (0.9-1.1)	640 (594-688)
¥*PetH*	*rpoZ191*	25.12 25.18 25.11	25.13 ± 0.04	14.58 ± 0.06	0.32 ± 0.06	1.25 (1.19-1.31)	4.1 (3.9-4.3)
	wt	24.81 24.85 24.71	24.78 ± 0.09	14.25 ± 0.10	0.00 ± 0.10	1.0 (0.9-1.1)	5.1 (4.8-5.5)
Normalizer							
†*18S*	*rpoZ191*	11.03 10.84 10.93	10.89 ± 0.06				
	wt	11.15 10.79 10.94	10.86 ± 0.11				
¥*18S*	*rpoZ191*	10.53 10.52 10.60	10.55 ± 0.04				

Table 23. (continued).

Gene	Sample	C_T	*Avg C_T
	wt	10.60 10.54 10.51	10.55 ± 0.05

* Used for calculating ΔC_T.
[a] $\Delta C_T = (C_{T\ sample} - C_{T\ normalizer})$.
[b] $\Delta\Delta C_T = (\Delta C_{T\ mutant} - \Delta C_{T\ wild\text{-}type})$
† Denotes genes and normalizer loaded on the same plate.
¥ Denotes genes and normalizer loaded on the same plate.

Table 24. Real-time PCR values in the seeds of wild-type and *rpoZ191* mutant

				Plastid Genes			
Gene	**Sample**	**C_T**	***Avg C_T**	**[a]ΔC_T**	**[b]$\Delta\Delta C_T$**	**$2^{-\Delta\Delta CT}$**	**$2^{-\Delta CT}$ ($X10^5$)**
[§]*rpoA*	*rpoZ191*	22.19 22.15 22.21	22.18 ± 0.03	10.52 ± 0.0	0.69 ± 0.07	1.6 (1.5-1.7)	68 (65-72)
	wt	21.58 21.53 21.52	21.54 ± 0.03	9.83 ± 0.24	0.00 ± 0.24	1.0 (0.8-1.2)	110 (93-130)
[†]*rpoC1*	*rpoZ191*	24.89 24.83 24.89	24.86 ± 0.04	12.18 ± 0.15	2.11 ± 0.15	4.3 (3.9-4.8)	22 (20-24)
	wt	21.28 21.20 21.26	21.23 ± 0.04	10.07 ± 0.07	0.00 ± 0.07	1.00 (0.95-1.05	93 (89-97)
[†]*rps14*	*rpoZ191*	23.07 23.12 23.13	23.11 ± 0.03	10.42 ± 0.15	0.01 ± 0.15	1.0 (0.9-1.1)	73 (66-80)
	wt	21.71 21.50 21.52	21.58 ± 0.12	10.42 ± 0.13	0.00 ± 0.13	1.0 (0.9-1.1)	73 (67-80)
[†]*rps15*	*rpoZ191*	24.68 24.64 24.78	24.70 ± 0.07	12.01 ± 0.16	1.61 ± 0.16	3.2 (2.9-3.6)	24 (22-27)
	wt	21.72 21.48 21.50	21.56 ± 0.13	10.41 ± 0.14	0.00 ± 0.14	1.0 (0.9-1.1)	77 (68-87)
[†]*rps16*	*rpoZ191*	27.00 26.74 26.78	26.76 ± 0.03	14.07 ± 0.14	1.59 ± 0.14	3.02 (2.73-3.33)	5.8 (5.3-6.4)
	wt	23.62 23.65 23.64	23.64 ± 0.01	12.48 ± 0.05	0.00 ± 0.05	1.00 (0.96-1.04)	17.5 (16.9-18.2)

Table 24. (continued).

Gene	Sample	C_T	*Avg C_T	[a]ΔC_T	[b]$\Delta\Delta C_T$	$2^{-\Delta\Delta CT}$	$2^{-\Delta CT}$ ($X10^5$)
†*rpl32*	*rpoZ191*	24.45 24.38 24.60	24.42 ± 0.05	11.73 ± 0.15	1.84 ± 0.15	3.4 (3.2-4.0)	29 (27-33)
	wt	21.09 21.10 21.12	21.11 ± 0.02	9.89 ± 0.11	0.00 ± 0.11	1.0 (0.9-1.1)	105 (97-114)
¥*rrn16*	*rpoZ191*	13.12 13.04 13.04	13.07 ± 0.05	0.72 ± 0.06	0.30 ± 0.06	1.23 (1.19-1.28)	61000 (59000-63000)
	wt	11.43 11.44 11.53	11.46 ± 0.05	0.41 ± 0.06	0.00 ± 0.06	1.00 (0.96-1.04)	75000 (72000-78000)
†*trnC-GCA*	*rpoZ191*	26.33 26.21 26.30	26.26 ± 0.06	13.57 ± 0.16	2.54 ± 0.16	5.8 (5.2-6.5)	8.2 (7.4-9.1)
	wt	22.16 22.21 22.19	22.19 ± 0.02	11.03 ± 0.06	0.00 ± 0.06	1.00 (0.96-1.04)	47.9 (46.0-49.8)
†*trnE-UUC*	*rpoZ191*	27.16 26.83 26.65	26.74 ± 0.12	14.06 ± 0.19	0.43 ± 0.19	1.3 (1.2-1.5)	5.9 (5.1-6.7)
	wt	24.81 24.73 24.82	24.79 ± 0.05	13.63 ± 0.08	0.00 ± 0.08	1.00 (0.95-1.05)	7.9 (7.5-8.3)
†*trnfM-CAU*	*rpoZ191*	25.73 26.29 25.87	25.80 ± 0.10	13.11± 0.17	0.28 ± 0.17	1.2 (1.1-1.4)	11 (10-13)
	wt	24.04 23.98 23.95	23.99 ± 0.05	12.83 ± 0.07	0.00 ± 0.07	1.00 (0.95-1.05 0	13.7 (13.0-14.4)
†*trnS-GCU*	*rpoZ191*	23.09 23.17 23.00	23.09 ± 0.09	10.40 ± 0.17	1.20 ± 0.17	2.3 (2.1-2.6)	74 (66-83)
	wt	20.42 20.32 20.34	20.36 ± 0.05	9.20± 0.08	0.00 ± 0.08	1.00 (0.95-1.05)	170 (161-179)

Table 24. (continued).

Gene	Sample	C_T	*Avg C_T	[a]ΔC_T	[b]$\Delta\Delta C_T$	$2^{-\Delta\Delta CT}$	$2^{-\Delta CT}$ ($X10^5$)
†*trnV-GAC*	*rpoZ191*	25.26 25.78 25.13	25.19 ± 0.09	12.51± 0.17	0.92 ± 0.17	2.0 (1.7-2.1)	17 (15-19)
	wt	22.87 22.67 22.69	22.74 ± 0.11	11.58 ± 0.12	0.00 ± 0.12	1.0 (0.9-1.1)	33 (30-35)
†*trnW-CCA*	*rpoZ191*	22.49 22.42 22.42	22.44 ± 0.04	9.76± 0.04	0.14 ± 0.04	1.08 (1.07-1.13	115 (112-119)
	wt	20.76 20.77 20.80	20.78 ± 0.02	9.62± 0.02	0.00 ± 0.02	1.00 (0.98-1.02)	127 (125-129)
†*atpA*	*rpoZ191*	22.07 22.04 22.01	22.04 ± 0.03	9.35 ± 0.15	0.54 ± 0.15	1.4 (1.3-1.6)	153 (138-169)
	wt	19.97 19.96 19.97	19.97 ± 0.01	8.81± 0.05	0.00 ± 0.05	1.00 (0.96-1.04)	222 (214-231)
†*atpB*	*rpoZ191*	26.11 24.06 24.07	24.06 ± 0.01	11.38 ± 0.14	1.73 ± 0.14	3.3 (3.0-3.5)	38 (34-41)
	wt	20.82 20.82 20.76	20.80 ± 0.03	9.64± 0.06	0.00 ± 0.06	1.00 (0.96-1.04)	125 (120-131)
†*ndhA*	*rpoZ191*	24.04 23.95 23.87	23.95 ± 0.09	11.26	1.79 ± 0.17	3.5 (3.1-3.9)	41 (36-46)
	wt	20.68 20.57 20.64	20.63 ± 0.06	9.47	0.00 ± 0.08	1.00 (0.95-1.05)	141 (134-149)
†*ndhB*	*rpoZ191*	32.26 31.70 32.39	32.32 ± 0.09	19.63 ± 0.17	1.28 ± 0.17	2.4 (2.2-2.7)	0.12 (0.11-0.14)
	wt	29.48 29.54 29.76	29.51 ± 0.04	18.35 ± 0.0	0.00 ± 0.07	1.00 (0.95-1.05)	0.30 (0.29-0.31)

Table 24. (continued.

Gene	Sample	C_T	*Avg C_T	[a]ΔC_T	[b]$\Delta\Delta C_T$	$2^{-\Delta\Delta CT}$	$2^{-\Delta CT}$ ($X10^5$)
†*ndhF*	*rpoZ191*	27.22 25.51 25.61	25.56 ± 0.07	12.88 ± 0.16	1.34 ± 0.16	2.5 (2.3-2.80	13 (12-15)
	wt	22.75 22.69 22.64	22.69 ± 0.06	11.54 ± 0.08	0.00 ± 0.08	1.00 (0.95-1.06)	34 (32-36)
†*ndhJ*	*rpoZ191*	23.39 23.33 23.31	23.34 ± 0.04	10.66 ± 0.15	1.09 ± 0.15	2.1 (1.9-2.4)	62 (56-69)
	wt	20.73 20.73 20.72	20.73 ± 0.01	9.57± 0.05	0.00 ± 0.05	1.00 (0.96-1.04)	132 (127-137)
†*petA*	*rpoZ191*	24.07 23.96 24.00	24.01 ± 0.06	11.33 ± 0.15	1.08 ± 0.15	2.1 (1.9-2.3)	39 (35-43)
	wt	21.77 21.42 21.38	21.40 ± 0.03	10.25 ± 0.06	0.00 ± 0.06	1.00 (0.96-1.04)	82 (79-86)
†*psaA*	*rpoZ191*	20.91 20.70 20.64	20.67 ± 0.04	7.98 ± 0.15	1.01 ± 0.15	2.0 (1.8-2.2)	396 (357-439)
	wt	18.19 18.32 18.07	18.13 ± 0.09	6.97± 0.10	0.00 ± 0.10	1.0 (0.9-1.1)	796 (743-854)
†*psaB*	*rpoZ191*	20.46 20.44 20.38	20.43 ± 0.04	7.74 ± 0.15	1.06 ± 0.15	2.1 (1.9-2.3)	467 (421-517)
	wt	17.85 17.62 17.82	17.84 ± 0.02	6.68 ± 0.06	0.00 ± 0.06	1.00 (0.96-1.04)	975 (937-1015)
†*psaJ*	*rpoZ191*	23.65 23.75 23.64	23.68 ± 0.06	10.99 ± 0.16	0.04 ± 0.16	1.0 (0.9-1.1)	49 (44-55)
	wt	22.08 22.14 21.87	22.11 ± 0.04	10.95 ± 0.07	0.00 ± 0.07	1.00 (0.95-1.05)	50 (48-53)

Table 24. (continued).

Gene	Sample	C_T	*Avg C_T	[a]ΔC_T	[b]$\Delta\Delta C_T$	$2^{-\Delta\Delta CT}$	$2^{-\Delta CT}$ ($X10^5$)
¥*psbA*	*rpoZ191*	17.17 17.11 17.11	17.13 ± 0.04	4.81 ± 0.05	1.27 ± 0.05	2.42 (2.34-2.50)	3570 (3450-3690)
	wt	14.55 14.61 14.59	14.59 ± 0.03	3.54 ± 0.04	0.00 ± 0.04	1.00 (0.97-1.03)	8630 (8380-8880)
¥*psbD190*	*rpoZ191*	22.34 22.31 22.29	22.31 ± 0.02	9.99 ± 0.04	0.83 ± 0.04	1.80 (1.73-1.82)	98 (96-101)
	wt	20.25 20.14 20.25	20.21 ± 0.06	9.16 ± 0.07	0.00 ± 0.07	1.00 (0.95-1.05)	175 (166-183)
†*psbDLRP*	*rpoZ191*	26.49 26.92 26.49	26.63 ± 0.25	13.95 ± 0.29	0.91 ± 0.29	1.9 (1.5-2.3)	6 (5-8)
	wt	24.21 24.27 24.11	24.20± 0.08	13.04 ± 0.10	0.00 ± 0.10	1.0 (0.9-1.1)	12 (11-13)
¥*rbcL*	*rpoZ191*	20.55 20.52 20.74	20.54 ± 0.02	8.21 ± 0.03	-0.59 ± 0.03	1.51 (1.47-1.54)	337 (329-345)
	wt	20.07 19.91 19.80	19.92 ± 0.14	8.80 ± 0.14	0.00 ± 0.14	1.0 (0.9-1.1)	224 (203-247)
¥*accD*	*rpoZ191*	24.86 24.79 25.03	24.83 ± 0.05	12.50 ± 0.06	1.03 ± 0.06	2.04 (1.95-2.12)	17.2 (16.5-18.0)
	wt	22.46 22.49 22.56	22.53 ± 0.05	11.48 ± 0.06	0.00 ± 0.06	1.00 (0.96-1.04)	35 (34-37)
§*clpP*	*rpoZ191*	19.14 19.15 19.19	19.16 ± 0.03	7.50 ± 0.07	0.50 ± 0.07	1.4 (1.3-1.5)	554 (528-582)
	wt	18.67 18.66 18.77	18.70 ± 0.06	6.99 ± 0.25	0.00 ± 0.25	1.0 (0.8-1.2)	786 (661-935)

Table 24. (continued).

Nuclear Genes

Gene	Sample	C_T	Avg C_T	ΔC_T	$\Delta\Delta C_T$	$2^{-\Delta\Delta CT}$	$2^{-\Delta CT}$ ($X10^5$)
¥*Lhca 1*	*rpoZ191*	29.73 29.78 29.74	29.75 ± 0.03	17.43 ± 0.04	-0.98 ± 0.04	2.0 (1.9-2.0)	0.57 (0.55-0.58)
	wt	29.47 29.40 29.51	29.46 ± 0.05	18.41 ± 0.06	0.00 ± 0.06	1.00 (0.96-1.04)	0.29 (0.28-0.30)
†*Lhcb 1.2*	*rpoZ191*	27.48 27.42	27.45 ± 0.04	14.76 ± 0.15	-3.66 ± 0.15	12.6 (11.4-14.0)	3.60 (3.25-3.99)
	wt	29.57 29.59	29.58 ± 0.01	18.42 ± 0.05	0.00 ± 0.05	1.00 (0.96-1.04)	0.29 (0.27-0.30)
†*Rbcs*	*rpoZ191*	32.08 32.22	32.15 ± 0.10	19.46 ± 0.17	1.50 ± 0.17	2.8 (2.5-3.2)	0.14 (0.12-0.16)
	wt	28.98 29.27	29.12 ± 0.21	17.96 ± 0.21	0.00 ± 0.21	1.0 (0.9-1.2)	0.39 (0.34-0.45)
¥*PetH*	*rpoZ191*	34.54 34.87 34.27	34.41 ± 0.19	22.08 ± 0.19	0.08 ± 0.19	1.06 (0.93-1.21)	0.023 (0.020-0.026)
	wt	33.00 33.06 33.09	33.05 ± 0.04	22.00 ± 0.05	0.00 ± 0.05	1.00 (0.96-1.04)	0.024 (0.023-0.025)

Normalizer

†*18S*	*rpoZ191*	12.75 12.95 12.35	12.69 ± 0.14				
	wt	11.34 11.20 11.12	11.22 ± 0.11				

Table 24. (continued).

Gene	Sample	C_T	*Avg C_T
¥*18SA*	*rpoZ191*	12.31 12.35 12.31	12.32 ± 0.02
	wt	11.01 11.03 11.07	11.04 ± 0.03
§*18S*	*rpoZ191*	11.71 11.62 11.15	11.67 ± 0.07
	wt	11.54 12.19 11.88	11.71 ± 0.24

* Used for calculating ΔC_T.
[a] $\Delta C_T = (C_{T\ sample} - C_{T\ normalizer})$.
[b] $\Delta\Delta C_T = (\Delta C_{T\ mutant} - \Delta C_{T\ wild\text{-}type})$
† Denotes genes and normalizer loaded on the same plate.
¥ Denotes genes and normalizer loaded on the same plate.
§ Denotes genes and normalizer loaded on the same plate.

Table 25. Real-time PCR values of the *RpoT* genes in *the* wild-type and *rpoZ191* mutant

Siliques

Gene	Sample	C_T	*Avg C_T	[a]ΔC_T
†*RpoT;1*	*rpoZ191*	28.48 28.47 28.62	28.53 ± 0.08	17.64 ± 0.10
	wt	28.90 29.02 29.03	28.98 ± 0.07	18.12 ± 0.13
†*RpoT;2*	*rpoZ191*	26.12 26.23 26.26	26.20 ± 0.07	15.31 ± 0.09
	wt	26.17 26.13 26.23	26.18 ± 0.05	15.31 ± 0.12
†*RpoT;3*	*rpoZ191*	34.30 32.50 32.64	32.57 ± 0.10	22.26 ± 0.12
	wt	27.16 27.19 27.23	27.19 ± 0.03	16.33 ± 0.11

Normalizer

†*18S*	*rpoZ191*	11.03 10.84 10.93	10.89 ± 0.06	
	wt	11.15 10.79 10.94	10.86 ± 0.11	

Seeds

Gene	Sample	C_T	*Avg C_T	[a]ΔC_T
†*RpoT;1*	*rpoZ191*	29.50 29.29 29.68	29.49 ± 0.19	16.81 ± 0.24
	wt	27.96 27.93 27.97	27.96 ± 0.02	16.80 ± 0.06

Table 25. (continued).

Gene	Sample	C_T	*Avg C_T	[a]ΔC_T
[#]*RpoT;2*	*rpoZ191*	26.97 27.08 27.05	27.04 ± 0.06	15.37 ± 0.09
	wt (1)	27.51 27.22 27.06	27.26 ± 0.23	15.39 ± 0.40
	wt (2)	27.08 27.15 27.25	27.20 ± 0.07	15.51 ± 0.09
	wt (3)	26.52 26.35 26.58	26.46 ± 0.16	15.17 ± 0.17
	wt (4)	27.04 26.76 26.95	26.86 ± 0.14	15.47 ± 0.14
[#]*RpoT;3*	*rpoZ191*	47.00 47.00 47.00		
	wt (1)	26.14 26.14 26.13	26.13 ± 0.01	14.42 ± 0.24
	wt (2)	26.29 26.27 26.28	26.28 ± 0.01	14.59 ± 0.05
	wt (3)	26.07 26.13 26.15	26.12 ± 0.04	14.82 ± 0.08
	wt (4)	26.33 26.42 26.28	26.34 ± 0.07	14.96 ± 0.07

Normalizer

Gene	Sample	C_T	*Avg C_T
[†]*18S*	*rpoZ191*	12.75 12.95 12.35	12.69 ± 0.14
	wt	11.34 11.20 11.12	11.22 ± 0.11

Table 25. (continued).

Gene	Sample	C_T	*Avg C_T	[a]ΔC_T
[#]*18S*	*rpoZ191*	11.71 11.62 11.15	11.67 ± 0.07	
	wt (1)	11.54 12.19 11.88	11.87 ± 0.33	
	wt (2)	11.65 11.74 11.67	11.69 ± 0.05	
	wt (3)	11.35 11.22 11.32	11.30 ± 0.07	
	wt (4)	11.37 11.39 11.36	11.38 ± 0.02	

2-day seedlings

Gene	Sample	C_T	*Avg C_T	[a]ΔC_T
[#]*RpoT;1*	*rpoZ191*	25.09 25.11 25.17	25.12 ± 0.04	14.45 ± 0.07
	wt	27.25 27.33 27.26	27.28 ± 0.04	16.14 ± 0.06
[†]*RpoT;2*	*rpoZ191*	24.10 24.09 24.05	24.08 ± 0.03	13.68 ± 0.05
	wt	26.30 26.23 26.28	26.27 ± 0.04	15.75 ± 0.16
[†]*RpoT;3*	*rpoZ191*	32.04 32.26 31.90	32.07 ± 0.18	21.67 ± 0.18
	wt	25.40 25.46 25.48	25.47 ± 0.02	14.95 ± 0.16

Table 25. (continued).

Normalizer

Gene	Sample	C_T	*Avg C_T
†*18S*	*rpoZ191*	10.95 10.42 10.37	10.39 ± 0.04
	wt	10.88 10.41 10.63	10.52 ± 0.16
#*18S*	*rpoZ191*	10.66 10.72 10.63	10.67 ± 0.05
	wt	10.75 11.17 11.11	11.14 ± 0.05

5-day seedlings

Gene	Sample	C_T	*Avg C_T	[a]ΔC_T
#*RpoT;1*	*rpoZ191*	25.17 25.16 25.12	25.15 ± 0.03	14.46 ± 0.08
	wt	26.48 26.51 26.56	26.52 ± 0.04	15.48 ± 0.06
†*RpoT;2*	*rpoZ191*	24.32 24.34 24.30	24.32 ± 0.02	13.92 ± 0.06
	wt	24.32 24.34 24.30	25.67 ± 0.40	14.45 ± 0.42
†*RpoT;3*	*rpoZ191*	33.16 32.46 33.27	33.22 ± 0.08	22.81 ± 0.10
	wt	25.01 24.91 25.01	24.96 ± 0.07	13.74 ± 0.14

Table 25. (continued.

Gene	Sample	C_T	*Avg C_T	$^{a}\Delta C_T$
Normalizer				
†*18S*	*rpoZ191*	10.39 10.36 10.47	10.40 ± 0.06	
	wt	11.30 11.13 10.77	11.22 ± 0.12	
#*18S*	*rpoZ191*	11.08 10.64 10.74	10.69 ± 0.07	
	wt	11.07 11.24 11.01	11.04 ± 0.04	
10-day cotyledons				
†*RpoT;2*	*rpoZ191*	31.72 31.86 30.97	31.79 ± 0.10	15.02 ± 0.11
	wt	28.23 27.87 28.77	28.05 ± 0.25	15.75 ± 0.26
†*RpoT;3*	*rpoZ191*	35.50 35.31 35.45	35.42 ± 0.10	18.65 ± 0.10
	wt (1)	26.29 26.25 26.18	26.24 ± 0.06	13.95 ± 0.08
	wt (2)	25.38 25.30 25.30	25.33 ± 0.05	14.05 ± 0.08
	wt (3)	24.17 24.18 24.23	24.19 ± 0.03	13.12 ± 0.04

Table 25. (continued).

Normalizer

Gene	Sample	C_T	*Avg C_T	
†*18S*	*rpoZ191*	16.79 16.75 16.76	16.77 ± 0.02	
	wt (1))	12.23 12.35 12.30	12.29 ± 0.06	
	wt (2)	11.31 11.20 11.33	11.28 ± 0.07	
	wt (3)	11.07 11.09 11.07	11.08 ± 0.01	

12-day cotyledons

Gene	Sample	C_T	*Avg C_T	[a]ΔC_T
†*RpoT;2*	*rpoZ191*	28.54 28.58 28.74	28.62 ± 0.11	15.04 ± 0.11
	wt	27.75 28.18 28.00	28.09 ± 0.13	15.50 ± 0.13
†*RpoT;3*	*rpoZ191*	35.09 34.03 35.45	35.27 ± 0.26	21.69 ± 0.26
	wt (1)	25.68 25.45 25.45	25.53 ± 0.13	12.93 ± 0.14
	wt (2)	26.37 26.45 26.50	26.44 ± 0.07	14.06 ± 0.17

Normalizer

Gene	Sample	C_T	*Avg C_T
†*18S*	*rpoZ191*	13.57 13.59 13.56	13.58 ± 0.02

Table 25. (continued).

Gene	Sample	C_T	*Avg C_T	
	wt (1)	12.57 12.56 12.65	12.59 ± 0.05	
	wt (2)	12.56 12.35 12.24	12.38 ± 0.16	
		15-day cotyledons		
Gene	**Sample**	**C_T**	***Avg C_T**	**[a]ΔC_T**
†*RpoT;2*	*rpoZ191*	25.57 25.58 25.68	25.61 ± 0.07	14.70 ± 0.30
	wt	25.81 25.95	25.88 ± 0.10	14.55 ± 0.11
†*RpoT;3*	*rpoZ191*	28.31 28.28 28.25	28.28 ± 0.04	17.37 ± 0.29
	wt	24.50 24.51 24.56	24.53 ± 0.03	13.20 ± 0.05
		Normalizer		
Gene	**Sample**	**C_T**	***Avg C_T**	
†*18S*	*rpoZ191*	11.11 10.70 10.68	10.91 ± 0.29	
	wt	11.30 11.38 11.31	11.33 ± 0.04	
		15-day rosette leaves		
Gene	**Sample**	**C_T**	***Avg C_T**	**[a]ΔC_T**
†*RpoT;2*	*rpoZ191*	26.03 25.74 25.98	25.86 ± 0.17	14.88 ± 0.22

Table 25. (continued).

Gene	Sample	C_T	*Avg C_T	[a]ΔC_T
	wt	26.97 27.25 26.99	26.98 ± 0.02	15.88 ± 0.05
†*RpoT;3*	*rpoZ191*	31.51 31.72 31.36	31.44 ± 0.10	20.45 ± 0.18
	wt	23.65 23.69 23.67	23.67 ± 0.02	12.57 ± 0.05

Normalizer

Gene	Sample	C_T	*Avg C_T
†*18S*	*rpoZ191*	10.88 11.08 10.74	10.98 ± 0.14
	wt	11.09 11.06 11.16	11.10 ± 0.05

35-day rosette leaves

Gene	Sample	C_T	*Avg C_T	[a]ΔC_T
†*RpoT;2*	*rpoZ191*	25.50 25.51 25.49	25.50 ± 0.01	13.77 ± 0.06
	wt	25.12 25.21 25.23	25.19 ± 0.06	13.42 ± 0.11
†*RpoT;3*	*rpoZ191*	30.88 31.57 31.21	31.39 ± 0.26	19.66 ± 0.26
	wt	24.71 24.87 24.69	24.76 ± 0.10	12.99 ± 0.13

Table 25. (continued).

Normalizer

Gene	Sample	C_T	*Avg C_T
†*18S*	*rpoZ191*	11.73 11.78 11.67	11.73 ± 0.06
	wt	11.67 11.84 11.79	11.77± 0.09

35-day cauline leaves

Gene	Sample	C_T	*Avg C_T	$^{a}\Delta C_T$
†*RpoT;2*	*rpoZ191*	25.14 24.94	25.04 ± 0.14	13.79 ± 0.16
	wt	24.70 24.66 24.67	24.68 ± 0.02	13.48 ± 0.03
†*RpoT;3*	*rpoZ191*	30.68 31.31 30.70	30.69 ± 0.01	19.44 ± 0.07
	wt	23.93 23.95 23.96	23.95 ± 0.02	12.75 ± 0.03

Normalizer

Gene	Sample	C_T	*Avg C_T
†*18S*	*rpoZ191*	11.30 11.20	11.25 ± 0.07
	wt	11.22 11.18	11.20 ± 0.03

5-day roots

Gene	Sample	C_T	*Avg C_T	$^{a}\Delta C_T$
¥*RpoT;1*	*rpoZ191*	25.27 25.23 25.29	25.26 ± 0.03	14.57 ± 0.17

Table 25. (continued).

Gene	Sample	C_T	*Avg C_T	[a]ΔC_T
	wt	26.60 26.69 26.80	26.70 ± 0.10	15.65 ± 0.10
[†]*RpoT;2*	*rpoZ191*	24.22 24.09 24.16	24.16 ± 0.07	12.88 ± 0.18
	wt	25.53 25.44 25.46	25.47 ± 0.05	14.30 ± 0.10
[†]*RpoT;3*	*rpoZ191*	34.23 35.24 33.19	34.74 ± 0.71	23.46 ± 0.73
	wt	26.52 26.52 26.72	26.59 ± 0.12	15.42 ± 0.14

Normalizer

Gene	Sample	C_T	*Avg C_T
[†]*18S*	*rpoZ191*	11.47 11.19 11.16	11.28 ± 0.17
	wt	11.17 11.26 11.09	11.17 ± 0.09
[¥]*18S*	*rpoZ191*	10.73 10.51 10.84	10.69 ± 0.17
	wt	11.01 11.07 11.07	11.05 ± 0.03

40-day roots

Gene	Sample	C_T	*Avg C_T	[a]ΔC_T
[¥]*RpoT;1*	*rpoZ191*	26.06 26.02 26.10	26.06 ± 0.04	15.37 ± 0.09
	wt	25.55 25.65 25.56	25.59 ± 0.05	14.81 ± 0.08

Table 25. (continued).

Gene	Sample	C_T	*Avg C_T	[a]ΔC_T
†*RpoT;2*	*rpoZ191*	24.38 24.35 24.38	24.37 ± 0.02	13.31 ± 0.17
	wt	24.24 24.26 24.30	24.27 ± 0.03	13.02 ± 0.11
†*RpoT;3*	*rpoZ191*	33.84 34.18 34.78	34.27 ± 0.48	23.21 ± 0.51
	wt	25.66 25.59 25.66	25.64 ± 0.04	14.39 ± 0.11
		Normalizer		
Gene	**Sample**	**C_T**	***Avg C_T**	
†*18S*	*rpoZ191*	11.24 10.90 11.03	11.06 ± 0.17	
	wt	11.30 11.12 11.31	11.25 ± 0.11	
¥*18S*	*rpoZ191*	10.59 10.75 10.71	10.68 ± 0.08	
	wt	10.74 10.85 10.76	10.78 ± 0.06	

* Used for calculating ΔC_T.
[a] $\Delta C_T = (C_{T\ sample} - C_{T\ normalizer})$.
† Denotes genes and normalizer loaded on the same plate.
¥ Denotes genes and normalizer loaded on the same plate.
§ Denotes genes and normalizer loaded on the same plate.
wt (1), wt (2), wt (3), and wt (4) represent different wild-type sample preparations each analyzed in triplicate.

VITA

Aglaia Chandler
c/o Department of Biochemistry & Biophysics
Texas A & M University, 2128 TAMU
College Station, TX 7743-2128

Education

Doctor of Philosophy
Biochemistry
Texas A&M University, College Station, TX
Date of Graduation: August 2005

Master of Science
Molecular Biology
Midwestern State University, Wichita Falls, TX
Date of Graduation: May 1997

Bachelor of Science (summa cum laude)
Biology
Midwestern State University, Wichita Falls, TX
Date of Graduation: May 1993

Teaching Experience

Texas A&M University, College Station, TX:

Laboratory Teaching Assistant – Biochemistry Laboratory 1997-1998

Grader – General Biochemistry 1997-1998; 2001

Midwestern State University, Wichita Falls, TX

Instructor – Anatomy & Physiology 1996 – 1997

Laboratory Teaching Assistant – Biochemistry Laboratory 1994

Laboratory Teaching Assistant / *Laboratory Coordinator* – Anatomy & Physiology,

Comparative Anatomy of Vertebrates 1992-1996